THE UNIVERSITY
of EDINBURGH

The role of the metabolic enzyme fumarate hydratase in aged haematopoiesis and malignant transformation

Theoni I Panagopoulou

A thesis submitted in fulfilment of the requirements for the degree of Doctor of Philosophy

University of Edinburgh

2017

Author's Declaration

This is to certify that that the work contained within has been composed by me and is entirely my own work. No part of this thesis has been submitted for any other degree or professional qualification.

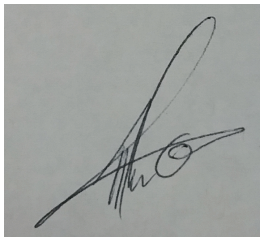

Theoni Panagopoulou,

February 2017

Abstract

The finely tuned regulation of haematopoiesis is crucial in order to maintain life-long haematopoiesis. The disruption of the balance among cell fates, can lead to malignant transformation. It has become increasingly evident that the metabolic regulation haematopoietic stem cells is critical for stem cell fate decisions. Haematopoietic stem cells reside in a hypoxic microenvironment within the bone marrow and are thought to mainly utilize glycolysis rather than oxidative phosphorylation in order to maintain their pool. However recent evidence suggests that oxidative phosphorylation is critical for quiescent HSCs and in several cases, for leukaemic stem cells (LSCs).

One of the key parts of mitochondrial respiration is the tricarboxylic cycle (TCA), providing co-factors for its efficient activity. The TCA functions by catalysing the oxidation of pyruvate via key enzymatic activities.

A key component of the TCA cycle is fumarate hydratase *(Fh1)* which catalyses the hydration of fumarate into malate within the mitochondria, but also catalyses the same reaction in the cytoplasm. FH is a tumour suppressor in human lyomeioma and renal kidney cancer (HLRCC). Previous work conducted by our team has shown that *Fh1* is essential for foetal and adult haematopoiesis, as *Fh1* deletion within the haematopoietic system is embryonic lethal. Furthermore, conditional deletion of *Fh1* in donor cells of the *Mx1-Cre* system that were injected in lethally irradiated recipients, resulted in the complete reduction of their chimerism in the peripheral blood of recipient mice. Mechanistically, these phenotypes were mostly associated with supra-physiological levels of fumarate as a result of *Fh1* deletion. Interestingly, by employing mice that ubiquitously express the human cytosolic isoform of FH (FH^{Cyt}, which lacks the mitochondrial targeting sequence and therefore is excluded from the mitochondria), we rescued the embryonic lethality that *Fh1* causes, and reduced the levels of fumarate. Importantly, although FH^{Cyt} expression restored fumarate-associated lethality, it did not restore the mitochondrial defects, allowing us to study the importance of genetically intact TCA in the context of haematopoiesis.

Here I investigated the impact that a genetic truncation of the TCA cycle (as a result of the lack of the mitochondrial isoform of *Fh1*) has on leukaemic transformation and on aged haematopoiesis. *Fh1*$^{fl/fl}$*; FH*^{Cyt}*; Vav-iCre* mice of approximately 60 weeks old displayed and expansion in the pool of early stem and progenitor compartment (Lin$^-$ Sca-1$^+$ c-Kit$^+$), as well as in the early progenitors HPC-1 (LSK CD48$^+$ CD150$^-$) and HPC-2 (LSK CD48$^+$ CD150$^+$). Furthermore, the mice exhibited a drastic depletion of B cells (CD19$^+$ B220$^+$) and an expansion in the frequency of the myeloid compartment (Mac-1$^+$ Gr1$^+$).

In order to assess the importance of the TCA cycle in malignant transformation, I isolated stem and progenitor cells from *Fh1*$^{fl/fl}$*; FH*^{Cyt}*; Vav-iCre* (and control (*Fh1*$^{fl/fl}$*; FH*^{Cyt} *Vav-iCre* negative or *Fh1*$^{fl/fl}$ *Vav-iCre* negative)) E 14.5 day old embryos and infected them with retroviruses expressing *Meis1* and *Hoxa9*, and generated pre-leukaemic cells (pre-LCs). Genetically intact TCA was required for the efficient generation of leukaemia-initiating cells (LICs), as injection of pre-LCs lacking mitochondrial *Fh1* into sub-lethally irradiated recipient mice, resulted in 76 % of leukaemia-free mice while injection of *control* pre-LCs resulted in 25 % of leukaemia-free mice. However, the genetic perturbation of the TCA did not exert and effect on the long-term self-renewal capacity of LICs. Inducible deletion of mitochondrial *Fh1* in established LICs of the *Mx1-Cre* background using poly (I:C) did not affect their ability to generate AML in primary and secondary recipient mice. These data indicate that genetically intact TCA is required for the efficient generation of LICs *in vivo* but is dispensable for their long-term self-renewal capacity, highlighting the metabolic rewiring that occurs at different stages of leukaemic transformation.

In an effort to understand whether, similarly to HLRCC, *Fh1* plays a tumour-suppressive role in malignant haematopoiesis, I isolated LSK cells from the foetal liver of E 14.5 old embryos lacking both isoforms of *Fh1*. *Fh1*$^{fl/fl}$*; Vav-iCre* cells transduced with *Meis1*/*Hoxa9* or *MLL-AF9*, *MLL-ENL*, *AML-ETO* (chromosomal translocations involved in AML development) -expressing retroviruses, failed to generate colonies in methylcellulose, indicating that stem and progenitor cells require *Fh1* to undergo *in vitro* transformation by these oncogenes. Furthermore, acute

deletion of *Fh1* (via the use of lentivirally-expressed Cre) in pre-LCs generated using the *Meis1*/*Hoxa9* retroviruses, rendered them unable to generate colonies in methylcellulose, indicating that *Fh1* is required for the self-renewal capacity of pre-LCs *in vitro*. Similarly, when LICs (*Fh1$^{fl/fl}$; Vav-iCre* negative*)* isolated from primary recipient mice were infected with Cre to induce deletion of *Fh1*, they were unable to generate colonies indicating that *Fh1* is required for the self-renewal capacity of LICs *in vitro*. Finally, in order to identify whether *Fh1* is important for LIC self-renewal *in vivo* I generated *Fh1$^{fl/fl}$; Mx1-Cre* pre-LCs by infecting stem and progenitor cells of E 14.5 embryos with *Meis1*/*Hoxa9* retroviruses, and injected them into sub-lethally irradiated mice. After the mice developed AML, I induced the deletion of *Fh1*, by injecting the mice with poly (I:C). Interestingly, the percentage of LICs in the peripheral blood of recipient mice was drastically decreased, leaving recipient mice leukaemia-free for the remaining time they were monitored. Surprisingly however, approximately 50 % of the recipient mice exhibited a drastic increase in LIC chimerism after two weeks post poly (I:C). Assessment of LICs isolated from recipient mice indicated that *Fh1* was fully deleted. These data indicate that while in some cases *Fh1* is required for LIC self-renewal *in vivo*, in other cases it is dispensable. Therefore, the tumour-suppressive roles of *Fh1* are likely tissue-specific and do not extend to haematopoietic cells.

Overall, this study agrees with published work supporting the notion that intact mitochondrial respiration is important (in varying degrees), in both the contexts of normal and malignant haematopoiesis.

Lay Summary

It has become increasingly evident that the metabolic regulation of haematopoietic stem cells (HSCs) is critical for stem cell fate decision. HSCs reside in a low oxygen environment within the bone marrow and are thought to utilise glycolysis rather than mitochondrial respiration in order to maintain their pool. However recent evidence suggests that mitochondrial respiration is critical for quiescent HSCs and in several cases, for leukaemia initiating cells (LICs). One of the key components of mitochondrial respiration is the tricarboxylic cycle (TCA) that provides essential co-factors for its efficient activity. A key component of the TCA is the enzyme fumarate hydratase (Fh1 in mouse and FH in humans), that also functions in the cytoplasm. Fh1 converts the metabolite fumarate into malate. Furthermore, FH is a tumour suppressor in human lyomeioma and renal kidney cancer (HLRCC) but its role in haematopoiesis is unknown.

Here I investigated the role of *Fh1* in aged haematopoiesis and in leukaemic transformation. Haematopoiesis-specific deletion of the mitochondrial isoform of *Fh1* in mice aged for approximately 60 weeks, resulted in an expansion of the early stem and progenitor cell populations. Furthermore the aged mice exhibited a depletion of the B cell compartment with the myeloid and T cell compartments remaining relatively unaffected. These results indicate that efficient fumarate metabolism is important for B cell development or survival.

Deletion of the mitochondrial isoform of *Fh1* did not impact the generation of pre-leukaemic cells as indicated by *in vitro* experiments. However, the mitochondrial isoform of *Fh1* was required for the efficient generation of LICs, as injection of pre-leukaemic cells lacking mitochondrial *Fh1* into sub-lethally irradiated recipient mice, resulted in 76 % of leukaemia-free mice while injection of *control* pre-LCs resulted in 25 % of leukaemia-free mice. The genetic deletion of the mitochondrial isoform of *Fh1* did not exert an impact on the long-term self-renewal capacity of LICs as indicated by *in vivo* experiments using an inducible system. Finally, in an effort to understand whether, similarly to HLRCC, Fh1 plays a tumour-suppressive role in malignant haematopoiesis, both lentivirally inducible and non-inducible *in vitro* methods were utilised. *In vitro* leukaemia initiation and propagation were not

possible in the absence of Fh1, indicating that Fh1 does not act as a tumour suppressor in the haemaopoieic system.

Overall, this study agrees with published work supporting the notion that intact mitochondrial respiration is important (in varying degrees), in both the contexts of normal and malignant haematopoiesis.

Contents

List of Tables

List of Figures

Related Publications

*Guitart A, *Panagopoulou T, Vukovic M, Sepulveda C, Sas Z, Gonzalez MV, Allen L, Armesilla--Diaz A,Edwards--Hicks J, Wills J, Easterbrook A, Corman D, Pollard P, Morton N, Carter R, Finch A, Kranc KR. Fumarate hydratase is a critical metabolic regulator of haematopoietic stem cell functions. Journal of Experimental Medicine. Accepted.
(*authors contributed equally to this work)

Vukovic M, Subramani C, Sepulveda C, Guitart A, Allen L, Panagopoulou T, Holyoake T, Ratcliffe PJ, Kranc KR. Adult haematopoietic stem cells lacking Hif--1α self--renew normally. Blood. 2016; 127, 2841--2846.

Vukovic M, Guitart AV, Sepulveda C, Villacreces A, O'Duibhir E, Panagopoulou T, Ivens A, Menendez--Gonzalez J, Iglesias JM, Allen L, Glykofrydis F, Subramani C, Armesilla--Diaz A, Post AE, Schaak K, Gezer D, So CW, Holyoake TL, Wood A, O'Carroll D, Ratcliffe PJ, Kranc KR. Hif--1α and Hif--2α synergize to suppress AML development but are dispensable for disease maintenance. J Exp Med. 2015 Dec14;212(13):2223--34.

List of Abbreviations

2-HG	2-hydroxyglutarate
2OG	2-oxoglutarate
ABL1	Abelson murine leukaemia 1
ACO2	Aconitase 2
ADCs	Antibody-drug conjugates
AF4	ALL-1 fused gene on chromosome 4
AF9	ALL-1 fused gene on chromosome 9
AGM	Aorta-gonad mesonephros
ALL	Acute lymphobastic leukaemia
AML	Acute myeloid leukaemia
AMPK	AMP-activated protein kinase
ASXL1	Additional sex combs like 1
ATP	Adeno tri phosphate
BCL-2	B cell CLL/Lypmhoma 2
BCOR	BCL6 Corepressor
BET	Bromodomain and extraterminal motif
BM	Bone marrow
c-Kit	Tyrosine-protein kinase (mast/stem cell growth factor receptor (SCFR) or CD117)
CBF	Core binding factor
CD	Cluster of differentiation
CEBPA	CCAAT/enhancer binding protein alpha
CEMP	CXCL12 expressing mesenchymal progenitor cells
CLL	Chronic lymphocytic leukaemia
CLP	Common lymphoid progenitor
CML	Chronic myeloid leukaemia
CMP	Common myeloid progenitor
CPT1	Carnitine palmitoytransferase
CXCL12	CXC motif chemokine 12
DMEM	Dulbecco's Modified Eagle's Medium
DNMT3	DNA (cytosine-5)-methyltransferase 3
dsRNA	Double-stranded RNA
E	Embryonic day
EBF1	Early B cell factor 1
ECAR	Extracellular acidification rate
EKLF	Erythroid kryppel-like factor
ELL	Eleven-nineteen lysine rich leukaemia
EMkMPP	Erythroid-megakaryocyte primed multipotent progenitor
EMT	Epithelial to mesenchymal transition
ENL	Eleven–nineteen-leukaemia gene
EoMP	Eosinophil-mast cell progenitor

Er(y)	Erythoid
ETO	Eight Twenty One gene
FAB	French-American-British classification
FACS	Fluorescence-activated cell sorting
FAD	Flavin adenine dinucleotide
FADH2	Flavin adenine dinucleotide
FAO	Fatty acid oxidation
FBS	Foetal bovine serum
FCCP	Carbonyl cyanide-p-trifluoromethoxyphenylhydrazone
FH	Fumarate hydratase
FIH	HIF-inhibitory protein
FL	Foetal liver
FL-HSCs	Foetal liver haematopoietic stem cells
Fli1	Friend leukaemia integration 1
FLT3	Fms Related Tyrosine Kinase 3
FOG1	Friend of GATA 1
G-CSF	Granulocyte-stimulating colony factor
GDP	Guanosine phosphate
GM	Granulocyte/macrophage
GM-CSF	Granulocyte-macrophage colony-stimulating factor
GMP	Granulocyte/macrophage progenitor
GSH	Glutathione
GTP	Guanosinetriphosphate
H3K4	Histone 3 lysine 4
HDAC	Histone deacetylase
HIF	Hypoxia inducible factor
HLRCC	Hereditary leiomyoma and renal cancer
HMOX1	Haem-oxygenase 1
HOX	Homeobox
HPC-1	Haematopoietic progenitor cell-1
HPC-2	Haematopoietic progenitor cell-2
HSC	Haemopoietic stem cell
HSPC	Haemopoietic stem and progenitor cell
iCre	Improved Cre recombinase
IDH1/2	Isocitrate dehydrogenase1/2
IL	Interleukin
IMDM	Iscove's Modified Dulbecco's Medium
ITD	Internal tandem mutation
KEAP1	Kelch-like ECH associated protein 1
LDHA	Lactate dehydrogenase A
LKB1	Liver kinase B1
LMPP	Lymphoid-primed multipotent progenitors
LSC	Leukaemic stem cell

LT-HSC	Long-term haemopoietic stem cell
LTR	Long terminal repeat
mTOR	Mammalian target of rapamycin
MAPK	Mitogen activated protein kinase
MDS	Myelodysplastic syndrome
MEFs	Mouse embryonic fibroblasts
MEIS	Myeloid ectropic insertion site
MEP	Megakaryocyte/erythroid progenitors
Mk	Megakaryocyte
MkE-GM	Megakaryocyte-erythroid-granulocyte-macrophage progenitors
MLL	Mixed Lineage leukaemia
MLL-AF9	Mixed-Lineage Leukaemia translocated AF9 protein
MPN	Myeloproliferative neoplasms
MPP	Multipotent progenitor
MSC	Mesenchymal stem cells
MSCV	Murine stem cell virus
MTCH2	Mitochondrial carrier homologue 2
MX1	Mixovirus resistance-1
MYH11	Myosin heavy chain 11
NADH	Nacotinamide adenine dinucleotide
NMP	Neutrophil-macrophage progenitor
NMP1	Nucleophosmin 1
NRF2	Nunclear erythroid-related factor 2
OCR	Oxygen consumption rate
ON	Overnight
OXPHOS	Oxidative phosphorylation
PB	Peripheral blood
PBS	Phosphate-buffered saline
PBX1	Pre-B cell leukaemia homeobox 1
PDK	Pyruvate dehydrogenase
PHD	Prolyl hydroxylase
PKM2	M2 pyruvate kinase isoform
PML	Progressive multifocal leukoencepathy
PPAR	Peroxisome-proliferator activated receptor
PPP	Pentose phosphate pathway
Pre LSC/LC	Pre-leukaemic (stem) cell
Pre NM	Pre neutrophil-macrophage
PRS	Prognosis risk score
PTEFb	Positive transcription elongation factor beta
RAD21	Cohesin sunbunit
RARA	Retonoic acid receptor alpha
ROS	Reactive oxygen species
RT	Room temperature
RUNX1	Runt-related transcription factor 1

SCA-1	Stem cells antigen-1
SCF	Stem cell factor
SF3B1	Splicing factor 3b subunit 1
SLAM	Signalling lymphocyte activation molecule
SLC1A5	Solute carrier family 1, member 5A
SMC1A	Structural maintenance chromosome
SMC3	Structural maintenance chromosome 3
Snai2	Snail family zinc finger 2
SO	Superoxide
SRSF2	Ser/Arg-rich splicing factor 2
ST HSC	Short term haematopoietic stem cells
STAG1/2	Cohesin sunbunit 1A
TCA	Tricarboxylic cycle
TEL	Translocation–Ets–leukaemia orETV6
TET	Ten-eleven-translocation gene
TF	Transcription factor
TGF	Transforming growth factor
TIF2	Transcriptional intermediary factor 2
U2AF1	U2 Small Nuclear RNA Auxiliary Factor 1
U2AF65	U2 small nuclear ribonucleoprotein auxiliary factor 65-kilodalton subunit
VHL	Von-Hippel-Lindau
VWF	Von Willebrand factor
WHO	World health organisation
WT	Wild type
WT1	Wilmuts tumour 1
Zeb	Zinc finger E box binding homeobox
ZRSR2	Zinc-finger CCCH-Type
α-KG	Alpha ketoglutarate

Acknowledgements

First and foremost, I would like to thank my primary supervisor Kamil R Kranc for giving me the opportunity to do my PhD in this lab and for putting up with my fiery temperament. Furthermore, I would like to thank the members of my committee, Lesley Forrester and Andy Finch for their guidance.

I would also like to thank the university of Edinburgh for sponsoring me during the last three years.

Amelie and Milica, needless to say that I wouldn't be here without you. You have taught me everything I know. You have supported me, given me guidance and truly invested into me. I really don't have words to describe how grateful I am for everything that you have done for me. I admire you both so much, you really are my role models.

Catarina, what can I say. Your positive vibe always keeps me sane. There is one particular memory of you that I think I will always remember. I was sleepless and I had a ton of work to do that day. Towards the end of the day, I ended up making a labelling mistake, broke down and sat on the TC floor, digging through the garbage in order to find all the different eppendorfs I had labelled. For some reason you walked into the room and all you did is smile, sit down on the floor with me, and started looking through the garbage to help me find those bloody eppendorfs. Your friendship means so much to me. I have never laughed as much as I have with you.

Lewis, oh Lewis! You are my favourite, man. I am so happy you joined our lab two years ago! I will never forget the DNA-extraction competitions we had and all the cat videos we have watched together. Thank you for all your help throughout these past years, the "genotyping express" especially, saved me so many times! Most of all though, thank you for putting up with me.

Hannah, I am so thankful for you! We became good friends so fast, it would have been great to have you join the lab earlier than what you did. It's been great to have someone that I can geek out about space and science with!

Arnaud, thank you so much for all of your help, especially during the last month of my thesis-writing time and while I was preparing for the viva. You are a wise man.

Jasmin, our champion! Thank you for your help and for all the delicious baking that you've done.

Fiona Rossi and Claire Cryer, thank you for all your help! Thank you for all those last-minute or over-time sorting slots. You always helped me regardless of whether it was easy to do so or not.

Finally, I would like to thank my family. I would not have done it without their support. You have always believed in me. Uncle Labros, Mimis and aunt Marika, you've always been proud of everything that I have done. Angela, thank you for sending me all those care-packages from Greece. The delicious cookies and cakes really helped, especially during my write-up time. You are the best, I am so lucky my dad met you.

I would like to dedicate this thesis to my father, Tasos. All of this would not have been possible without him, as he is the one that stood by my side since the age of 6, making sure I always did my homework. Every day, he would always come over after working two jobs (an office job and a nightclub job), just so he can pay for my tutoring lessons.
He has put me through school and university. The following paragraph is for him:

Μπαμπά,

Αυτή η πτυχιακή είναι αφιερωμένη σε σένα. Από την ημέρα που η κυρια Χρυσουλα σου είπε πως δεν τα πηγαίνω καλά στο σχολειο (ημουν 6 ετων τοτε), το έβαλες στόχο της ζωής σου να μάθω γράμματα. Τα χρονια περνουσαν και συ ησουν εκει, κάθε μεσημερι μετα τη δουλεια. Ακομη και όταν δούλευες δυο δουλείες, μια βραδινή και μια πρωινή, για να πληρώνουμε το φροντιστήριο (ημουν σκραπας στα μαθηματικα οποτε επρεπε καποιος να μου τα μάθει), πάλι ήσουν εκεί κάθε μέρα μετά τη δουλειά. Με τα χρονια, εφτασα λοιπον στην τελευταια ταξη του Λυκειου και όπως θα θυμασαι..πατωσα στις εξετασεις! Αντι να μου θυμωσεις, αρχισες να ψαχνεις για ιδιωτικα κολλεγια μπας και αρχισω καπου. Κανενα δεν σου αρεσε, θυμασαι αυτον τον περιεργο πρυτανη που πηγαμε να δουμε? Μολις βγηκαμε από το γραφειο του μου ειπες «Αυτος είναι απατεωνας, δεν θα γραφτεις εδω». Λες και το ξερες ρε μπαμπα, μετα από λιγους μηνες εκλεισε αυτο το κολλεγιο και οι μαθητες εμειναν στον τοπο, και εχασαν και τα λεφτα που του ειχαν πληρωσει. Με τα πολλα-πολλα λοιπον, αποφασίσαμε πως ισως είναι καλη ιδεα να παω στο εξωτερικο να σπουδασω. Για ποτε γραφτηκα και για ποτε έφυγα από τη Ελλαδα για Γλασκωβη, ουτε που το καταλαβαμε. Εσυ μου εμαθες γραμματα, εσυ με σπουδασες. Μονος σου. Μπαμπα, χωρις εσενα δεν θα ημουν ε δ ώ. Ολες μου οι επιτυχιες (τωρινές και μελλοντικες) οφείλονται σε εσενα.

CHAPTER 1
Introduction

1 Introduction

1.1 The haematopoietic hierarchy

The blood system serves as a paradigm for understanding tissue stem cells. Differentiated blood cells are short lived, and therefore, a constant replenishment throughout life is provided by haematopoietic stem cells (HSCs) and multilineage progenitors. HSCs are defined as cells with self-renewal and differentiation potential (Till et al., 1964). Accumulating evidence demonstrates that HSCs are a heterogeneous population in varying aspects, including their self-renewal potential (Guenechea et al., 2001; Ema et al., 2005), differentiation pattern (Muller-Sieburg et al., 2012; Compley et al., 2012) and lifespan (Osawa et al., 1996; Morrison et al., 1997; Yang et al., 2005). Retroviral-based studies indicate that HSCs clonally give rise to all cells of the haematopoietic system and also self-renew, unequivocally proving the existence of HSCs in the bone marrow (Dick et al., 1985; Keller et al., 1985; Lemischka et al., 1986). In the traditional view of the haematopoietic hierarchy, long-term haematopoietic stem cells (LT-HSC) provide life-long haematopoiesis, while short-term HSCs (ST-HSC) support haematopoiesis for approximately four months (Morrison and Weissman, 1994). It has become increasingly evident that LT-HSCs are functionally heterogeneous. Muller-Sieburg et al identified the presence of myeloid-biased HSCs (My-bi HSCs), lymphoid-biased HSCs (Ly-bi HSCs), and balanced HSCs (Bala HSCs) (Challen et al., 2010; Muller-Sieburg et al, 2004; Muller-Sieburg et al., 2012). On the other hand Eaves et al have identified these HSCs as α, β, γ, and δ (Benz et al., 2012; Dykstra et al., 2007). Both types of classification are defined based on myeloid and lymphoid reconstitution ratios, but the criteria used to make these classifications are different. α HSCs are thought to correspond to My-bi HSCs, β to Bala HSCs, and γ/δ to Ly-bi HSCs.

In the traditional view, LT-HSCs give rise to multipotent progenitor cells (MPP) that exhibit a lower self-renewal capacity and can give rise to all subsequent lineages (Morrison et al., 1997; Adolfson et al., 2001). MPPs in turn give rise to common

lymphoid (CLP) and common myeloid progenitors (CMP), segregating myeloid and lymphoid lineages early in haematopoiesis, thus constituting the initial step of lineage commitment. CMPs give rise to granulocyte-monocyte progenitors (GMP), which become committed to the granulocyte-monocyte fate, and MEPs, which only produce erythroid and megakaryocyte cells. On the lymphoid side, CLPs give rise to B cell precursors and early progenitors for T and natural killer (NK) lineages (Akashi et al., 2000; Kondo et al., 1997). However recent evidence suggests that lymphoid progenitors (LMPP-like population) are mostly T cell restricted, potentially suggesting that CLPs are not common progenitor for both B and T cells (Luis et al., 2016). Although the standard model is still extensively used as an operational paradigm, further purification and functional assays have led to key revisions to the model (Figure 1-1). The identification of lymphoid-primed multipotent progenitors (LMPPs) argued that megakaryocyte-erythrocyte potential is the first branch lost in lympho-myeloid specification, as LMPPs give rise to macrophage-granulocyte and T-B lineages but not megakaryocyte-erythrocyte lineages (Adolfson et al., 2005; Mansson et al., 2007). However, lineage tracing studies have shown that LMPPs can in fact differentiate into megakaryocyte-erythrocyte progenitors (Forsberg et al., 2006; Boyer et al., 2011). Furthermore, paired-daughter HSC cell divisions have demonstrated that megakaryocyte-erythrocyte progenitors can be derived from HSCs directly, without the conventional progression through MPPs and CMPs (Yamamoto et al., 2013). Furthermore, Sten Eric Jacobsen's group provided evidence for a megakaryocyte-biased HSC population by using a transgenic mouse model with a GFP reporter driven by the megakaryocyte-associated gene, VWF (Sanjuan-Pla et al., 2013). The authors specifically showed that the VWF-positive HSCs exhibited a strong platelet bias and contribution to the myeloid lineage, but with very limited (short-term) lymphoid potential. Evidence for megakaryocyte-biased HSCs has also been provided by the Waskow and Park groups (Grinenko et al., 2014; Shin et al., 2014). Finally, a recent study separated cells of the haematopoietic system based on their *Gata1* expression, highlighting the heterogeneity within already immunophenotypically defined cell populations (Drissen et al., 2016). More specifically, *Gata1*-expressing pre granulocyte-monocyte progenitors (pre-GMs) and granulocyte-monocyte progenitors (GMPs) gave rise to mast cells and eosinophils,

but lacked monocyte-macrophage and had little or no neutrophil potential. Conversely, *Gata1*-non expressing pre-GMs and GMPs (as well as LMPPs) generated monocytes and neutrophils, but no mast cells and few eosinophils. Notably, monocyte-neutrophil and mast cell-eosinophil potentials segregated prior to separation from other blood lineages, as *Gata1*-expressing pre-GMs generated megakaryocytes and erythroid cells, whereas LMPPs contained robust B- and T-lineage potential. The authors termed the *Gata-1*-expressing pre-GMs and GMPs erythroid-megakaryocyte-primed multi-potent progenitors (EMkMPP) and eosinophil-mast cell progenitors (EoMPs) respectively, and the *Gata1*-non expressing pre-GMs and GMPs pre-neutrohil monocyte-progenitors (pre-NM) and neutrophil-monocyte progenitors (NMPs) (Figure 1-1). Their findings therefore identified an early blood lineage fate decision segregating lymphoid-macrophage-neutrophil potential from mast cell-eosinophil-megakaryocytic-erythroid potential, establishing separate myeloid-erythroid and myelo-lymphoid differentiation pathways, and generating two distinct myeloid-restricted progenitor subsets, instead of a common GMP harboring all monocyte-macrophage and granulocyte potentials (Drissen et al., 2016).

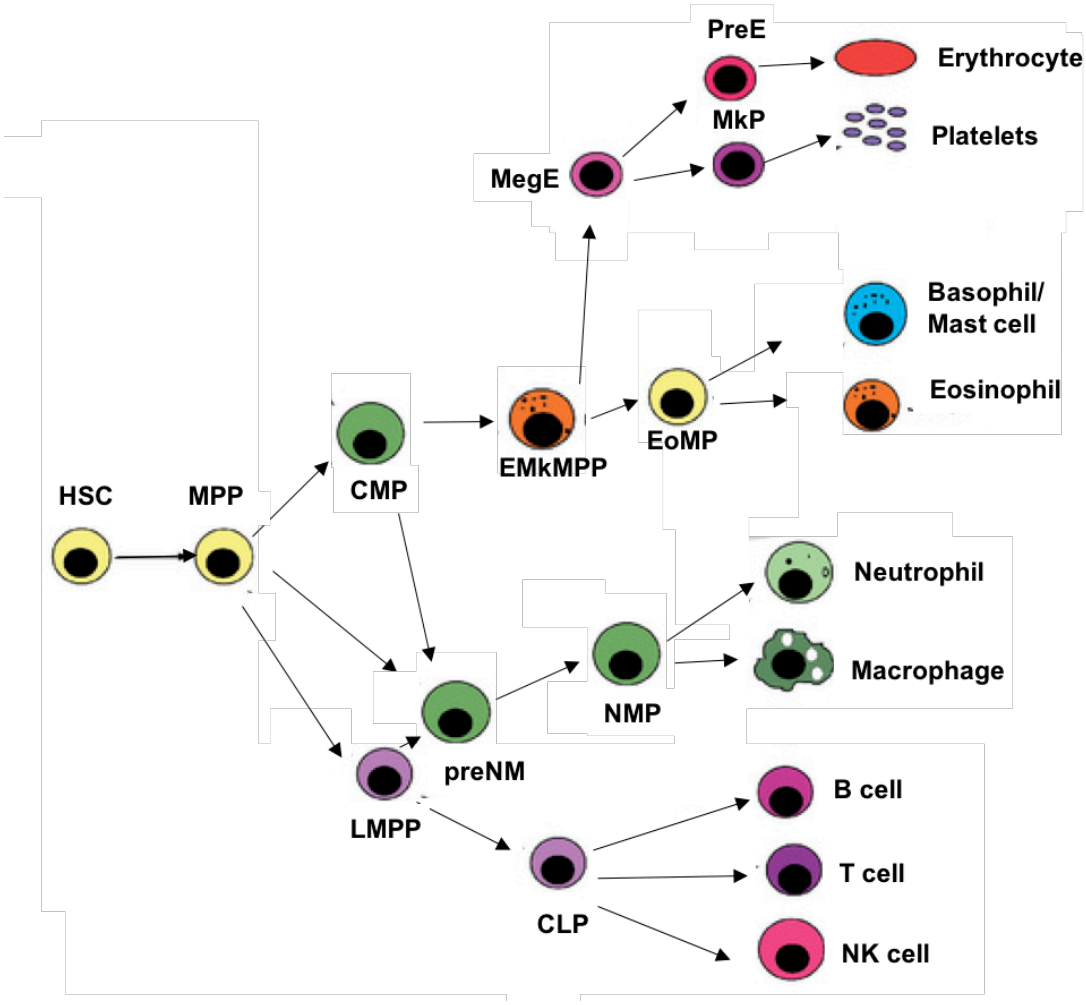

Figure 1-1. Recently proposed model of haematopoiesis. Immunophenotypically defined heterogeneous HSC populations with respect to lineage potential give rise to the immediate progeny of multipotent progenitors (MPP) that then give rise to lymphoid-primed progenitors (LMPP), common myeloid progenitors (CMP) and pre neutrophil-macrophage progenitors (pre NM). LMPPs give rise to common lymphoid progenitors (CLP) and pre NMs that give rise to neutrophil-macrophage progenitors (NMP). NMPs and CLPs then give rise to differentiated cells. CMPs also give rise to erythroid-megakaryocyte primed multi-potent progenitors (EMkMPP) which in turn give rise to eosinophil-mast cell (and likely basophil) fate (EoMP) or to megakaryocyte-erythrocyte progenitors (MegE) that then give rise to oligopotent megakaryocyte (MkP) and erythrocyte (PreE) progenitors giving, rise to erythrocytes and platelets respectively. (Adapted from Drissen et al., 2016).

1.1.1 Reconceiving the haematopoietic hierarchy

The majority of the work that has been conducted so far has been based on transplantation assays. However, although the transplantation assay is considered as

the "golden standard" for the analysis of the haematopoietic system, it comes with considerable caveats. To begin with, it detects only the cells that are able to home to the bone marrow and proliferate rapidly. Furthermore, given the immense stress that transplanted cells endure during isolation, engraftment and transplantation, it is questionable whether these cells share the same characteristics as cells present in physiological, non-transplant haematopoiesis. As a result, more recent studies that utilise novel tracking techniques were able to challenge the long-standing view of the haematopoietic hierarchy (Sun et al., 2014; Notta et al., 2016; Drissen et al., 2016; Biasco et al; 2016).

In their study, Sun et al utilised *in situ* labelling and clonal tracking of murine haematopoietic cells. Based on their study, the authors propose that in an unperturbed system, LT-HSCs have limited contribution to blood production during adulthood, while MPPs provide constant replenishment of the blood lineages (Sun et al., 2014). In a study published earlier this year, the authors studied the myeloid-erythroid-megakaryocyte differentiation process, using human cord blood, foetal liver tissue and adult bone marrow (Notta et al., 2016). Intriguingly, in their model they challenge the existence of oligopotent progenitors such as CMPs and GMPs, inferring that multipotent cells differentiate into unipotent cells directly. More specifically, they suggested that in cord blood and the bone marrow, most megakaryocytes emerged as part of mixed clones from HSC/MPPs, indicating that megakaryocytes branch directly from multipotent progenitors (Notta et al., 2016). This study therefore provided major insight into the myeloid-erythroid-megakaryocyte lineage, suggesting that these cells can differentiate directly from primitive cells.

In another study, Biasco and colleagues utilised an *in vivo* tracking system in order to study the clonal expansion of human haematopoietic cells in early and late stages of autologous transplantation (Biasco et al., 2016). Based on their data, they were able to conclude that the initial, short-term haematopoiesis was maintained by lineage-committed progenitor cells. However, after approximately 6 months post transplantation, they observed a switch in haematopoiesis where the first wave of cells was exhausted, and LT-HSCs progressively took over, generating a stable

output up to 3 years post-transplantation (Biasco et al., 2016). This study provided invaluable insight of what occurs after human transplantations and parallels well with animal studies, thereby validating some long-standing models regarding haematopoiesis but also shedding new light on the clonal dynamic of blood cells.

Overall, these studies indicate that haematopoietic cells exhibit immense plasticity and that perhaps one firm model of the haematopoietic hierarchy is not sufficient to describe the true complexity of haematopoietic differentiation.

1.2 Immunophenotypic characterisation of HSCs and progenitor cells

Prospective isolation of cellular subsets based on expression of cell-surface markers and functional characterisation using *in vivo* and *in vitro* assays has provided key insights into the haematopoietic development (Weissman, 2000). HSCs have been highly enriched as Thy-1^{lo} Sca-1^{+} Lineage^{-} c-Kit^{+} or as $CD34^{-}$ Sca-1^{+} Lineage^{-} c-Kit^{+} (Spangrude et al., 1988; Morrison and Weissman, 1994; Osawa et al., 1996). Furthermore, early progenitors of the haematopoietic system also reside within the Lineage^{-} Sca-1^{+} c-Kit^{+} (LSK) compartment (Ikuta and Weissman, 1992; Li and Johnson, 1995; Spangrude et al., 1988; Weissman et al., 2001). More recently, LT-HSCs and early progeny have been classified based on the SLAM family of surface markers (Kiel et al., 2005). These markers include CD48, CD150 and CD244 and have been extensively used over the past decade to isolate LT-HSCs (LSK $CD48^{-}$ $CD150^{+}$ $CD244^{-}$), multipotent primitive progenitors (LSK $CD48^{-}$ $CD150^{-}$ $CD244^{+}$) and committed progenitor cells (HPC-1: LSK $CD48^{+}$ $CD150^{-}$ $CD244^{+}$; HPC-2: LSK $CD48^{+}$ $CD150^{+}$ $CD244^{+}$) (Kiel et al., 2005). Furthermore, LT-HSCs and early progenitor cells can also be isolated based on CD34 and Flt3 expression (Adolfson et al., 2001; 2005). LT-HSCs lack the expression of CD34 and Flt3, whereas short-term HSCs (ST-HSCs) are $CD34^{+}$ and $Flt3^{-}$ (Adolfson et al., 2001; 2005; Osawa et al., 1996). Additionally, CD34 and Flt3 expression has allowed the prospective isolation of a population of early progenitors that possess B-cell, T-cell and granulocytic monocytic (GM) potential but lack significant megakaryocyte erythrocyte (MegE) potential can be isolated.

This population is double positive for CD34 and Flt3 (LSK $CD34^{+}$ $Flt3^{+}$) and is

referred to as lymphoid-primed multipotent progenitors (LMPP) (Adolfsson et al., 2005). Committed progenitor cells that arise from the Lineage $^{-}$ c-Kit^{+} Sca-1^{-} (LK) population, can be discriminated based on their expression of CD34 and CD16/32 (receptor-II/III (FcgR)) (Akashi et al., 2000). CD16/32 is an important marker for myelomonocytic cells and CD34 marks the fraction of haematopoietic stem and progenitor cells (Osawa et al., 1996; Lacaud et al., 1998). The resultant populations are the common myeloid progenitors (CMP, CD16/32^{-} CD34^{+}), granulocyte-monocyte progenitors (GMP, CD16/32^{+} CD34^{+}) and megakaryocyte-erythrocyte progenitors (MkEP, CD16/32^{-} CD34^{-}). Finally, Drissen et al. made use of *Gata1*expression in order to segregate EMkMPPs, EoMPs, pre-NMs and NMPs. EMkMPPs, EoMPs are *Gata1*$^{+}$ while pre-NMs and NMPs are *Gata1*$^{-}$ (Drissen et al., 2016). The surface makers used to immunophenotypically mouse haematopoietic stem and progenitor cells are summarized in Figure 1-2.

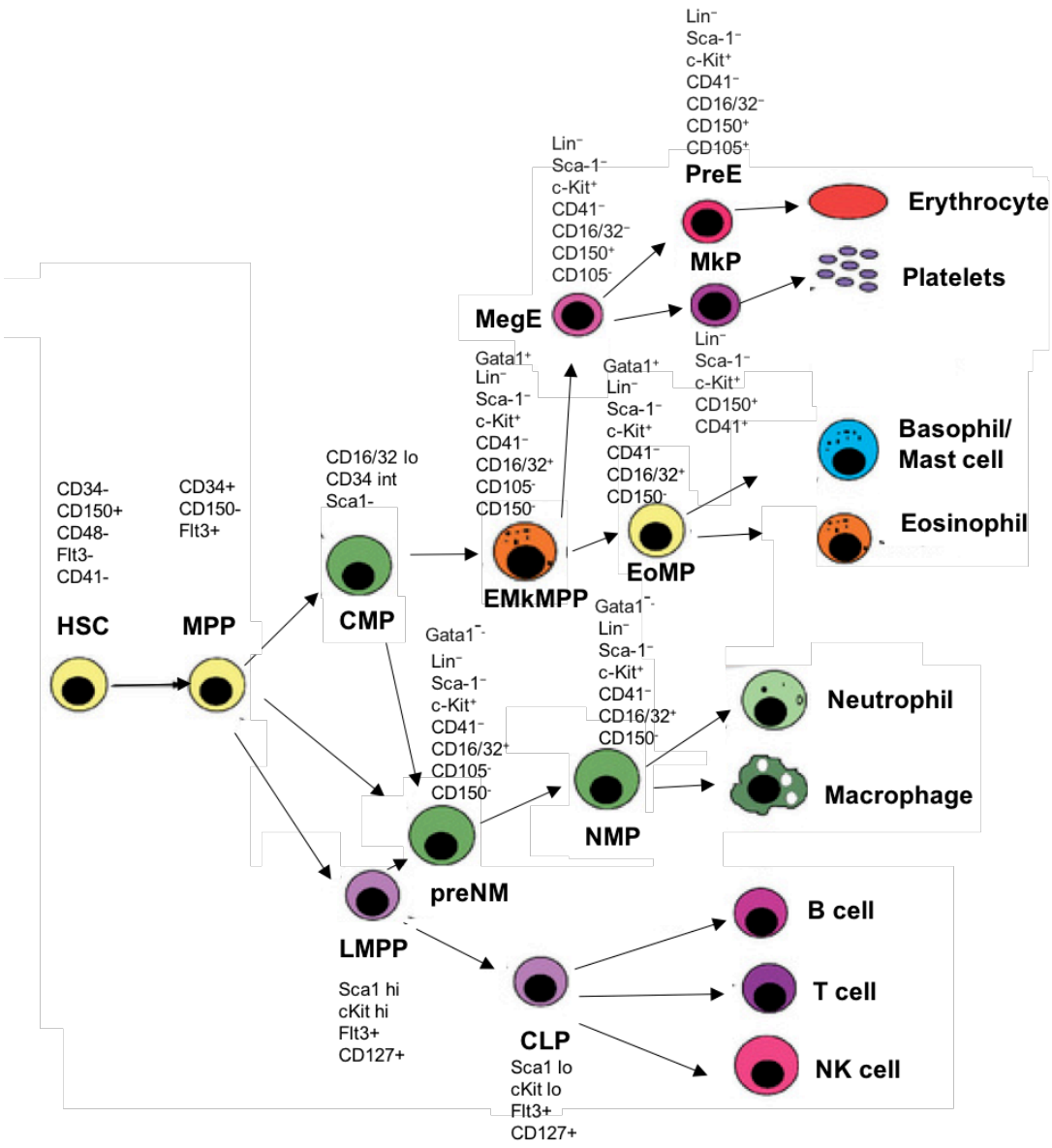

Figure 1-2. Surface marker expression on stem and progenitor cell compartments of mouse haematopoiesis. EMkMPPs and pre-NMs are defined as $Lin^{-}Sca\text{-}1^{-}c\text{-}Kit^{+}$ $CD41^{-}$ $CD16/32^{+}$ $CD150^{-}$ $CD105^{-}$ whereas EoMPs and NMPs are defined as $Lin^{-}Sca\text{-}1^{-}c\text{-}Kit^{+}$ $CD41^{-}$ $CD16/32^{+}$ $CD150^{-}$. Finally, EMkMPPs, EoMPs, pre-NMs and NMPs are segregated based on their *Gata1* expression. EMkMPPs, EoMPs are $Gata1^{+}$ while pre-NMs and NMPs are $Gata1^{-}$. (Adapted from Doulatov et al., 2012; Drissen et al., 2016).

1.3 HSC ageing

Ageing of HSCs is associated with reduction in function. Aged HSCs exhibit increased number/frequency (Rossi et al., 2005; Harrison et al.,1989) and reduced self-renewal capacity, determined by serial transplantation assays (Jansen et al., 2006; Kamminga et al., 2005). Furthermore, when aged HSCs are transplanted with young HSCs into lethally irradiated recipient mice, aged HSCs contribute to multilineage haematopoiesis less efficiently (Morrison et al., 1996; Chen et al., 2000), and exhibit a two-fold reduced ability to home to the bone marrow (Liang et al., 2005). In terms of differentiation potential, aged HSCs are deficient in their ability to support erythropoiesis, they generate B and T cells less efficiently and exhibit a bias towards the myeloid lineage (Dykstra et al., 2007; 2011; Benz et al., 2012; Cho et al., 2008). With respect to lineage skewing, it is proposed that myeloid-biased HSCs increase in the expense of lymphoid-bias or balanced HSC clones upon ageing (Beerman et al., 2010; Challn et al., 2010; Sienburgh et al., 2004; Morita et al., 2010).

1.4 Early haematopoiesis

In mammals, haematopoiesis occurs in multiple waves in distinct anatomical sites during embryonic development (Johnson and Moore, 1975; Medvinsky and Dzierzak, 1996; Metcalf & Moore, 1972) (Figure 1-3). The initial wave of blood production occurs in the mammalian yolk sac, at day 7.5 of embryonic development (E 7.5), and is termed as “primitive” haematopoiesis (Russell and Bernstein, 1966). Primitive haematopoiesis involves the production of red blood cells that facilitate oxygenation of the tissue as the embryo rapidly grows (Russell and Bernstein, 1966). Furthermore, during primitive haematopoiesis, megakaryocytes and macrophages are generated presumably to scavenge apoptotic cells and debris during development. The second or “definitive” wave also occurs in the yolk sac and is characterised by the presence of myeloid lineages, at E8.25. The next site of definitive haematopoiesis is the aorta-gonad-mesonephros (AGM) region of the embryo, where definitive HSCs arise, at E10.5 of embryonic development (Medvinski and Dzierzak, 1996; Muller et al, 1995). The definitive HSCs then migrate to the foetal liver and by E12.5

of embryonic development, the foetal liver is the major site of haematopoiesis (Kumaravelu et al, 2002; Morrison et al., 1995). Subsequent definitive haematopoiesis takes place in the spleen, the thymus and ultimately the bone marrow at E16-E17. Thereafter, the bone marrow is the main site of haematopoiesis soon after birth and throughout adult life (Clapp et al., 1995 Zanjani et al., 1993).

1.4.1 Foetal liver haematopoiesis

Although foetal liver HSCs are considered as the "definitive" HSCs that colonise the bone marrow, they nevertheless exhibit differences when compared to adult bone marrow HSCs. For instance, foetal liver HSCs display faster expansion kinetics when grafted in adult bone marrow, compared to long term-HSCs isolated from the bone marrow of adult mice (8 weeks old; Morrison et al., 1995). Furthermore, foetal liver HSCs undergo more symmetrical self-renewing cell divisions compared to adult (8 weeks old) long-term HSCs (Harrison et al, 1997; Dykstra et al, 2007), and foetal liver progenitors, appear to follow the same differentiation hierarchy as bone marrow progenitors (Traver et al., 2001). More recently, it was demonstrated that foetal liver HSCs rely more on oxidative phosphorylation whereas adult bone marrow HSCs rely on glycolysis in order to self-renew (Manesia et al, 2015; Suda et al, 2011). It is also interesting that the spectrum of clonal differentiation is different for foetal and adult sources (Benz et al., 2012). In the developing foetal liver, the lymphoid-deficient α-HSCs constitute less than 5 % of all HSCs and less than 10 % of the HSCs with durable self-renewal activity. However, they are much more prevalent in the initial HSC population that can be detected in the bone marrow just before birth (Benz et al., 2012). Finally, foetal liver HSCs and adult bone marrow HSCs also differ immunophenotypically. For instance, while Mac-1 marks foetal liver HSCs, in the adult bone marrow it is a marker of myeloid cells (Morrison et al., 1995; Jordan ET AL., 1990; Kim et al, 2006). Haematopoietic cells of the foetal liver exist in a specific microenvironment that controls their proliferation and differentiation. This microenvironment is created by different cell populations including epithelial cells, macrophages, cells that undergo epithelial-to mesenchymal transition, and various stromal cells such as fibroblasts, mesenchymal stromal cells, hepatic cells and vascular smooth muscle cells (Paiushina et al., 2012).

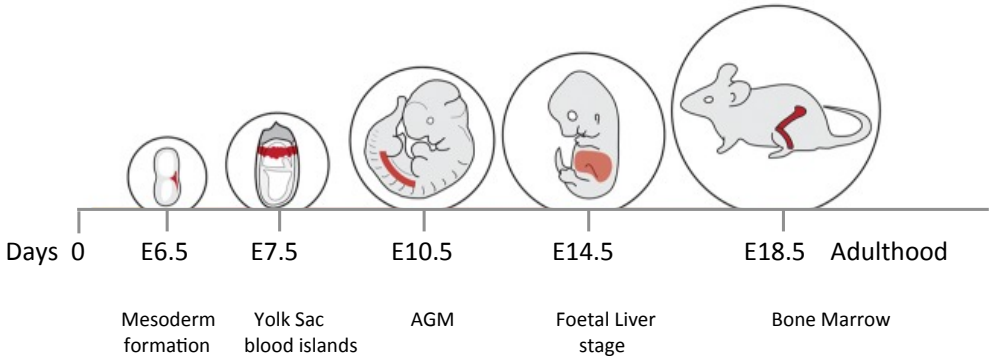

Figure 1-3. Sites of haematopoiesis during murine development. The mesoderm forms during gastrulation at day E6.5; development of the yolk sac blood islands occurs at day E7.5; emergence of HSCs in the aorta-gonad-mesonephros (AGM) region occurs at day E10.5; active haematopoiesis occurs at the foetal liver at day E14.5; haematopoiesis in the bone marrow of the late gestation embryo occurs at day E18.5 and throughout adulthood (Adapted from Baron et al., 2012).

1.5 Regulation of HSCs

1.5.1 Transcription factors regulating HSC emergence and lineage specification

A complex network of various transcription factors (TFs) regulate the early development of HSCs and the self-renewal of adult HSCs. Generally, TFs are classified as basic helix-loop-helix TFs, homeobox TFs, Ets TFs and zinc finger TFs. Some critical factors include stem cell leukaemia (Slc), runt-related transcription factor 1 (Runx1), mixed lineage leukaemia (Mll), globin transcription factor 2 (Gata2), myeloid ecotropic viral integration site 1 (Meis1) and homeobox A9 (Hoxa9) (described in section 4.1), Lim only domain 2 (Lmo2), Ets-related gene (Erg), c-Myb, and are described below.

Scl encodes a basic helix-loop-helix transcription factor required for haematopoietic development, as mutation of Scl results in severe defects in blood formation and lack of all haematopoietic lineages in mice (Porcher et al., 1996). Runx1 is a core-binding factor and is shown to be required for definitive haematopoiesis, and its transient expression is correlated with the emergence of HSCs in the AGM (North et al., 1999). Runx1 continues to be expressed in HSCs during subsequent development and in adult life (North et al., 1999; Teitell et al., 2006; North et al., 2004). Runx1-null embryos lack foetal liver haematopoietic progenitor cells, indicating that it is important in definitive haematopoiesis (North et al., 1999; Teitell et al., 2006; North et al., 2004). Similarly to Runx1, Mll that encodes for a SET-domain containing histone methyltransferase, is essential for the development of HSCs in the AGM (McMahon et al., 2007). Lmo2 is a protein required for erythropoiesis in the yolk sac, as *ex vivo* differentiation of erythroid development was impaired in yolk sac tissue. Furthermore, Lmo2 plays a critical role in definitive haematopoiesis as Lmo2-null cells do not contribute to any of the haematopoietic lineages (Yamada et al., 1998). Erg is a member of the ETS family and has been shown to play a significant role in the endothelial and haematopoietic development (McLaughlin et al., 2001;

Murakami et al., 1993). Erg was shown to be a positive regulator of Gata2 and Runx1 gene expression once haematopoiesis progressed to the foetal liver, and to be involved in HSC self-renewal (Taoudi et al., 2011). Furthermore, Erg is required to maintain the adult HSC pool and reconstitution ability, and differentiation to committed progenitors (Loughran et al., 2008; Ng et al., 2011). C-Myb plays an important role in adult HSC self-renewal. Its conditional deletion causes a defect in HSC proliferation and loss of reconstitution ability (Lieu et al., 2009). Gfi1 is a transcriptional repressor that promoters HSC quiescence, and maintains HSC self-renewal and reconstitution potential (Zeng et al., 2004; Hock et al., 2004).

HSC lineage-priming transcription factors promote their own lineage differentiation while simultaneously suppressing other factors. For instance, Gata1 and Pu1 promote erythroid-megakaryocyte-eosinophil and myeloid differentiation, respectively. The proteins physically interact and antagonize each other's actions. The complementary roles of these two transcription factors have been exhibited in zebrafish. Inhibition of GATA1 expression in morpholinos shifted the haematopoietic progenitors towards a myeloid differentiation, whereas the opposite occurred upon inhibition of PU1 expression (Galloway et al., 2005; Rhodes et al., 2005). In a similar fashion, C/EBP and friend of Gata1 (Fog1) control eosinophil and multipotential cell fates (Querfurth et al., 2000). Erythroid kruppel-like factor (Eklf) and Fli1 are critical for erythroid and megakaryocyte choice (Starck et al., 2003), GATA3 and T-bet for T helper 1 and 2 cells (Usui et al., 2006), and growth factor independent-1 (Gfi1) and PU1 for neutrophil versus monocyte outcomes (Dahl et al., 2007).

Lineage commitment in B-cell development is orchestrated in a regulatory network of key transcription factors. Pu1 and E2A are critical for lymphoid cell fate determination and induce specific B-lineage commitment factors like early B-cell factor 1 (Ebf1) and Pax5. Ebf1 is a primary determinant of B-cell fate and its expression is controlled by high expression of Ikaros (regulator of lymphoid lineage priming in HSCs) and E2A in conjunction with Pu1 and by extrinsic signals provided by the IL-7 receptor (Seet et al., 2004; Kwon et al., 2008)

T-lymphoid development depends upon Notch signalling and principally acts by repressing factors such as Pu1. Notch signalling turns LMPPs into early T-cell

progenitors by inducing a pro-T-cell developmental program with the activation of Gata3, Tcf7 and other T-cell restricting genes. Furthermore, although Gata3 has been viewed as a T-cell specific transcription factor, recent evidence indicates that it functions only within the context of Notch (Rothernberg, 2007).

1.5.2 Regulation of HSC functions by the bone marrow niche

The bone marrow microenvironment is uniquely adapted to support the properties of HSCs. The idea of a stem cell niche was initially proposed by Scofield and colleagues in 1978. In this model, a niche comprised of specialised cells of the bone marrow, physically interact with HSCs and provide signals that support their function (Schofield, 1978). These cells include mesenchymal stem cells (MSCs), endothelial cells and osteoblasts. Furthermore, other cells of the bone marrow such as glial cells, adipocytes and neuronal cells are thought to also regulate haematopoiesis (Figure 1-4).

The location of HSCs within the bone marrow remains controversial. Initial studies utilising labelled HSCs for transplantation assays suggested that HSCs mostly reside in the endosteal location of the bone marrow (Nilsson et al., 2001; Xie et al., 2009). In contrast, by immunophenotypically defining HSCs ($CD150^+$ $CD48^-$ $CD41^-$ lineage $^-$), Kiel et al demonstrated that HSCs are in contact with cells of the endothelium (Kiel et al., 2005). Consistent with this report, a recent study suggested that HSCs and early progenitor cells are localised near the sinusoidal endothelium, with a preference for the endosteal region (Nombela-Arrieta et al., 2013). Collectively, these studies suggest that the majority of HSCs reside in the perivascular region and are enriched in the highly vascular endosteal region. The niche cells that support HSC function are outlined below.

The endosteal niche contains osteoblasts as the main supportive cell type for HSC maintenance. Osteoblasts secrete cytokines implicated in HSC regulation including thrombopoietin (Qian et al., 2007; Yoshihara et al., 2007) and C-X-C motif chemokine 12 (CXCL12) (Jung et al., 2006). The role of osteoblastic cells in the maintenance of HSCs is controversial. Conditional ablation of osteoblastic cells has been associated with loss of HSCs in the bone marrow and extramedullary

haematopoiesis (Visnjic et al., 2004). Furthermore, expansion of osteoblastic cells through expression of the parathyroid hormone receptor 1 or through conditional deletion of bone morphogenic protein receptor 1 (Calvi et al., 2003), is associated with an expansion of HSCs (Zhang et al., 2003). In contrast, treatment of mice with the bone stimulating agent, strontium, leads to expansion of mature osteoblasts but does not affect the numbers of HSCs (Lymperi et al, 2008). Finally, deletion of SCF or CXCL12 from mature osteoblasts had no effect on HSCs (Ding et al., 2013; Greenbaum et al., 2013; Ding et al., 2012). The apparent discrepancy between studies can be partially attributed to the fact that osteoblasts are a heterogeneous population comprising of both mature and immature cells. In particular, it was recently demonstrated that immature osteoblastic cells express higher levels of SCF and CXCL12 than more differentiated osteoblasts (Nakamura et al., 2010), suggesting that mature osteoblasts do not regulate HSCs but immature osteoblasts do.

The perivascular location of most HSCs has focused recent attention to the stromal cells that reside in the perivascular niche. Apart from endothelial cells, the perivascular niche contains mesenchymal stem cells (MSCs) and a heterogeneous population of stromal cells that express high levels of CXCL12. This population is defined by transgene expression using stromal-specific promoters. These stromal populations include the CXCL12-abundant reticular (CAR) cells, leptin^{+} receptor stromal cells and nestin-GFP^{+} stromal cells and are referred to as CXCL12-expressing mesenchymal progenitors (CEMP) cells.

CAR cells are mesenchymal progenitors that exhibit adipogenic and osteogenic potential *in vitro* (Omatsu et al., 2010). CAR cells are the major source of SCF and CXCL12 in the bone marrow, and ablation of these cells is associated with a significant loss of SCF and CXCL12. Conditional ablation of CAR cells using transgenic mice expressing the diphtheria toxin receptor under the control of *Cxcl12* regulatory elements resulted in a reduction of HSC numbers and long-term reconstitution capacity of HSCs (Omatsu et al., 2010).

Lineage mapping using *Cre* recombinase under the expression of the leptin receptor identified another perivascular stromal population in the bone marrow (Ding et al.,

2013). Similarly to CAR cells, leptin$^+$ stromal cells express high levels of SCF and CXCL12. Deletion of SCF from the leptin$^+$ stromal cells resulted in loss of HSCs, indicating that these cells are important for the regulation of HSCs (Ding et al., 2012).

Nestin-GFP$^+$ cells are perivascular stromal cells that express high levels of GFP under the nestin promoter (Mendez-Ferrer et al., 2010). Nestin-GFP$^+$ cells are enriched for MSCs and express several genes implicated in HSC maintenance such as CXCL12, SCF and angiopoietin. Conditional deletion of nestin-expressing cells results in loss of HSCs (Mendez-Ferrer et al., 2010).

Bone marrow endothelial cells express several genes implicated in HSC maintenance including CXCL12, SCF and angiopoietin (Chute et al., 2006). Deletion of the endothelial-specific adhesion molecule E-selectin, results in increased HSC quiescence, suggesting that endothelial cells regulate HSC proliferation (Winkler et al., 2012). Furthermore, SCF deletion in endothelial cells results in loss of HSCs, indicating that endothelial cells are key components of the HSC niche (Ding et al., 2012).

Adipocytes are also part of the bone marrow niche and are thought to exert an inhibitory effect on HSCs, as adipose-rich bone marrows have decreased HSC numbers compared to adipose-poor bone marrows (Naveiras et al., 2009).

Recent studies have shown that the sympathetic nervous system contributes to HSC trafficking from the bone marrow by regulating local production of CXCL12 (Katayama et al., 2006). Another recent study has also implicated glial cells, specifically non-myelinating Schwann cells, in the regulation of HSCs (Yamazaki et al., 2011). More specifically, glial cells are thought to be a major source of the transforming growth factor beta (TGF-beta). TGF-beta is an important regulator of HSC function as it induces quiescence *in vitro*. Furthermore, loss of TGF-beta signalling in HSCs results in impaired long-term repopulation capacity (Yamazaki et al., 2011). Finally, surgical disruption of the sympathetic nervous system, resulting in loss of Schwann cells, is associated with a decreased expression of TGF-beta and

consequent loss of HSCs (Yamazaki et al., 2011). A summary of the bone marrow HSC niche is presented in the figure below (Figure 1-4).

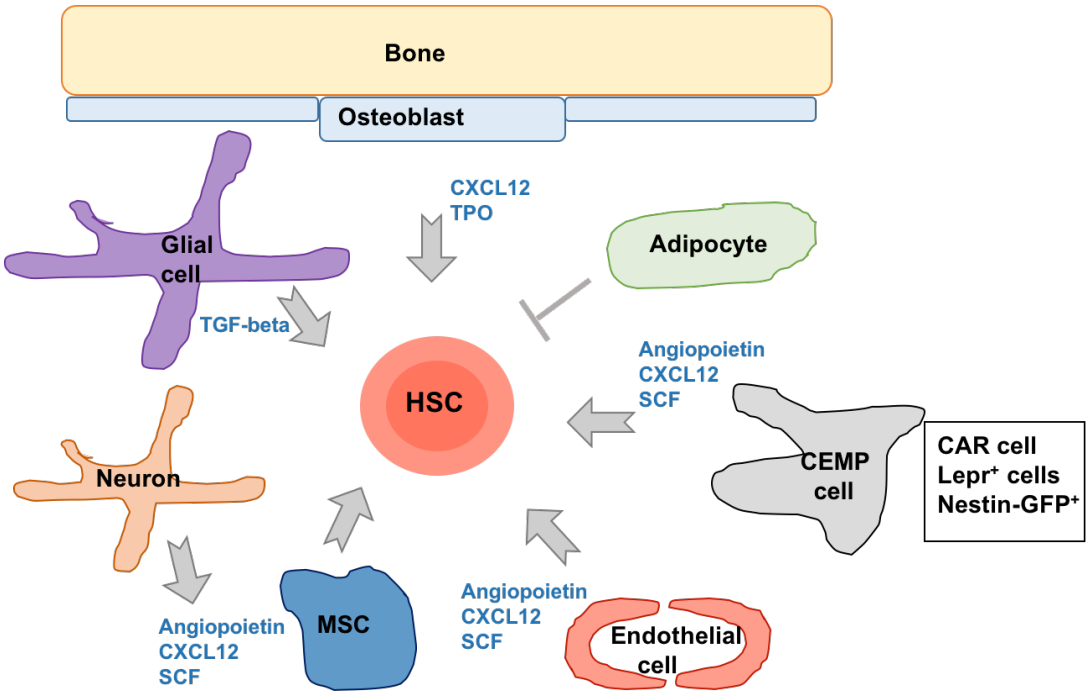

Figure 1-4. Stromal cell populations in the bone marrow contributing to HSC maintenance. Endothelial cells, mesenchymal stem cells (MSCs), and CXCL12-expressing mesenchymal progenitor (CEMP) cells have been identified as CAR cells, leptin receptor^{+} cells (Leptr^{+}), and nestin-GFP^{+} cells. Osteoblasts produce several factors that support HSC function such as thrombopoietin (TPO) and CXCL12. Synpathetic neurons indirectly regulate HSCs by targeting CXCL12 expression. Glial cells regulate HSCs through production of active TGF-beta, and adipocytes are likely to exert inhibitory effects on HSCs (Adapted from Anthony and Link, 2014).

1.6 Hypoxia and the stem cell niche

The bone marrow is considered to be a tissue with limited oxygen supply and as a result the prevailing view is that HSCs are maintained in a hypoxic environment (Nombela-Arrieta et al., 2013; Spencer et al., 2014; Kiel et al., 2003). The proposed view is that the endosteal niche might provide a hypoxic environment for maintaining HSCs in a quiescent state whereas the perivascular niche allows HSCs to proliferate and differentiate in an environment where more oxygen is available (Wilson et al., 2008; Suda et al., 2011). However, in a recent study, live *in vivo* imaging of oxygen concentration provided evidence that the most hypoxic region is actually located 40 μm from the bone in the perisinusoidal region, and there is a modest increase in oxygen concentration within 20 μm of the bone in the endosteal region (Spencer et al., 2014). Furthermore, higher oxygen tension is found near nestin-GFP^{+} vessels, which harbor quiescent HSCs (Kunisaki et al., 2013). Interestingly, haematopoietic stem and progenitor cells display a hypoxic profile (as evidenced by pimonidazole retention and expression of HIF-1α) regardless of their location in the bone marrow, suggesting that hypoxia might be HSC autonomous (Nombela-Arrieta et al., 2013). In fact, SCF (Pedersen et al., 2008) and thrombopoietin (Kirito et al., 2005) are known to increase HIF-1α levels, which could alter the distribution of hypoxic HSCs. Therefore, intrinsic metabolic properties rather than localisation in a hypoxic microenvironment may define the hypoxic prolife of HSCs.

1.7 HIF-1α as a regulator of HSCs

Oxygen homeostasis is key for the normal development and physiology of the vast majority of multicellular organisms. As mentioned in the previous section, HSCs reside in a hypoxic niche within the bone marrow (Nombela-Arrieta et al., 2013; Spencer et al., 2014; Kiel et al., 2003). The understanding of how oxygen is sensed at the cellular level has recently been intensely investigated. Oxygen sensing primarily occurs through the hypoxia inducible factors (HIF), a family of transcription factors that act as key regulators of a hypoxic response (Parmar et al., 2007; Semenza et al.,

2000; Simsek et al., 2010; Smith et al., 2008; Spencer et al., 2014; Takubo et al., 2010). Under normoxic conditions, HIF is mainly regulated by propyl hydroxylase domain enzymes (PHDs) that mark HIFs for proteosomal degradation via the von Hippel-Lindau tumour (VHL) suppressor protein (Epstein et al., 2001; Jaakkola et al., 2001; Masson et al., 2001). Furthermore, HIF action is also regulated by the factor inhibiting HIF-1 (FIH-1), via asparagine residue hydroxylation (Elvidge et al., 2006; Schodel et al., 2011).

Several studies have investigated the role of HIF in HSC fate decisions (Takubo et al., 2010; Simsek et al., 2010; Guitart et al., 2013; Speth et al., 2014; Vukovic et al., 2016). Our lab has for many years investigated the role of HIF in both normal and malignant haematopoiesis (Guitart et al., 2013; Vukovic et al., 2015; Vukovic et al., 2016). In contrast with other reports (Takubo et al., 2010; Speth et al., 2014; Forristal et al., 2015), our work has conclusively demonstrated that HIF is dispensable for HSC maintenance, as deletion of *Hif-1a*, *Hif-2a* or both had no impact on the survival or maintenance of HSCs in both steady-state haematopoiesis or under stress conditions (Guitart et al., 2013; Vukovic et al., 2016).

1.8 Metabolic regulation of HSCs

In mammalian cells, ATP is mainly produced by the mitochondrial respiratory chain oxidative phosphorylation (OXPHOS). The remaining ATP is provided by anaerobic cytosolic degradation of nutrients, mainly by glycolysis (Papa et al., 2012). In order for OXPHOS to take place, necessary co-factors such as NADH and $FADH_2$ need to be generated that will act as electron carriers during OXPHOS and will generate ATP. NADH and $FADH_2$ are mainly generated by the tricarboxylic acid (TCA) cycle, a key part of mitochondrial respiration. The TCA cycle is essentially the carboxylation of carbon-based entities which occurs through a combination of multiple steps, catalysed by several enzymes. An outline of the TCA cycle and glycolysis are presented in Figure 1-5.

Emerging evidence has linked metabolic activity of HSCs with their functional behaviour (Folmes et al, 2012). Previous studies have shown that quiescent HSCs reside in a hypoxic microenvironment and rely on glycolysis in order to meet their

energy demands (Simsek et al, 2010; Suda et al., 2011). More recently, studies have shed light on the metabolic regulation of HSCs, providing a better understanding of how metabolic regulators dictate HSC fate and function. Below, I describe some of the most recent advances regarding our understanding about the metabolic regulation of haematopoietic cells.

In a recent study, genetic deletion of pyruvate dehydrogenase (Pdk), one of the key enzymes of the glycolytic pathway, drove murine HSCs out of quiescence. Furthermore, HSCs lacking Pdk were unable to reconstitute the haematopoiesis of recipient mice (Takubo et al., 2013). The results of this study highlight a key feature of HSCs, which is their need to maintain glycolysis in order to remain at a quiescent state. However, in another recent study, genetic deletion of pyruvate kinase isoform 2 (Pkm2), a key enzyme of the glycolytic pathway that catalyses the conversion of phosphoenol pyruvate to pyruvate, did not affect the function or survival of HSCs (Wang et al., 2014).

Considering that glycolysis is an inefficient way for ATP production, how can HSCs undergo differentiation? In another seminal study, conditional deletion of *Ptpmt1*, a PTEN-like mitochondrial phosphatase, using the *Mx1-Cre* model that allows conditional deletion of *Ptpmt1* in haematopoietic cells, resulted in disruption of mitochondrial respiration and a complete block in HSC differentiation, and ultimately HSC failure (Yu et al., 2013). Surprisingly, this was not due to the loss of the HSC compartment, but rather to the complete inability of HSCs to undergo differentiation. This study highlights another essential feature of self-renewing HSCs, which is that they cannot undergo efficient differentiation when mitochondrial respiration is impaired. This statement has been supported by other studies (Maryanovich et al., 2015). Loss of the mitochondrial carrier homologue 2 (MTCH2) which acts as a negative regulator of OXPHOS, using the haematopoiesis-specific deleter *Vav*, resulted in cell cycle entry of HSCs and progenitor cells, and HSC exhaustion (Maryanovich et al., 2015). This study supports the view that metabolism plays a key role in co-ordinating HSC fates such as self-renewal and differentiation. Recently, the importance of liver kinase B1(LKB-1), an important promoter of

mitochondrial biogenesis, for HSC functions was highlighted by three independent laboratories (Gurumurthy et al., 2010; Gan et al., 2010; Nakada et al., 2010).

Targeted conditional deletion of *Lbk1* in mice of either *Mx1-Cre* background or *Rosa26-ERT*, severely compromised HSC functions. Loss of Lkb1 resulted in bone marrow failure, preceded by an increase in proliferation and subsequent loss of HSC quiescence (Gurumurthy et al., 2010; Gan et al., 2010; Nakada et al., 2010). Importantly, the authors demonstrated that HSCs exhibited defective mitochondrial bioenergetics, indicating that Lkb1 acts as a metabolic checkpoint, balancing HSC proliferation and quiescence. In another study, the authors looked at the importance of fatty acid oxidation (FAO) in HSC functions. FAO takes place within the mitochondria and is effectively the breakdown of fatty acids in order to generate NADH and $FADH_2$, which are necessary for ATP synthesis. Inhibition of the peroxisome-proliferator activated receptor (PPARδ)-FAO pathway using the FAO inhibitor etimoxir, profoundly reduced the absolute numbers of HSCs *in vivo*. Mechanistically, depletion of *Pparδ* resulted in the symmetric division of HSCs while *Pparδ* activation increased asymmetric division (Ito et al., 2012), highlighting the importance of FAO for the regulation of HSC self-renewal and differentiation.

Cell differentiation is associated with proliferation and an increase in energy demands. As a result, quiescent HSCs need to switch from glycolysis to OXPHOS in order to support the energetically-expensive differentiation process. Furthermore, progenitors and more differentiated cells exhibit a different metabolic profile from HSCs (Piccoli et al., 2013). Therefore, studies have focused on understanding the precise metabolic profiles of HSCs and progenitor cells. For instance, genetic deletion of the M2 pyruvate kinase isoform (*Pkm2*) in mice, which favours glycolysis and synthesis of macromolecules, impaired progenitor function without perturbing HSCs. In contrast, deletion of lactate dehydrogenase A (*Ldha*), a key enzyme directly driving glycolysis, affected the function of both HSCs and progenitor cells (Wang et al., 2014). Furthermore, recent studies have shown that different metabolic pathways are key for specific lineages of the haematopoietic system. Oburoglu et al demonstrated that human HSCs and progenitor cells that are committed to the erythroid lineage, are strictly dependent on glutamine metabolism (Oburoglu et al.,

2014). Furthermore, inhibition of glutamine uptake by blocking the glutamine transporter ASCT2, drove human HSCs towards myeloid differentiation, highlighting the importance of metabolic processes in lineage specification.

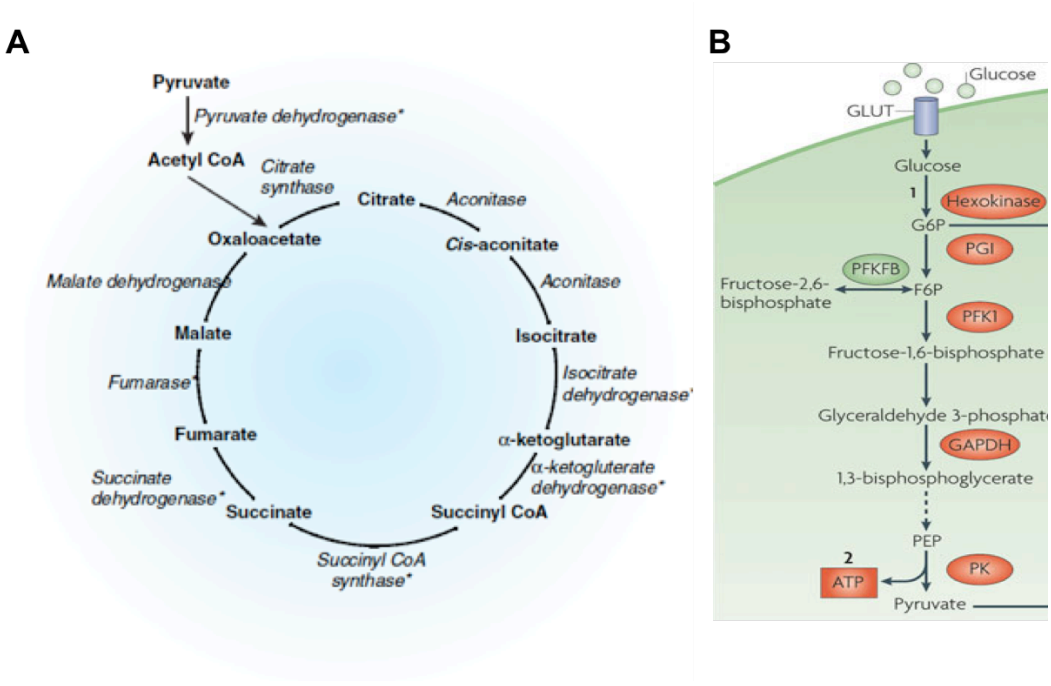

Figure 1-5. Illustration of the TCA cycle and glycolysis. (A) The TCA cycle begins with the reaction between acetyl-coA and the four carbon oxaloacetate that form six carbon citrate. In the second step, citrate is converted to its isomer, isocitrate through a two-step process by a loss and then addition of a water molecule. In the first step, citrate is converted to cis-aconitase which is then converted to isocitrate. In the third step, isocitrate is oxidised, producing a five carbon molecule, a-ketoglutarate (a-KG), together with a molecule of carbon dioxide (CO_2), two electrons, which reduce NAD^+ to NADH + H^+. a-KG is then converted to succinyl group which binds to a molecule of CoA to form succinyl-CoA, while carboxylation of a-KG results in the release of another CO_2 molecule and the reduction of NAD^+ to NADH + H^+. Step five involves the removal of CoA from succinyl CoA and is replaced by a phosphate group. The phosphate group is then removed and attached to guanosine diphosphate (GDP), thereby forming guanosine triphosphate (GTP). The final product from the removal of CoA from succinyl CoA is succinate. The sixth step involves the oxidation of succinate to fumarate, while Flavin adenine dinucleotide (FAD) is reduced and forms $FADH_2$ in the process. The seventh step involves the hydration of fumarate into malate and during the eighth step malate is oxidized, forming oxaloacetate, the initial substrate of the cycle, while NAD^+ is reduced to NADH+ H^+ in the process. (Image taken from Munnich, 2008). (B) Glycolysis. Glucose enters the cell and is phosphorylated to glucose-6-phosphate (G6P) by hexokinase (1). G6P either proceeds through glycolysis to produce ATP, NADH and pyruvate (2), or through the PPP, producing ribose-5-phosphate and NADPH. G6P dehydrogenase (G6PD) dictates entry of G6P into the pentose phosphate pathway (PPP), and G6P oxidation produces NADPH. NADPH is an important cellular antioxidant and is a cofactor in the reductive biosynthesis of fatty acids, nucleotides and amino acids. Pyruvate produced by glycolysis is converted to acetyl-CoA, which enters the TCA cycle and produces two ATP molecules and six NADH molecules per glucose. (Image taken from Buchakjian and Kornbluth, 2010).

1.8.1 Oxidative stress and redox regulation in HSCs

Reactive oxygen species (ROS) are highly reactive free radicals that act as key regulators of the oxidoreductive state, and are generated as by-products of normal physiological processes (Chance et al., 1979). They are short-lived oxygen-derived molecules mainly represented superoxide anions (O_2^-), hydrogen peroxide (H_2O_2), and hydroxyl radicals (OH). Hydrogen peroxide is the most important ROS, involved in signalling and acting as a second messenger in cells, and is mostly generated by the dismutation of O_2^- to H_2O_2. (Loschen et al., 1974). Superoxide anions can be produced by NADPH oxidases (NOXs, NOX1-NOX5), by the mitochondrial complexes I and III of the electron transport chain, or by physical stimuli such as ultraviolet radiation. NOXs were first identified in 1999 and constitutively generate low levels of ROS through electron transfer from NADPH to molecular oxygen (Suh et al., 1999). However, upon specific stimuli or growth factors, NOX enzymes can increase ROS production.

ROS are functionally involved in the control of the biological activity of HSCs. Murine HSCs with low ROS production are quiescent and exhibit an increased self-renewal capacity, while HSCs with higher ROS production have a reduced self-renewal capacity (Jang and Shakris, 2007; Ludin et al., 2014). Recent studies have provided strong evidence that low levels of ROS are strictly required in order to maintain HSC quiescence and stemness, while increased ROS levels favour HSC differentiation. The molecular mechanism underlying the implication of ROS in self-renewal of HSCs has been recently elucidated, revealing the involvement of the p38 MAPK and mammalian target of rapamycin (mTOR) pathways. Activation of p38 MAPK in response to elevated ROS, limited the life-span of murine HSCs *in vivo* and drove HSCs out of quiescence (Ito et al., 2006). Inhibition of either of those pathways rescued the ROS-induced effects in the repopulating capacity of HSCs (Ito et al., 2006). Furthermore, prolonged treatment with an antioxidant extended the lifespan of HSCs from wild-type mice in transplantation experiments. Conversely, stimulation of ROS triggered HSC differentiation in murine models (Jang et al., 2007; Ito et al., 2006). In addition, a study exploring the ROS production in different

progenitor cells found that while production of ROS remained low in HSCs. CMPs were classified according to their ROS expression, to high ROS and low ROS CMPs. High ROS CMPs differentiated into GMPs whereas low ROS differentiated into MEPs. (Shinohara et al., 2014). Additionally, after culturing low ROS CMPs with H_2O_2 in semi-solid media, the authors observed a decrease in MEP colony production. In contrast, when they cultured high ROS CMPs with catalase, a ROS scavenger, they observed an increased generation of GMP colonies, at the expense of MEP colonies (Shinohara et al., 2014). Further studies have shown the importance of ROS in granulopoiesis (Segal et al., 2005), platelet production and megakaryopoiesis (McCrann et al., 2009; Motohashi et al., 2010).

1.9 AML

Leukaemias are a heterogeneous group of diseases characterised by the infiltration of immature blood cells into the blood, bone marrow, spleen and other tissues such as the liver, lungs and lymph nodes. These clonal haematopoietic malignancies arise from stem and progenitor cells of the haematopoietic system and are characterised by impaired differentiation and enhanced proliferation of immature cells. Leukaemias are classified based on the speed of the disease and the particular blood lineage cell of origin. As a result, leukaemias are classified as chronic myeloid leukaemia (CML), chronic lymphoblastic leukaemia (CLL), acute myeloid leukaemia (AML) and acute lymphoblastic leukaemia (ALL). AML represents the largest group of haematopoietic malignancies, accounting for 80 % of all acute leukaemias in adults. As such, our lab is interested in understanding how AML develops and whether it can be eradicated using novel strategies.

AML is an aggressive type of leukaemia that is characterised by the rapid expansion of immature myeloid cells that accumulate in the bone marrow and infiltrate secondary organs such as the spleen and the lymph nodes (Wang and Dick, 2005; Andersson et al., 2015; Khwaja, 2016; Metzeler et al., 2016). The incidence of AML increases with age, with people over 60 years of age being most affected. Although AML is mostly prevalent in adults, AML accounts for approximately 20 % of all

leukaemia cases in children (De Kouchkovsky & Abdul-Hay, 2016; Kelly & Gilliland, 2002).

1.9.1 Pathophysiology of AML

Expansion of the immature blast cells cause the initial clinical symptoms of the disease, including haemorrhage, fatigue and recurrent infections as a result of decreased numbers of platelets, red blood cells and neutrophils. Infiltration of leukaemic cells in secondary organs such as the lungs, liver, spleen, lymph nodes and the central nervous system, results in a variation of other symptoms including shortness of breath, excessive sweating and weight loss (Lowenberg et al., Downing, 1999). In the clinic, patients are diagnosed with AML when there are at least 20 % of blast cells present in the bone marrow (Estey and Döhner, 2006).

1.9.2 The cell of origin of AML

Leukaemias and solid tumours are known to exhibit tumour heterogeneity and the mechanism by which malignancies are maintained has been the focus of intense investigation. More than 50 years ago the idea of a 'cancer stem cell' model arose, describing the notion that cancers arise from one cell that exhibits self-renewal capacity. Seminal studies using ^{3}H-thymidine showed that only a small fraction of cells in AML patients proliferate (AML-CFU), and were enriched exclusively in the $CD34^{+}$ $CD38^{-}$ fraction (Bhatia et al., 1997; McCulloch, 1983; Griffin, 1986). As the normal HSCs are found within the same compartment, it was proposed that leukaemic stem cells (LSCs) arise exclusively from HSCs (Bhatia, 1997; Hope and Dick, 2004).

However, the idea that LSCs can only arise from HSCs was challenged by a series of studies, some of which are described below. A series of recent reports it has been demonstrated that progenitor cells retrovirally transduced with oncogenic fusion proteins (such as MLL-AF9, MLL-ENL, MOZ-TIF2 fusions), are capable of propagating AML (Huntly et al, 2004; Cozzio et al, 2003; Somervaille and Cleary 2006; Krivstov et al, 2006). The MOZ-TIF2 chromosomal translocation has been identified in subsets of AML and is a fusion between the histone acetyltransferase MOZ and the nuclear receptor transcriptional intermediary factor 2 (TIF) (Carapeti et

al., 1998). Transformation of murine CMP cells with the human MOZ-TIF2 conferred a proliferative advantage of CMPs *in vitro* in serial-replating assays. Furthermore, transplantation of the cells generated AML in primary recipient mice (Huntly et al, 2004). In a similar study, Cozzio et al isolated murine HSCs, GMPs, CMPs and MEPs and transformed them *in vitro* with the human MLL (mixed lineage leukaemia) fusion protein MLL-ENL (eleven nineteen leukaemia), the third most common MLL translocation in AML (Tkachuk et al., 1992; Cozzio et al., 2003). MLL-ENL- transduced stem and progenitor cells generated colonies *in vitro* and exhibited granulocyte/monocyte potential. Upon transplantation of these populations in recipient mice, apart from MEPs, they all generated AML with a similar latency of average of 90 days (Cozzio et al., 2003). More recently, by utilising a transgenic MLL-ENL mouse model, Ugale et al demonstrated that AML developed from multiple progenitor cells, but not HSCs (Ugale et al., 2014). In another study, by utilising a transgenic mouse model of human MLL-AF9, a frequently occurring MLL fusion oncogene (Swansbury et al., 1998), it was demonstrated that LSCs from the MLL-AF9 mouse model were neither rare nor resembled HSCs (Somervaille and Cleary 2006). Specifically, the authors showed that the LSCs were not derived from the HSC compartment as none of the cells displayed an LSK immunophenotype. By using a similar model, Krivstov et al., isolated GMPs from wild-type mice and transduced them with retroviruses expressing the human MLL-AF9 fusion protein (Krivstov et al, 2006). Injection of the MLL-AF9-transduced cells generated AML in primary and secondary recipient mice and shared a common genetic signature with normal GMPs. However, a subset of genes normally expressed in HSCs was re-activated in the GMP-derived LSCs, indicating that a self-renewal-associated signature, similar to that of normal HSCs, can be activated. Amongst others, *HoxA5, HoxA9, HoxA10, Runx2* and *Meis1* exhibited increased expression in the GMP-derived LSCs. In a more recent study carried out by the same group, the authors utilised the human MLL-AF9 knock-in mouse model that has a defined cell of origin (Krivstov et al., 2013). Their findings showed that MLL-AF9-mediated transformation differed when HSCs were the cells of origin as compared with GMPs. Specifically, although they were immunophenotypically similar, the LSCs arising from these two populations exhibited differences in gene expression and DNA

methylation status. More specifically HSC-derived LSCs were expressing "stemness-associated" genes such as *Evi1*, *c-Jun*, *Fos1*, *Bcl6* while the GMP-derived LSCs were not. Additionally, HSC-derived LSCs exhibited an elevated global 5-hydroxy-methylcytosine (5-hmC) profile when compared to GMP-derived LSCs. Furthermore, LSCs derived from HSCs, were less responsive to the chemotherapy drug cytarabicine when treated *in vitro* (Krivstov et al., 2013). These data demonstrate that the cell of origin can influence the gene expression profile, epigenetic profile and response to chemotherapy, highlighting the true heterogeneity of AML as well as the clinical relevance of identifying the cell of origin of different AML subtypes.

Overall, it is evident that AML does not exclusively originate from a single cell population such as the HSC but rather, frequently arises from committed progenitor cells such as GMPs.

1.9.3 Mutations and chromosomal translocations in AML

1.9.3.1 FAB and WHO classifications of AML

A classification for AML, originally proposed in 1976, provided a consistent morphological and cytogenetic framework in which the significance of the genetic abnormalities could be appreciated (Bennet et la., 1976). The classification was referred to as French- American- British (FAB) classification and is outlined in Table 1. However genetic and morphological correlations are not always perfect and in many cases, cannot be identified. Furthermore, the underlining genetic and molecular defects cannot be identified. For that reason, a new way of classifying AML was developed by the world health organization (WHO), that was later updated (Hossfeld et al., 2002; Swerdlow et al., 2008). The WHO classification is outlined in Table 2.

Pioneering work led by Janet Rowley established that AML is a genetic disease, with the discovery of somatic chromosomal abnormalities, including balanced translocations in patient samples (Rowley et al., 1973; 1977). These studies set the stage for the identification of the genes involved at the chromosomal breakpoints, providing major insight into the cytogenetic abnormalities found in AML. However, approximately 40 % of AML patients present a normal karyotype, suggesting that there are molecular changes that cannot be identified using cytogenetics (Grimwade

et al., 2010). However, over the course of the past 20 years, major technological advances have been made such as whole exome sequencing, thus allowing us to better characterise the mutational landscape of AML.

Table 1- FAB classification of AML (Adapted from cancer.org).

The French-American-British (FAB) classification of AML	
FAB subtype	**Name**
M0	Undifferentiated acute myeloblastic leukemia
M1	Acute myeloblastic leukemia with minimal maturation
M2	Acute myeloblastic leukemia with maturation
M3	Acute promyelocytic leukemia (APL)
M4	Acute myelomonocytic leukemia
M4 eos	Acute myelomonocytic leukemia with eosinophilia
M5	Acute monocytic leukemia
M6	Acute erythroid leukemia
M7	Acute megakaryoblastic leukemia

Table 2- WHO classification of AML (Adapted from Arber et al., 2016).

Acute myeloid leukemia (AML) and related neoplasms
AML with recurrent genetic abnormalities AML with t(8;21)(q22;q22.1);RUNX1-RUNX1T1 AML with inv(16)(p13.1q22) or t(16;16)(p13.1;q22);CBFB-MYH11 APL with PML-RARA AML with t(9;11)(p21.3;q23.3);MLLT3-KMT2A AML with t(6;9)(p23;q34.1);DEK-NUP214 AML with inv(3)(q21.3q26.2) or t(3;3)(q21.3;q26.2); GATA2, MECOM AML (megakaryoblastic) with t(1;22)(p13.3;q13.3);RBM15-MKL1 Provisional entity: AML with BCR-ABL1 AML with mutated NPM1 AML with biallelic mutations of CEBPA Provisional entity: AML with mutated RUNX1
AML with myelodysplasia-related changes
Therapy-related myeloid neoplasms
AML, Not Otherwise Specified

1.9.3.2 Genetic mutations in AML

Next-generation sequencing and whole-exome sequencing have led to the discovery of numerous recurrent mutated genes in AML (Ley et al., 2008). Furthermore, the Cancer Genome Atlas consortium studied the mutational status of 200 AML patient samples and found a large proportion to be "significantly mutated", at a higher than expected frequency (The Cancer Genome Atlas (TCGA), 2013). Although the functional significance of many of these mutations is not fully understood yet, these mutations can become clinically useful, as they could be used as biomarkers. Below, I outline the classes of the most common mutations that have been implicated in AML development in Figure 1-6. Broadly speaking, the identified mutations fall under the following categories: mutations involving components of signalling pathways, mutations in epigenetic modifiers, splicing factor gene mutations and CEBPA, NPM1 and RUNX1 mutations.

1.9.3.3 Mutations in signalling pathway components

A major step forward was the discovery that the receptor tyrosine kinase fms-like tyrosine kinase 3 (FLT3) is mutated in a third of all AML cases (Grimwade et al., 2016). These mutations involve in-frame duplications within the juxtamembrane region (FLT3-ITD), and point mutations in the tyrosine kinase domain (FLT3-TKD) in 25 % and 7 % of AML, respectively. Both classes of mutation lead to constitutive activation of the receptor, yet surprisingly carry different prognostic implications. FLT3-ITD mutations are associated with a poorer prognosis while FLT3-TKD are associated with a more favorable prognosis (Mead et al., 2007). Following studies established that a number of other genes encoding signalling pathway components such as RAS and cKIT, are recurrent mutations in AML (Grimwade et al., 2016).

1.9.3.4 Epigenetic modifier mutations

Recent studies have identified a number of epigenetic modulators to be mutated in AML. Alterations include a number of genes such as *DNMT3A, TET2, WT1* and *IDH1/2* mutations (Grimwade et al., 2016). DNMT3A, is a methyltransferase generating *de novo* DNA methylation, mutated in approximately 30 % of all AML

cases (Ley et al., 2010) and often appears in conjunction with *NPM1* (Slush et al., 2014) and *FLT3* mutations (Thiede et al., 2006). Most *DNMT3A* mutations are heterozygous and alter the R882 catalytic domain, suggesting the possibility of dominant-negative consequences (Russler-Germain et al., 2014).

Recently, mutations in other epigenetic modifiers such as *TET2*, *WT1* and *IDH1/2* have been identified as well. Mutations in these genes were found to be mutually exclusive but shared similar signatures in terms of DNA methylation profiling (Figuoeroa et al., 2010; Wang et al., 2015; Rampal et al., 2014). The key downstream target is TET2, which is mutated in 8 % of all AML cases. *IDH1* mutations affecting R132 are found in 7 % of all AML cases while *IDH2* mutations are found in 9 % of all AML cases (TCGA, 2013).

IDH enzymes catalyze the conversion of isocitrate to alpha-ketoglutarate. However, *IDH* mutations not only reduce the formation of alpha-ketoglutarate but also exhibit a neomorphic activity, altering the enzyme's function to produce the "oncometabolite" 2-hydroxyglutarate, which inhibits the function of TET2 (Xiao et al., 2011). *WT1* mutations are found in 9 % of all AML cases and has been recently identified as a binding partner of TET2 (TCGA, 2013; Wang et al., 2015; Rampal et al., 2014). These studies collectively demonstrate that the IDH/WT1/TET2 axis plays an important role in AML pathogenesis.

1.9.3.5 *CEBPA, NPM1*, and *RUNX1* mutations

Major insight into the molecular pathogenesis of AML was provided by the discovery of mutations in genes encoding CCAAT/enhancer binding protein alpha (CEBPA) and nucleophosmin (NPM1). These mutations were recognised by the WHO in 2008 classification and define prognostically relevant subsets in AML (Swerdlow et al., 2008). CEBPA encodes a myeloid transcription factor and mutations of CEBPA are found in approximately 10 % of all AML cases (TCGA, 2013). CEBPA mutations result in the expression of a truncated version, potentially acting in a dominant-negative manner (Pabst et al., 2001).

NPM1 is the single most commonly mutated gene in AML, found in approximately 35 % of all AML (Falini et al., 2005; Thiede et al., 2006). The *NPM1* gene encodes a nucleoplasmic shuttling protein with prominent localisation in the nucleus. However,

mutation in *NPM1* result in an aberrant cytoplasmic localisation (Fallini et al., 2005). Although *NPM1* mutations are very frequent in AML, the exact molecular mechanisms by which they contribute to AML is not fully understood yet. Finally, *NPM1* mutations are frequently associated with alterations in *FLT3, DNMT3A* and *IDH1/2* genes (Dohter et al., 2005; Schnittger et al., 2005).

RUNX1 is a relatively common mutation target in cytogenetically abnormal AML. Germ-line mutations of *RUNX1* lead to familial platelet disorder and predispose to AML (Lam et al., 2012). In adult AML, *RUNX1* mutations tend to be mutually exclusive with balanced chromosomal translocations and mutations involving *NPMT1*, *IDH2* and *CEBPA* mutations (Lam et al., 2012).

1.9.3.6 Splicing factor gene mutations

Recently, mutations in genes encoding members of the pre- messenger RNA splicing machinery were identified in myelodysplastic syndromes (MDS) (Yoshida et al., 2011; Papaemmanuil et al., 2011). MDS are a heterogeneous group of myeloid neoplasms characterised by deregulated blood cell production with evidence of myeloid dysplasia and a predisposition to AML (Yoshida et al., 2011). The most common mutations of splicing factors involve *SF3B1, SRSF2*, *ZRSR2, SF3B1* and *U2AF1* (TCGA, 2013; Yoshida et al., 2011; Lindsley et al., 2015). A recent study focusing on *SRSF2* showed that the mutation impaired normal differentiation *in vivo.* Specifically, the mutation resulted in missplicing of targets such as *EZH2* (Kim et al., 2015). Further insights into the functional consequences of splice factor mutations came from *in vivo* studies involving *U2AF1* (Shirai et al., 2015). Shirai et al found that *U2AF1* mutations altered haematopoiesis by missplicing genes involved in AML and MDS, such as *MLL* and *BCOR* (Shirai et al., 2015). Splice factor mutations are the most frequent mutations in MDS, where they are considered to be an initiating event (Papaemmanuil et al., 2013), but are much less common in AML (found in 5-10 % of all AML cases) (TCGA, 2013; Yoshida et al., 2011).

1.9.3.7 Mutations in cohesin complex members

By the use of whole exome sequencing, genes encoding components of the cohesin complex were identified as recurrent mutations in AML (TCGA, 2013; Tho et al., 2014; Kon et al., 2014). The cohesin complex is a ring-like structure composed of

SMC1A, SMC3, RAD21 and one of either STAG1 or STAG2 (Nasmyth et al., 2009). The cohesin complex is involved in sister chromatid exchange during anaphase, regulation of DNA repair, and transcriptional control by coordinating interaction between promoters, via DNA looping (Kagey et al., 2010; Degner et al., 2011; Schaaf et al., 2013). Interestingly, cohesin mutations are associated with altered transcriptional regulation in the development of AML and are detected in 20 % of AML patients. Cohesin complex mutations are often associated with mutations involving *RUNX1*and *ASXL1* (Thota et al., 2014). For an overview of the most common mutations in AML, please refer to Figure 1-6.

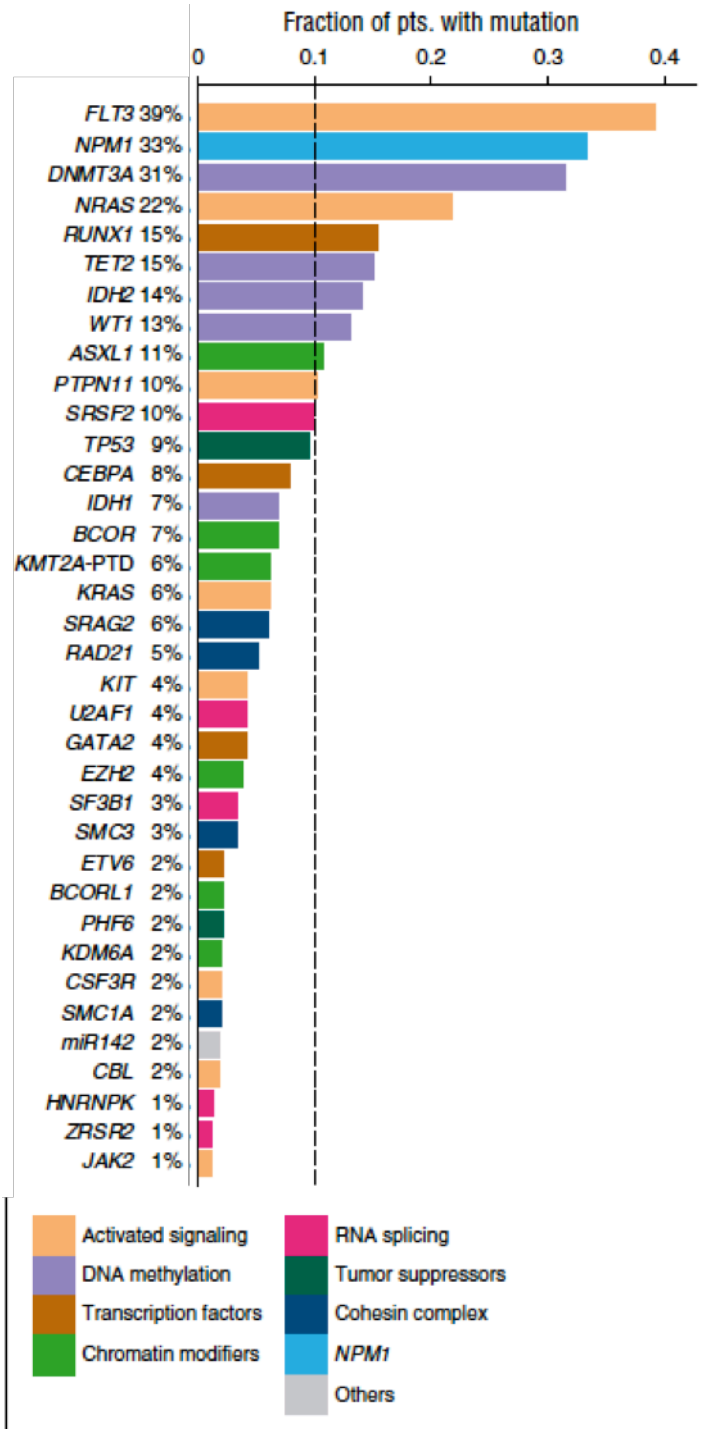

Figure 1-6. Overview of the most common mutations identified in AML patients (Adapted from Metzeler et al., 2016).

1.9.3.8 Cytogenetic characterisation of AML

1.9.3.8.1 Chromosomal rearrangements and translocations

Balanced chromosomal rearrangements are detected in approximately 25-30 % of all adult AML and give rise to in-frame chimeric fusion genes. Frequently targeted genes encode haematopoietic transcription factors such as RARA, RUNX1 or the CBFb subunit of the core binding factor complex, components of the nuclear pore complex (NUP98, NUP214) and epigenetic regulators such as MLL (Grimwade et al., 2016; Mrozek et al., 2008). The most common balanced chromosomal rearrangements in AML are: (1) the t (8;21) translocation resulting in RUNX1-ETO fusion protein, (2) inv(16)/ t(16;16) resulting to the core binding factor beta (CBFB) fusion with the muscle myosin heavy chain (MYH11) gene (Liu et al., 1993; Shurtleff et al., 1995), (3) the t (15;17) translocation creating the PML-RARA gene fusion (de The et al., 1990).

1.9.3.8.2 t (8;21)/ RUNX1-ETO

Approximately 10 % of AML cases carry the t(8;21) translocation, which involves the *RUNX1* and *ETO* genes, and express the DNA- binding transcription factor, crucial for normal haematopoietic differentiation (Erickson et al., 1992; Mrozek et al., 2008; Cameron et al., 2004), while ETO is a protein acting as a transcriptional repressor (Davis et al., 2003). The fusion protein is suggested to function as a transcriptional repressor that blocks RUNX1-dependent transactivation of various promoters, suggesting that the fusion protein might act as a dominant negative regulator of wild-type RUNX1 (Meyers et al., 1995; Bulchi et al., 2014).

1.9.3.8.3 Inv (16)/ CBFB-MYH11

Inv (16) is found in 8 % of AML cases and fuses the first 165 amino acids of CBFB to the C-terminal coiled-coil region of MYH11 (Liu et al., 1993; Shurtleff et al., 1995). CBFB-MYH11 fusion protein is suggested to co-operate with RUNX1 to repress transcription (Lutterbach et al., 1999; 2000).

1.9.3.8.4 t (15;17)/ PML-RARA

The PML-RARA oncogenic fusion protein is found in approximately 95 % of all M3FAB (APL) subtypes of AML, and acts as a transcriptional repressor that interferes with gene expression programs involved in normal differentiation, self-renewal and apoptosis (Jing et al., 2004; Licht, 2006).

1.9.3.8.5 MLL rearranged leukaemias

The MLL gene is located on chromosome 11 and is a frequent target for chromosomal rearrangements and translocations (Ziesmin-van der Poel et al., 1991; de Boer et al. 2013; Martin et al., 2003; Rao &Dou, 2015). MLL is a trithorax-related histone methyltransferase (H3K4), homologous to yeast Set1, the first H3K4 methylase that was identified (Djabali et al., 1992; Miller et al., 2001).

MLL has been found in 73 different translocations and 54 partner genes have been cloned (TCGA, 2013). MLL rearrangements are found in approximately 80 % of all infant ALL cases and in 10 % of all adult leukaemia cases (Mohan et al., 2010). MLL fusion proteins underline some of the most aggressive human leukaemias and represent the most frequent translocations found in both myeloid and lymphoid leukaemias (Garcia-Cuellar et al., 2016; Cano et al., 2007; Cozzio et al., 2003). As a result, most of the leukaemias harboring MLL rearrangements are associated with poor prognosis (Mohan et al., 2010; Anderson et al., 2015). Over 90 % of all MLL cases are accounted for by gene fusion with AF4 (42 %), AF9 (16 %), ENL (11 %), AF10 (7 %) and ELL (4 %) (Mayer et al., 2009).

Expression of the MLL promoter after translocation produces an MLL fusion protein consisting of the N-terminus of MLL and the C-terminus of the fusion protein, which does not contain H3K4 methyltransferase activity (Marschalek, 2010). MLL fusion proteins appear to interfere with normal transcriptional regulators and mediate leukaemogenesis. Four of the most common fusion partners of MLL, namely AF4, AF9, ENL and ELL participate in a common biological reaction known as the positive transcription elongation factor b (P-TEF-b)- dependent transcriptional activation cycle of RNA polymerase II, converting a “promoter-arrested RNA polymerase II”, into “elongating RNA polymerase II” (Peterlin and Price, 2006). These factors along with the polymerase associated factor 1 complex, the H3K79

methyltransferase DOTL1, and the BET family protein BRD4, are thought to form a large complex and transcriptionally alter target genes (Yokomama et al., 2010; Biswas et al., 2011; Milne et al., 2010; Jang et al., 2005). MLL fusion proteins appear to promote leukaemogenesis through a common molecular mechanism that involves aberrant transcriptional elongation of target genes involved in proliferation, differentiation and survival (Wang et al., 2011). Furthermore, MLL fusion proteins target transcriptional regulators of HSC self-renewal, in particular *MEIS1* and *HOXA9* (described in more detail in section 4.1) (Kawagoe et al., 1999; Imamura et al., 2002; Ayton and Cleary, 2003).

Finally, although MLL fusions may contribute to leukaemogenesis via a common molecular mechanism to dysregulate transcription of target genes, many of these target genes are likely to be unique to the particular MLL fusion partner, and may depend on the cell of origin and additional mutations that may be present, thus explaining the heterogeneity in the pathology of the different MLL leukaemias.

1.9.3.9 Mutational evolution of AML

Next generation sequencing studies have documented the stepwise acquisition of mutations by identifying differences in the relative proportion of co-occurring mutations in the bulk AML cells at the time of diagnosis (Mardis et al., 2009; Walter et al., 2012). Longitudinal sequencing studies using samples at the time of diagnosis as well as relapse of the same patient, have shown that the patterns of relapse are heterogeneous. Relapse was shown to occur from the expansion of both major and minor clones that were present in diagnosis, or from new clones that did not share ancestry with the diagnostic clone (Ding et al., 2012; Wong et al., 2015).

Recent studies have identified several mutations that arise as initiating or secondary events (Jan et al., 2012; Corces-Zimmerman et al., 2014; Slush et al., 2014). For instance, mutations in *DNMT3A, TET2, IDH1/2* and *ASXL1* are thought to occur in progenitor and haematopoietic stem cells without affecting the normal characteristics of the cells. However, upon the acquisition of secondary mutations such as a mutation of the NPM1 gene, lead to the generation of AML (Slush et al., 2014). Pre-leukaemic mutations such as *DNMT3A, TET2* and *ASXL1* are associated with poorer prognosis (Slush et al., 2014).

Taken together, recent studies have identified early mutations and mutations that persist after treatment failure, therefore pointing towards the critical molecular drivers that need to be therapeutically targeted.

1.9.4 Two hit model

AML is considered to develop in a "two hit" fashion. This view suggests that the development of AML is a multistep process, where initial and secondary mutations are required (Papaemmanuil et al., 2016; Kelly and Gilliland, 2002). More specifically, initial mutations occurring in stem or progenitor cells lead to the generation of pre-leukaemic stem cells (pre-LSCs). In murine models, pre-LSCs are characterised by their ability to generate disease in primary recipient mice with varying latency. Secondary mutations then lead to the generation of leukaemic stem cells (LSCs), and the founding clone(s) of AML. LSCs are defined by their self-renewal capacity and their ability to propagate disease with very short latency. The mutations are broadly classified in type I and type II mutations, with type I conferring a survival and proliferative advantage, and type II mutations impairing normal haematopoietic differentiation (Kelly and Gilliland, 2002). However, more recent studies have identified epigenetic mutations that do not necessarily fall under either of those categories, challenging the simplicity of the "two hit" model (TCGA 2013; Metzeler et al., 2016). While the mutational status and cytogenetic abnormalities involved in AML are well described, the metabolic properties of AML cells are only recently better understood. Below I describe the most recent studies that aim to uncover the metabolic properties of AML cells.

1.9.5 Current treatments for AML

Standard therapy for AML patients is delivered in two phases. The first phase is the "induction" phase, and the second phase is the "consolidation" phase that eradicates any residual disease in order to achieve lasting remission. The induction phase consists of a standard "7+3" treatment that consists of a 7-day continuous infusion with cytarabicine (interfering with DNA synthesis), followed by 3 days of treatment with anthracycline (inhibiting RNA and DNA synthesis, as well as topoisomerase II, ultimately blocking DNA replication and transcription). The "7+3" regimen is generally offered to patients with a favorable or intermediate prognosis. The

"consolidation" phase normally involves a sequence of higher doses of cytarabicine, with 40 % of young patients remaining in complete remission for approximately 5 years (Burnett et al., 2011). This treatment is repeated approximately every 4 weeks, of a total of 3 to 4 cycles. Young patients can also undergo allogeneic stem cell transplant (ASCT) after "induction" therapy. ASCT has been found to reduce the risk of patient relapse but comes with serious complications, including the risk of treatment-associated death. Older patients are often not able to tolerate such intensive "consolidation" treatment and as a result are treated with fewer cycles (1 or 2) of cytarabicine. Some of the novel agents currently used as first-line AML treatment and those currently being developed for the clinic include: FLT3-ITD inhibitors (such as Sorafenib, Midostaurin and Quizartinib), STAT inhibitors (such as C188-9), and IDH1/IDH2 small molecule inhibitors (such as Clofarabine) (Dombret and Gardin, 2016; Kouchkovsky and Abdul-hay, 2016). Emerging therapies for AML currently include inhibitors for histone deacetylase (HDAC), DOTL1, BCL-2 and BET bromodomain inhibitors. Finally, antibody-drug conjugates (ADCs) are also in early-phase clinical trials (Sten and Tallman, 2016).

1.10 Abnormalities in the metabolism of LSCs

1.10.1 OXPHOS in LSCs

Elevated ROS production has been associated with various myeloid malignancies, including CML and AML (Hole et al., 2011). The use of experimental mouse models has provided evidence that ROS production contributes to leukaemogenesis. For example, in murine breakpoint cluster region-abelson (BCR-ABL) models, expression of BCR-ABL induced the production of ROS, which contributed to malignant transformation (Sattler et al., 2000; Kim et al., 2005). Transformation of the haematopoietic cell lines, Ba/F3, 32Dcl3 and MO7e with retrovirally expressed BCR-ABL, resulted in an increase of ROS (Sattler et al., 2000). The authors showed that the increase in ROS was a direct consequence of BCR-ABL expression, since treatment of the cell lines with an ABL-specific tyrosine kinase inhibitor, decreased ROS levels. Finally, stimulation of untransformed MO7e cells with H_2O_2 (to mimic increase of ROS), increased the phosphorylation of components of the BCR-ABL pathway, including c-ABL, SHC and SHP-2 (Sattler et al., 2000). A more recent

study suggested that elevated ROS is dependent on BCR-ABL-dependent increase in glucose metabolism, as treatment of BCR-ABL-transformed Ba/F3 and MO7e cells with the glycolysis inhibitor 2-deoxy-glucose, reduced ROS levels (Kim et al., 2005).

Similarly, human AML cell lines MOLM13 and MV4-11 that express FLT3-ITD, exhibited increased levels of ROS that was attributed to high transcript expression of NOX4. Knock-down of NOX4 in these cell lines resulted in diminished colony forming potential *in vitro*. Furthermore, the essential role of ROS in FLT3-ITD-mediated leukaemia was supported by the fact that in a murine model of FLT3-ITD, *NOX4*-targeting compounds had an inhibitory effect on the development of AML *in vivo* (Jayavelu et al., 2016). Interestingly, in another study, Lagadinou et al demonstrated that ROS production is heterogeneous in primary human AML cells. In particular, the authors isolated LSCs based on their ROS expression via flow cytometry. While ROS-low cells were quiescent and exhibited functional LSC properties, ROS-high cells proliferated more and did not possess LSC properties (Lagadinou et al., 2013). Ectopic expression of the Ras oncogene via retroviral vectors in $CD34^+$ cells isolated from healthy donors, promoted ROS production as indicated by a superoxide-sensitive chemiluminescent probe (Hole et al., 2010). Furthermore, ROS production was attributed to the activation of NOX enzymes. More importantly, the authors showed that Ras-expressing $CD34^+$cells exhibited augmented proliferation that was specifically attributed to ROS production, as treatment with the antioxidants DPI and NAC, supressed the proliferation of the cells (Hole et al., 2010).

In another study primary cells isolated from the peripheral blood or bone marrow of AML patients, exhibited a strong elevation of ROS (specifically superoxide), when compared to cord blood $CD34^+$ cells of healthy donors (Hole et al., 2013). Furthermore, the elevated ROS production was attributed to increased expression of NOX2/4 enzymes and inhibitors of such, decreased the concentration of superoxide. Finally, treatment of the human AML cell lines MV4-11 and KG1 (that normally exhibit low levels of ROS) with H_2O_2, in order to mimic elevated ROS increased the proliferation of the cells in a dose-dependent manner (Hole et al., 2013). Overall, this

study demonstrated that primary AML cells exhibit a strong ROS signature and that NOX-derived ROS production promotes the proliferation of AML cells (Hole et al., 2013).

Skrtic et al. also analysed mitochondrial function in primary AML cells and found that these cells exhibited greater mitochondrial mass when compared to normal progenitor cells (Skrtic et al., 2011). Interestingly, the AML cells with the greater mitochondrial mass selectively underwent apoptosis when treated with tigecycline, an antimicrobial agent that blocks mitochondrial respiration (Skrtic et al., 2011). The same authors extended their study and found that the increased mitochondrial mass was not concomitant with the increase of respiratory chain activity. Furthermore, the cells exhibited low spare respiratory capacity and were thus more sensitive to oxidative stress (Sriskanthadevan et al., 2015). The authors took advantage of this sensitivity and selectively killed the AML cells by treating them with the fatty acid palmitate, which increases the flux of electrons through the electron transport chain, eliciting oxidative stress (Sriskanthadevan et al., 2015).

1.10.2 Mitochondrial metabolism alterations in AML cells

Recent efforts have been made in order to understand the biochemical mechanisms responsible for the apparent increased dependence of cancer cells on aerobic glycolysis (i.e. reliance on glycolysis even in the presence of oxygen). An interesting hypothesis that has emerged from recent studies, indicate that mitochondrial uncoupling (the uncoupling of ATP synthesis from mitochondrial membrane potential), could promote the shift to aerobic glycolysis. When culturing AML cell lines on a layer of feeder MSC cells, Samudio et al demonstrated OCI-AML3 and MOLM13 cells were more resistant to chemotherapy and decreased the entry of pyruvate into the TCA cycle, without compromising oxidative phosphorylation (Samudio et al, 2008; 2009). This observation suggested that the shift to oxidation of non-glucose nutrients could be mainly sustained by fatty acids. Consistent with this notion, pharmacological inhibition of fatty acid oxidation (FAO) sensitised human primary AML cells to apoptosis, by induction of the molecule ABT-737, a molecule that releases pro-apoptotic Bcl-2 proteins (Samudio et al., 2010). The rate-limiting

step of FAO, is carried out by the enzyme carnitine palmitoytransferase 1 (CPT1). Inhibition of FAO, using a CPT1 inhibitor, resulted in mitochondrial damage, growth arrest and apoptosis of primary AML cells derived from bone marrow aspirates and cell lines (Ricciardi et al., 2014). More recently, avocatin B, a lipid derived from the avocado fruit, was shown to exert cytotoxic effects *in vitro* on the AML cell lines TEX and OCI-AML2, as well as on primary AML cells. Interestingly, avocatin B exerted its cytotoxic effects via inhibition of FAO, highlighting the fact that AML cells rely on FAO in order to sustain their energy demands (Lee et al., 2015).

Apart from lipids, glutamine also represents an important source of carbon molecules in order to sustain oxidative phosphorylation. Recently, the importance of glutamine metabolism for AML cells was highlighted by the observation that knock-down of the glutamine transporter SLC1A5 induced apoptosis in the AML cell lines MV4-11 and OCI-AML13 and inhibited AML development in a xenotransplantation mouse model, without affecting normal $CD34^+$ cells (Willems et al., 2013; Jacque et al., 2015). Interestingly, glutamine deprivation in the AML cell lines HL-60, THP-1 and K-562, induced upregulation of enzymes involved in serine metabolism, namely phosphoglycerate dehydrogenase and phosphoserine aminotransferase (Polet et al., 2016). This observation potentially highlights new therapeutic windows via the inhibition of glutamine and serine metabolism.

Finally, in an effort to identify members of the mitochondrial proteome for which inhibition may reduce the viability of AML cells, Cole et al identified the caseinolytic mitochondrial matrix protease CIcp, a mitochondrial protease, being overexpressed in approximately half the AML samples (Cole et al., 2015). Down-regulation of CIcp in primary AML samples, selectively induced apoptosis while sparing normal haematopoietic cells (Cole et al., 2015).

1.10.3 Abnormalities of the glycolytic pathways in AML cells

Similarly to other cancers, the level of glycolytic metabolism is high in AML patient samples (Herst et al., 2011). Interestingly, the level of the glycolytic pathway was

variable between patients, separating patients into two groups. One group exhibited high glycolytic activity and the other group exhibited moderate levels of glycolytic activity as measured by a dye-reduction assay *in vitro* (Herst et al., 2011). These findings were corroborated by another study that measured the concentration of different metabolites from the sera of AML patients (Chen et al., 2014). Based on their metabolomics study, Chen et al identified a total of 6 metabolites representing a glucose metabolism signature. Based on these metabolites, the authors were able to separate patients into a high- and low- prognostic risk score (PRS). Low-PRS patients had a poor prognosis and were characterised by an increase in the levels of lactate, pyruvate, 2-oxoglutarate, 2-hydroxyglutarate and glycerol-3-phosphate and decreased levels of citrate, thereby suggesting a truncation of the TCA cycle and an augmentation of glycolysis (Chen et al., 2014). Inhibition of glycolysis using 2-deoxyglucose decreased survival of AML cells and increased their sensitivity to the anti-leukaemic agent arabinofuranosyl cytidine (Chen et al., 2014).

Given these observations, efforts have been made to evaluate whether blocking enzymes of the glycolytic pathway, would exert an inhibitory effect on leukaemic cells in terms of their survival. Pyruvate dehydrogenase kinase-1 (PDK1), is a key enzyme of the glycolytic pathway, regulating the flux of pyruvate into the TCA cycle. PDK1 is often over-expressed in cancer cells. Recently, it was shown that the use of a PDK1 inhibitor, dichloroacetophenone, induced apoptosis of the AML cell line U937, and inhibited their growth when transplanted in nude mice (Qin et al., 2016).

PKM2, is another key enzyme of the glycolytic pathway most predominantly expressed in cancer cells. Genetic deletion of *Pkm2* in mice decreased survival of LSCs but had no effect on normal haematopoietic cells (Wang et al., 2014). Lactate dehydrogenase A (LDHA) catalyzes the final step in the glycolysis pathway (oxidation of pyruvate to lactate). The authors furthered their study by genetically deleting *Ldha* in mice using the transgenic *Mx1-Cre* mouse model, which affected the survival of both leukaemic and normal cells, indicating that lactate production is important for both cell types (Wang et al., 2014).

Other studies have also investigated the activation of the pentose phosphate pathway

(PPP) in AML. Based on the Cancer Genome Atlas AML dataset, in 61 % of AML cases, PPP genes are upregulated. Furthermore, inhibition of PPP in leukaemic cells suppressed growth and invasion of AML but not colony growth (Chen et al, 2016).

Cancer metabolism is an intense area of investigation that could offer the potential of new therapeutic windows. Increasing evidence suggests that oxidative phosphorylation is an important source of energy for leukaemic cells, thus underscoring the importance of elucidating the exact mechanisms by which it contributes to leukaemogenesis and to normal haematopoiesis. With that in mind, my project focuses on unravelling the importance of OXPHOS in both normal haematopoietic cells and leukaemic cells, by deleting one of the key enzymes of the TCA cycle, fumarate hydratase Figure 1-5.

1.11 Fumarate hydratase

1.11.1 FH identified as a tumour suppressor in HLRCC

Fumarate hydratase (FH in humans, Fh1 in mice) is an enzyme of the TCA cycle catalysing the hydration of the metabolite fumarate into malate (Figure 1-7 A). Although FH is generally considered a mitochondrial enzyme, it is also expressed in the cytoplasm where it participates in various macromolecular processes such as the urea, nucleotide and amino acid cycles and in the nucleus where it is thought to be part of the DNA damage response (Sass et al, 2001; Yogef et al, 2012). FH has been classified as a tumour suppressor in hereditary leiomyomas and renal cell cancer (HLRCC) as affected individuals inherit a germline mutation while tumours exhibit loss of the wild-type copy of the gene (Tomlison et al, 2002). Biallelic loss of *FH* was initially identified in patients with HLRCC and has been recently identified in patients with paragangliomas and pheochromocytomas (Tomlison et al, 2002; Vega et al, 2013). Fumarate, which is highly accumulated in FH-deficient cells, is considered a major pro-oncogenic factor in HLRCC. Initial studies proposed that the stabilisation of the hypoxia-inducible factors (HIFs), caused by the fumarate-dependent inhibition of propyl-hydroxylases (PHDs) that negatively regulate HIFs, was instrumental for tumour formation (Isaacs et al, 2005; Pollard et al, 2005). However, it was demonstrated that neither HIF-upregulation nor PHD inactivation was required for renal cyst formation in *Fh1*-deficient cells, challenging their

implication in tumour formation in this context, suggesting that HIF-independent oncogenic pathways might be involved (Adam et al., 2013). The functions of fumarate identified up to date are outlined in Figure 1-7 B.

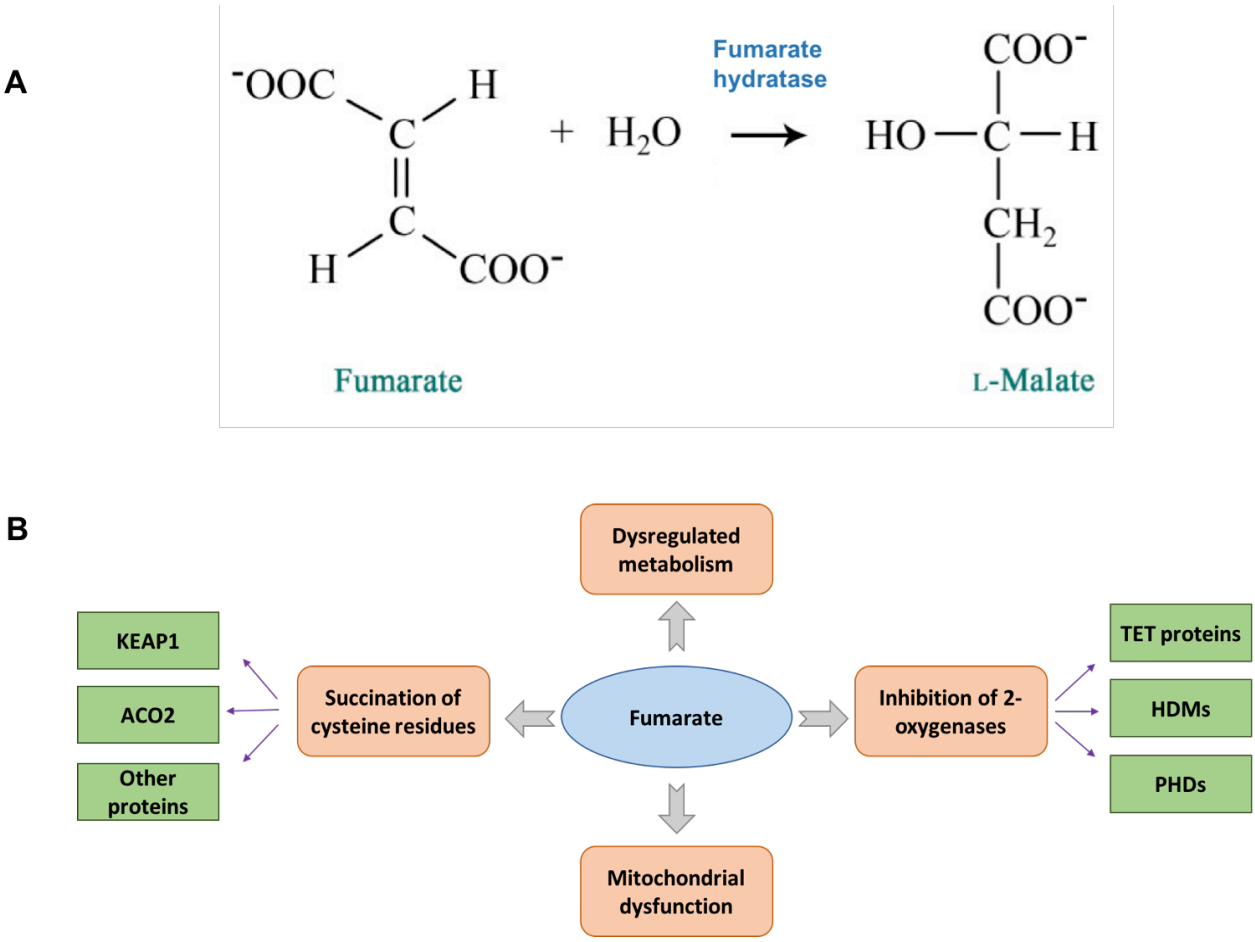

Figure 1-7. The catalytic reaction of fumarate hydratase and the cellular consequences of elevated fumarate. (A) Fumarate hydratase catalyses the hydration of the four carbon fumarate to the four carbon malate. (B) Loss of fumarate hydratase activity results in intracellular accumulation of fumarate. Dysregulated metabolism is linked with fumarate hydratase deletion due to a biochemical truncation of the TCA cycle. Fumarate has been shown to act as a competitive inhibitor of a-KG-dependent dioxygenases, including histone demethylases (HDMs), TET proteins and the negative regulator of HIF hydroxylases, propyl-hydroxylases. Succination of cysteine residues that could lead to the loss of protein functions has been associated with the elevation of intracellular fumarate. The proteins identified so far include Kelch-like ECH-associated protein 1(KEAP1) and aconitase 2 (ACO2) (Adapted from Yang et al., 2012).

1.11.2 Fumarate causes protein succination

Fumarate is a natural nucleophile that can covalently (and irreversibly) bind to cysteine residues of proteins under physiological conditions, by a process termed succination (2SC; Figure 1-8) (Alderson et al., 2006). Interestingly, succination is a feature of *FH*-deficient cells, where fumarate accumulates to very high levels (Bardella et al., 2011). The Kelch-like ECH-associated protein 1 (KEAP1), an E3 ubiquitin ligase and an inhibitor of the transcription factor nuclear erythroid-related factor 2 (NRF2), was recently identified as a target of protein succination in *FH*-deficient cells (Adam et al., 2011). Its consequent inhibition led to the activation of NRF2 and a subsequent strong antioxidant response (Adam et al., 2011; Ooi et al., 2011). Although KEAP1 succination could provide an explanation for the antioxidant phenotype observed in *FH*-deficient cells, other oxidation-related mechanisms could contribute to this response. In particular, the loss of *FH* has been previously associated with an increase in ROS (Sudarshan et al., 2009), where accumulation of fumarate leads to the formation of a covalent adduct between fumarate and glutathione (GSH), leading to oxidative stress (Sullivan et al., 2013). In contrast however, in a recent study Zheng et al proposed that the oxidative stress observed in *FH*-deficient cells is a result of an alternate mechanism (Zheng et al., 2015). Specifically, the authors proposed that succination of GSH increases the demands of NADPH in order to sustain GSH biosynthesis. This reaction in turn negatively affects redox homeostasis and as a compensatory mechanism, *FH*-deficient cells enhance cysteine uptake and GSH biosynthesis, causing chronic oxidative stress (Zheng et al., 2015). The precise mechanisms by which oxidative stress is caused in *FH*- deficient cells and how it contributes to tumorigenesis, is not fully understood but recent evidence suggests that oxidative stress indirectly activates the oncogene abelson murine leukaemia 1 (ABL1), which in turns promotes nuclear translocation of NRF2, potentially contributing to malignancy (Sourbier et al., 2014) (described in more detail in section 1.9.3- Metabolic disruption as a result of FH deletion).

In an effort to identify more succinated proteins, Ternette et al searched for other 2SC targets that could contribute to pathogenesis of *FH*-associated disease (Ternette

et al., 2013). Hence, they conducted a large proteomic screen for 2SC in *Fh1*-deficient mouse embryonic fibroblasts (MEFs) and in mouse kidney tissue, where *Fh1* had been deleted from the kidney tubules. The authors identified 94 succinated proteins, including some that were succinated on functional cysteine residues (Ternette et al., 2013). In particular, they investigated the succination of three key cysteine residues in the TCA cycle enzyme, mitochondrial aconitase hydratase (ACO2). The consequences of ACO2 inhibition are described in detail in section 1.11.3- Metabolic disruption as a result of FH deletion.

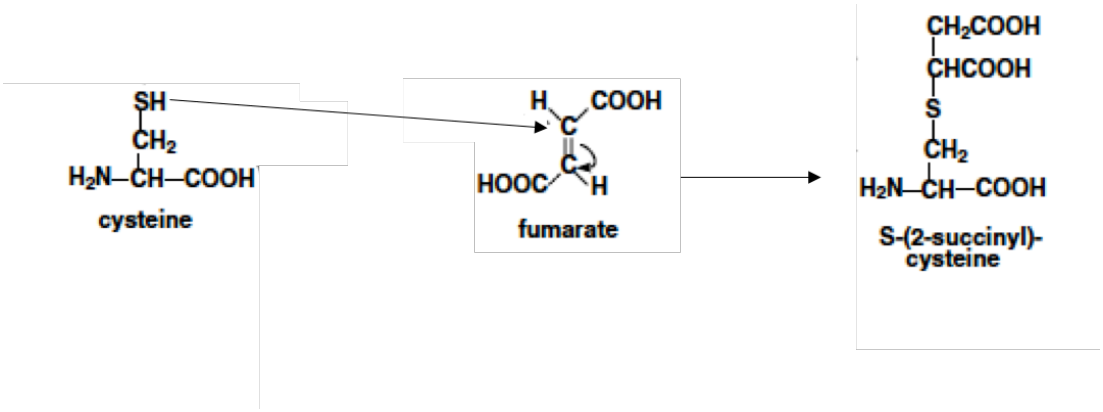

Figure 1-8. Succination reaction. Fumarate is a natural electrophile and as a result spontaneously reacts by a Michael addition reaction with free sulfhydryl groups to generate a thioether linkage with cysteine residues of proteins. This results in the formation of S-(2-succino) cysteine (2SC), a process termed succination (Adapted from Alderson et al., 2006).

1.11.3 Metabolic disruption as a result of FH deletion

The TCA cycle dysfunction caused by the loss of FH, poses significant challenges to cells in meeting their energetic demands, in the generation of macromolecular precursors and in their survival. Metabolic characterisation of *Fh1*-deficient cells using isotope labelling, has provided great insight about how these cells can function with a truncated TCA cycle. Because the TCA cycle is a major source for mitochondrial NADH, the truncation of the TCA cycle may have severe bioenergetic outcomes. Indeed, in *Fh1*- deficient cells, NADH levels were lower compared to control cells (Frezza et al., 2011). Furthermore, *Fh1*- deficient cells exhibit impaired respiration as indicated by a decrease in oxygen consumption (Frezza et al., 2011). However, despite the biochemical block of the TCA cycle, *Fh1*-deficient kidney cells and MEFs are still able to generate sufficient NADH for survival.

The decrease in respiration in *Fh1*- deficient cells has been associated with upregulation of glycolysis as indicated by an increase in lactate production, as well as increased uptake of glucose (Sudarshan et al., 2009; O'Flaherty et al., 2010; Tong et al, 2011; Sourbier et al., 2014). Much effort has been put forward to better understand the glycolytic phenotype of *Fh1*-deficient cells, and how it confers a growth advantage to HLRCC tumours. Metabolic analysis of the human cell line UOK262 and HLRCC tumours has provided valuable information. Tong et al., showed that UOK262 and HLRCC tumours exhibit an increase in glycolysis and low AMPK levels, which in turn reduces p53 levels. Low AMPK activity in turn decreases the expression of the iron transporters, resulting in a lower iron uptake. Finally, the reduced cytosolic iron levels and fumarate accumulation are expected to inhibit PHD activity and therefore stabilize Hif-1a expression, leading to a glycolytic phenotype (Tong et al., 2011). As a result, the glycolytic shift coupled with low AMPK levels could offer a proliferative advantage in HLRCC cells. The same group furthered their findings regarding how glycolysis contributes to the aggressive phenotype of HLRCC tumours (Sourbier et al., 2014). The authors begun by performing an unbiased drug screen to identify drugs that would selectively kill HLRCC cells. Through their screen, they identified vandetanib, which was highly cytotoxic to UOK262 kidney cancer cells. When they looked into the mechanism by

which vandetanib killed UOK262 cells, they identified a reduction in the expression of the oncogene ABL1 known to promote glycolysis, by regulating the mTOR pathway. Furthermore, *Fh1*-deficient (and human UOK262 cells) exhibit increased levels of ABL1 expression, and have been previously shown to exhibit increased levels of mTOR concomitantly with increased glycolysis (Tong et al., 2011). The authors therefore concluded that vandetanib acts against *FH*-deficient cells by decreasing the glycolytic pathway (through the reduced expression of the mTOR regulator ABL1), necessary for survival. Finally, by using a xenograft UOK262 mouse model, the authors showed that treatment with vandetanib reduced tumour burden *in vivo*, by decreasing the expression of ABL1-mediated glycolysis. Overall, this study showed that ABL1 is a key modulator in response to fumarate accumulation, partially providing a mechanistic explanation of *FH*-mediated tumorigenesis.

Further insight into the metabolic reprogramming of *Fh1*-deficient cells has been provided by Frezza et al. Through isotope labelling, it has been suggested that *Fh1*-deficient renal cells exhibit increased glutaminolysis (Frezza et al., 2011). More importantly, through an *in silico* model, Frezza et al predicted that the haem-metabolism pathway is critical for the survival of *Fh1*-deficient cells (Frezza et al., 2011). The model predicted genes for which elimination together with *Fh1* would affect the growth ability of *Fh1*-deficient cells. Haem biosynthesis is a cataplerotic pathway that uses TCA-derived carbon to generate haem, whereas the haem degradation pathway generates bilirubin that can be excreted from the cells. Therefore, haem biosynthesis and degradation generates a linear pathway starting with glutamine uptake and ending with bilirubin excretion, allowing some generation of mitochondrial NADH in order to support minimal mitochondrial respiration. Indeed, the activation of the haem pathway was validated in *Fh1*-deficient cells by identifying an increase of bilirubin excretion using mass-spectrometry (Frezza et al., 2011). In support of these findings, knock-down of a key enzyme involved in the haem pathway, haem oxygenase-1 (*Hmox-1*), resulted in the death of *Fh1*-deficient cells (Frezza et al., 2011).

Recently, as described in the previous section, Ternette et al identified that mitochondrial ACO2 function is abolished in *Fh1*-deficient murine MEFs and kidney cells (Ternette et al., 2013). Mitochondrial ACO2 functions as part of the TCA cycle, catalyzing the conversion of citrate to isocitrate. In their system, Ternette et al observed a decrease in the levels of citrate and isocitrate, supporting the observation that ACO2 function was decreased as a result of its cysteine residue succination. Furthermore, when the authors cultured the cells in deuterium-labelled glutamine, which labels hydrogens and thus allowed them to determine whether the oxidative (i.e. reversed) flux of the TCA cycle functions properly, they observed labelling incorporation in fumarate, malate and isocitrate but not in citrate. Some cancer cells display altered metabolism by utilizing glutamine-dependent reductive carboxylation to produce citrate, which can be used for fatty acid generation and for anaplerosis of the TCA cycle (Metallo et al., 2012, Mullen et al., 2012, Wise et al., 2011). This pathway utilizes IDH1/2 to reductively carboxylate α-KG to isocitrate and is considered to occur both in the mitochondria and the cytoplasm (Mullen et al., 2012).

The results obtained by Ternette et al suggested that α-KG can be converted to isocitrate by reversal of the IDH-catalyzed reaction, but that isocitrate cannot be further metabolized to citrate, due to impaired activity of ACO2. As a result, *Fh1*-deficient MEFs may not be able to utilize reductive carboxylation. Finally, the absence of citrate labelling suggests that both mitochondrial and cytoplasmic isoforms of ACO2 are potentially inactive.

Further insight has been provided regarding the metabolic changes that *Fh1* deletion cause in kidney cells. A recent study found that *Fh1*-deficient kidney cells and tissues exhibit dysregulation in the urea cycle and arginine metabolism and accumulate high levels of argininosuccinate via the reversal of the activity of argininosuccinate lyase. (Adam et al., 2013; Zheng et al., 2013). Furthermore, *Fh1*-deficient cells exhibit increased sensitivity to arginine deprivation, indicating that arginine is an important energy source for these cells (Adam et al., 2013). The overall metabolic alterations as a result of *Fh1* deficiency, are outlined in Figure 1-9.

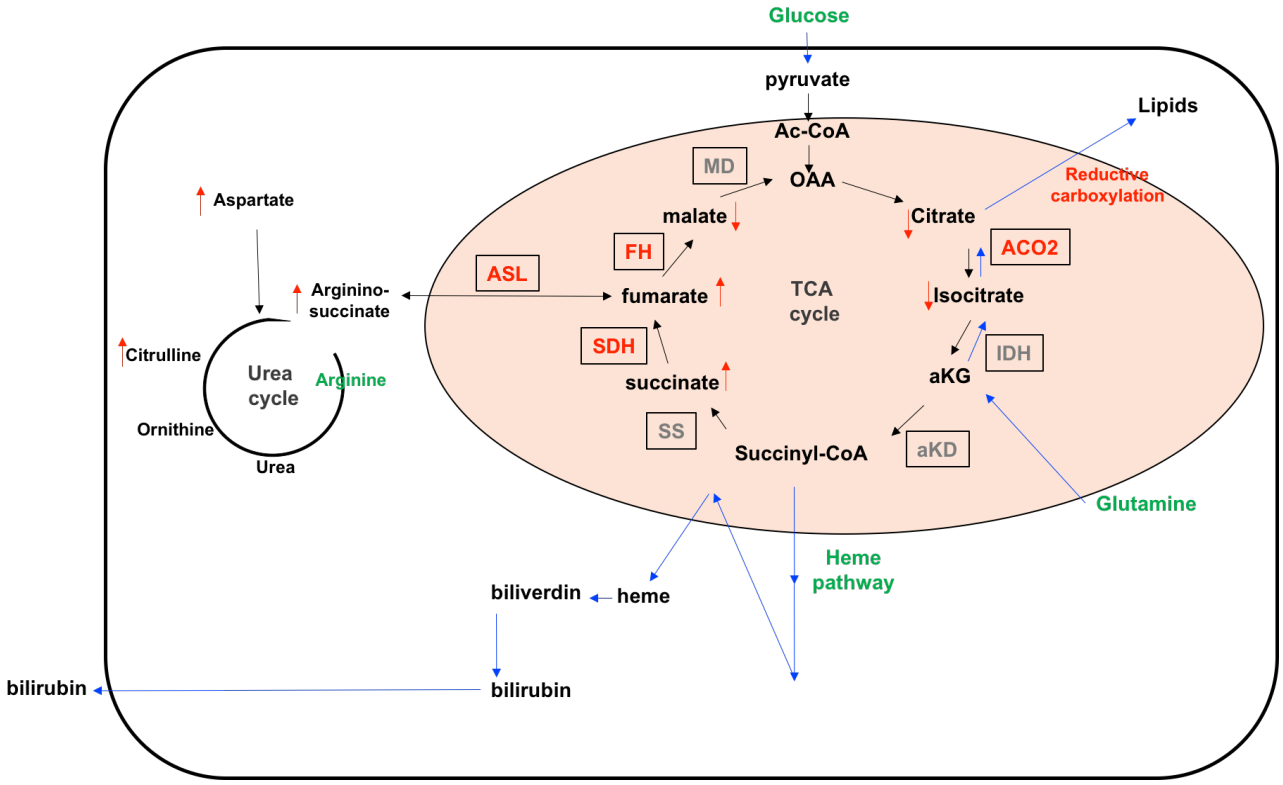

Figure 1-9. The metabolic changes occurring in *Fh1*- deficient cells. Enzymes are shown within boxes. The enzymes highlighted in red are inhibited in *Fh1*-deficient cells. The pathways which *Fh1*- deficient cells critically rely on or are upregulated are highlighted in green, whereas the pathways that are inhibited are highlighted in red. The red arrows next to metabolites indicate either increased levels (arrow pointing upwards), or decreased levels (arrow pointing downwards). Glycolysis, glutaminolysis and the haem pathway are upregulated in *Fh1*-deficient cells, whereas reductive carboxylation is inhibited as a result of aconitase 2 (ACO2) succination. Citrate and isocitrate levels are reduced as a result of decreased ACO2 function. Succinate and fumarate levels are increased, while malate levels are decreased as a result of the inactivation of fumarate hydratase (FH). Succinate dehydrogenase activity (SDH) is decreased possibly due to fumarate accumulation. The haem pathway is upregulated, generating enough NADH for minimal mitochondrial respiration. Arginino-succinate (and indirectly aspartate and citrulline) levels are increased due to reversal of the enzyme argininosuccinate lyase (ASL). *Fh1*-deficient cells are critically reliant on arginine.

1.11.4 Fumarate as an epigenetic modifier

Recent studies have identified another potential mechanism of how *FH* (and *Fh1*) deletion and subsequent fumarate accumulation could contribute to tumorigenesis. Excess fumarate is known to inhibit a-KG-dependent enzymes, a large family of enzymes with diverse functions. Apart from PHDs, fumarate has been shown to inhibit epigenetic modifiers such as TET proteins (Xiao et al., 2012). TET proteins are DNA hydroxylases that play a central role in epigenetic control, as TET proteins (specifically TET1 and TET2) are responsible for the oxidation of 5mC to 5-hydroxymethylcytosine (5hmC) (Tahiliani et al., 2009), whereas TET3 is mainly involved in the oxidation of 5mC to 5hmC in zygotic parental DNA after fertilization (Gu et al., 2011). The inhibition of TET proteins by the accumulation of fumarate has been supported by recent studies (Xiao et al., 2012; Hoekstra et al., 2015; Laukka et al., 2016;). In human smooth-muscle tumours, inhibition of TET proteins, as a result of fumarate accumulation, lead to a decrease of overall 5hmC and in an increase of the repressive histone trimethylation H3K9me3 signatures, leading to epigenetic remodelling (Hoekstra et al., 2015). Similar observations were made using the human neuroblastoma cell line SK-N-BE cell line, and by knocking down FH in the human cell lines HEK293T and Hela cells, where global 5-hmC levels were reduced as a result of TET inhibition (Laukka et al., 2016).

More recently, Sciacovelli et al., performed an unbiased proteomics analysis on *Fh1*-deficient kidney cells and the kidney cancer cell line UOK262 in order to identify oncogenic features associated with the loss of *Fh1* (and *FH*) (Sciacovelli et al., 2016). Gene expression profiling followed by gene enrichment analysis, confirmed an epithelial-to-mesenchymal transition (EMT) signature, where genes associated with EMT, such as *vim* (gene encoding for the EMT marker vimentin), snail family zinc finger 2 (*Snai2)*, and the zinc-finger E-box binding homeobox proteins *Zeb1* and *Zeb2*, were upregulated. The expression of these EMT-associated genes is suppressed by the antimetastatic micro RNA, mir-200 (De Craene and Berx, 2013), which was downregulated in *Fh1*-deficient cells and UOK262 cells. Interestingly, the authors found that the downregulation of mir-200 was a result of the Tet-mediated demethylation of its regulatory region, as a result of fumarate accumulation. Finally,

by re-expressing *Fh1* in *Fh1*-deficient cells, mir-200 expression was rescued and the EMT phenotype was reversed, highlighting a novel means by which fumarate could contribute to the metastatic phenotype of HLRCC tumours (Sciacovelli et al., 2016).

1.11.5 Fumarate hydratase in normal haematopoiesis

Genetic evidence indicates that rare recessive mutations in the *FH* gene result in severe developmental abnormalities, including haematopoietic defects (Bourgeron et al., 1994; Tregoning et al., 2013). Consistent with a previous report (Bourgeron et al., 1994), monozygous twins with recessive *FH* mutations, display leukopenia and neutropenia, therefore suggesting a role for FH in the regulation of haematopoiesis (Tregoning et al., 2013).

Previous work in our lab has demonstrated that *Fh1* is critical for the haematopoietic system (Guitart, unpublished). Deletion of *Fh1* specifically in the haematopoietic system using the *Vav Cre* deleter strain results in embryonic lethality. $Fh1^{fl/fl}$*; Vav-iCre* embryos at embryonic day 14.5 are pale, exhibit reduced foetal liver cellularity and are unable to generate colonies *in vitro* when plated in semi-solid media (Figure 1-10 A, B, D). Furthermore, analysis of the haematopoietic system showed that *Fh1*-null embryos exhibit significant reduction in the lineage positive compartment (indicating a reduction in the differentiated cells), and a significant expansion in LT-HSC numbers (Figure 1-10 B, C). Furthermore, *Fh1* loss results in the complete inability of foetal liver HSCs to reconstitute the haematopoietic system, in lethally irradiated recipient mice (Figure 1-10 E). Apart from foetal haematopoiesis, *Fh1* is also essential for adult haematopoiesis. Lethally irradiated mice were injected with $Fh1^{fl/fl}$; *Mx1-Cre* donor cells, and after efficient reconstitution was achieved, poly:I:poly:C administration of the recipient mice resulted to a progressive decline of donor-derived cell chimerism, and a complete failure of *Fh1*-deficient cells to contribute to primitive and mature haematopoietic compartments of the recipients (Figure 1-10 F).

Finally, mass-spectrometry analysis showed that fumarate and argininosuccinate are significantly elevated in *Fh1*$^{fl/fl}$*; Vav-iCre* stem and progenitor cells (Figure 1-11 A, B).

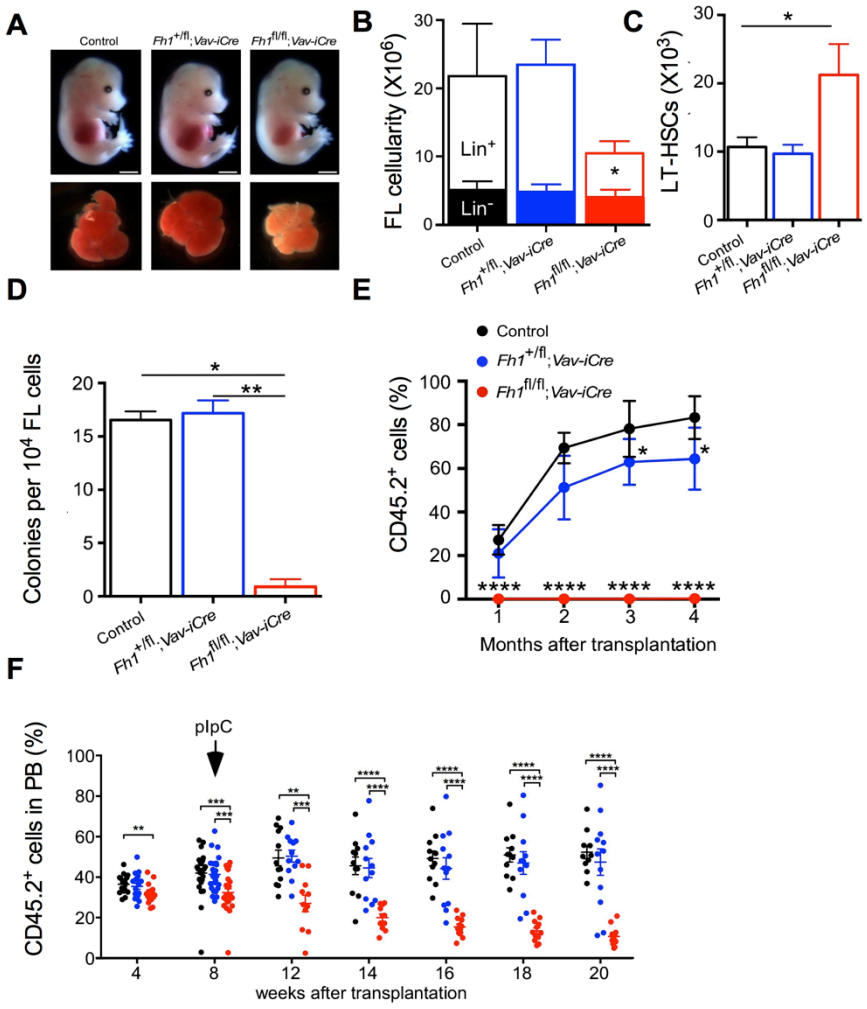

Figure 1-10. *Fh1* is essential in foetal and adult haematopoiesis. (A) FLs from 14.5dpc *Fh1*$^{fl/fl}$*; Vav-iCre* embryos are smaller and paler compared to *Fh1*$^{+/fl}$*;Vav-iCre* and *control* embryos (magnification: ×3 for upper panels, x6 for bottom panels). **(B)** Total cellularity (the sum of Lin+ and Lin−cell numbers) of nucleated cells in 14.5dpc FLs from embryos of the indicated genotypes. (C) Total numbers of LT-HSC (LSK CD48^{-}CD150^{+}) cells in FLs of day 14.5 old embryos (*control* n = 17, to *Fh1*$^{+/fl}$*; Vav-iCre* n = 11 and *Fh1*$^{fl/fl}$*; Vav-iCre* n = 9). (D) Colony forming cell (CFC) assay using 10^4 total FL cells. (*control* n = 11, *Fh1*$^{+/fl}$*; Vav-iCre* n = 8 and *Fh1*$^{fl/fl}$*; Vav-iCre* n = 4). (E) Percentage of CD45.2^{+} cells in PB after transplantation of 100 FL HSCs (n = 5-8 recipients per genotype, at least 3 biological replicates were used per genotype). (F) Percentage of donor derived CD45.2+ cells in PB (n = 5-10 recipient mice per biological replicate (n = 2)). Data are mean ± S.E.M., *p<0.05, **p<0.005, ***p<0.001, Mann-Whitney test.

Mechanistically, the phenotypes observed upon *Fh1* deletion could result from the genetic block in the TCA cycle, or the accumulation of cellular fumarate. To differentiate between those two mechanisms, we generated mice that ubiquitously express the human cytosolic isoform of FH (FH^{Cyt}, which lacks the mitochondrial targeting sequence and therefore is excluded from the mitochondria). Expression of FH^{Cyt} rescued embryonic lethality and reduced the levels of fumarate and argininosuccinate (Figure 1-11 A, B). Furthermore, the resulting *$Fh1^{fl/fl}$; FHCyt; Vav-iCre* mice exhibited normal bone marrow cellularity (Figure 1-11 C), normal numbers of myeloid cells (Figure 1-11 D), and depleted B cells (Figure 1-11 E). Finally, *$Fh1^{fl/fl}$; FHCyt; Vav-iCre* mice exhibited an increase in the LSK and LT-HSC compartments (Figure 1-11 F, G).

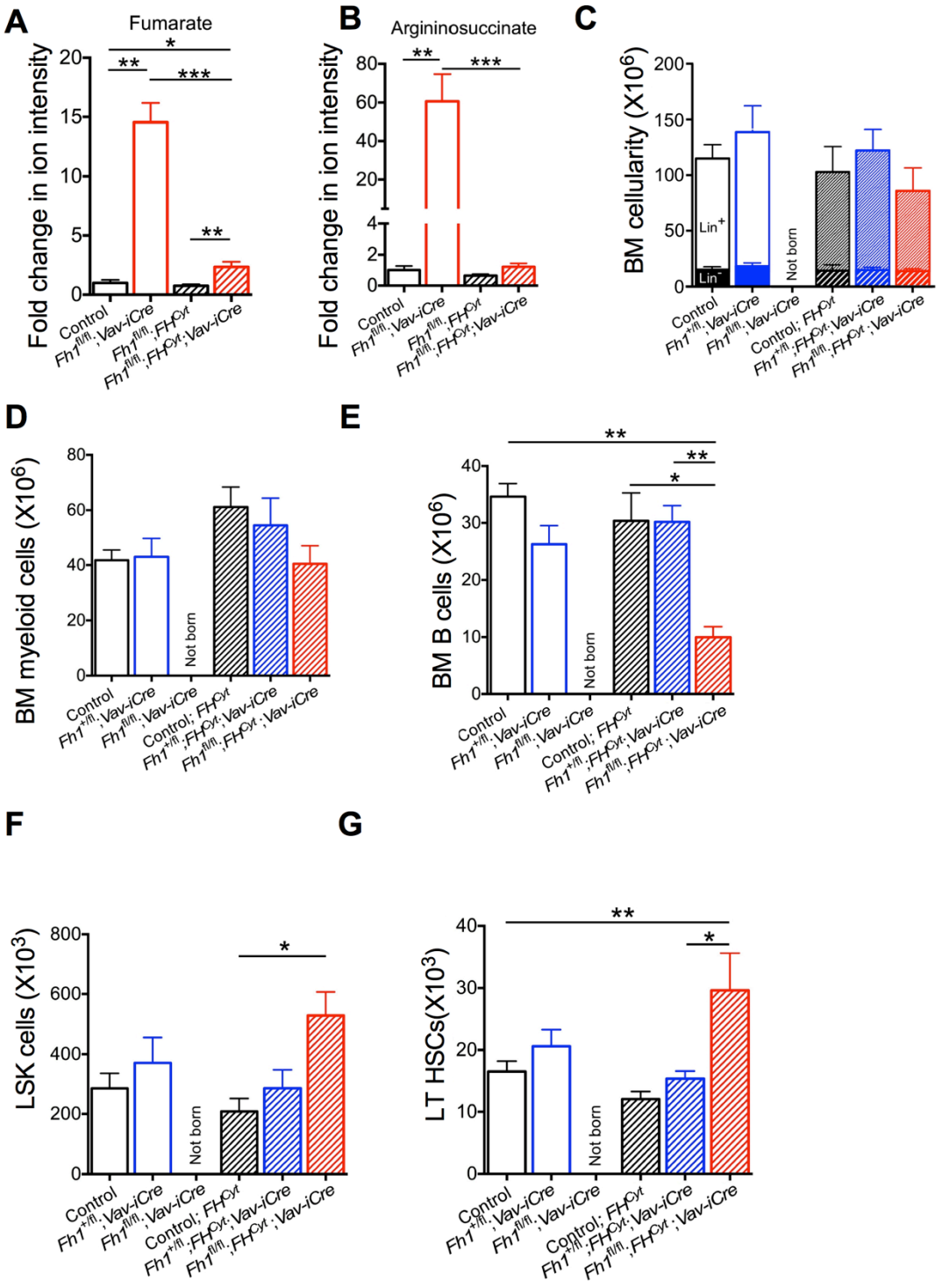

Figure 1-11.Cytosolic isoform of Fh1 rescues normal steady-state haematopoiesis in *Fh1$^{fl/fl}$;Vav-iCre* mice. (A) Fumarate levels in FL c-Kit+ cells of indicated genotypes measured by liquid chromatography–mass spectrometry (LC-MS). (*control* n = 6, *Fh1$^{fl/fl}$; Vav-iCre* n = 4, *control; FH^{Cyt}* n = 6 and *Fh1$^{fl/fl}$; FHCyt;*

Vav-iCre n = 13). (B) Argininosuccinate levels in FL c-Kit^{+} cells measured using LCMS. (*control* n = 6, *Fh1$^{fl/fl}$; Vav-iCre* n = 4, *control; FH^{Cyt}* n = 6 and *Fh1$^{fl/fl}$;FH^{Cyt}; Vav-iCre* n = 13). (C) Total number of BM nucleated cells obtained from two tibias and two femurs of 8-10 week old mice. (D) Total numbers of Mac-1^{+} Gr1^{+} myeloid cells. (E) Total CD19^{+} B220^{+} cells. (F) LSK cells (G) LT-HSC cells. Data are mean ± S.E.M. n = 3-4 per genotype. *p<0.05, **p<0.005, ***p<0.001, Mann-Whitney test.

The data generated from our lab in conjunction with previous reports (Bourgeron et al., 1994; Tregoning et al., 2013), strongly indicate that fumarate hydratase plays a critical role in regulating haematopoiesis, and could also play a role in leukaemic transformation. With that in mind, the aim of this project was to identify the roles of *Fh1* in the generation and development of AML, as well as identify the role of the mitochondrial isoform of *Fh1* in normal haematopoiesis.

1.12 Defining the nomenclature utilised in this thesis

Throughout this thesis, I will be referring to "genetically intact TCA cycle", denoting that the TCA cycle has not been genetically manipulated and therefore it operates normally. Furthermore, the term "genetically truncated TCA" or "genetic truncation of the TCA cycle" is used to describe the fact that genetic deletion of mitochondrial *Fh1* generates a genetic truncation in the TCA cycle. The reason I specifically refer to a "genetic" truncation on the TCA cycle, is because I haven't performed any metabolite analyses in order to identify the biochemical consequences that mitochondrial *Fh1* deletion has (for example a build-up or reduction in the levels of TCA metabolites that would have biochemical consequences). However, this has been previously conducted for non-transformed stem and progenitor cells (Guitart, unpublished) (see Figure 1-11).

Finally, throughout my thesis, I have chosen to refer to "leukaemia-initiating cells (LICs)", rather than "leukaemic stem cells (LSCs)". The term LSC was originally coined to describe a very rare population of leukaemic cells, that shared a lot of similarities with HSCs, as described by seminal work conducted John Dick's group (Lapidot et al., 1994). There are two prevailing models of leukaemogenesis. In the first "hierarchical" model, similarly to HSCs, LSCs are thought to reside at the top of the leukaemic hierarchy and produce more differentiated, heterogenic leukaemic blasts, that feature a high proliferative potential, a block in terminal differentiation and defective apoptosis, leading to the accumulation of blasts and clinical disease (Reya et al., 2001; Huntly and Gilliland 2005; Riether et al., 2015). The second

"stochastic" model proposes that every leukaemic cell has the ability to self-renew and recapitulate disease phenotype, given that it enters a permissive environment, an event which has very low probability (Huntly and Gilliland, 2005; Reya et al., 2001).

Furthermore, it has been convincingly demonstrated that LSCs can arise from more differentiated progenitor cells such as CMPs and GMPs (Cozzio et al., 2003; Huntly et al., 2004; Somerville and Cleary; 2006; Kristov et al., 2006; 2013). There is a possibility that both models of leukaemogenesis occur, depending on the cell-of-origin and the type of leukaemia (e.g. CML versus AML). I therefore believe that the term "LSC" might be a bit misleading as not all leukaemia-initiating cells possess the characteristics of a true stem cell.

CHAPTER 2
Materials and Methods

2 Materials and methods

2.1 Mouse strains

All mice were on the C57BL/6 genetic background. *Vav1-iCre* and *Mx1-Cre* mice were purchased from Jackson Laboratory. *Vav1-iCre* mice were originally developed by De Boer et al., 2003. According to Jackson Laboratory, *Vav1-iCre* is also known as *Vav-iCre*. As a result, for simplicity reasons throughout this thesis I will be referring to *Vav1-iCre* as *Vav-iCre*. $Fh1^{fl/fl}$; *Vav-iCre* mice were generated by crossing $Fh1^{fl/fl}$ mice to $Fh1^{+/+}$; *Vav-iCre*, and then breeding littermates that were $Fh1^{+/fl}$; *Vav-iCre*. $Fh1^{fl/fl}$; *Mx1-Cre* mice were generated in the same manner. Non-conditional $Fh1^{fl/fl}$; FH^{Cyt}; *Vav-iCre* mice were generated by crossing FH^{Cyt}; *Rosa26* mice that were generated by Adam et al., 2013, with $Fh1^{+/+}$; *Vav-iCre* mice. All transgenic and knockout mice were $CD45.2^{+}$. Congenic recipient mice were female $CD45.1^{+}/CD45.2^{+}$. All experiments on animals were performed under UK Home Office authorization. Irradiation protocol: Recipient mice received one dose of irradiation (7 gy) using a 33% attenuator.

2.2 DNA extraction

Genomic DNA from animal tissue (mouse ear notch, BM, blood) or cultured cells was extracted using ISOLATE II Genomic DNA Kit (BIO-52067, Bioline), according to the manufacturer's instructions. A pre-lysing step was used for animal tissue samples where lysis buffer and proteinase K was added and the sample incubated at 56 ^{o}C overnight (ON). Lysis buffer and an incubation step of 10 - 15 minutes at 70 ^{o}C were used to lyse cultured cells. After the lysis, ethanol (96 - 100 %) was added and the samples were vortexed. DNA was bound to the silica membrane of the spin column (centrifuged for 1 minute at 11,000 x g) and washed twice (GW1, GW2 buffers). The silica membrane was dried by centrifugation (1 minute at 11, 000 x g) and DNA was eluted using preheated (70 ^{o}C) PCR water (DNAse/RNAse free) (1 minute at 11,000 x g). Concentration of eluted DNA was measured by nanodrop spectrometer (Nanodrop ND1000 Spectrophotometer; Lab tech International Ltd, East Sussex, UK) by recording absorbance at wavelength 260

nm. The DNA purity was assessed through the ratio of absorbance at 260 nm and 280 nm. DNA with A260/A280 ratio of 1.7 - 1.9 was considered as pure.

2.3 Maxiprep of plasmids

Maxiprep of all plasmids was conducted using the HiSpeed plasmid kit (Qiagen), according to the manufacturer instructions. Briefly, a starter culture was left overnight at 37 ^{o}C in 500 ml of LB media. The bacteria were harvested by centrifugation at 6,000 x g for 15 minutes at 4 ^{o}C. Bacterial pellet was then re-suspended in 10 ml of buffer P1 (lysis step), followed by addition of buffer P2 and incubated at room temperature for 5 minutes. 10 ml of pre-chilled P3 buffer were added and then lysate was transferred into the QIAfilter Cartridge and incubated at room temperature for 10 minutes. The lysate was then poured into the HiSpeed Maxi tip and entered the resin by gravity flow. The Maxi tip was then washed with 60 ml of buffer QC and DNA was eluted with 15 ml of buffer QF. DNA was precipitated by adding 10.5 ml isopropanol. DNA was isolated by running the precipitated DNA through a QIAprecipitator Maxi module in a final volume of 0.5 ml. Concentration of eluted DNA was measured by nanodrop spectrometer (Nanodrop ND1000 Spectrophotometer; Labtech International Ltd, East Sussex, UK) by recording absorbance at wavelength 260 nm. The DNA purity was assessed through the ratio of absorbance at 260 nm and 280 nm. DNA with A260/A280 ratio of 1.7 - 1.9 was considered as pure.

2.4 Genotyping and PCR primers

The PCR for *Vav-iCre*, *Mx-Cre*, and *Fh1* was prepared using MangoMix™ (BIO - 25033), a 2x Reaction Mix containing MangoTaq™ DNA Polymerase, MgCl2 and ultra-pure dNTPs. Water and primers were added to the MangoMix™. For FH^{Cyt} the Hot Start kit from Qiagen was used (Qiagen-203443) according to the manufacturer's protocol. All primers were at a concentration of 100 μM. The PCR programs were as follows: 5 minutes at 95 ^{o}C (double strand DNA denaturation); 30 - 39 cycles of 95 ^{o}C for 30 seconds - 1 minute, 57 - 67 ^{o}C for 40 seconds - 60 seconds (primer annealing, temperature dependant on the primers) and 72 ^{o}C for 30 seconds - 60 seconds (initial extension); 72 ^{o}C for 5 minutes (final extension) and tubes were held at 10 ^{o}C. The sequence of the primers, the exact PCR program and

the expected band size of each PCR reaction is demonstrated below (Table 3). The reactions were carried in the PCR cycler Biometra.

Table 3- PCR programs and primer sets.

Vav-iCre		*MxCre*		*FH^{Cyt}*		*Fh1*	
95ºC	5 min	95ºC	5 min	95ºC	15 min	95ºC	5 min
94ºC	40 sec	95ºC	30 sec	95ºC	1 min	95ºC	30 sec
64C	40 sec	67ºC	45 sec	60ºC	1 min	57ºC	45 sec
72ºC	30 sec	72ºC	1 min	72ºC	1 min	72ºC	45 sec
x30		x39		x35		x35	
72ºC	5 min	72ºC	5 min	72ºC	5 min	72ºC	5 min
10ºC	continuous	10ºC	continuous	10ºC	continuous	10ºC	continuous
Primer sets							
Forward 5'-CCGAAGGGCCA AGTGAGAGG -3'		Forward 5'-CGTTTTCTGAGC ATACCTGGA-3'		Forward 5'-AACATGATCGTTGG ATGCACACAGG-3'		Forward 5'-GCTCAGTCACC CATCCAAAT-3'	
Reverse 5'GGAGGGCAGGC AGGTTTTGGTG-3'		Reverse 5'-ATTCTCCCACCG TCAGTACG-3'		Reverse 5'-GCCTCTGCTAACC ATGTTCATGCCTTCT-3'		Reverse 1 5'-ACCCTGCTAGG TGTCACCAC-3'	
						Reverse 2 5'-CCTGGCACTGCA GACTACAA-3'	
Expected product size							
400bp		400bp		510bp		Floxed: 500bp KO: 420bp WT: 260bp	

2.5 RNA extraction

RNA was extracted and purified using RNeasy micro Kit (Qiagen - 74004) according to the manufacturer's instructions. Briefly cells were harvested and 350 µl RLT buffer (Qiagen) was added to cell pellets, followed by 350 µl 70 % ethanol. The mixture was spun down in RNeasy MinElute spin columns (Qiagen) for 15 seconds at 8,000 x g 350 µl RWI buffer (Qiagen) was added and spun down for 15 seconds at 8,000 x g 80 µl of DNase I incubation mix (Qiagen) was added and left at room temperature for 15 minutes. 350 µl RWI buffer (Qiagen) was added and spun down for 15 seconds at 8,000 x g. 500 µl RPE buffer (Qiagen) was added and spun down for 15 seconds at 8,000 x g. Subsequently, 500 µl 80 % ethanol was added and spun down for 2 minutes at 8,000 x g to wash the spin column membrane. The spin column was centrifuged at full speed for 5 minutes to dry the membrane. Finally, 15 µl RNAse free water was added and spun down for 1 minute at 8,000 x g to elute RNA. RNA concentration was measure by NanoDrop 1000 Spectrophotometer.

2.6 RT-PCR

RT-PCR was performed in order to transcribe the RNA into cDNA using reverse transcriptase. The High-Capacity cDNA Reverse Transcription Kit was used for all RT-PCR reactions (Applied BiosystemsTM - 4368813). The mix consisted of 2.0 µL 10X RT buffer, 0.8 µL dNTP mix (100 mM), 2.0 µL 10X RT random primers, 1.0 µL reverse transcriptase, 0.5 µL RNase inhibitor, and 3.7µL distilled water (DNase and RNase free; gibco®, ThermoFisher Scientific - 10977-035). The samples were processed using TProfessional Basic Thermocycler, using the cDNA synthesis program that ran at 25 ^{o}C for 10 minutes, 37 ^{o}C for 120 minutes and 85 ^{o}C for 5 minutes.

2.7 qPCR

Equal concentrations of RNA were reverse transcribed as indicated in 2.4. mRNA levels were quantified for *Meis1* and *Hoxa9* of pre-LCs after the third serial re-plating. β-actin was used as a housekeeping gene (Table 4). Technical triplicates of each sample were analysed and reactions were performed in a 5 µL volume. Each

well was filled with 2.5 µL TaqMan® Universal PCR Master Mix (Applied BiosystemsTM, ThermoFisher Scientific, Cat. 4304437), 0.25 µL of the TaqMan ® probe/primer set for each gene (see Table 4 below), 1.25 µL distilled water, and 1 µL of the cDNA sample. The samples were analysed using LightCycler® 480 (Roche), using the following program: 50 °C for 2 minutes, 95 °C for 10 minutes, followed by 40 cycles of 95 °C for 15 seconds and 60 °C for 1 minute. Finally, 60 °C for 5 minutes and 40 °C for 5 minutes. All signals were quantified using the ΔΔCt method using β -actin as the housekeeping gene.

Table 4- TaqMan probes for *Meis1/Hoxa9* expression.

Gene	TaqMan probe
Beta-actin	Mm00607939_s1
Hoxa9	Mm00439364_m1
Meis1	Mm00487664_m1

2.8 Preparation of bone marrow, spleen and thymus cell suspensions

Tibias and femurs of both hind legs were taken from adult mice. These were crushed using a pestle and mortar until a homogeneous cell suspension was achieved. Cells were collected in PBS (2 % FBS) and filtered through a 70 µm nylon strainer (BD Falcon, 352340). Spleen and thymus were retrieved and disaggregated in PBS (2 % FBS). All cell counts were performed by an automatic cell counter (MEK 6500K, Nihon Kohden) and used in subsequent assays.

2.9 Imunophenotypic characterisation of blood cells

SLAM staining: $10x10^6$ BM cells were incubated in CD16/CD32 (Fc Block) antibody in 50 µl of cold phosphate-buffered saline supplemented with 2 % heat-inactivated foetal bovine serum (PBS (2 %FBS)) for 5 min on ice. 50 µL of 2X antibody mix containing a biotin conjugated lineage cocktail (CD3, CD5, CD4, CD8a, Gr-1, CD19, B220, Ter119) and Sca-1, c-Kit, CD48 and CD150 was added (Table 5). After 20 minutes of incubation at 4 ^oC (protected from light), cells were

washed in cold PBS (2 % FBS) and spun down at 500 x g for 5 minutes. The pellet was then re-suspended in 100 μL of Streptavidin - PerCP. After 15 minutes, the cells were washed and re-suspended in cold PBS (2 % FBS).

Progenitor staining: $6x10^6$ BM cells were incubated in 100 μL of an antibody mix containing a biotin conjugated lineage cocktail (CD3, CD5, CD4, CD8a, Gr-1, CD19, B220, Ter119 (Ter119 is absent in myeloid-erythroid progenitor staining)) and Sca-1, c-Kit, CD127, CD16/32, CD34, Flt3 (committed progenitors). After 20 minutes of incubation at 4 ^oC (protected from light), cells were washed in cold PBS (2 % FBS) and spun down at 500 x g for 5 minutes. The pellet was then re-suspended in 100 μL of Streptavidin - Pacific Blue. After 15 minutes, cells were washed and re-suspended in cold PBS (2 % FBS).

Lineage staining: $2x10^5$ of BM, spleen or thymus cells were incubated with antibody mix: myeloid (CD11b, Gr-1); B-lymphoid (CD19, B220), T-lymphoid (CD4, CD8) and incubated for 20 minutes at 4 ^oC (protected from light) (Table 5). Cells were then washed in cold PBS (2 % FBS) and spun down at 500 x g for 5 minutes.

For all experiments, cells were acquired on FACSFortessaV (BD). Data were acquired through BD FACSDiva (BD Biosciences) and analysed by Flowjo software (Tree Star Inc., USA). The gating strategy for subsequent cell sorting and analysis was performed based on single stainings, as no isotype controls were used.

Table 5- List of antibodies used for flow cytometry.

	Antibody	Conjugate	Catalogue number	Clone	Manufacturer
Lineage Cocktail	CD4	biotin	553649	H129.19	BD Biosciences
	CD5	biotin	553019	53-7.3	BD Biosciences
	CD8a	biotin	553029	53-6.7	BD Biosciences
	CD11b	biotin	553309	M1/70	BD Biosciences
	CD45R/B220	biotin	553086	RA3-6B2	BD Biosciences
	Ter119	biotin	553672	TER-119	BD Biosciences
	Gr-1/Ly-6G/C	biotin	553125	RB6-8C5	BD Biosciences
HSPCs and committed progenitors	CD117/c-Kit	APC	105812	2B8	Biolegend
	CD117/c-Kit	BV510	135119	ACK2	Biolegend
	Sca-1/Ly-	APC-Cy7	122513	E13-161.7	Biolegend
	Sca-1/Ly-	PE-Cy7	122514	E13-161.7	Biolegend
	CD48	APC	103411	Hm48-1	Biolegend
	CD150	PE-Cy7	115914	TC15-	Biolegend
	CD16/32	APC-Cy7	101328	93	Biolegend
	CD127	BV605	112324	A7R34	Biolegend
	CD135/Flt3	PE	135306	A2F10	Biolegend
	CD34	FITC	553733	RAM34	BD Biosciences
B cells	CD19	APC-Cy7	115530	6D5	Biolegend
	CD45R / B220	PE	103236	RA3-6B2	Biolegend
Myeloid cells	CD11b	Pacific Blue	101224	M1/70	Biolegend
	CD11b	APC	101212	M1/70	Biolegend
	Gr-1/Ly-6G/C	PE-Cy7	108416	RB6-8C5	Biolegend
T cells	CD4	PE	130310	H129.19	Biolegend
	CD8a	PE	100708	53-6.7	Biolegend
	CD8a	APC	100712	53-6.7	Biolegend
	CD45.1	FITC	110706	A20	Biolegend
	CD45.2	Pacific Blue	109820	104	Biolegend
	Strepavidin	Pacific Blue	405225	-	Biolegend
	Strepavidin	PerCP	405213	-	Biolegend
	CD16/32 FC block	none	553142	2.4G2	BD Pharmagen

2.10 *Meis1/Hoxa9* driven AML: transplantation assays

Pre-LCs from CFC3 were harvested and counted. 100,000 c-Kit$^+$ pre-LCs (CD45.2$^+$) were injected into sub-lethally irradiated CD45.1$^+$/CD45.2$^+$ syngeneic recipient mice (7 Gy). The mice were monitored for AML development by blood sampling (via tail vein) every 2-4 weeks after transplantation. For secondary transplantation assays 10,000 LICs (CD45.2$^+$c-Kit$^+$ cells) were sorted from primary recipients and transplanted into secondary CD45.1$^+$/CD45.2$^+$ sub-lethally irradiated (7 Gy) recipient mice.

2.10.1.1 Monitoring AML development

AML development was assessed by tracking the chimerism of CD45.2$^+$ cells in the peripheral blood (Figure 2-1). Mice were bled every 2-4 weeks and white blood cells were stained for flow cytometry: CD45.2 (LICs), CD45.1/CD45.2 (remaining haematopoiesis), CD11b and Gr-1 (myeloid cells). Sick mice were harvested when showing signs of disease: high percentage of LICs in the blood, hunched posture, weight loss, difficulties in breathing and anaemia.

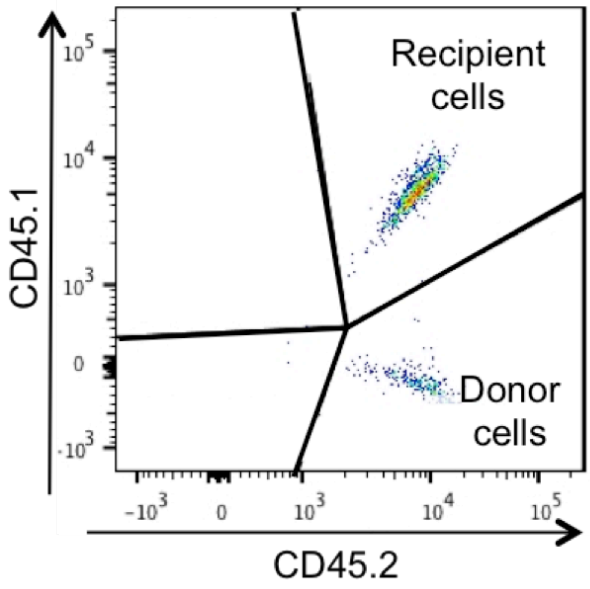

Figure 2-1. Syngeneic model that allows tracking of LIC cells in mice.

2.11 Blood sampling

To assess multilineage haematopoiesis reconstitution, peripheral blood samples were taken from the tail vein every 4 weeks. Blood was collected using capillary blood collection tubes coated with EDTA (Microvette® CB 300 K2E - 16.444, Sarstedt).

2.12 Inducible *Mx1-Cre*-mediated gene deletion

After the transplanted mice reached 20-30 % of LIC chimerism in the peripheral blood, the mice were administered with 6 - 8 doses of polyinosinic-polycytidylic acid (poly (I:C); GE Healthcare; 0.3 mg per dose) every other day. Mice injected with PBS were used as controls.

2.13 Isolation of haematopoietic stem and progenitor cells from foetal liver of E 14.5 dpc embryos

Embryos were aseptically removed and placed in PBS (2 % FBS). The foetal liver was extracted and placed in a 70 μm strainer in a 35 mm petri dish (Sterilin - 121V). Cells were extracted in 10 mL of PBS (2 % FBS) by gently pushing them through the strainer using a plunger. Red blood cells were lysed by a 1 minute incubation with NH_4Cl (Stem Cell Technologies - 07850). The reaction was stopped by adding PBS (2 %FCS). Cells were re-suspended in 100 μl PBS (2 % FBS) per $100x10^6$ cells and incubated with immunomagnetic microbeads, conjugated to monoclonal anti-mouse CD117 (c-Kit) antibodies (isotype: rat IgG2b) (Mylteni Biotec - 130-091-224) for 15 minutes at 4 °C. Cells were applied to a MACS LS column (Mylteni Biotec - 130-042-401) placed on a QuadroMACS (Miltenyi Biotec) separator, and washed four times with PBS (2 % FBS). PBS (2 % FBS) was added and the column was removed from the magnet, and the c-kit enriched fraction was flushed out.

2.13.1 Isolation of LSK cells via flow cytometry

In order to isolate LSK cells, HSPCs were incubated in Fc block and then stained with antibodies listed on Table 5. Briefly, following Fc block, HSPCs were stained with the biotinylated lineage markers anti-CD4, anti-CD5, anti-CD8a, anti-B220, anti-Gr1 and anti-Ter119 antibodies (but excluding CD11b as it marks embryonic HSCs) together with APC-conjugated anti-c-Kit, APC/Cy7-conjugated anti-Sca-1, PE-conjugated anti-CD48 and PE-Cy7-conjugated anti-CD150 antibodies. Biotin-

conjugated antibodies were then stained with Pacific Blue-conjugated streptavidin. Cell sorting was performed on a FACSAria Fusion (BD). 10,000 LSK cells were isolated from every foetal liver (Figure 2-2) and were retrovirally transduced using the Retronectin method (See section 2.14.4).

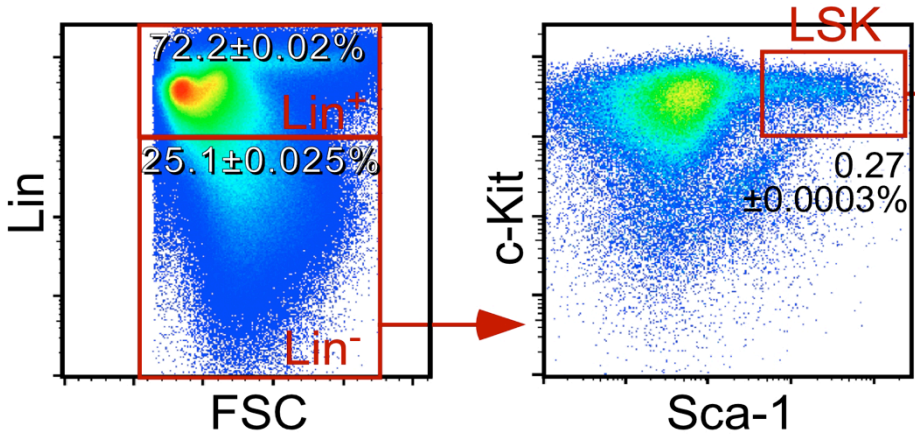

Figure 2-2. Representative FACS plots showing gating strategy for LSK isolation in foetal livers from 14.5 dpc embryos.

2.13.2 Cell lines and primary murine cells

For virus production, two packaging cell lines were used, one for retroviral production (platinum E) and one for lentiviral production (HEK 293T). An overall schematic of lentiviral production is shown in (Figure 2-3).

For retroviral production, no packaging plasmid was added, as Platinum E cells already stably express packaging proteins.

Platinum E - cell line generated based on 293T cell line that ensures high and stable expression of *gag, pol, env* (packaging viral structural proteins) through EF1α promoter. This cell line was used as retrovirus packaging cell line, and allows for retroviral packaging with a single plasmid transfection.

HEK 293 T- highly transfectable cell line from human embryonic kidney 293 cells that contains the SV40 T-antigen.

NIH3T3 – mouse embryo fibroblast cells, were used for retroviral titration. All cell lines used were cultured in Dulbecco's Modified Eagle's medium (DMEM) supplemented with 10 % FBS, 2.0 mM L-glutamine and 1 % penicillin/streptomycin (100 units/mL).

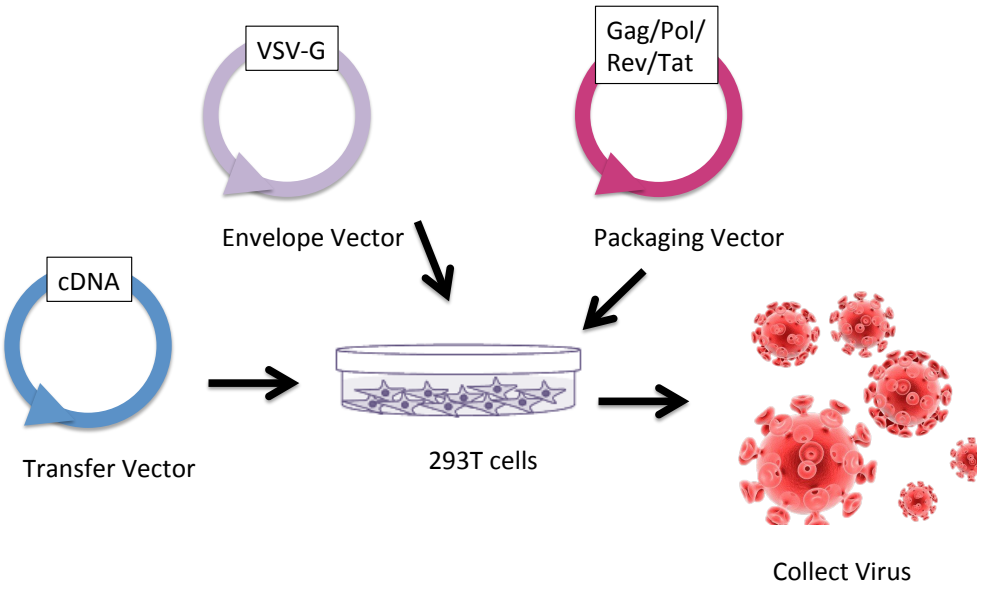

Figure 2-3. Lentiviral production schematic. Adapted from https://www.addgene.org/viral-vectors/lentivirus/lenti-guide/.

2.13.3 Retroviral constructs

Retrovirus production was conducted using Platinum E cells expressing the structural proteins of the virus *gag, pol, env* (Figure 2-4).

2.13.4 Transfer vectors and components

MSCV-Meis1-puro. cDNA encoding murine *Meis1* was cloned into the MSCV (murine stem cell virus) vector, MSCVPGK. PGK (phosphoglycerate kinase internal promoter) controls the expression of the puromycin resistance cassette and the long terminal repeat (LTR) region drives the expression of *Meis1* gene (Kroon et al., 1998a).

***MSCV-HoxA9-neo*.** cDNA encoding murine *HoxA9* fragment was inserted at BamHI-XhoI site of a pMSCVneoEB (neomycin (G418) resistance) (Kroon et al., 1998). The LTR region controls the expression of *HoxA9* gene and PGK promoter drives the expression of the neomycin resistance cassette.

***MSCV-MLL-ENL-neo*.** cDNA encoding for human *MLL-ENL* fusion transcript was inserted into a MSCV vector (ECORI site) under the transcriptional control of LTR. The MSCV/*MLL–ENL* encodes a neomycin resistance gene (Lavau et al., 1997).

MSCV-AML-ETO9a-neo cDNA encoding for human *AML/ETO9a* was cloned into MSCV-PGK-Neo vector (Xho and ECOR1 sites) (Zuber et al., 2009).

MSCV-MLL-AF9-neo. A retroviral construct encoding *MLL-AF9* was generated by fusion of the carboxy-terminal 91 amino acids of human AF9 (accession number BC036089) in-frame with the amino-terminal 1395 amino acids of human MLL in the retroviral vector MSCV-PGK-Neo (DiMartino et al., 2002).

PGK – the phosphoglycerate kinase (PGK) promoter drives the expression of antibiotic resistance genes thus enabling selection of infected cells on the basis of antibiotic resistance.

MSCV –the Murine Stem Cell Virus (MSCV) retroviral vector is optimized for introducing and expressing target genes in pluripotent cells, including murine haematopoietic cells.

LTR – the retroviral long terminal repeat (LTR) contains promoters that drive gene expression in many infected cell types, including multiple haematopoietic lineages.

Subcomponents of LTR: U3-R-U5- element. U3 and U5 are found at the end of the viral genomic RNA and contain sequences necessary for activation of viral genomic RNA transcription.

2.13.5 Packaging vectors and components

VSV-G- Vesicular stomatitis virus G glycoprotein is the envelope vector that determines the tropism of the virus (broad tropism envelope protein).

Gag- precursor structural protein of the retroviral/lentiviral particle containing matrix, capsid and nucleocapsid components.

Pol- precursor protein containing reverse transcriptase and integrase components.

Lentiviral constructs

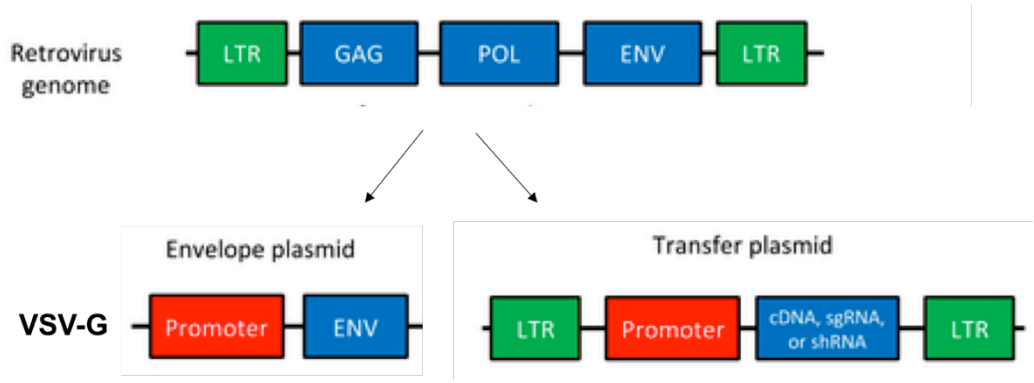

Figure 2-4. Components for retrovirus generation. The envelope plasmid (in this case VSV-G) determines the tropism of the virus. The transfer plasmid contains the gene of interest located in between LTR sites that will allow integration into the host genome, and the promoter that will allow for expression of the protein of interest. Taken from https://www.addgene.org/viral-vectors/lentivirus/lenti-guide/.

2.13.6 Packaging vectors and components

Lentivirus production was made using HEK 293T cells and the following constructs: **PsPax2**- expresses the HIV *gag*, *pol*, *rev* and *tat* genes that are necessary for the packaging of the lentivirus (Figure 2-5).

VSV-G- Vesicular stomatitis virus G glycoprotein is the envelope vector that determines the tropism of the virus (broad tropism envelope protein).

Gag- Gag is a precursor structural protein of the retroviral/lentiviral particle containing matrix, capsid and nucleocapsid components.

Pol- Pol is a precursor protein containing reverse transcriptase and integrase components.

Tat- Tat facilitates the activation of transcription from the LTR promoter.

Rev- Rev binds to the Rev response element in order to facilitate nuclear export.

2.13.7 Transfer vectors and components

pRRL vectors contain CMV-HIFV5' LTRs and vector backbones in which the SV40 polyadenylation and enhancerless origin of replication sequences have been included downstream of the HIV 3'LTR, replacing most of the human sequence remaining from the HIV integration site. These vectors are very efficient as transfer vectors (Dull et al., 1998).

p-RRL-iVenus- empty transfer vector with fluorescent selection marker iVenus. This vector was a kind gift from Sten Eirik Jacobsen.

p-RRL-Cre-iVenus- p-RRL-iVenus vector in which Cre is expressed under the CMV promoter. This vector was a kind gift from Sten Eirik Jacobsen.

LTR- long terminal repeats flank the insert of interest and facilitate host genome integration. The 5' LTR acts as an RNA pol II promoter. The 3' LTR terminates transcription that started by 5' LTR by the addition of a poly A tract.

RRE- Rev responsive element; sequence to which Rev binds.

IRES- The internal ribosome entry site; Bicistronic vectors constitutively express the protein of interest (Cre) and a reporter protein (iVenus). Expression is driven by the constitutively active bidirectional human cytomegalovirus promoter.

CMV- bidirectional human cytomegalovirus promoter.

Subcomponents of LTR: U3-R-U5- element. U3 and U5 are found at the end of the viral genomic RNA and contain sequences necessary for activation of viral genomic RNA transcription.

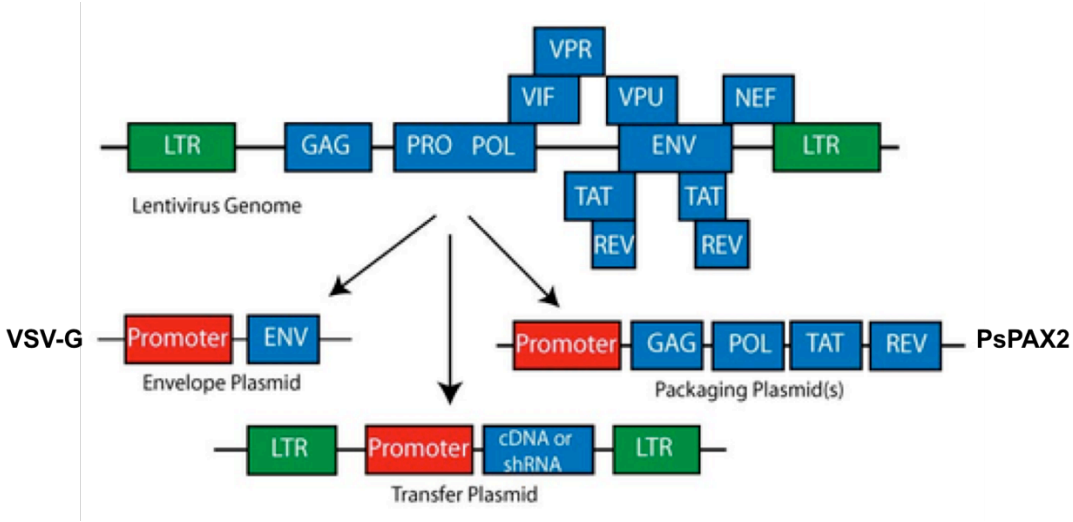

Figure 2-5. Components for lentivirus generation. The envelope plasmid determines the tropism of the virus. The transfer plasmid contains the gene of interest located in between LTR sites that will allow integration into the host genome, and the promoter that will allow for expression of the protein of interest. The packaging plasmid contains the necessary viral genes (*gag*, *pol, tat*, *rev*). Adapted from https://www.addgene.org/viral-vectors/lentivirus/lenti-guide/.

2.13.8 Preparing and testing virus

Plat-E or HEK 293T cells were transfected by Calcium Phosphate method, a method that involves the formation of calcium phosphate-DNA precipitates that facilitate the binding of condensed DNA to the cell surface, allowing the DNA to enter the cell by endocytosis (Kingston et al., 2003). The supernatant (containing viral particles) was collected at 24 and 48 hours after transfection, filtered through a 0.45 mm non-protein binding filter and snap frozen in dry ice and stored at -80 ^{o}C. In order to test virus efficiency, NIH3T3 cells were plated in 6 well plates (1.8×10^{5} cells per well) and incubated with the virus for 12 hours. The efficacy of infection was assessed by comparing the number of live cells of infected and non-infected cells after antibiotic selection or based on the fluorescence signal determined by flow cytometry (in the case of *pRRL-iVenus*).

2.13.9 Retroviral/Lentiviral transduction of murine HSPC/LSK cells

c-Kit^{+} cells were incubated overnight in Iscove's Modified Dulbecco's Medium (IMDM) with 10 % FCS, 40 ng/mL of mouse recombinant stem cell factor (SCF) (carrier-free) (Biolegend, Cat. 579702), 20 ng/mL of recombinant mouse IL-3 (carrier-free) (Biolegend, Cat. 575502) and IL-6 (Biolegend, Cat. 575702) to promote cell cycle entry and proliferation of cells (in the case cells were infected with retrovirus).

LSK cells were isolated via FACS and maintained in Iscove's Modified Dulbecco's Medium (IMDM) with 10 % FCS, 100 ng/mL of mouse recombinant stem cell factor (SCF) (carrier-free) (Biolegend - 579702), 100 ng/mL of recombinant mouse TPO (carrier-free) (Biolegend - 593306) and Flt3 ligand (Biolegend - 550704). The cells were transduced using the RetroNectin® (Takara, Cat. T100A/B) method.

RetroNectin® is a recombinant human fibronectin fragment used to efficiently enhance retroviral mediated gene transduction through co-localization of target cells and virions (Figure 2-6). 48 well plates (non-tissue culture treated) were coated with

RetroNectin® and left overnight at 4 ^{o}C. The next day, RetroNectin® was removed from each well and 1 mL of retroviral supernatant was added on the coated wells. The plate was spun for 2 hours, 2,000 x g at 32 ^{o}C in order for the viral particles to bind on the plate (this method is ideal for low titre retroviruses). After centrifugation, the viral supernatant was removed and 200,000 c-Kit^{+} or 10,000 LSK cells were seeded on the virus-coated plates (in IMDM with 10 % FCS, and 100 ng/mL SCF, TPO and Flt3 ligand) and left overnight at 37 ^{o}C, 5% CO_2. The next morning, a second plate was similarly prepared and cells were washed off the first plate and transferred on the second plate. The cells were left overnight at 37 ^{o}C, 5 % CO_2. 48 hours after the initiation of the infection, the cells were transferred on a plate containing no retronectin or virus, and were left for 24 hours to recover and also start expressing the antibiotic resistance genes. The next morning, the cells were seeded in media containing the appropriate antibiotic as well as the cytokine cocktail described earlier. Cells infected with both *Meis1* and *Hoxa9* were selected both for puromycin and neomycin (puromycin: 1.5 μg/mL; neomycin:1mg/mL). Cells infected with *MLL-ENL*, *MLL-AF9* and *AML-ETO9A* were selected for neomycin resistance. Antibiotic selection process lasted for 3 days. Finally, cells infected with the pRRL vectors were selected based on iVenus expression (GFP) via flow cytometry.

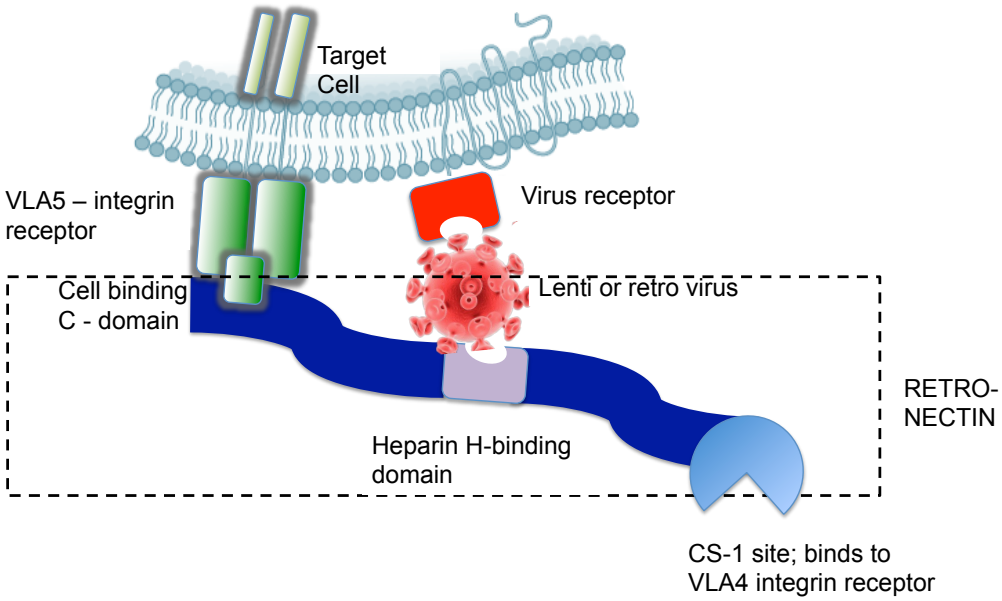

Figure 2-6. Retronectin reagent. Retronectin is a human fibronectin fragment that contains three functional domains: the cell binding domain (C-domain), the heparin binding domain (H-domain) and the CS-1 sequence. The viral particles bind retronectin via the H-domain, and the target cells bind through the interaction of the surface integrin receptors VLA-5 and VLA-4 with the C-domain and CS-1 sites respectively (Adapted from:

http://www.clontech.com/GB/Products/Viral_Transduction/Haematopoietic_Cell_Transduction/xxclt_displayImage.jsp?imgCntId=11249&sitex=10030:22372:US).

2.13.10 Generation of pre-leukaemic cells: colony forming assay

Meis1/Hoxa9 transduced HSPCs were counted by trypan blue viability staining. Live cells were plated in MethoCult™ M3231 (Stem cell technologies, Cat. 03231) supplemented with 20mL IMDM; 20 ng/mL of SCF; 10 ng/mL of IL-3; 10 ng/mL of IL-6 and 10 ng/mL of GM-CSF (granulocyte-macrophage colony stimulating factor; Biolegend - 576302), 100 Units/mL penicillin and 100 mg/mL streptomycin. *Meis1/Hoxa9* transduced HSPCs seeding concentration: 2,500 cells/mL; *MLL-ENL, MLL-AF9-, AML-ETO9a-*, *pRRL-Cre-iVenus-* (and control) transduced HSPCs seeding concentration: 25,000 cells/mL. Selection antibiotics were added according to the resistance of the retrovirus/retroviruses in use (puromycin (1.5 μg/mL) and/or neomycin (1mg/mL)). Empty wells were filled with PBS in order to avoid evaporation of the semi-solid medium. After 6 days in culture (CFC1), colonies were counted and re-plated at the same concentration and using the same culture conditions (CFC2, CFC3).

2.13.10.1 Colony size assessment

500 cells/well were seeded on a 96 well plate (5 technical replicates). After 3,4 and 5 days after seeding the size of the colonies was measured using the Operetta high-content automated microscope analyses (Operetta® High Content Imaging). For each well, six fields of view were acquired at each of the five focal planes separated by 150 μm, ensuring no double counting of colonies. Colony size was calculated in an unbiased way by the Operetta microscope software at day 3,4 and 5 after plating using the Harmony texture-based image analysis software. All data from the Operetta high content automated microscope are represented as mean ± SEM.

2.13.11 Cell cycle analyses

For cell cycle analyses, cells were incubated with DAPI (containing 0.1 % Triton) (5 μg/mL; Sony Biotecnhology Inc.) solution for 1 - 2 minutes at room temperature and acquired on FACSFortessaV (BD). Figure 2-7 shows a cell cycle profile obtained from CFC3 *Meis1/Hoxa9* transformed cells. G1 phase reflects cell growth; S phase,

cell prepares for division by increasing the number of copies of its chromosomes; this is followed by G2/M phase where the duplicated chromosomes are checked and the cell divides. Cells that are not dividing leave the cell cycle and stay in G0. Gating was performed using the built-in Watson algorithm (Watson et al., 1987) , available on the FlowJo software.

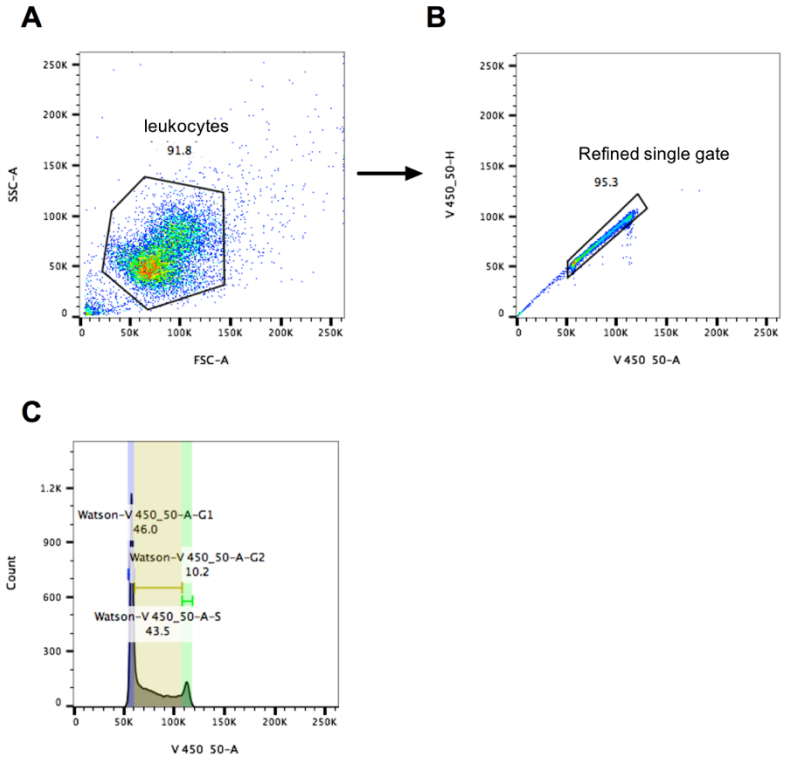

Figure 2-7. Gating strategy for cell cycle. Cells were gated based on the side and forward scatter (A) and gating was then refined in order to exclude doublets (B). Cell cycle analysis was performed by applying Watson's algorithm on the DAPI channel histogram.

2.13.12 Apoptosis assay

Cells were washed in ice-cold PBS, re-suspended in 100 µL of Annexin binding buffer 1X (BD, Cat.556454) containing 5 µL of Annexin V (BD, conjugated with FITC, Cat. 556420) and incubated for 20 minutes at room temperature. Before sample acquisition on FACSFortessaV (BD) DAPI was added (final concentration 10 µg/mL) and incubated for 1 minute at room temperature. The dot plots below, indicate the gating strategy used as well as individually stained cells with AnnexinV-FITC or DAPI (or unstained) (Figure 2-8). $DAPI^-$/ $AnnV\text{-}FITC^-$ are live cells, $DAPI^-$ / $AnnV\text{-}FITC^+$ are early apoptotic cells and $DAPI^+$/ $AnnV\text{-}FITC^+$ are late apoptotic cells. It is important to note that accurately measuring apoptosis using in vitro assays is difficult as cell debris can influence the percentage of apoptotic cells.

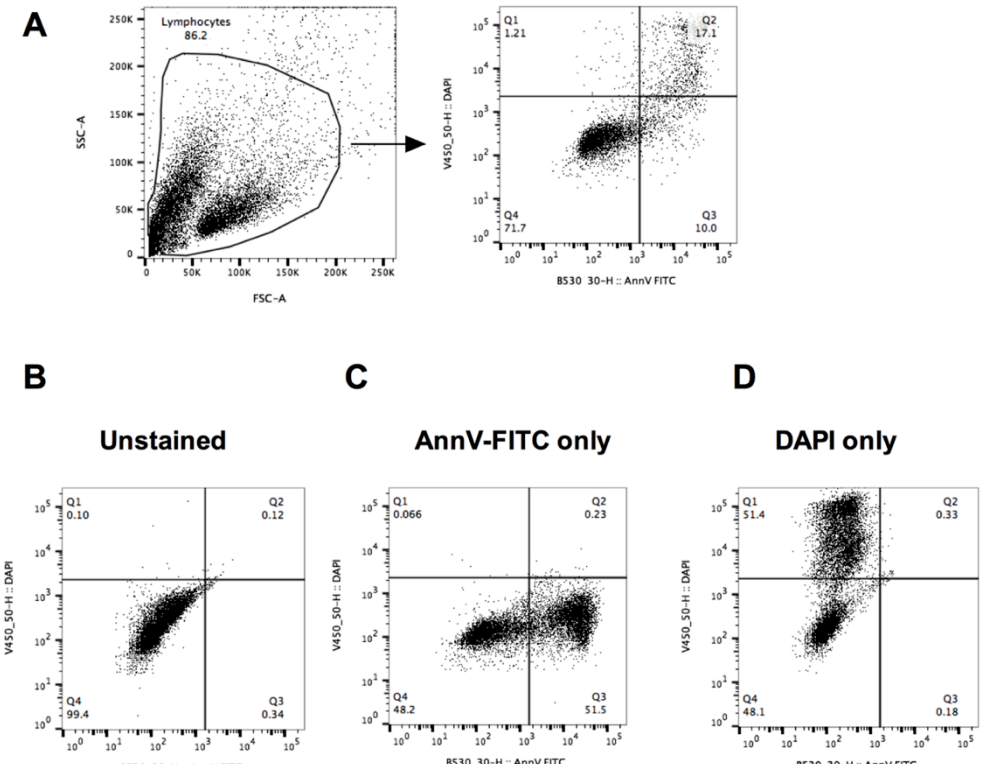

Figure 2-8. Annexin V apoptosis assay. (A) Gating strategy for annexin V apoptosis assay. (B) unstained control, (C) cells only stained with annexinV-FITC and (D) cells only stained with DAPI.

2.14 Proliferation assay

The proliferation assays were performed with cells at a concentration of 150,000 cells/ml. The cells were seeded on a 96 well plate in triplicate, in Iscove's Modified Dulbecco's Medium (IMDM) with 10 % FCS, 40 ng/mL of mouse recombinant stem cell factor (SCF) (carrier-free) (Biolegend - 579702), 20 ng/mL of recombinant mouse IL-3 (carrier-free) (Biolegend - 575502) and IL-6 (Biolegend - 575702). Counting of cells was performed with trypan blue exclusion or via acquisition using BD Accuri flow cytometer.

2.15 Seahorse assay

Oxygen consumption rate (OCR) measurements were made using a Seahorse XF-24 analyser (Seahorse Bioscience) and the XF Cell Mito Stress Test Kit. Briefly, LICs isolated from the bone marrow of sick recipient mice were plated in XF-24 microplates pre-coated with cell-tak (BD) at 250,000 cells per well in XF Base Medium supplemented with 2 mM pyruvate and 10 mM glucose (pH 7.4). OCR was measured 2 times every 6 minutes for basal value and after each sequential addition of oligomycin (1μM), FCCP (4 μM) and finally concomitant rotenone and antimycin A(1μM). Oxygen consumption measurements were normalised to cell counts performed before and after each assay. Extracellular acidification rate (ECAR) was measured after the addition of 2-deoxy glycose (100 μM).

CHAPTER 3

The role of mitochondrial *Fh1* and the TCA cycle in aged haematopoiesis

3 The role of mitochondrial *Fh1* and the TCA in aged haematopoiesis

3.1 Introduction

The defining characteristics of HSCs are their capacity to self-renew and provide life-long replenishment of the haematopoietic system. Recent studies have indicated that specific metabolic properties govern the fates of HSCs, such as self-renewal and differentiation (For detailed description, see section 1.8). Self-renewing HSCs suppress the flow of glycolytic metabolites into the TCA cycle and are known to rely on glycolysis in order to remain in a quiescent state (Takubo et al., 2013; Suda et al., 2011; Wang et al., 2014). Furthermore, HSCs switch from glycolysis to oxidative phosphorylation during the differentiation process (Yu et al., 2013). Thus, it is of interest to clearly identify metabolic regulators of such HSC fates.

3.1.1 Fumarate hydratase

Fumarate hydratase (FH) is an essential part of the TCA cycle within the mitochondria where it catalyses the hydration of fumarate into malate. Although FH is considered a TCA cycle enzyme, it is also expressed in the cytoplasm and the nucleus (Yogef et al., 2012). Autosomal dominant mutations in FH have been associated with hereditary leiomyomatosis and renal cell cancer (HLRCC), indicating that FH functions as a tumour suppressor (Tomlinson et al., 2002).

In order to study the role of the mitochondrial and cytoplasmic isoforms of FH in haematopoiesis, we generated a mouse model that lacks mitochondrial *Fh1* but expresses the cytosolic isoform of human FH (for details, please see section 3.3). Consequently, haematopoietic cells are able to efficiently metabolise fumarate, while exhibiting a genetic truncation of the TCA cycle in their mitochondria (Figure 3-3).

From a young age (8 weeks), preliminary analysis of mice lacking the mitochondrial *Fh1* but expressing the cytosolic isoform, exhibited an expansion of the myeloid compartment in the peripheral blood (Figure 3-1), indicating a potential myeloproliferative disorder. In humans, myeloproliferative disorders often develop

into AML, with an average onset between 64 and 68 years (Heaney and Soriano, 2013). Case reports dating back to the 1950s document patients with a history of myeloproliferative disorders, progressing to AML (Skversky et al., 1957; Bank et al., 1966). The AML that arises as a consequence of myeloproliferative disorders is generally aggressive and resistant to conventional therapy (Heaney and Soriano, 2013). With that in mind, we aged the mice lacking the mitochondrial isoform of *Fh1*, mice in order to observe whether they would develop AML.

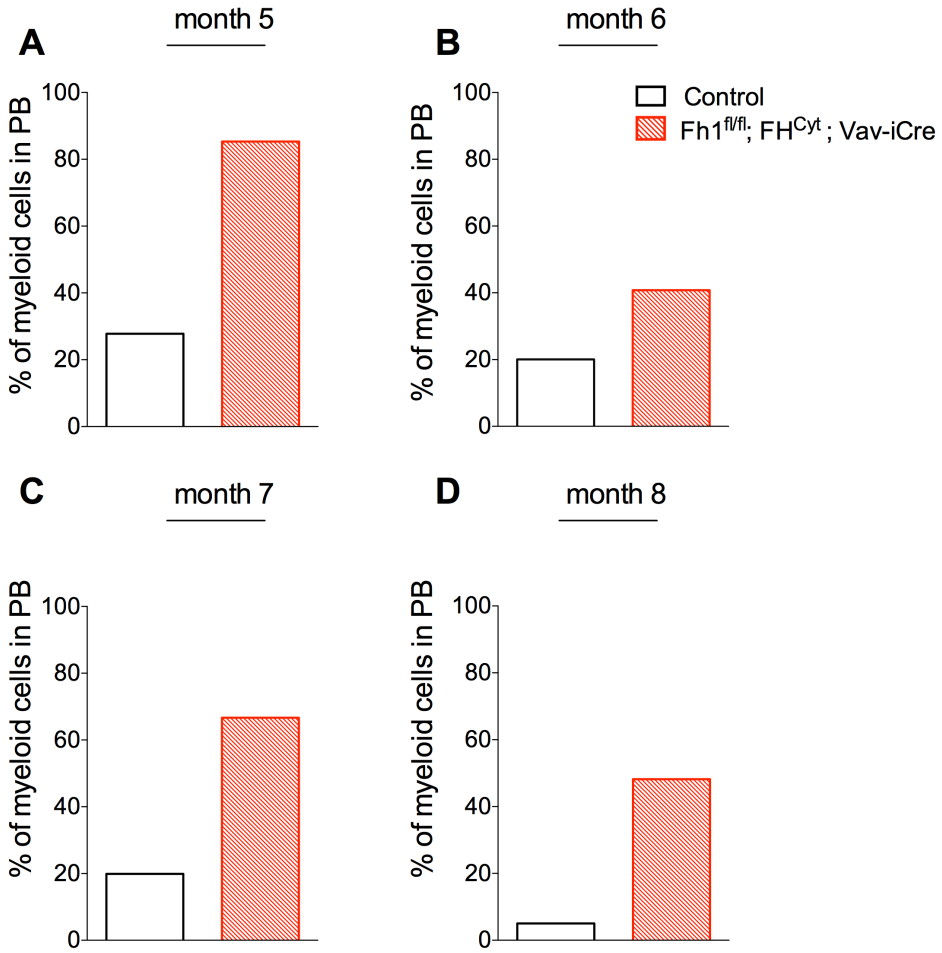

Figure 3-1. *Fh1*$^{fl/fl}$; *FH*^{Cyt}; *Vav-iCre* mice exhibit an expansion of the myeloid compartment within the peripheral blood. We generated mice lacking the mitochondrial *Fh1* specifically within the haematopoietic system but expressing the cytosolic isoform (*Fh1*$^{fl/fl}$; *FH*^{Cyt}; *Vav-iCre* mice). Mice were bled from month 5-8 every 4wks and blood was phenotypically analysed for myeloid cells (Mac-1^{+}Gr1^{+} white blood cells (WBC)). Age- matched wild-type mice were used as controls. n = 1.

3.2 Aims

The aim of this chapter was to age *Fh1$^{fl/fl}$; FH^{Cyt}; Vav-iCre* mice (and age-matched controls) in order to observe whether these cohorts would spontaneously develop AML. As controls we used mice that were expressing the wild type mitochondrial and cytosolic isoforms of *Fh1* (here after referred to as *control* mice) and mice that were expressing both isoforms of *Fh1* but also expressing the human cytosolic isoform of FH (here after referred to as *control; FH^{Cyt}*). At the age between 56-60 weeks, the mice were sacrificed and the bone marrow as well as extramedullary haematopoietic sites such as the spleen and the thymus were immunophenotypically analysed. We specifically looked at the primitive, the progenitor and the differentiated cell compartments.

3.3 Experimental design

In order to investigate the role of mitochondrial and extra mitochondrial FH we utilised an *in vivo* mouse model that specifically deletes *Fh1* in the haematopoietic system, while simultaneously expressing the extra mitochondrial human FH. The transgenic mouse was generated by crossing *Fh1$^{fl/fl}$; Vav-iCre* mice with mice expressing *FH* cDNA lacking the mitochondrial targeting sequence and therefore preventing its mitochondrial localisation, in the *Rosa26* locus (Adam et al, 2013). The utilisation of the *Vav* promoter allows for haematopoiesis-specific deletion, shortly after the emergence of HSCs during embryonic development (deBoer et al, 2003). The resulting genotypes that were used throughout this chapter are indicated in Figure 3-3. *Control* mice, (expressing wild type mitochondrial and cytosolic isoforms of *Fh1) control; FH^{Cyt}* (expressing both isoforms of *Fh1* but also expressing the cytosolic isoform of human *Fh1* (FH)), and *Fh1$^{fl/fl}$; FH^{Cyt}; Vav-iCre* mice (lacking the murine mitochondrial and cytosolic isoforms of *Fh1* but expressing the human cytosolic isoform of *Fh1* (FH)). The absence of Fh1 protein in *Fh1$^{fl/fl}$; FH^{Cyt}; Vav-iCre* mice has been previously validated in our team (Figure 3-2 A). Similarly, the exclusion of the FH^{Cyt} from the mitochondria was also validated by our team and other laboratories (Figure 3-2 B; Adam et al, 2013).

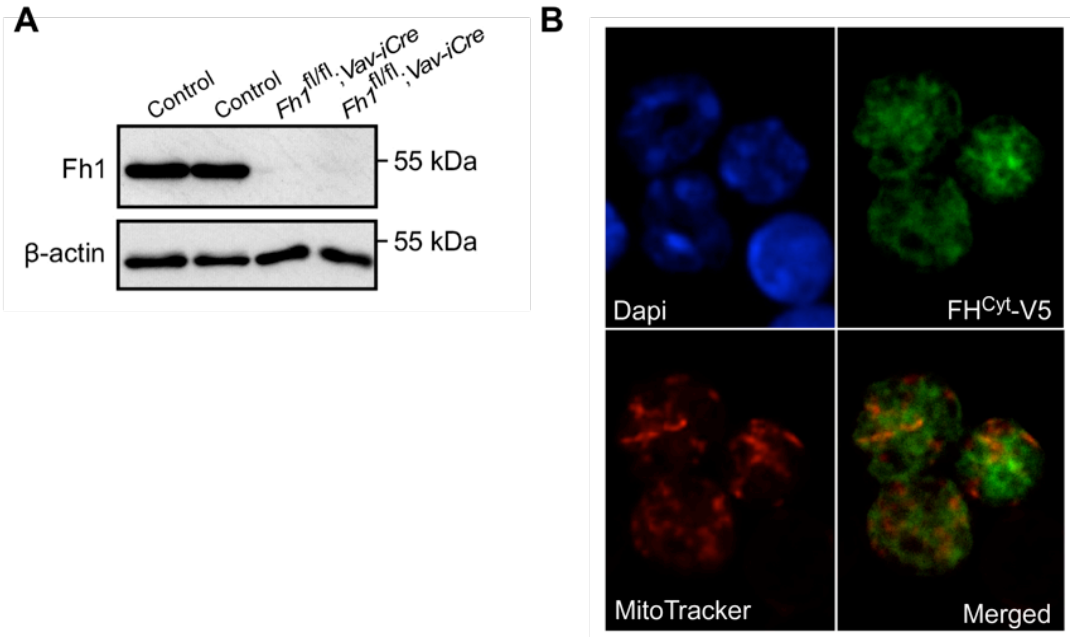

Figure 3-2. Validation of *Fh1$^{fl/fl}$; FH^{Cyt}; Vav-iCre* mice. (A) Western blot analysis indicating absence of Fh1 protein in c-Kit^{+} cells. (B) Validation of FH^{Cyt} localisation. Representative immunofluorescence performed on total BM cells of *control* and *control; FH^{Cyt}* stained with Dapi (blue), anti-V5-FH^{Cyt} (green) and MitoTracker (Red) confirming that FH^{Cyt} is excluded from the mitochondria.

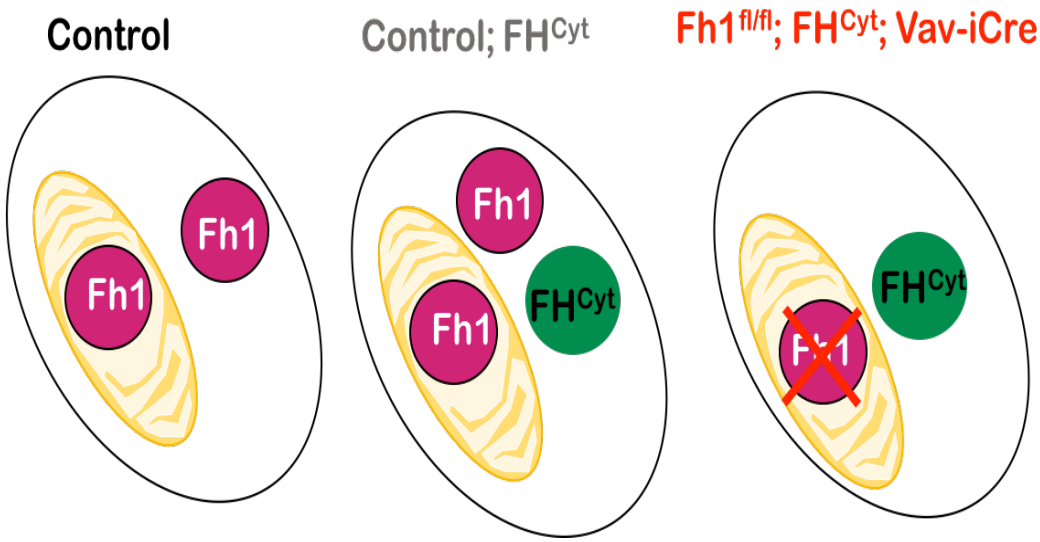

Figure 3-3. Generation of *Fh1$^{fl/fl}$; FH^{Cyt}; Vav-iCre* mice. We generated mice lacking the mitochondrial *Fh1* specifically within the haematopoietic system but expressing the cytosolic isoform (*Fh1$^{fl/fl}$; FH^{Cyt}; Vav-iCre* mice). The transgenic mouse was generated by crossing *Fh1$^{fl/fl}$; Vav-iCre* mice with mice expressing FH cDNA lacking the mitochondrial targeting sequence, in the *Rosa26 locus* (Adam et al., 2013).

3.4 Results

3.4.1 Aged $Fh1^{fl/fl}$; FH^{Cyt}; Vav-iCre mice exhibit an expansion of the myeloid compartment with a concomitant decrease in the B cell compartment

A combination of both male and female mice were aged for approximately nine months and were bled in order to assess the myeloid compartment within the peripheral blood. Mice lacking mitochondrial *Fh1* while simultaneously expressing the cytosolic isoform of FH exhibited a bias towards the myeloid compartment in the blood (Figure 3-4).

Immunophenotypic analysis of the bone marrow at the point of sacrifice revealed lower bone marrow cellularity (WBC count) of *$Fh1^{fl/fl}$; FH^{Cyt}; Vav-iCre* mice compared to *control* and *control; FH^{Cyt}* mice (Figure 3-5A). Interestingly, although the mice exhibited a myeloid bias in both the peripheral blood and the spleen at the point of sacrifice, they exhibited a comparable frequency of myeloid cells in the BM to that of *control* and *control; FH^{Cyt}* mice (Figure 3-5 B-G; also see representative FACS profile in Figure 3-6).

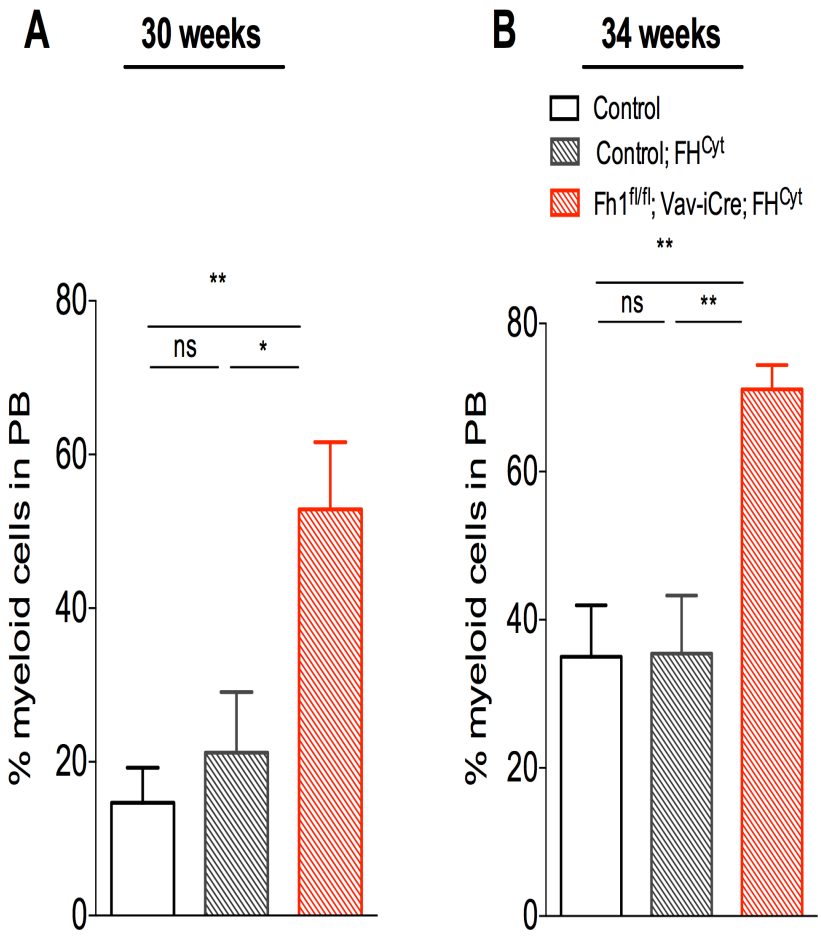

Figure 3-4. *Fh1*$^{fl/fl}$; *FH*^{Cyt}; *Vav-iCre* mice exhibit expansion of the myeloid compartment in the peripheral blood. Graphs show the frequency of the myeloid compartment in aged mice at 30 weeks (A) and 34 weeks of age (B) in the peripheral blood. Myeloid cells are defined as the sum of Mac-1^{+}/ Gr1^{+} and Mac-1^{+} cells. n = 4-6 biological replicates per genotype. Graphs show mean ± S.E.M *p<0.05, **p<0.01, Mann-Whitney test. PB; peripheral blood.

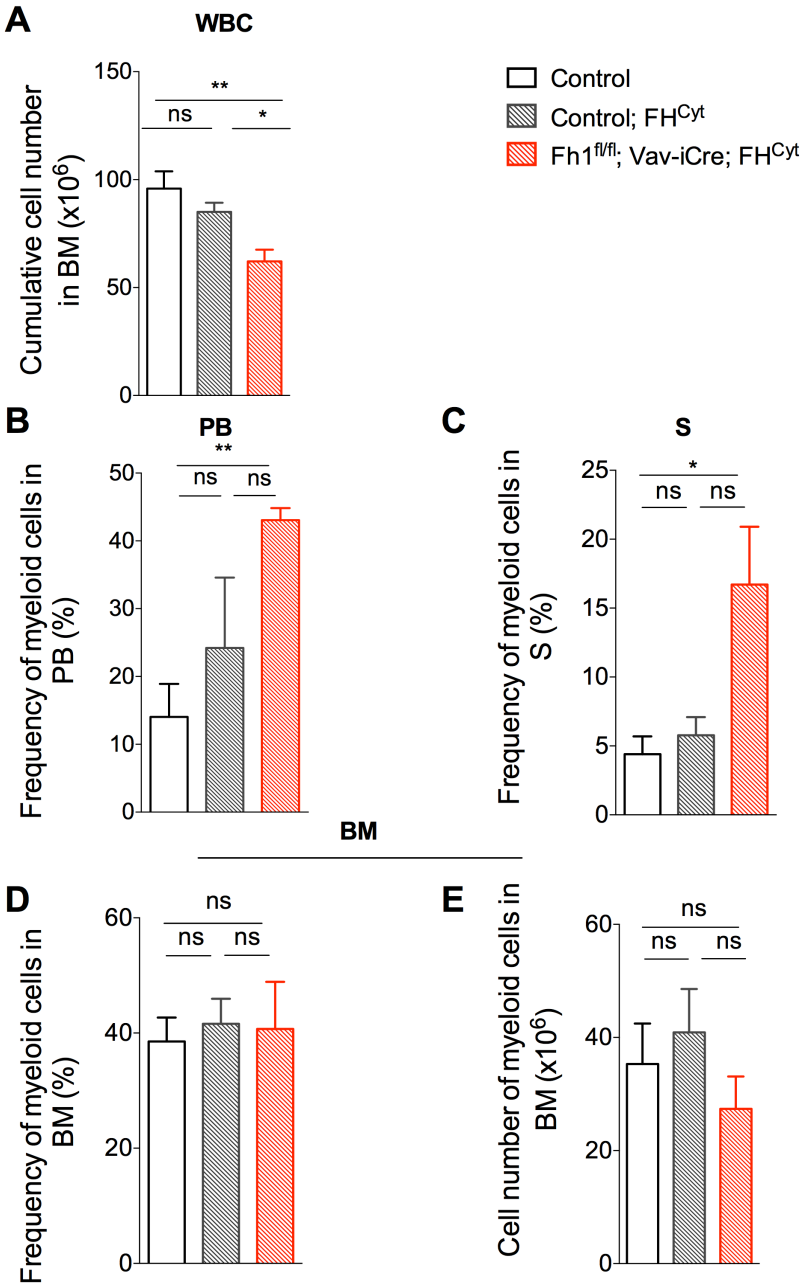

Figure 3-5. *Fh1*$^{fl/fl}$; *FH*^{Cyt}; *Vav-iCre* mice exhibit lower bone marrow cellularity and myeloid expansion in extramedullary haematopoietic sites. (A) The graph shows the total cell number of the bone marrow (WBC) of aged mice (per 1 femur and 1 tibia). All cell counts were performed by an automatic cell counter (MEK 6500K, Nihon Kohden). (B, C, D) Graphs show the frequency of the myeloid cells in the peripheral blood (B), the spleen (C), and the bone marrow (D). (E) Graph shows absolute numbers of myeloid cells in the BM. Myeloid cells were defined as the sum of Mac-1^{+} Gr1^{+} and Mac-1^{+}. n = 4-6 biological replicates per genotype. Mice were analysed at 56-60 weeks. Graphs show mean± S.E.M. *p<0.05, **p<0.01, Mann-Whitney test. WBC; white blood cells, BM; bone marrow, PB; peripheral blood, S; spleen.

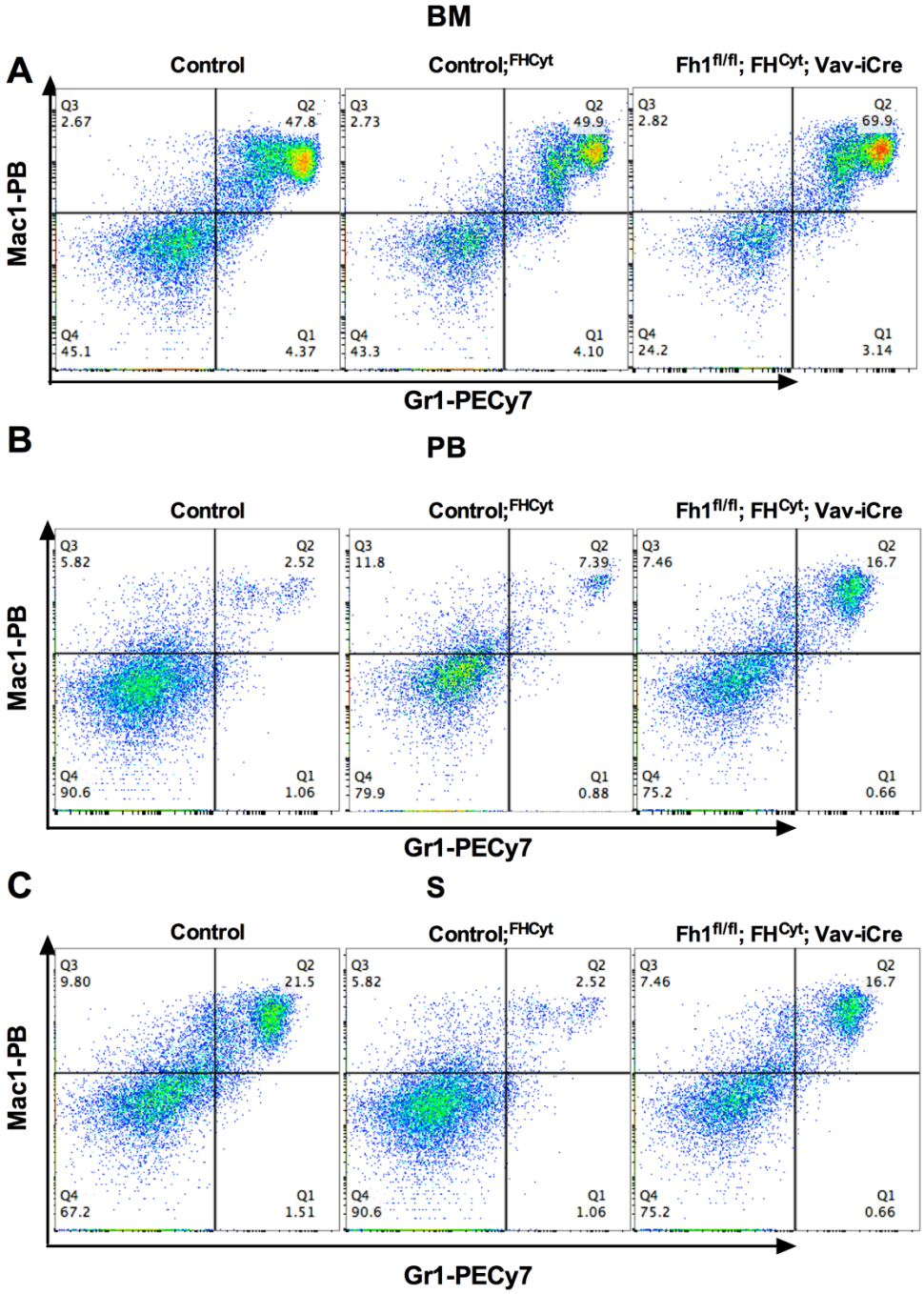

Figure 3-6. Representative FACS plots of the myeloid compartment at the time of sacrifice. (A) Representative FACS plots of the myeloid compartment in the bone marrow, (B) spleen and (C) peripheral blood of aged mice at the point of sacrifice. FACS plots are for *control* (left panels), *control; FH*^{Cyt} (middle panels) and *Fh1*$^{fl/fl}$*; FH*^{Cyt}*; Vav-iCre* (right panels). PB; peripheral blood, BM; bone marrow, S; spleen Axes are at a logarithmic scale.

Analysis of the lymphoid compartment revealed that aged *Fh1$^{fl/fl}$; FH^{Cyt}; Vav-iCre* mice had a much lower frequency of B cells compared to *control* and *control; FH^{Cyt}* mice (identified based on the markers B220 and CD19). More specifically, a drastic decrease of B cell frequency and numbers was observed in the peripheral blood, bone marrow and spleen (Figure 3-7; also see representative FACS profile in Figure 3-8). Furthermore, the frequency of T cells (the sum of $CD4^+$ and $CD8^+$ cells) was unaffected in the peripheral blood, but was significantly decreased in the spleen (Figure 3-9; also see representative FACS profile in Figure 3-8). Of note, *control; FH^{Cyt}* mice also exhibited a lower frequency of T cells compared to the *control* mice (Figure 3-9). Maturation of the T cell lineage takes place in the thymus. As a result, we assessed the thymic T cell compartment. *Fh1$^{fl/fl}$; FH^{Cyt}; Vav-iCre* mice exhibited a comparable frequency of mature T cells in the thymus to *control* and *control; FH^{Cyt}* mice (Figure 3-10A, C). Furthermore, the frequency of the double positive population of $CD4^+$ $CD8^+$ representing immature thymocytes (Bosselut, 2004), was also comparable between all three genotypes.

Overall, these data indicate that the *Fh1$^{fl/fl}$; FH^{Cyt}; Vav-iCre* mice exhibit a decrease of the B cell compartment, possibly explaining the increased frequency of the myeloid compartment.

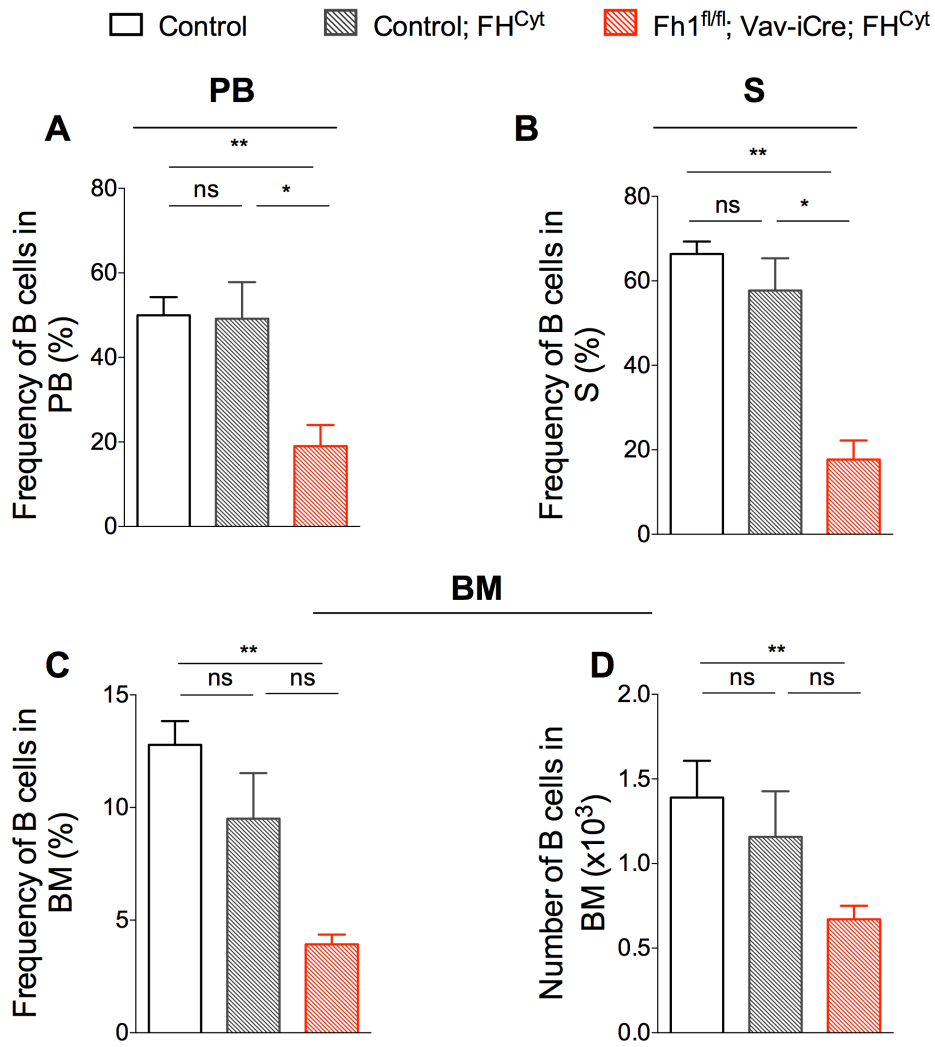

Figure 3-7. The B cell lineage is compromised in aged *Fh1$^{fl/fl}$; FH^{Cyt}; Vav-iCre* mice. Frequency of B cells in PB (A) S (B) and BM (C). (D) Total B cell numbers in BM of mice at the point of sacrifice. B cells are defined as B220^{+} CD19^{+} WBC, representing the mature B cells. n = 4-6 biological replicates per genotype. Mice were analysed at 56-60 weeks. Graphs show mean ± S.E.M. *p< 0.05, **p<0.01, Mann-Whitney test. PB; peripheral blood, BM; bone marrow, S; spleen.

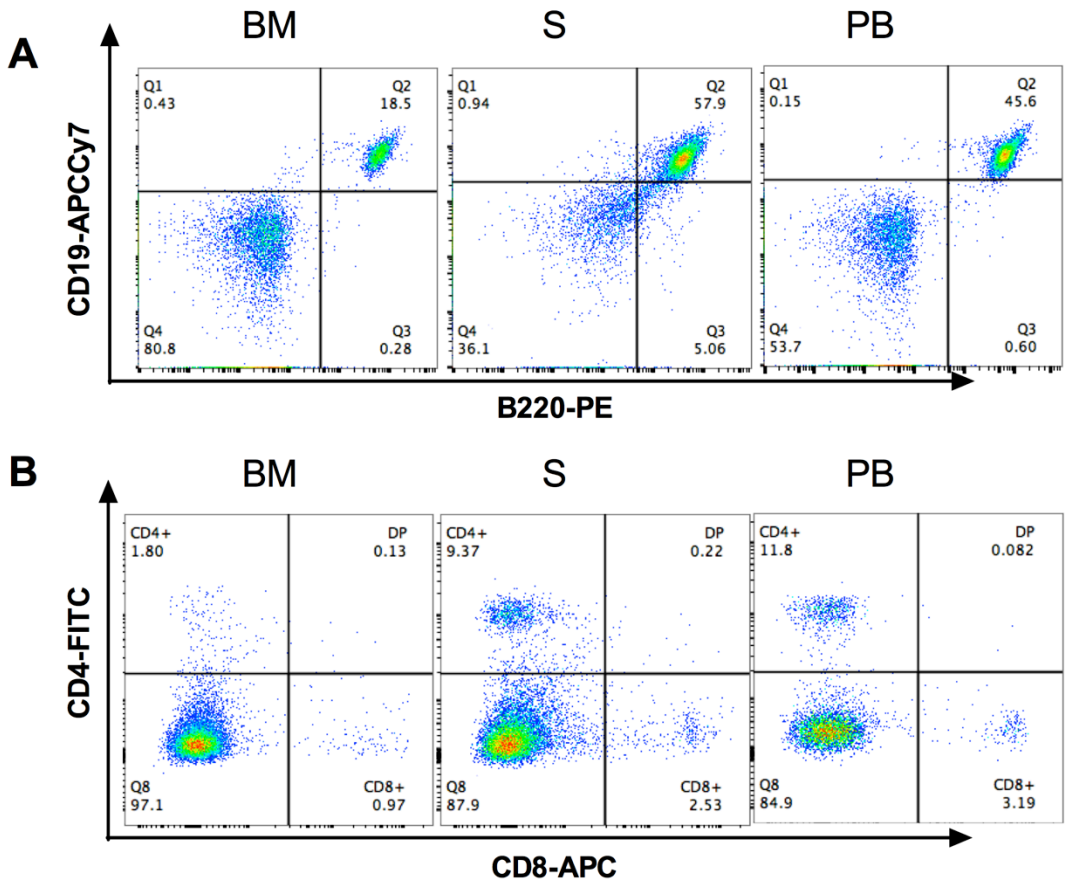

Figure 3-8. Representative FACS plots of lymphoid lineages. (A) FACS plots showing B cells (A) and T cells (B) present in the bone marrow (BM, left panels), spleen (S, middle panels) and peripheral blood (PB, right panels), at the point of sacrifice. Plots are representative for *control* mice. B cells: $CD19^{+}$ $B220^{-}$, $CD19^{+}$ $B220^{+}$, $CD19^{-}$ $B220^{+}$. T cells $CD4^{+}$, $CD8^{+}$. PB; peripheral blood, BM; bone marrow, S; spleen

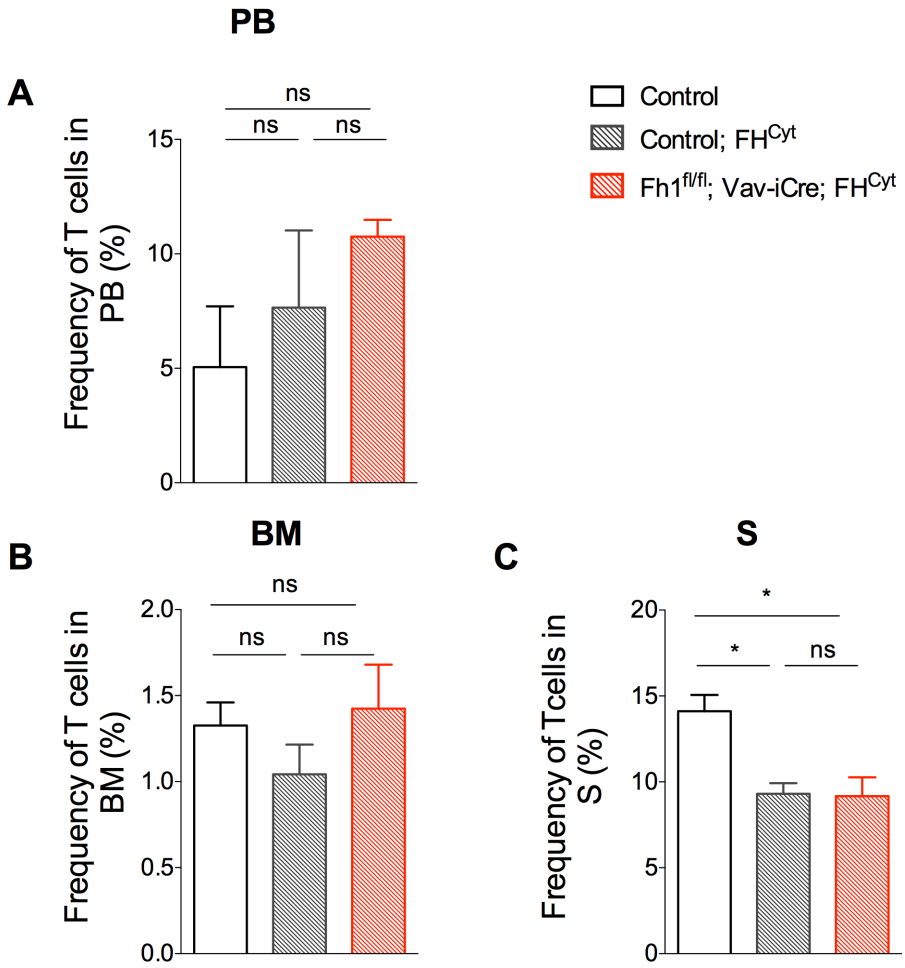

Figure 3-9. The T cell lineage is compromised in the spleen of aged *Fh1$^{fl/fl}$; FH^{Cyt}; Vav-iCre* mice. Frequency of T cells in PB (A), BM (B) and S (C) T cells are the sum of $CD4^+$ and $CD8^+$ cells. n = 4-6 biological replicates per genotype. Mice were analysed at 56-60 weeks. Graphs show mean ± S.E.M. *p< 0.05, Mann-Whitney test. PB; peripheral blood, BM; bone marrow, S; spleen.

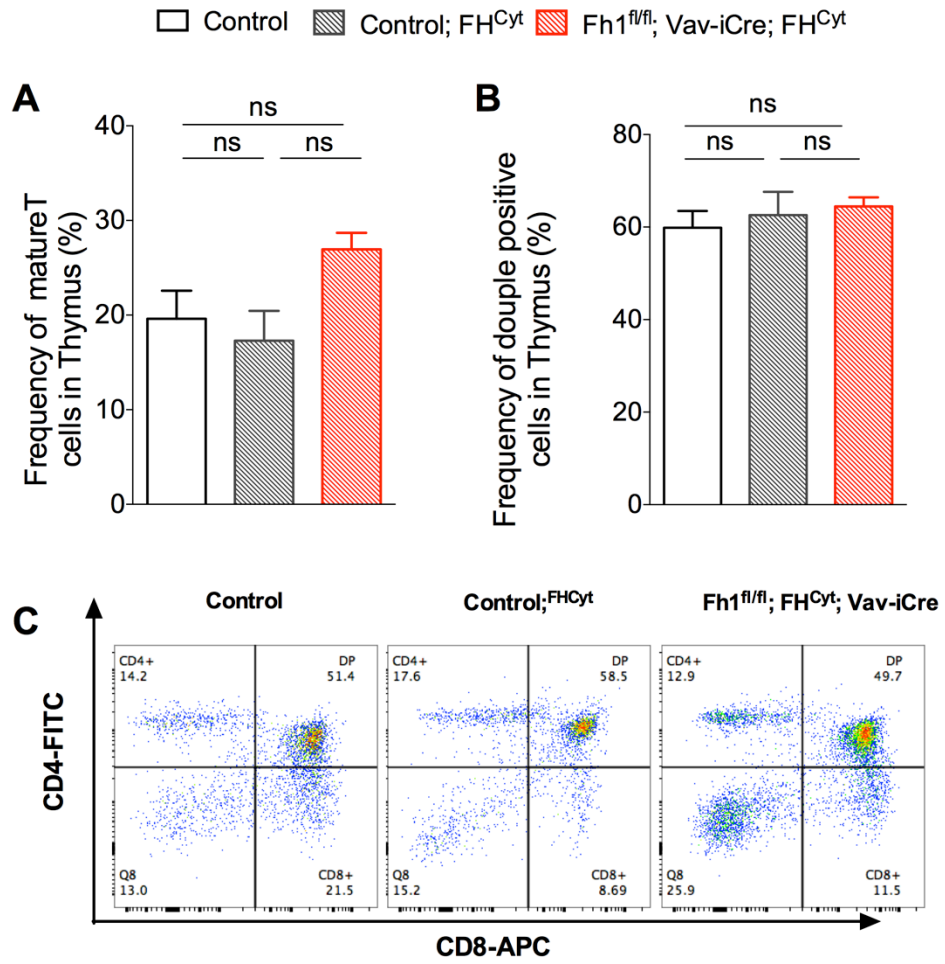

Figure 3-10. Frequency of T cells in the thymus of aged *Fh1$^{fl/fl}$; FH^{Cyt}; Vav-iCre* mice. (A) Frequency of mature T cells in the thymus. T cells are defined as a sum of CD4^{+} and CD8^{+} cells. (B) Frequency of double positive CD4^{+} CD8^{+} cells, denoting the immature thymocytes within the thymus. (C) Representative FACS plots of T cells and immature thymocytes within the thymus of *control* (left panel), *control; FH^{Cyt}* (middle panel) and *Fh1$^{fl/fl}$; FH^{Cyt}; Vav-iCre* (right panel). n = 4-6 biological replicates per genotype. Mice were analysed at 56-60 weeks. Graphs show mean ± S.E.M. *p< 0.05, Mann-Whitney test.

3.4.2 *Fh1*$^{fl/fl}$; *FH*^{Cyt}; *Vav-iCre* mice exhibit increased frequency of the early progenitors HPC-1 and HPC-2

We next wanted to determine the effect that mitochondrial deletion of *Fh1* would have on the primitive haematopoietic compartment. Analysis of the most primitive compartment of the haematopoietic hierarchy in *Fh1*$^{fl/fl}$*; FH*^{Cyt}*; Vav-iCre* mice revealed unaffected frequency and absolute cell numbers of the lineage negative population and the Lin$^-$Sca-1$^-$c-kit$^+$ (LK) population, representing the pool of committed progenitor cells (Figure 3-11A-B, D-E). However, the frequency (but not the absolute cells numbers) of Lin$^-$Sca-1$^+$c-Kit$^+$ (LSK) cells, containing the most primitive cell populations (stem and early progenitor cells), was significantly increased in *Fh1*$^{fl/fl}$*; FH*^{Cyt}*; Vav-iCre* mice when compared to *control* and *control; FH*^{Cyt} mice (Figure 3-11 C, F). Further analysis of the LSK population using the SLAM markers CD48 and CD150, revealed that the frequency and absolute cell number of long-term HSCs (CD48$^-$ CD150$^+$) was not significantly affected (Figure 3-12 A, C). In contrast however, LT-HSCs identified based on CD34 and Flt3 (LSK CD34$^-$ Flt3$^-$), appeared to be reduced both in frequency and absolute cell numbers (Figure 3-12 B, D; also see Figure *3-15* for representative FACS plots).

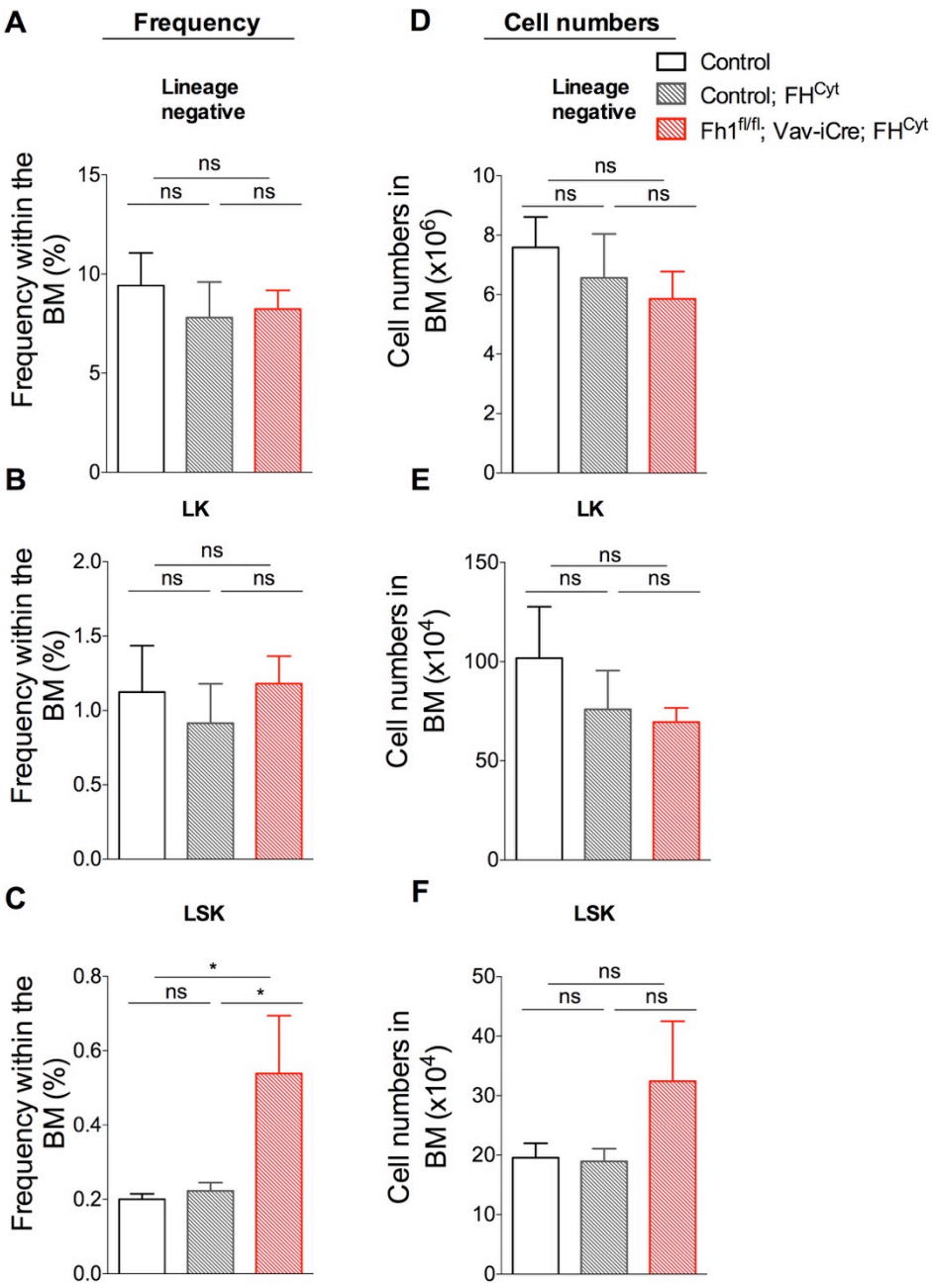

Figure 3-11. *Fh1*$^{fl/fl}$ *FH*^{Cyt}*; Vav-iCre* mice exhibit an increased frequency of LSK cells in the BM. (A-C) Frequency of (A) lineage negative cells (B) Lin$^-$Sca-1$^-$c-Kit$^+$ (LK) and (C) Lin$^-$Sca-1$^+$c-Kit$^+$ cells (LSK) within the bone marrow (1 femur, 1 tibia). (D-F) Total cell numbers of (D) lineage negative (E) LK and (F) LSK cells within the BM. n = 4-6 biological replicates per genotype. Mice were analysed at 56-60 weeks. Graphs show mean ± S.E.M. *p<0.05 Mann-Whitney test.

Additionally, the frequency (but not absolute numbers) of the haematopoietic progenitors-1 (HPC-1, LSK $CD150^{-}$ $CD48^{+}$) and haematopoietic progenitors -2 (HPC-2, LSK $CD150^{+}$ $CD48^{+}$) and HPC-2 were significantly increased (Figure 3-13 A-B, D-E). Furthermore, the frequency and absolute cell numbers of multipotent progenitors (MPP, LSK $CD150^{-}$ $CD48^{-}$) were comparable to that of *control* and *control;* FH^{Cyt} mice (Figure 3-13 C, F; also see representative FACS profile in Figure 3-14).

In summary, these data show that while the most primitive compartment was not dramatically altered, the frequency of the early progenitors HPC-1 and HPC-2, were significantly increased. Upon transplantation, HPC-1 an HPC-2 cells give rise to a mixture of cells, including both myeloid and lymphoid cells (Oguro et al., 2013). As a result, it is likely that the increase in these two populations result in the downstream perturbation of the haematopoietic hierarchy.

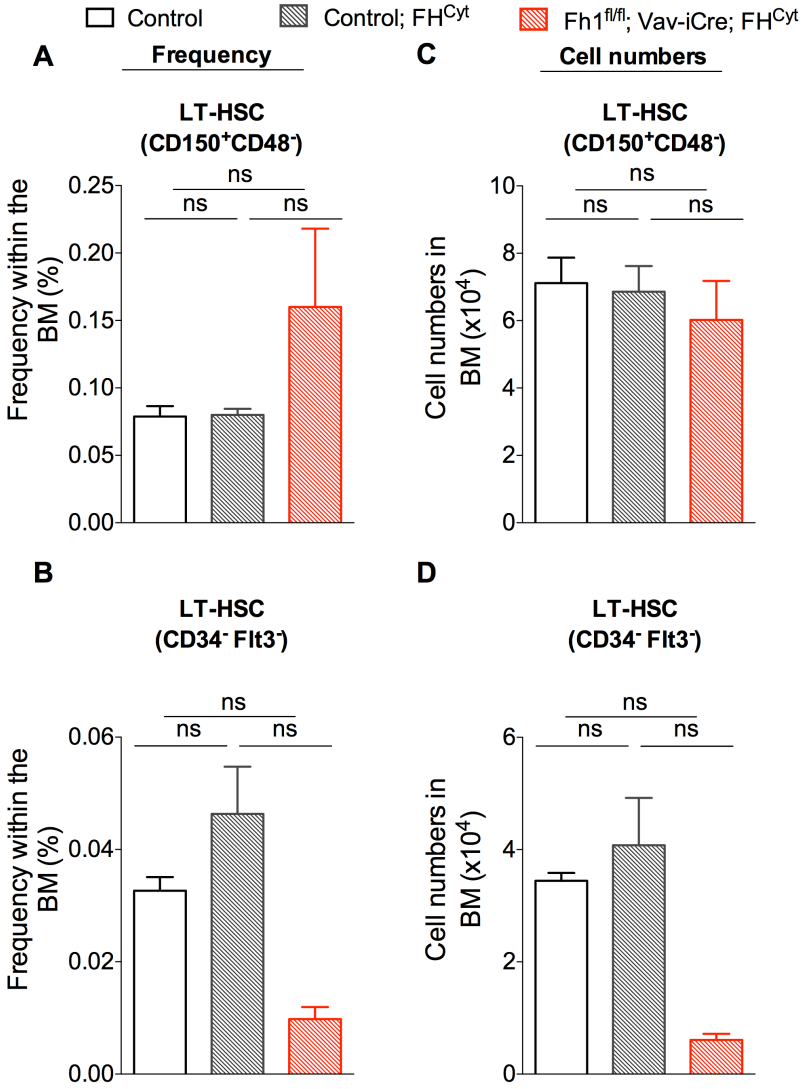

Figure 3-12. Frequency and cumulative cell number of LT-HSCs in the bone marrow of aged mice. This graphs show the frequency of LT-HSCs from the parental gate (LSK cells) (A-B) and total cell number of LT-HSCs. The cell number was estimated by multiplying the frequency of LT-HSCs in the WBC gate (not shown) by the total number of cells in the bone marrow (1 femur and 1 tibia). (C-D) LT-HSC characterisation based on expression of SLAM markers: haematopoietic stem cells (LT-HSCs: LSK $CD48^{-}CD150^{+}$); and CD34 and Flt3 markers: long-term HSCs (LT-HSCs: LSK $CD34^{-}Flt3^{-}$). n = 4 biological replicates per genotype. Mice were analysed at 56-60 weeks. Graphs show mean ± S.E.M. Data are not significant, Mann-Whitney test.

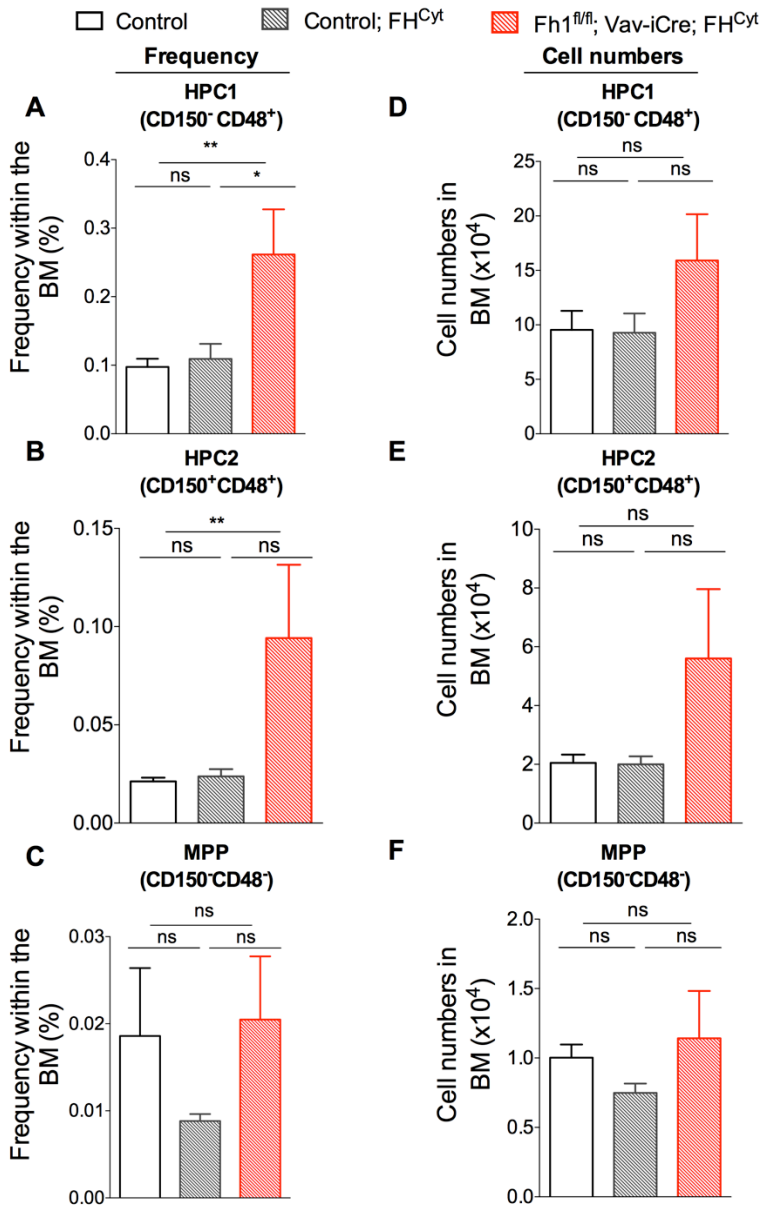

Figure 3-13. *Fh1*$^{fl/fl}$ *FH*^{Cyt}*; Vav-iCre* mice exhibit increased numbers of HPC-1 and HPC-2 compartments in the BM. These graphs show the frequency and total numbers of MPP and HPC compartments of the BM. (A, D) Frequency and total numbers of HPC-1 compartment in the BM. (B, E) Frequency and total numbers of the HPC-2 compartment in the BM. (C, F) Frequency and total numbers of the MPP compartment in the BM. n = 4-6 biological replicates per genotype. Mice were analysed at 56-60 weeks. Graphs show mean ± S.E.M. *p<0.05, **p<0.01, Mann-Whitney test. MPPs, LSKCD150^{-}CD48^{-}; HPC-1, LSKCD150^{-}CD48^{+} and HPC-2, LSK CD150^{+}CD48^{+}. HPC-1; haematopoietic progenitor cell-1, HPC-2; haematopoietic progenitor cell-2, MPP; multipotent progenitor.

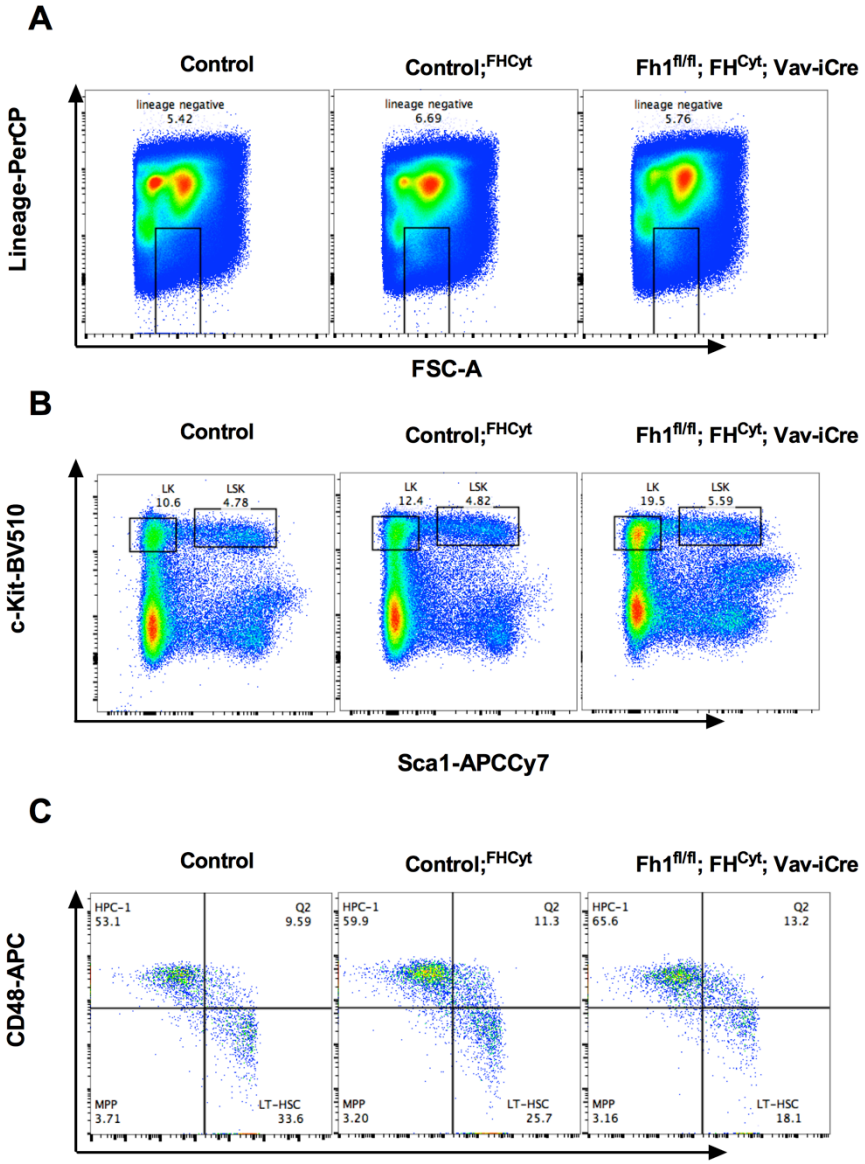

Figure 3-14. Representative FACS plots for stem and early progenitor cells. (A) FACS plots show the lineage negative population from which LK ($Lin^-c\text{-}Kit^+Sca\text{-}1^-$) and LSK ($Lin^-c\text{-}Kit^+Sca\text{-}1^+$) populations are isolated. (B) FACS plots show the LK and LSK populations. (C) FACS plots show the isolation of LT-HSCs and early progenitor cells using the SLAM markers. HPC-1 (LSK $CD150^-$ $CD48^+$), HPC-2 (LSK $CD150^+$ $CD48^+$), LT-HSC (LSK $CD150^+$ $CD48^-$), MPP (LSK $CD150^-$ $CD48^-$). Cells were isolated from the bone marrow of mice analysed at 56-60 weeks (1 femur and 1 tibia). n = 4-6 biological replicates per genotype. FACS plots show *control* (left panels), *control;* FH^{Cyt} (middle panels) and $Fh1^{fl/fl}$*;* FH^{Cyt}*; Vav-iCre* (right panels). LT-HSC; long-term haematopoietic stem cells. HPC-1; haematopoietic progenitor cell-1, HPC-2; haematopoietic progenitor cell-2, MPP; multipotent progenitor.

3.4.3 $Fh1^{fl/fl}$; FH^{Cyt}; Vav-iCre mice do not exhibit significant changes in the committed progenitor compartment

We next wanted to analyse the committed progenitor compartment that gives rise to the differentiated cells of the haematopoietic system. HSCs and immediate progeny are characterised as multipotent cells that in turn give rise to oligopotent progenitor cells of restricted lineage. These oligopotent progenitors will in turn give rise to the terminally differentiated cells of the haematopoietic system (Figure 3-16A).

Via immunophenotypic characterisation, committed progenitor cells that arise from the LK population, can be discriminated based on their expression of CD34 and CD16/32 (receptor-II/III (FcgR)) (Akashi et al., 2000). CD16/32 is an important marker for myelomonocytic cells and CD34 marks the fraction of haematopoietic stem and progenitor cells (Osawa et al., 1996; Lacaud et al., 1998). The resultant populations are the common myeloid progenitors (CMP, CD16/32^{-} CD34^{+}), granulocyte-monocyte progenitors (GMP, CD16/32^{+} CD34^{+}) and megakaryocyte-erythrocyte progenitors (MkEP, CD16/32^{-} CD34^{-}). Furthermore, via the use of CD34 and Flt3 a population of progenitors that possess B-cell, T-cell and GM (granulocytic monocytic) potential but lack significant MegE (megakaryocyte erythrocyte) potential can be isolated. This population is double positive for CD34 and Flt3 (LSK CD34^{+} Flt3^{+}) and is referred to as lymphoid-primed multipotent progenitors (LMPP) (Adolfsson et al., 2005).

Immunophenotypic analysis of the bone marrow, showed that *$Fh1^{fl/fl}$; FH^{Cyt}; Vav-iCre* mice exhibited a trend in the increase of the LMPP, CMP and GMP frequencies when compared to *control* and *control; FH^{Cyt}* mice (Figure 3-16 B, C; also see Figure 3-15 and Figure 3-17). Additionally, MkEP and CLP progenitors in *$Fh1^{fl/fl}$; FH^{Cyt}; Vav-iCre* mice were comparable to *control* and *control; FH^{Cyt}* mice (Figure 3-16 B, C; also for representative FACS plots see Figure 3-17).

Overall, given the fact that we observed a drastic decrease in the B cell compartment with a concomitant bias towards the myeloid compartment, it is surprizing that we

did not observe any dramatic changes in the committed progenitor compartment. To that end, it is possible that the metabolic changes that may have occurred due to the deletion of mitochondrial *Fh1*, affect mainly the differentiated cells rather than the more primitive compartments.

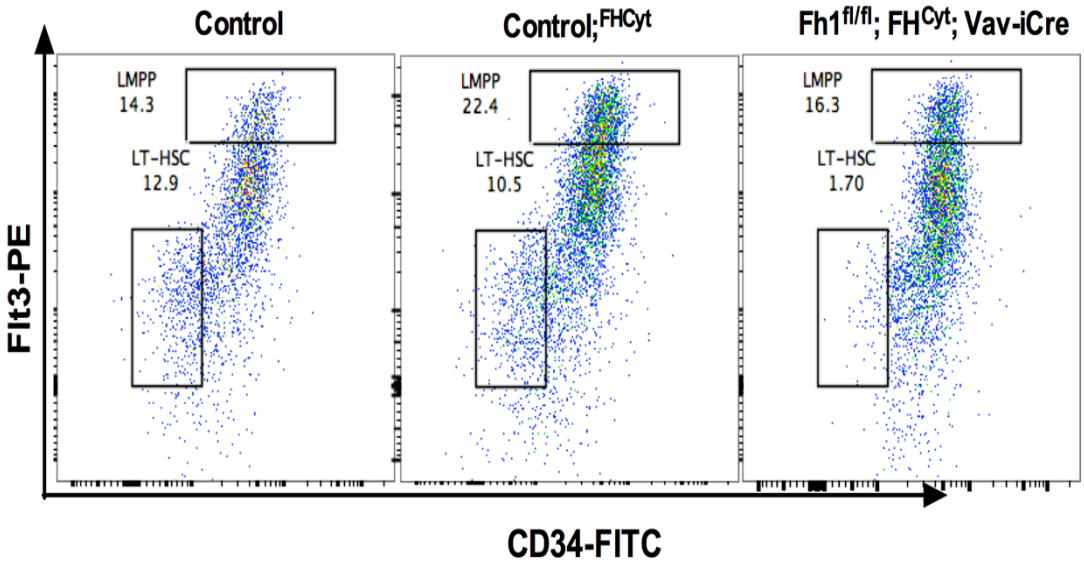

Figure 3-15. Representative FACS plots of the LMPP and LT-HSC compartments based on the CD34 and Flt3 markers. The graphs depict *control* (left panel), *control; FH*^{Cyt} (middle panel) and *Fh1*$^{fl/fl}$*; FH*^{Cyt}*; Vav-iCre* (right panel). LMPP: lymphoid-myeloid multipotent progenitor cells (LSK CD34^{+}Flt3^{+}), LT-HSC: long-term haematopoietic stem cells (LSK CD34^{-} Flt3^{-}).

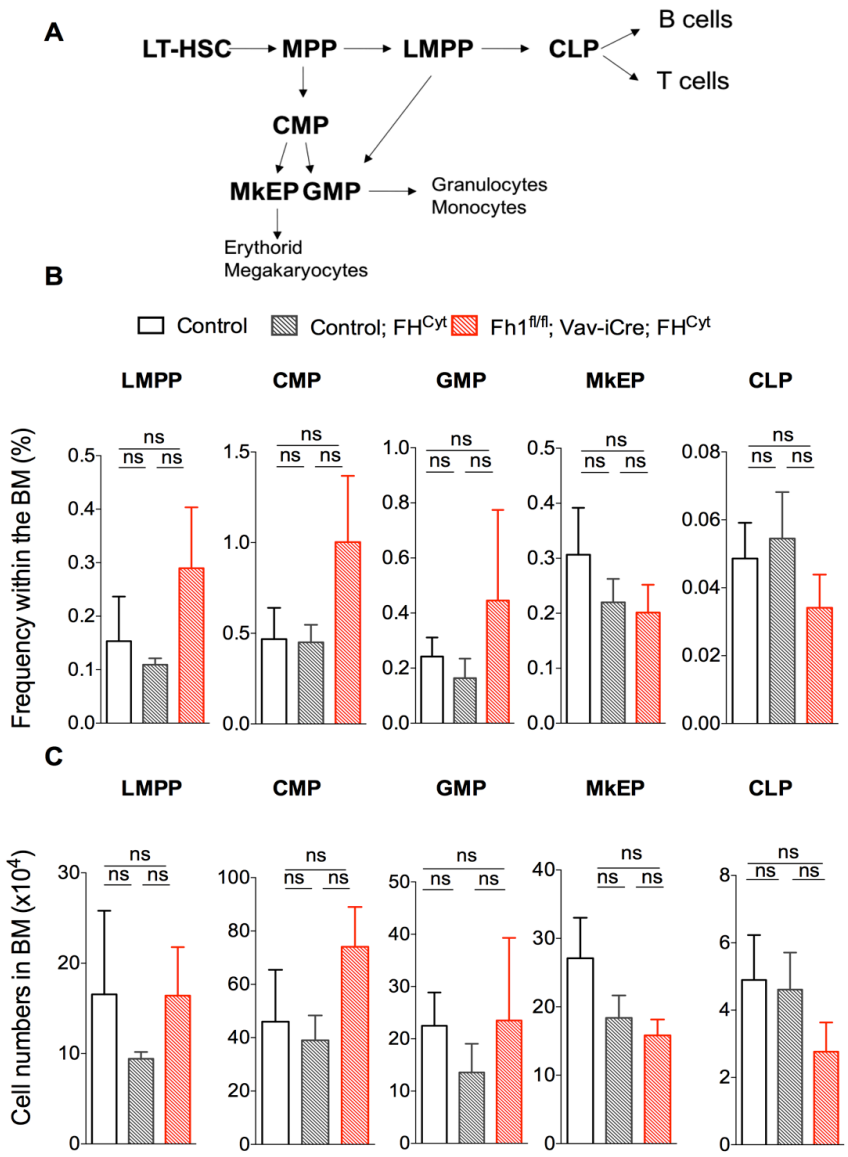

Figure 3-16. The distribution and absolute numbers of committed progenitor cells are not affected in *Fh1$^{fl/fl}$; FH^{Cyt}; Vav-iCre* mice. (A) Schematic representation of the haematopoietic hierarchy. LT-HSC; long-term haematopoietic stem cell, MPP; multipotent progenitor, LMPP; lymphoid-primed multipotent progenitor; CLP, common lymphoid progenitor, CMP; common myeloid progenitor, MkEP; megakaryocyte-erythrocyte progenitor, GMP; granulocyte-monocyte progenitor (Adapted from Adolfson et al., 2005). (B) Frequency and total cell numbers (C) of committed progenitor cells within the bone marrow of aged mice (per 1 femur and 1 tibia). LMPP (LSK CD34^{+} Flt3^{+}), CMP (Lin^{-}c-Kit^{+}Sca-1^{-} (LK) CD34^{+}CD16/32^{-}), GMP (LK, CD34^{+}CD16/32^{+}), MkEP (LK, CD34^{-} CD16/32^{-}), CLP (Lin^{-}c-Kit^{low}Sca-1^{low}CD127^{+}Flt3^{+}). The cell number was estimated by multiplying the frequency of each cell population by the total number of cells in the bone marrow. n = 4-5 biological replicates per genotype. Mice were analysed at 56-60 weeks. Graphs show mean ± S.E.M. ns, Mann-Whitney test.

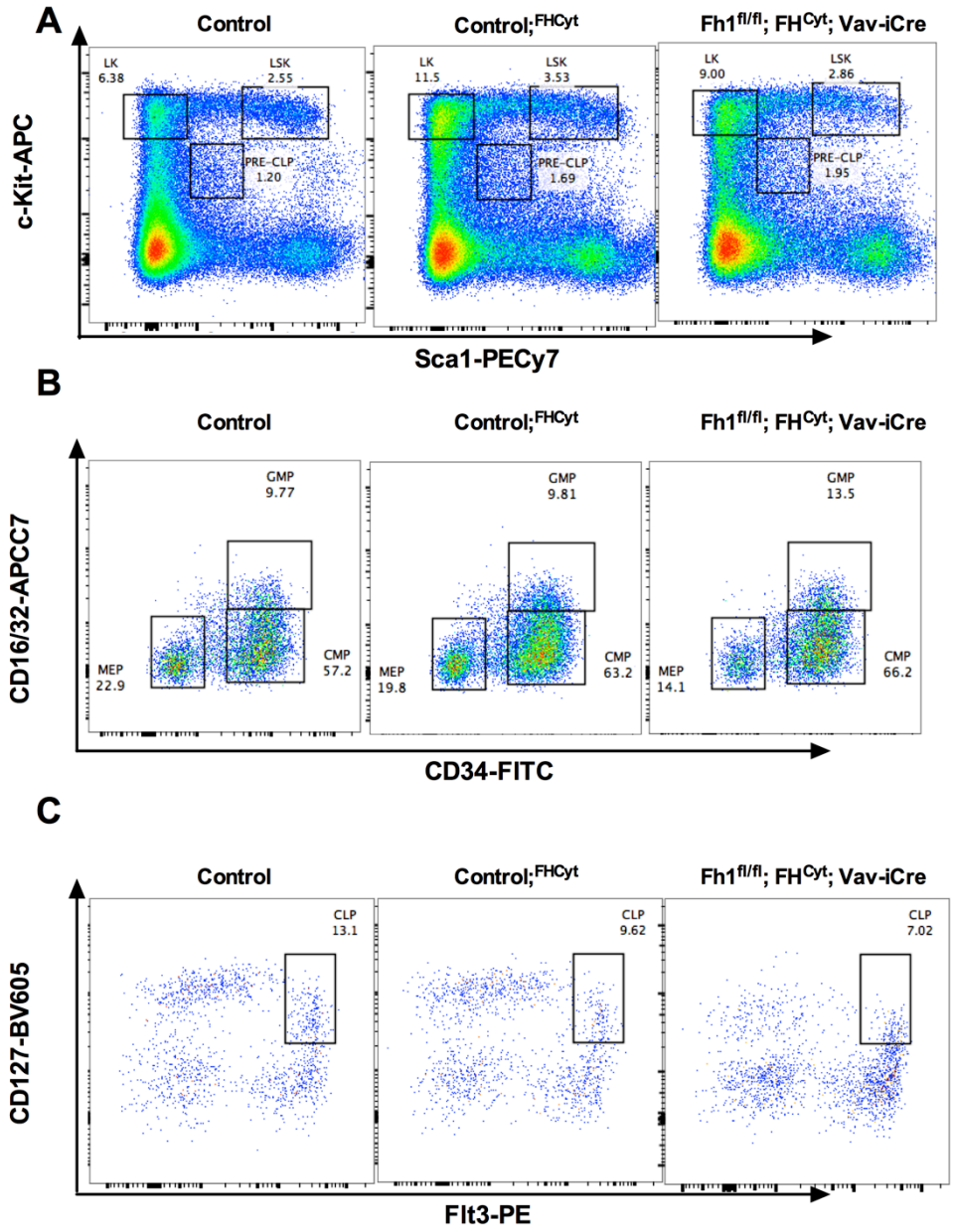

Figure 3-17. Representative FACS dot plots of committed progenitors. (A) This figure shows representative FACS plots for the isolation of LK ($Lin^-c\text{-}Kit^+Sca\text{-}1^-$) and pre-CLP ($Lin^-c\text{-}Kit^{low}Sca\text{-}1^{low}$) cells. (B) Shows representative FACS plots for the committed progenitor cells (GMP, CMP, MEP) arising from the LK gate. CMP ($Lin^-c\text{-}Kit^+Sca\text{-}1^-$ (LK) $CD34^+CD16/32^-$), GMP (LK, $CD34^+CD16/32^+$), MkEP (LK, $CD34^-CD16/32^-$). (C) Shows representative FACS plots for CLP progenitor cells ($Lin^-c\text{-}Kit^{low}Sca\text{-}1^{low}CD127^+Flt3^+$). FACS plots show *control* (left panels), *control; FH^{Cyt}* (middle panels) and *$Fh1^{fl/fl}$; FH^{Cyt}; Vav-iCre* (right panels).

3.5 Discussion

3.5.1 Primitive compartment of the haematopoietic system

In *Fh1*$^{fl/fl}$*; FH*^{Cyt}*; Vav-iCre* mice, the frequency of LSK cells, containing the most primitive compartment and the early haematopoietic progenitors, was increased. Within the LSK compartment, via the use of the SLAM markers CD48 and CD150 we observed a significant increase in the early progenitors HPC-1 and HPC-2. Based on transplantation studies, HPC-1 and HPC-2 cells contain a mixture of progenitor cells that can collectively give rise to all lineages (Oguro et al, 2013). More specifically, HPC-1 cells are able to transiently produce myeloid, B and T cells and to a lesser extent platelet cells. HPC-2 cells have a limited reconstitution capacity *in vivo* but are able to transiently produce erythrocytes and platelets and to a lesser extent myeloid and B cells (Oguro et al, 2013). However, even though their differentiation potential is somewhat understood, their relationship with oligopotent progenitor cells such as GMP, CMP or CLPs is not clear. As a result, we cannot infer whether the expansion of HPC-1 and HPC-2 cells has to correlate with a downstream expansion in one of the oligopotent compartments. It would have been of interest to investigate further the haematopoietic hierarchy in order to identify a potential deregulation in progenitor cells downstream of HPC-1 and HPC-2, which at the time of analysis was not considered. Specifically, it would be of interest to characterize the early erythroid-myeloid progenitors using the staining panel developed by Pronk et al (Pronk et al., 2007), in order to identify whether the expansion of HPC-1 and HPC-2 translates into an expansion of the erythroid-myeloid progenitors, therefore explaining the myeloid bias we observe. Finally, although I did not observe any significant changes in the frequency or the cell number of progenitor populations downstream of HPC-1 and HPC-2, there is a trend towards an increase in CMPs and a decrease in CLPs. Therefore, it is likely that if I utilised more biological replicates I would have observed a significant change, as there would be less variability within the biological replicates.

3.5.2 Lymphoid lineage

We showed that mice lacking mitochondrial *Fh1* exhibited a bias towards the myeloid compartment in expense of the B-cell lineage.

Recent studies have shown that lineage specification is dictated by distinct metabolic pathways. A recent study demonstrated that lineage commitment of human and murine HSCs is dependent on glutamine metabolism. Specifically, when the authors blocked the glutamine transporter ASCT2, erythropoietin-stimulated HSCs diverted to myelomonocytic differentiation, highlighting the importance of metabolic pathways in lineage commitments (Oburgoglu et al., 2014). In a similar manner, it is possible that, due to a genetic perturbation of the TCA cycle (as a result of *Fh1* deletion) HSCs are skewed towards a specific lineage.

In *Fh1*$^{fl/fl}$*; FH*^{Cyt}*; Vav-iCre* mice B cell (B220^{+} CD19^{+}) frequency and absolute cell numbers were decreased in the bone marrow, spleen and peripheral blood. However, the CLP and LMPP progenitors appeared normal in both frequency and absolute cell numbers in the *Fh1*$^{fl/fl}$*; FH*^{Cyt}*; Vav-iCre* mice, indicating that there might be a possible blockade downstream in the lymphoid differentiation.

B-cell development occurs in both the bone marrow and peripheral lymphoid organs such as the spleen. The initial stages of B cell differentiation occur within the bone marrow. In the bone marrow B cells that successfully go through the self-reactive checkpoint (checkpoint that eliminates autoreactive B cells), exit the bone marrow where they mature in peripheral organs. It would be interesting to decipher the exact stage at which B cell differentiation has been compromised in *Fh1*$^{fl/fl}$*; FH*^{Cyt}*; Vav-iCre* mice by using a larger panel of surface markers. However, it is clear that B cell differentiation or survival is compromised.

T cell maturation occurs in the thymus after CLP progenitors exit the bone marrow (Petrie et al., 2002). T cells then undergo differentiation steps typically defined by the expression of CD4 and CD8. To begin with, thymocytes start as double negative for CD4 and CD8 expression, then they become double positive and lastly maturing into single positive CD4^{+} or CD8^{+} (Anderson et al., 2001). Interestingly, the frequency of mature T cells (sum of single positive CD4 and CD8 cells) was not

altered in the thymus but was significantly decreased in the spleen. The spleen is an important site for lymphocyte traffic (Cesta et al, 2006). It is therefore possible that adhesion molecules involved in T cell homing to the spleen are absent in *Fh1*$^{fl/fl}$*; FH*^{Cyt}*; Vav-iCre* mice. For instance, lymphocytes lacking the lymphocyte- function associated antigen-1 (LFA-1) and alpha 4 beta 1 integrin, are unable to migrate to the white pulp of the spleen (Nolte et al., 2002; Lo et al., 2003).

Furthermore, it is interesting that we observed a significant dysregulation in B cell but not T lineage (with the exception of the decrease in the spleen that could be explained by the inability of cells to migrate to that site) in the organs that were analyzed. The difference we observed could be attributed to the differential metabolic requirements of these two lineages. B cells have been shown to utilise glycolysis and oxidative phosphorylation at equal rates. Conversely, in order for B cells to produce antibodies, they upregulate glycolysis to specifically convert pyruvate to lactate and inhibition of glycolysis leads to suppression of antibody production (Caro-Maldonado et al., 2014; Doughty et al., 2006). However, the importance of oxidative phosphorylation is not well understood, but literature highlights that a fine balance between glycolysis and oxidative phosphorylation is required for their maintenance. Given the fact that we deleted a key enzyme of the TCA cycle, it is possible that the fine-tuning of these pathways might be disrupted and as a result, B cell maturation is limited.

Conversely, relatively quiescent T cells primarily utilise oxidative phosphorylation and lipid oxidation (MacIver et al., 2013). However, activated T cells robustly proliferate and utilise glycolysis in order to meet their energetic demands (Chen et al., 2013; Pearce et al.,2013; MacIver et al., 2013; Caro-Maldonado et al., 2014). Overall, it is plausible that since T cells do not heavily rely on oxidative phosphorylation, they are not affected by deletion of mitochondrial *Fh1* (and thus the potential genetic perturbation of the TCA cycle). On the other hand, since B cells appear to require a fine-tuned ratio of oxidative phosphorylation and glycolysis it is possible that mitochondrial *Fh1* deletion would lead to deleterious effects on the B cell lineage.

3.5.3 Myeloid lineage

The disruption of the lymphoid lineage could result in a bias towards the myeloid lineage as a compensatory mechanism, rather than *Fh1* deletion having a direct effect on the myeloid lineage. Interestingly, recent findings indicate that myeloid cells exhibit a glycolytic rather than oxidative phosphorylation phenotype. Specifically, a recent study showed that neutrophils (and to a lesser extent monocytes), have little to no dependency on oxidative phosphorylation (Chacko et al., 2013). These conclusions were drawn based on the seahorse assay, that measures the oxygen consumption rate of cells, directly translating to what extent cells use oxidative phosphorylation.

Furthermore, is also worth noting that we only observed an expansion of the differentiated myeloid lineage in the peripheral blood and spleen of the mice and not in the bone marrow. Overall, these data suggest that since myeloid cells do not appear to critically rely on oxidative phosphorylation, mitochondrial *Fh1* deletion (and the resultant genetic perturbation of the TCA cycle), would not negatively impact the myeloid lineage. Most importantly, the most likely explanation regarding the increased frequency of the myeloid lineage, is the depletion of the B cell lineage.

3.6 Summary

In summary, even though we observed a persistent myeloid expansion in the peripheral blood of the $Fh1^{fl/fl}$; FH^{Cyt}; *Vav-iCre* mice, the mice did not spontaneously develop AML, potentially indicating that if mitochondrial *Fh1* deletion is involved in leukaemogenesis, it may be only one of the co-operative events required for AML development. Furthermore, while we observed only a minimal dysregulation in the most primitive haematopoietic compartment of these mice, we observed a drastic decrease in the B cell lineage but not the T cells lineage (Figure 3-18). Given the fact that mitochondrial *Fh1* deletion resulted in a genetic truncation of the TCA, these data could potentially highlight the distinct metabolic requirements of B, T and myeloid cells.

	Organ		Frequency	Cell number
Haematopoietic stem and early progenitor cells	Bone marrow		HPC-1 ↑↑ HPC-2 ↑↑	HPC-1 **ND** HPC-2 **ND**
Committed lineage progenitors	Bone marrow		**ND**	**ND**
Mature blood cells	Bone marrow		B cells ↓↓ T cells **ND** Myeloid cells **ND**	B cells ↓↓ T cells - Myeloid cells **ND**
	Peripheral blood		B cells ↓↓ T cells **ND** Myeloid cells ↑↑	-
	Spleen		B cells ↓↓ T cells ↓↓ Myeloid cells ↑↑	-
	Thymus		T cells **ND**	-

Figure 3-18. Summary of changes in the different haematopoietic compartments of *Fh1$^{fl/fl}$; FH^{Cyt}; Vav-iCre* mice. The table indicates changes between *Fh1$^{fl/fl}$; FH^{Cyt}; Vav-iCre* and *control* mice. ND: no difference observed, arrow pointing downwards indicates a decrease in the cell population while the arrow pointing upwards indicates an increase in the cell population, - indicates that analysis was not performed. LT-HSC: long-term haematopoietic stem cell, HPC-1: haematopoietic progenitor cell 1, HPC-2: haematopoietic progenitor cell 2.

CHAPTER 4

The role of mitochondrial *Fh1* and the TCA in leukaemic transformation

4 The role of mitochondrial *Fh1* and the TCA in leukaemic transformation

4.1 Introduction

Alterations in cellular metabolism represent a hallmark of cancer (Hanahan and Weinberg, 2011). Until recently, it was widely accepted that most cancer cells rely more on glycolysis rather than oxidative phosphorylation in order to meet their energy demands (Warburg, 1956), (Gatenby and Gillies, 2004).

However, recent studies have demonstrated that some cancer cells rely on oxidative phosphorylation rather than on glycolysis. For example, Sugamuma et al., showed that while some AML cell lines such as NB4 rely more on glycolysis, other cells such as THP1 rely more on oxidative phosphorylation, as demonstrated by the induction of cell death of THP1 cells through inhibition of ATP synthase (by treatment with oligomycin) (Suganuma et al., 2010). Similarly, a recent study showed that cells isolated from CLL patients primarily utilise oxidative phosphorylation and inhibition of such (using a benzodiazepine derivative that blocks ATP synthase), led to cell death (Jitschin et al., 2014). In another study, quiescent leukaemic stem cells (LSCs) exhibited low ROS, relied more on oxidative phosphorylation and underwent cell death when oxidative phosphorylation was inhibited (Lagadinou et al., 2013). Furthermore, in another study, to address whether loss of mitochondrial function *in vivo* impacts tumorigenesis, the authors crossed the Kras-driven lung cancer model with mice harbouring floxed alleles of the mitochondrial transcription factor *Tfam* (Weinberg et al., 2010s). TFAM is required for mitochondrial DNA replication and *Tfam*-null cells are deficient in electron transport and OXPHOS. *Cre*-treated Kras-G12D-*Tfam*-null mice exhibited smaller tumours, indicating that functional mitochondrial electron transport chain is required for tumorigenesis (Weinberg et al., 2010). Additionally, knock-down of p32, a mitochondrial membrane protein, in the breast carcinoma cell line MDA-MB-435 shifted their metabolism from OXPHOS, as indicated a decrease in the activity of complexes III and IV of the electron transport chain, to glycolysis, as indicated by

increased glucose consumption and lactate production, and reduced their viability *in vitro*. Furthermore, knock-down of p32 in the highly aggressive MDA-MB-231 D3H2LN breast cancer cell line, reduced tumour development in nude mice (Fogal et al., 2010). More recently, it was shown that when compared to normal haematopoietic cells, AML cell lines and patient samples exhibited low maximal respiration capacity and increased mitochondrial mass with no corroborative increase in the activity of the electron transport chain. As a result, the cells were more susceptible to oxidative stress and preferentially underwent cell death (Sriskanthadevan et al., 2015).

Collectively, the studies available suggest that there is a lot more to be understood about cancer metabolism and that there is wide heterogeneity when considering the metabolic properties of cancer cells. With that in mind, this chapter aims to uncover the importance of mitochondrial respiration through the genetic deletion of the key TCA enzyme *Fh1* in malignant haematopoiesis, utilizing the retroviral *Meis1/Hoxa9* AML model.

4.1.1 Meis1/Hoxa9 retroviral model

For the purpose of this chapter, I utilised the *Meis1/ Hoxa9* retroviral model. *Meis1* and *Hoxa9* are oncogenes frequently deregulated in AML patients. Furthermore, their over-expression leads to immortalisation of haematopoietic stem and progenitor cells (Zeisig and Wai Eric So, 2009). Out of 6817 genes, *Hoxa9* is the single most highly correlated gene with poor prognosis (Golub et al., 1999). The *Meis1/Hoxa9* retroviral AML mouse model is well characterised and is widely used in leukaemic studies (Kroon et al., 1998b) (Thorsteinsdottir et al., 2001) (Pineault et al., 2002) (Thorsteinsdottir et al., 2002). The use of this model has the advantage to study the requirement of *Fh1* in a step-wise manner. Below, I describe the implication of *Hoxa9* and *Meis1* genes in normal haematopoiesis and leukaemogenesis.

4.1.2 Hoxa9

The clustered Hox family of homeobox genes (class I homeobox genes) is an evolutionarily highly conserved set of genes encoding DNA-binding transcription factors that were first identified as key regulators in positional identification of cells

during development (Krumlaf et al, 1994). In mammals, there are 39 *Hox* genes organised into 4 distinct genomic clusters (A-D) located on four different chromosomes. Gene expression analyses showed that the majority of *Hox* genes are highly expressed in the most primitive compartment of the haematopoietic system while down regulated in more differentiated cells, suggesting that the *Hox* genes play key roles in primitive haematopoietic cells, and that dysregulation of such genes may impact leukaemic transformation (Sauvengeau et al., 1994; Pineault et al., 2002; Giampaolo et al., 1994; Kawagoe et al., 1999). Like most *Hox* genes *Hoxa9* is highly expressed in foetal liver (FL) and bone marrow (BM) primitive haematopoietic cells and is downregulated during differentiation (Sauvengeau et al., 1994; Pineault et al., 2002). Indeed, *Hoxa9*-deficient mice exhibited multilineage defects (Lawrence et al., 1997). Competitive repopulation assays revealed that the major defect of Hoxa9$^{-/-}$ animals was the inability of HSCs to repopulate haematopoiesis in recipient mice (Lawrence et al., 1997), suggesting that *Hoxa9* is crucial for HSC self-renewal. This was reinforced by the fact that overexpression of *Hoxa9* can enhance HSC regeneration *in vivo,* with additional defects in differentiation that eventually led to leukaemia (Thorsteinsdottir et al., 2002). HOX proteins, bind target DNA with little obvious selectivity (Argiropoulos et al., 2007). HOX cofactors have been shown to directly interact with HOX proteins to increase their DNA-binding affinity and to modify their transregulatory properties (Argiropoulos et al, 2007). HOX proteins from paralog groups 1-10 have been shown to interact with PBX1 while those from paralog groups 9-13 interact with Meis1a (Shen et al., 1997).

4.1.3 Meis1

Meis1 also belongs to the Hox family of homeobox genes and is expressed in foetal HSC compartments (Krumlaf et al, 1994; Azcoitia et al., 2005). Similarly to *Hoxa9*, *Meis1* is expressed in the most primitive haematopoietic subpopulations and is downregulated during differentiation (Argiropoulos et al., 2007; Pineault et al., 2002). Deletion of *Meis1* causes embryonic lethality by embryonic day 14.5, causing multiple vascular and haematopoietic effects. *Meis1* was first identified as a common viral integration site in myeloid leukaemic cells of BXH-2 mice (Moskow et al., 1995). The importance of MEIS1 in human leukaemogenesis was highlighted by the

finding that it was frequently up-regulated in primary AML and acute lymphoblastic leukaemia samples (Kawagoe et al., 1999; Imamura et al., 2002; Rozovskaia et al., 2001). Interestingly, *Meis1* has no transforming capacity alone (Kroon et al., 1998b).

Co-activation of HOXA9 with MEIS1 is a frequent occurrence in leukaemias associated with MLL rearrangements (Yeoh et al., 2002; Kohlmann et al.,2003; Fine et al., 2004; Tsutsumi et al., 2003). Indeed, co-overexpression of *Hoxa9* and *Meis1* in murine bone marrow cells recapitulates *MLL-ENL*-mediated immortalisation of myeloid progenitor cells (Zeisig et al., 2004). Furthermore, in another study the authors showed that the ability of MLL fusion proteins to induce and maintain leukaemic transformation in progenitor cells, was dependent and rate-limited by *Meis1* (Wong et al., 2007).

4.2 Aims

As described in chapter 3 $Fh1^{fl/fl}$; FH^{Cyt}; *Vav-iCre* cells lack the expression of the mitochondrial isoform of *Fh1* but express the human cytosolic isoform (FH^{Cyt}). This modification results in a genetic truncation of the TCA cycle while fumarate is metabolized efficiently in the cytoplasm. We have previously demonstrated in the lab that $Fh1^{fl/fl}$; *Vav-iCre* mice are not viable but the expression of the cytosolic isoform rescues lethality, indicating that the cytosolic expression of *Fh1* is essential. The aims of this chapter were to assess the importance of intact TCA cycle in:

- The generation of pre-LCs
- The generation of LICs
- Maintenance of LICs

4.3 Experimental design

4.3.1 Generation of pre-LCs and LICs

In order to address the points above I utilised the retroviral model *Meis1/Hoxa9,* as described in the previous chapter. Briefly, LSK cells were isolated from the foetal liver of *control* ($Fh1^{fl/fl}$, *Vav-iCre* negative), *control;* FH^{Cyt} ($Fh1^{fl/fl}$, *Vav-iCre* negative, expressing the cytosolic isoform of human *FH*) and $Fh1^{fl/fl}$; FH^{Cyt}; *Vav-*

iCre (*Fh1*$^{fl/fl}$*; Vav-iCre* positive cells that lack mitochondrial *Fh1* but express the cytosolic isoform of human *FH;* thereafter referred to as cells lacking mitochondrial *Fh1*) 14.5 dpc embryos and were infected with retroviruses over-expressing *Meis1/Hoxa9.* Cells over-expressing *Meis1* and *Hoxa9* were then selected based on their antibiotic resistance to puromycin and neomycin, respectively. Selected cells subsequently underwent three rounds of serial re-plating in semi solid media. The established pre-LCs were then injected into primary recipient mice (for the outline of the experimental design, see Figure 4-1 A).

4.3.2 Maintenance of LICs

In order to assess the role of mitochondrial *Fh1* in the maintenance of self-renewal capacity of LICs, I utilised the *Meis1/Hoxa9* model in an *Mx1-Cre* background, therefore allowing for the conditional deletion of *Fh1*. LSK cells (CD45.2^{+}) were isolated from the foetal liver of embryos at 14.5 dpc. The cells were isolated from embryos of the following genotypes: *control* (*Fh1*$^{fl/fl}$; *Mx1-Cre* negative), *control; FH*^{Cyt} (*Fh1*$^{fl/fl}$*; Mx1-Cre* negative cells that over-express the cytosolic isoform of FH) and *Fh1*$^{fl/fl}$*; FH*^{Cyt}; *Mx1-Cre* (*Fh1*$^{fl/fl}$*; Mx1-Cre* positive cells that over-express the cytosolic isoform of FH). After isolation, the cells were subsequently infected with retroviruses over-expressing *Meis1* and *Hoxa9.* The cells over-expressing *Meis1* and *Hoxa9* were then selected based on their antibiotic resistance to puromycin and neomycin, respectively. The cells were then serially re-plated in semi-solid media. 100,000 of the resultant pre-LCs were injected in sub-lethally irradiated recipient mice (CD45.1^{+}/CD45.2^{+}). Once the chimerism of leukaemic CD45.2^{+} cells reached 20-30 % in the peripheral blood of the recipient mice, the mice were intra-peritoneally injected 6-8 times every alternate day with 300μg poly (I:C), in order to induce the deletion of *Fh1*. This experiment allows for the study of the generation of LICs. In order to assess the maintenance of the self-renewal capacity of LICs, 10,000 LICs (CD45.2^{+}c-Kit^{+}) were transplanted into secondary sub-lethally irradiated recipient mice (for the outline of the experimental design, see Figure 4-1 B).

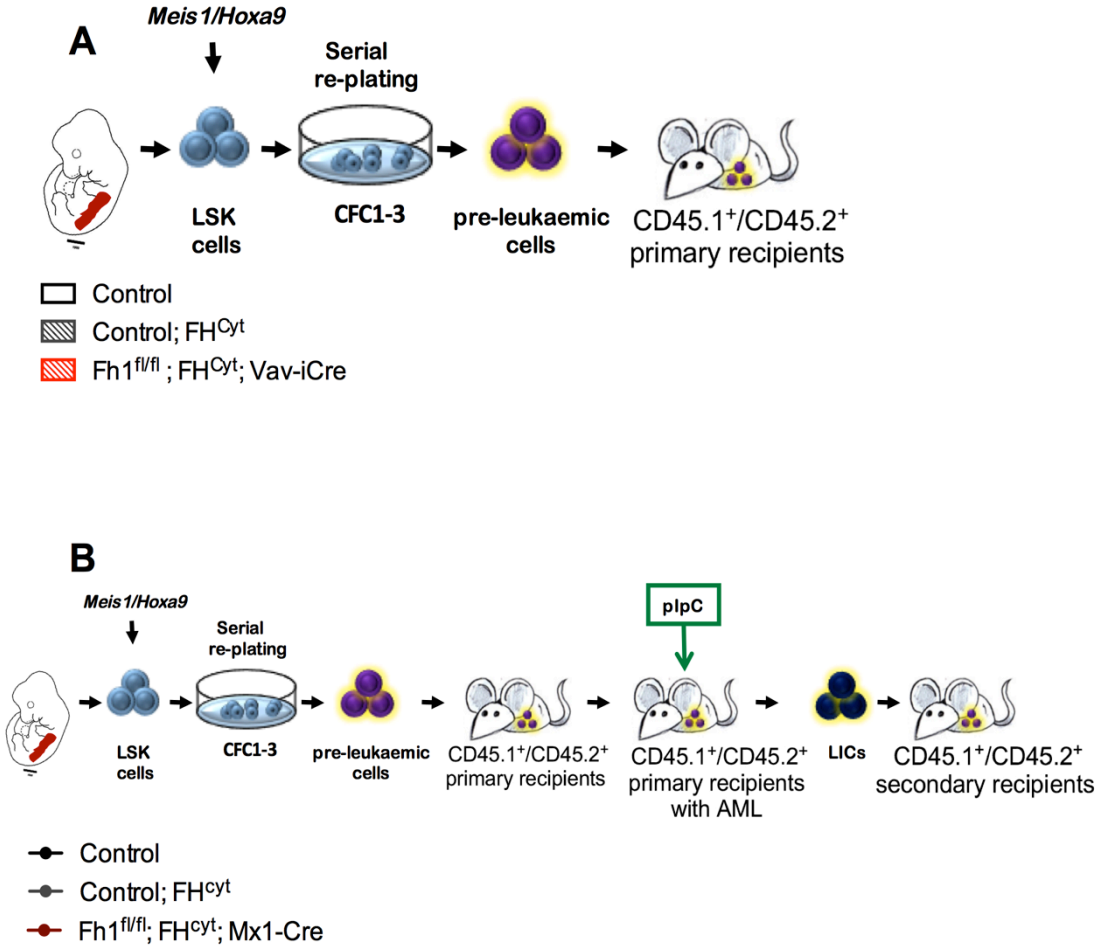

Figure 4-1. Experimental design. (A) LSK cells were isolated from the foetal liver of *control* (*Fh1*$^{fl/fl}$, *Vav-iCre* negative), *control; FH*^{Cyt} (*Fh1*$^{fl/fl}$, *Vav-iCre* negative, expressing the cytosolic isoform of human *FH*) and *Fh1*$^{fl/fl}$*; FH*^{Cyt}*; Vav-iCre* (*Fh1*$^{fl/fl}$*; Vav-iCre* positive cells that lack mitochondrial *Fh1* but express the cytosolic isoform of human FH; thereafter referred to as cells lacking mitochondrial *Fh1*) 14.5 dpc embryos and were infected with retroviruses over-expressing Meis1/Hoxa9. Cells over-expressing *Meis1* and *Hoxa9* were then selected based on their antibiotic resistance to puromycin and neomycin, respectively. Selected cells subsequently underwent three rounds of serial re-plating in semi solid media. The established pre-LCs were then injected into primary recipient mice**.** (B) LSK cells (CD45.2^{+}) were isolated from the foetal liver of embryos at 14.5 dpc. The cells were isolated from embryos of the following genotypes: *control* (*Fh1*$^{fl/fl}$*; Mx1-Cre negative*), *control; FH*^{Cyt} (*Fh1*$^{fl/fl}$*; Mx1-Cre* negative that over-express the cytosolic isoform of *FH*) and *Fh1*$^{fl/fl}$*; FH*^{Cyt}*; Mx1-Cre* (*Fh1*$^{fl/fl}$*; Mx1-Cre* positive cells that over-express the cytosolic isoform of *FH*). After isolation, the cells were subsequently infected with retroviruses over-expressing *Meis1* and *Hoxa9*. The cells over-expressing *Meis1* and *Hoxa9* were then selected based on their antibiotic resistance to puromycin and neomycin, respectively. The cells were then serially re-plated in semi-solid media. 100,000 of the resultant pre-LCs were injected in sub-lethally irradiated recipient mice (CD45.1^{+}/CD45.2^{+}). Once the chimerism of leukaemic CD45.2^{+} cells reached 20-30 % in the peripheral blood of the recipient mice, the mice were intra-peritoneally injected 6-8 times every alternate day with 300µg poly (I:C), in order to induce the deletion of *Fh1*.

4.4 Results

4.4.1 Mitochondrial Fh1 deletion does not affect the transforming capacity of cells

We wanted to assess the importance of mitochondrial *Fh1* deletion in leukaemic transformation. To address this aim, I isolated LSK cells from the foetal liver of *control*, *control; FH^{Cyt}* and *$Fh1^{fl/fl}$; FH^{Cyt}; Vav-iCre* 14.5 dpc embryos and infected them with retroviruses over-expressing *Meis1* and *Hoxa9,* in order to assess the transforming and clonogenic capacity of cells lacking mitochondrial *Fh1*. The cells were able to efficiently generate colonies *in vitro,* indicating that a genetically intact TCA is not necessary for leukaemic transformation, at least using the *Meis1/Hoxa9* retroviral model (Figure 4-2A). Pre-LCs lacking mitochondrial *Fh1* (but expressing FH^{Cyt}), had a smaller average colony size compared to *control* cells, potentially indicating a slower proliferation rate (Figure 4-2 B-E).

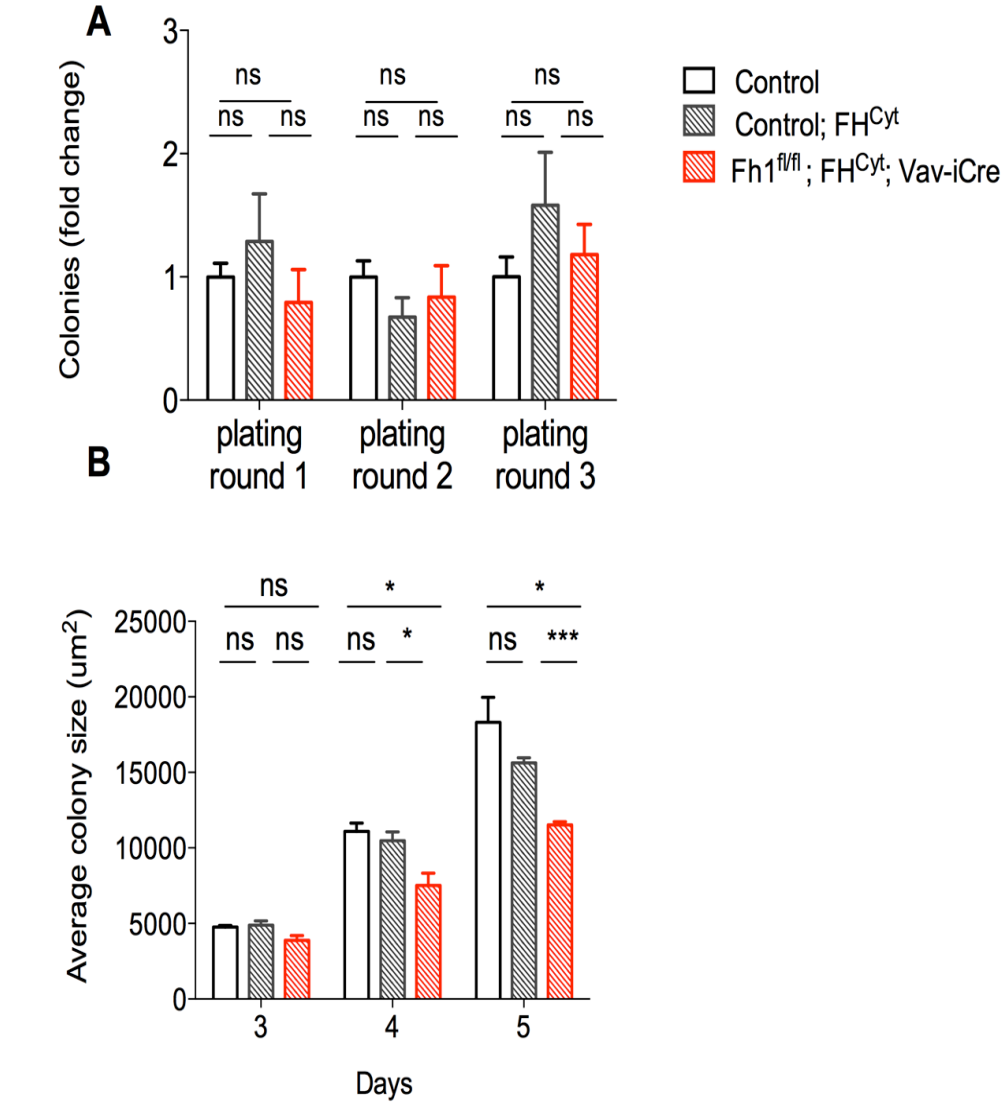

Figure 4-2. Assessing colony number and colony size of pre-LCs lacking mitochondrial *Fh1*. (A) CFC counts at each re-plating (plating round 1, 2 and 3) are shown. Data are mean ± S.E.M., n = 6-8 biological replicates per genotype. Cells were seeded at a density of 2,500 cells per well. Colonies were counted 6 days post seeding. (B) Graph shows average colony size in um^2. Data are mean ± S.E.M., n = 3 biological replicates per genotype. 500 cells per 96-well plate well were seeded. 5 technical replicates were seeded for each biological replicate. Counting of colonies was performed using the Perkin Elmer Operetta high content imaging system at day 3, 4 and 5 post seeding. (C-E) Representative colony images of *control* (C), *control; FH^{Cyt}*, (D) and *$Fh1^{fl/fl}$; FH^{Cyt}; Vav-iCre*. Images were at 4X magnification. Unpaired t test, * $p< 0.05$, ***$p< 0.001$

4.4.1.1 *In vitro* characterisation of pre-LCs lacking mitochondrial *Fh1*

In order to address the possibility of a slower proliferation rate in pre-LCs lacking mitochondrial *Fh1,* I performed a proliferation assay, counting the cumulative cell number over the span of 48 hours. $Fh1^{fl/fl}$; FH^{Cyt}; *Vav-iCre* cells had a proliferation rate comparative to that of *control* and *control;* FH^{Cyt} cells (Figure 4-3 A). Furthermore, in the span of 48 hours $Fh1^{fl/fl}$; FH^{Cyt}; *Vav-iCre* cells exhibited differences in the percentage of apoptotic cells compared to *control* and *control;* FH^{Cyt} cells (Figure 4-3 B). Specifically, $Fh1^{fl/fl}$; FH^{Cyt}; *Vav-iCre* cells had an average percentage of apoptotic and late apoptotic cells of 2.8 % and 6.3 % respectively, while *control* cells and *control;* FH^{Cyt} cells exhibited a percentage of 4.5 %, 18.8 % and 6.26 %, 19.1 % respectively. Of note, there was no difference in the cell cycle status of the pre-LCs lacking mitochondrial *Fh1* (Figure 4-4). Furthermore, the fraction of cells in the sub-G0 phase can be indicative of the fraction of apoptotic cells. Pre-LCs lacking mitochondrial *Fh1* had a significantly lower percentage of sub-G0 cells after 48 hours, corroborating well with the data obtained from the annexin V assay (Figure 4-5). Collectively, these data indicate that there is no difference in the proliferation rate or cell cycle status, but that a higher percentage of cells are alive within the $Fh1^{fl/fl}$; FH^{Cyt}; *Vav-iCre* population.

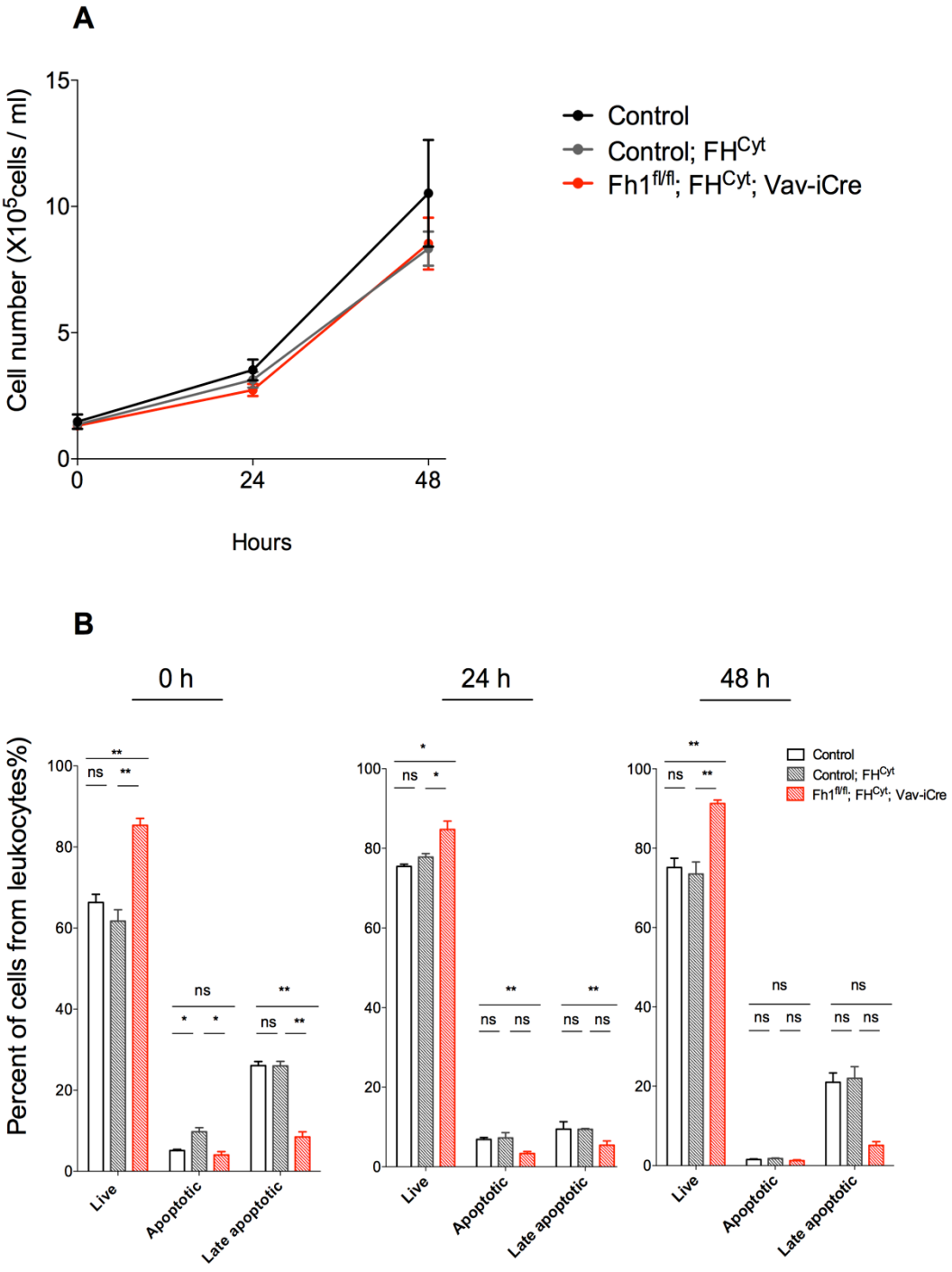

Figure 4-3. Pre-leukaemic cells lacking mitochondrial *Fh1* exhibit normal proliferation rate but lower cell death rate. (A) Proliferation curves of pre-leukaemic cells in liquid culture. Cell were seeded at a concentration of 150,000 cells/ml. ns, Unpaired t test performed between each time point (B) Apoptosis assay using annexin V-FITC and DAPI staining analysed using flow cytometry 0 (left), 24 (middle) and 48 hours (right) after seeding. Data are mean ± S.E.M, n = 3 biological replicates. unpaired t test, *p<0.05, ** p<0.001

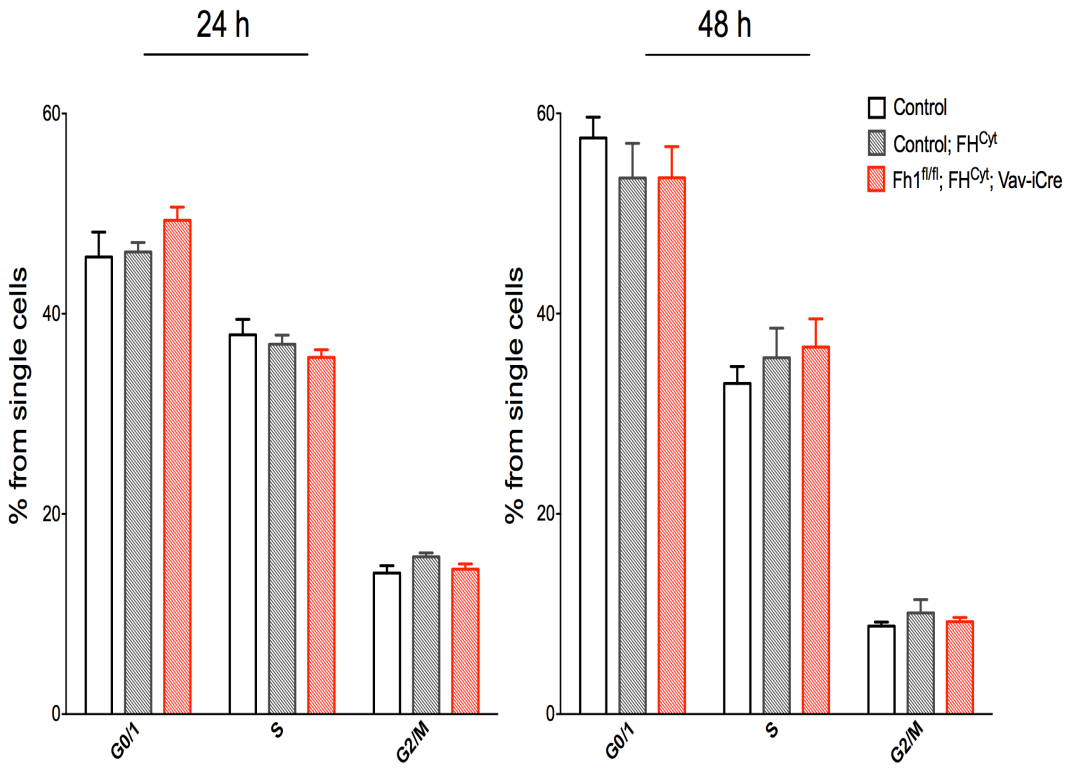

Figure 4-4. pre-LC cells lacking mitochondrial *Fh1* exhibit normal cell cycle status. Cell-cycle analysis of pre-leukaemic cells. Graph indicates percentage of cells (from the single cell gate) at each stage of the cell cycle at 24hours (left) and 48hours (right). Data are mean ± S.E.M., n = 3 biological replicates per genotype, 3 technical replicates. This is a representative experiment carried out twice. Analysis was performed using DAPI (containing 0.1% Triton) staining and cells were analysed via flow cytometry. ns, Unpaired t test. (For gating strategy see section 2.13.11).

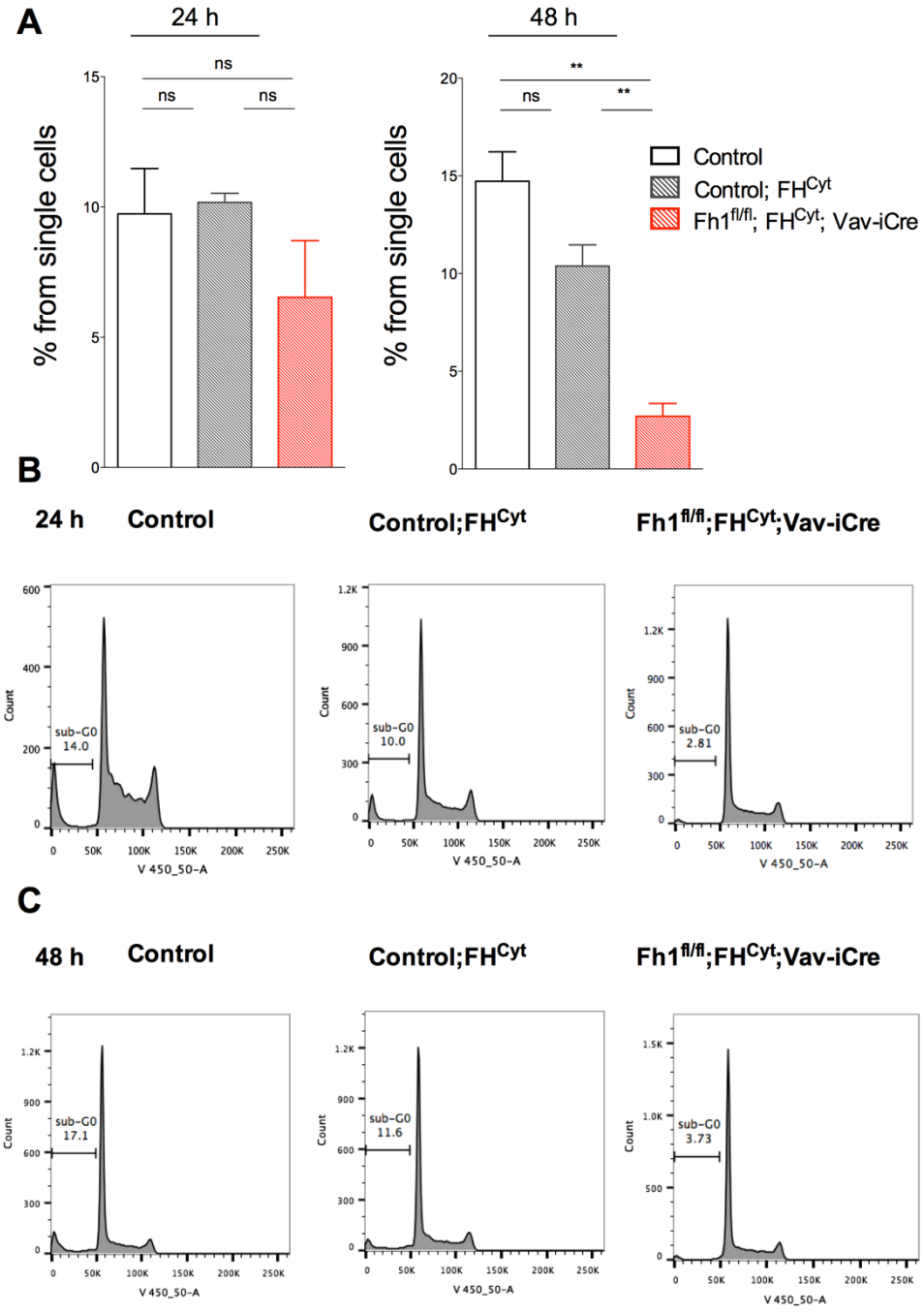

Figure 4-5. Sub-G0 phase of pre-LCs indicative of cell death rate. (A-B) Graphs indicate percentage of cells (from the single cell gate used to exclude doublets) in the sub-G0 phase of cell cycle. Sub-G0 fraction was determined based on the DNA content of cells, using DAPI and analysing cells via flow cytometry. (B-C) Representative histograms indicating how the sub-G0 phase was determined at 24 hours (B) and at 48 hours (C) for *control* (left), *control; FH^{Cyt}* (middle) and *Fh1$^{fl/fl}$; FH^{Cyt}; Vav-iCre* (right). Representative of two experiments. n = 3 biological replicates per genotype, Data are mean ± S.E.M, ** p<0.01, Unpaired t test.

4.4.2 Mitochondrial Fh1 and genetically intact TCA are required for AML generation in vivo

After characterising the pre-LCs lacking mitochondrial *Fh1 in vitro*, I wanted to assess whether mitochondrial *Fh1* (and effectively intact TCA) is required for AML propagation. To this end, 100,000 pre-LCs (myeloid cells that are $CD45.2^+$/ $c\text{-}Kit^+$) were injected into sub-lethally irradiated recipient mice ($CD45.1^+/CD45.2^+$) (Figure 4-6 A, B). Equal expression of *Meis1* and *Hoxa9* was confirmed via qRT-PCR (Figure 4-7 A, B). Interestingly, the percentage of surviving recipient mice that were injected with pre-LCs lacking mitochondrial *Fh1* was much higher than the mice injected with *control* or *control;* FH^{Cyt} pre-LCs (Figure 4-7 C). Specifically, while only 25 % and 30 % of *control* and *control;* FH^{Cyt} respectively recipient mice survived, 76 % of mice injected with pre-LCs lacking *Fh1* survived (Figure 4-7 D). At the point of sacrifice, the bone marrow and spleen of recipient mice were infiltrated with LICs expressing myeloid markers, confirming that the mice succumbed to AML (Figure 4-8 A-B). Furthermore, mice also exhibited splenomegaly at the time of sacrifice (Figure 4-8 C). These data indicate that mitochondrial *Fh1* and genetically intact TCA are required for efficient generation of LICs.

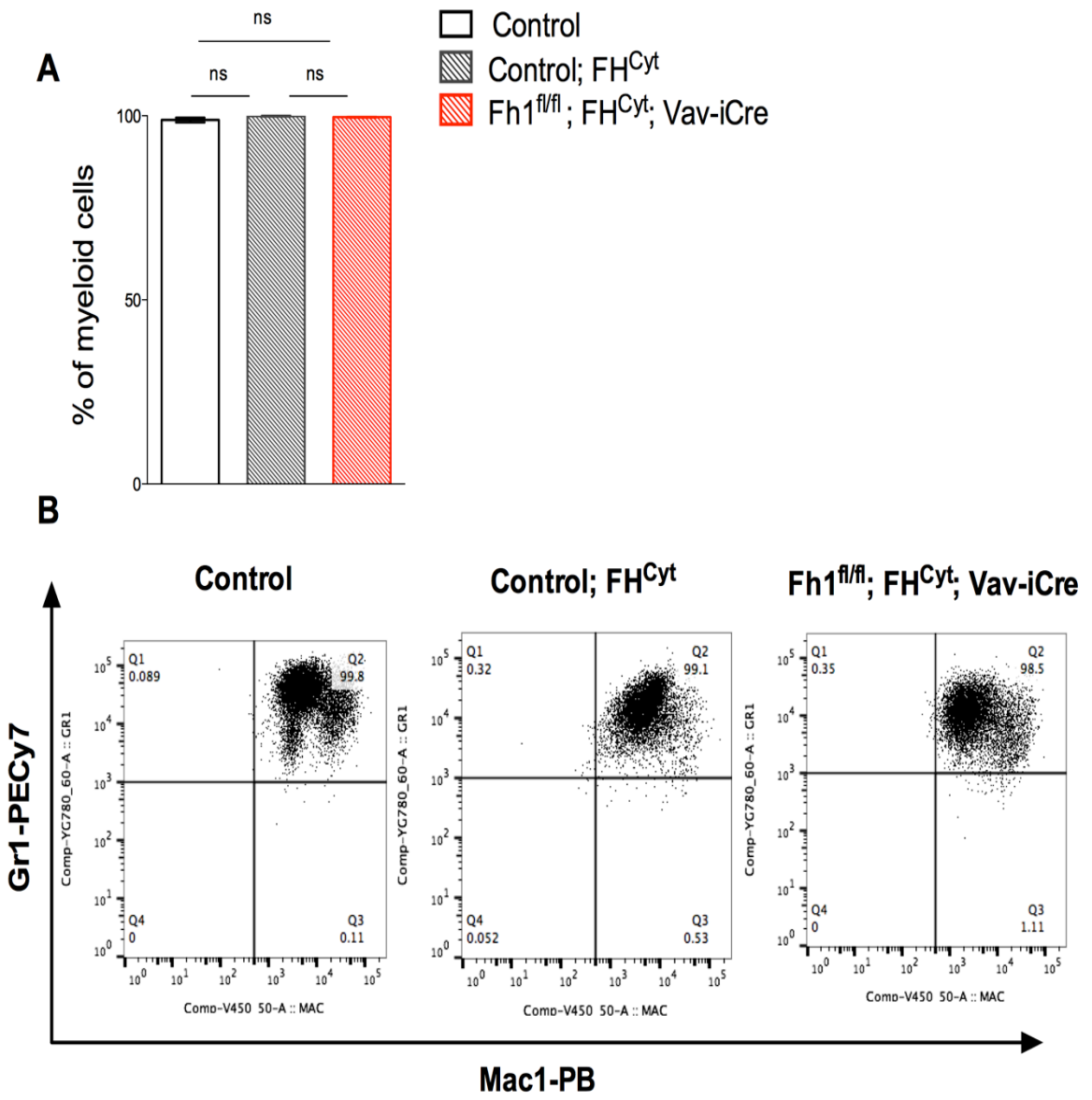

Figure 4-6. Flow cytometry profile of pre-LCs lacking mitochondrial *Fh1*. (A) Graph shows percentage of myeloid cells of pre-LCs of the indicated genotypes. Cells were analysed via flow cytometry after harvesting from the third serial re-plating. Myeloid cells are the sum of Mac-1^{+}/Gr1^{+} and Mac-1^{+}. (B) Representative flow cytometry profiles of *control* (left panel), *control; FH^{Cyt}*, (middle panel) and *Fh1$^{fl/fl}$; FH^{Cyt}; Vav-iCre* (right panel). n = 3 biological replicates per genotype. Graphs show mean ± S.E.M, ns, Mann-Whitney test.

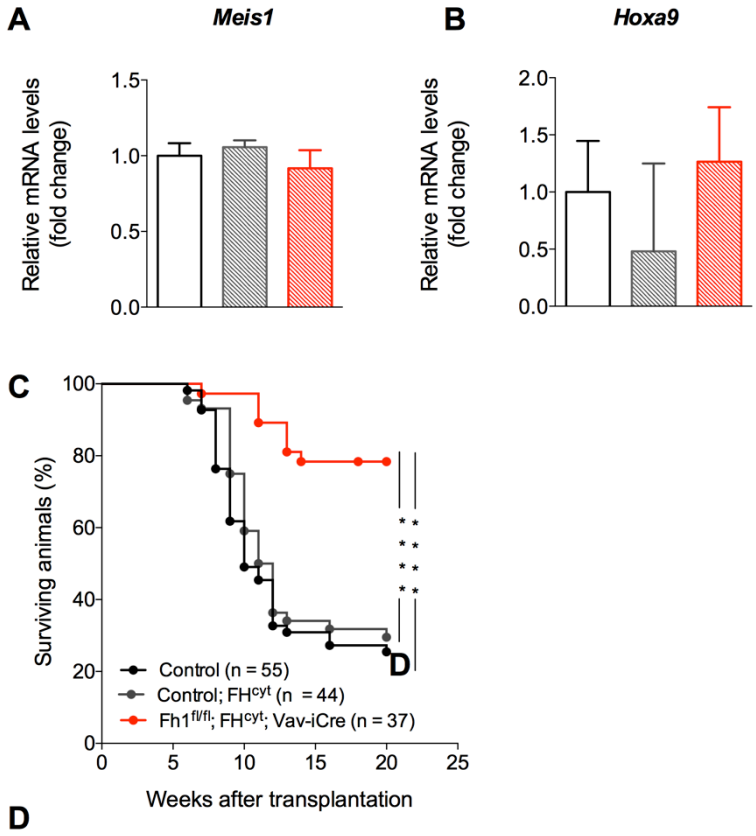

D

	Control	Control;FH^{Cyt}	Fh1$^{fl/fl}$; FH^{Cyt}; Vav-iCre
Surviving animals	14	13	28
Dead animals	41	31	9
% of surviving animals	25	30	76
Total animals	**55**	**44**	**37**

Figure 4-7. Mitochondrial *Fh1* is required for efficient LIC generation. (A-B) Relative mRNA expression of *Meis1* (A) and *Hoxa9* (B) in pre-LCs after CFC3, before transplantation into recipient mice. The analysis was performed using *control* as a reference point, and β -actin as a housekeeping gene (CT method). n = 3-6 biological replicates per genotype. (C) Kaplan-Meier survival curve of sub-lethally irradiated primary recipient mice transplanted with 100,000 c-Kit^{+} pre-leukaemic cells obtained from serial re-plating assays. (D) Table indicating recipient mice injected with LICs of the indicated genotypes, that succumbed to leukaemia or remained disease-free up to 20 weeks. n = 8-10 recipients per biological replicate, n = 4-6 biological replicates per genotype. **** p< 0.0001, Log-rank (Mantel-Cox) and Gehan-Breslow-Wicoxon tests.

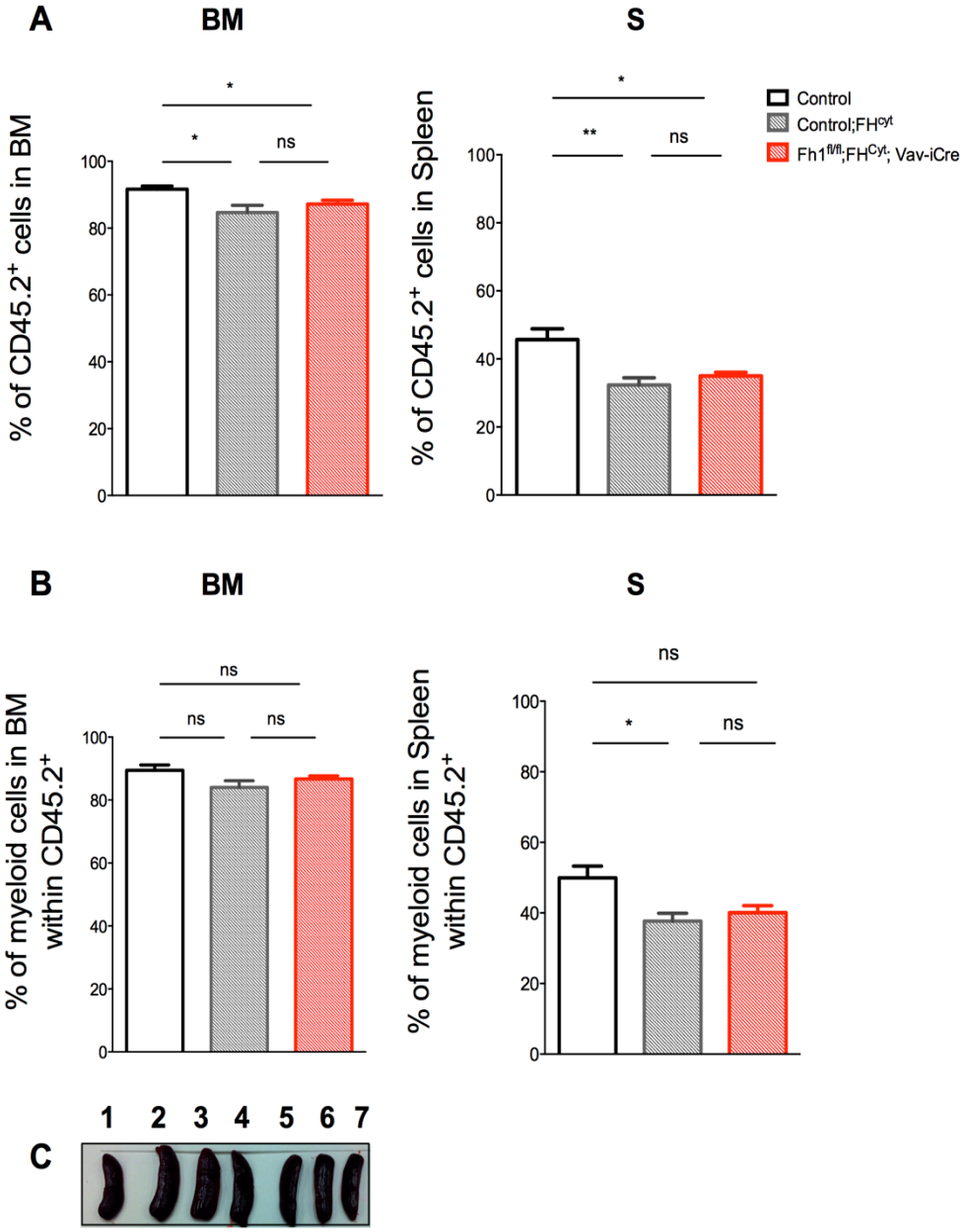

Figure 4-8. Infiltration of LICs in the bone marrow and spleen of recipient mice. (A) Percentage of CD45.2$^+$ LICs in the bone marrow (left) and spleen (right) of sick recipient mice at the point of sacrifice. (B) Percentage of myeloid cells in the bone marrow (left) and spleen (right) within the LIC compartment (myeloid cells were defined as the sum of Mac-1$^+$/Gr1$^+$ and Mac-1$^+$). (C) Representative image of spleens isolated from sick recipient mice at the point of sacrifice (lane 1 = *control*, lanes 2-4 = *control; FH^{Cyt}* mice, lanes 5-7 = *Fh1$^{fl/fl}$; FH^{Cyt}; Vav-iCre* mice). Graphs show mean ± S.E.M, n = 6-7 recipient mice per genotype, *p< 0.05, ** p<0.001, Mann-Whitney test.

4.4.3 LICs lacking mitochondrial Fh1 exhibit low spare respiratory capacity

Given the fact that mitochondrial *Fh1* is part of the TCA, and the TCA in an integral component of the electron transport chain, I wanted to assess whether deletion of such would result in dysfunction of mitochondrial respiration. To this end, I utilised seahorse technology (for a detailed explanation of how the Seahorse assay functions, see Figure 4-9). Briefly, the assay measures key parameters of mitochondrial function by directly measuring the oxygen consumption rate (OCR) of cells after the sequential addition of inhibitors of the electron transport chain. After the addition of each inhibitor, several values can be extracted and thus assess mitochondrial function. LICs were isolated from the bone marrow of sick recipient mice and their mitochondrial fitness was assessed using the Seahorse assay. Interestingly, although the basal respiration appeared to be at comparable levels to that of *control* and *control; FH^{Cyt}* cells, the spare respiratory capacity (SRC), was significantly lower in LICs lacking mitochondrial *Fh1* (Figure 4-10 A, B). SRC is the extra mitochondrial capacity available in a cell in order to produce energy under stress conditions, and is thought to be important for long-term survival and function (van der Windt et al., 2012) (Choi et al., 2009) (Ferrick et al., 2008) (Nicholls, 2009). The SRC reflects the difference between basal and maximal respiration, which is determined by measuring OCR before the treatment with oligomycin and after treatment with FCCP. Of note, in LICs lacking mitochondrial *Fh1* SRC had a negative value indicating that cells were not only incapable of displaying normal SRC but were also unable to reach the basal levels of their oxygen consumption rate (Figure 4-10 B).

Given the fact that cells lacking mitochondrial *Fh1* do not appear to be able to utilise mitochondrial respiration efficiently (reflected by the low SRC after FCCP addition that mimics physiological high stress conditions), we hypothesized that the cells must use a different metabolic pathway to do so. Since glycolysis is a pathway that many cancer cells utilise in order to meet their energy demands, we assessed the

glycolysis rates of LICs exhibiting low SRC. In order to do that, I measured the extracellular acidification rate (ECAR) of the cells, by utilising seahorse technology. ECAR can be measured in the surrounding media of the cells, which predominantly arises from the excretion of the lactic acid and is indicative of glycolysis taking place (TeSlaa and Teitell, 2014).

In order to measure changes in ECAR, 2-deoxy-glucose (2-DG) was injected into the media. 2-DG is a glucose analogue that cannot be metabolised therefore resulting to the inhibition of the glycolytic pathway (Zhong et al., 2009**)**. As a result, a decrease in ECAR after the addition of 2-DG will be specifically due to glycolysis shutdown. LICs lacking mitochondrial *Fh1* exhibited a greater drop in ECAR after 2-DG addition. Furthermore, LICs lacking mitochondrial *Fh1* exhibit higher basal levels of ECAR (Figure 4-11 A, B). These data suggest that cells could indeed rely more on the glycolytic pathway in order to meet their energetic demands.

A

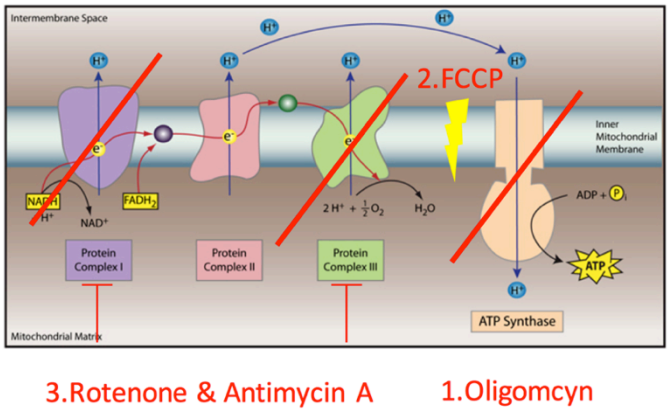

B

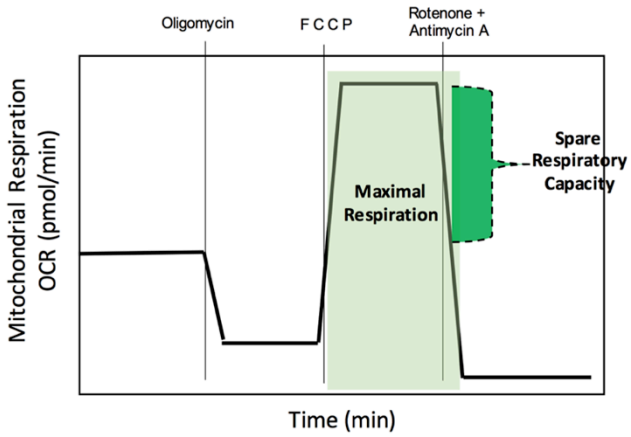

Figure 4-9. Outline of SeaHorse technology to assess mitochondrial fitness of LICs lacking mitochondrial *Fh1*. (A) The SeaHorse assay measures key parameters of mitochondrial function and directly measures oxygen consumption rate (OCR), after the sequential addition of compounds that inhibit different components of the electron transport chain. Initially, addition of oligomycin will inhibit ATP synthase, resulting in a drop of OCR. Then addition of FCCP, a mitochondrial membrane potential uncoupler, mimicks a pysiological high energy demand by stimulating the chain to operate at a maximum capacity, and therefore OCR will increase. The addition of FCCP allows for extraction of information about how well the cells can respond to high energy demand situations, or by measuring the spare respiratory capacity of the system (SRC). The third and final injection is a mix of rotenone and antimycin alpha that will inhibit complex I and III of the electron transport chain respectively. This combination shuts down mitochondrial respiration and as a result, OCR decreases. (B) Graph indicating how the trace of OCR is plotted after the sequential addition of electron transport chain inhibitors.

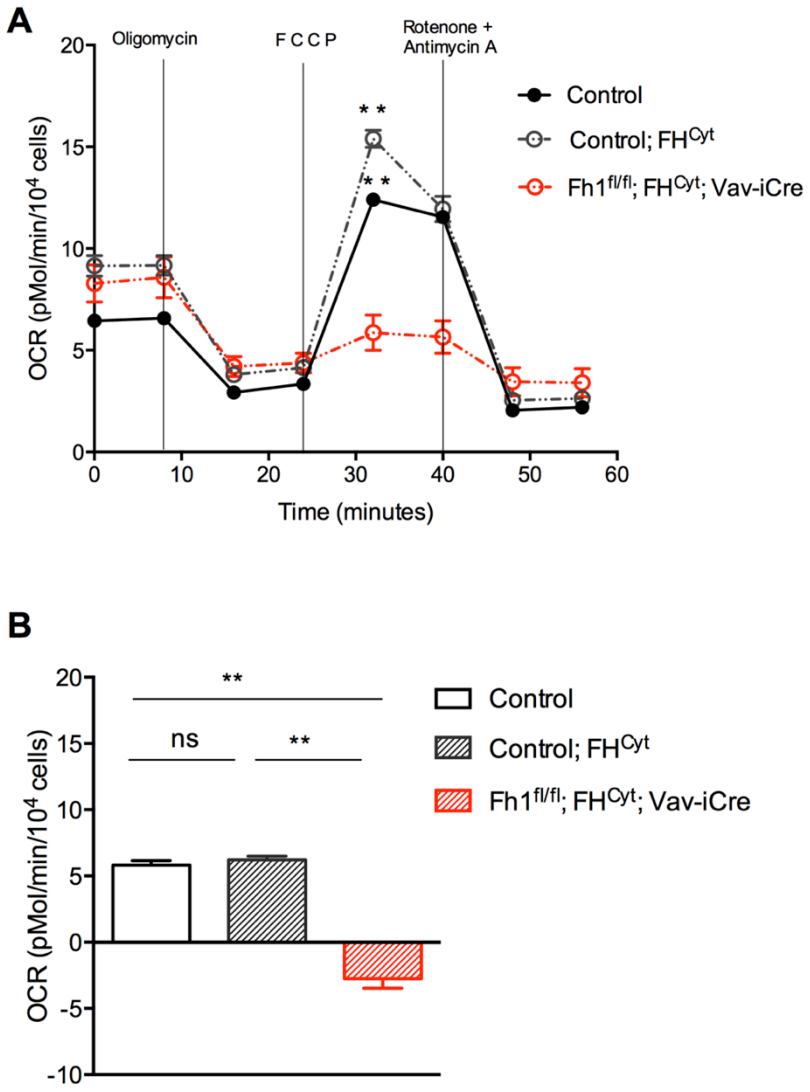

Figure 4-10. LICs lacking mitochondrial *Fh1* exhibit low spare respiratory capacity. (A) Oxygen consumption rate in LICs of the indicated genotypes under basal conditions and following the sequential addition of the ATP synthase inhibitor oligomycin, the uncoupler FCCP, and the electron transport chain inhibitors antimycin alpha and rotenone. 250,000 cells/well were used. Values were normalised against the number of cells per well using either trypan blue discrimination or propidium ionide exclusion by flow cytometry (B) Graph shows spare respiratory capacity (SRC) of indicated genotypes. SRC was calculated by substracting the value obtained right before the addition of oligomycin (i.e second measurement of basal respiration) from the value obtained after the addition of FCCP. OCR was measured using the Seahorse XF24 analyser. Data are mean ± S.E.M. n = 4-9 technical replicates per genotype. This is a representative graph of an experiment repeated 3 times using n = 3-4 biological replicates per genotype. ** $p<0.01$, Mann-Whitney test.

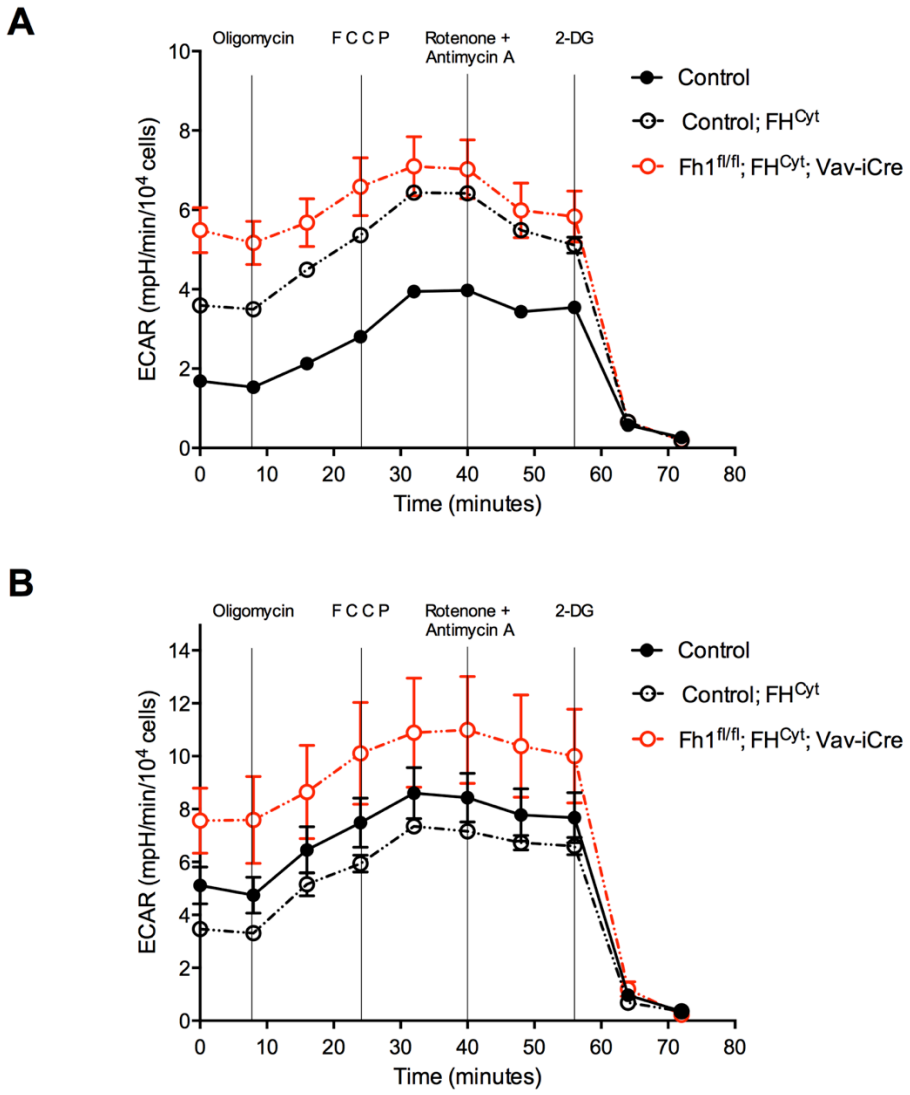

Figure 4-11. ECAR rate of LICs with low SRC. (A-B) The graphs show the same experiment performed twice using n = 1 biological replicate per genotype for (A) and n = 2 biological replicates per genotype for (B) with n = 4-9 technical replicates. ECAR is the extracellular acidification rate and is indicative of the glycolysis rate. 2-DG is a non-specific inhibitor of glycolysis. 250,000 cells/well were used and normalisation was done using the cell number/well. Cell numbers were determined using either trypan blue discrimination or propidium ionide exclusion by flow cytometry. ECAR was measured using the Seahorse XF24 analyser. LICs were isolated from the bone marrow of primary sick recipient mice. Graphs show mean ± S.E.M, Data are non-significant at time-point of 2-DG addition, Mann-Whitney test.

4.4.4 In vitro characterisation of LICs exhibiting low SRC

LICs isolated from the bone marrow of sick recipient mice were also assessed for their proliferation and apoptosis rates as well as cell cycle status. The proliferation rate of LICs with low SRC was comparable to that of *control* and *control; FH^{Cyt}* LICs (Figure 4-12). Furthermore, LICs with low SRC exhibited a trend of a lower percentage of late apoptotic (or early apoptotic) cells when assessed using the annexin V apoptotic assay (Figure 4-13 A-B change of axes on figure). Additionally, the fraction of sub-G0 cells of LICs exhibiting low SCR was significantly lower compared to *control* LICs, indicative of a lower apoptosis rate (Figure 4-14). Of note, when the experiment was repeated using two additional biological replicates, although the difference was not statistically significant, it was nevertheless of a similar trend. These data indicate that similarly to pre-LCs, LICs with low SRC exhibit a lower percentage of apoptotic cells. Additionally, based on the data of two independent experiments, LICs with low SRC exhibited more cells in G0/1 phase and fewer cells at the S and G2/M phases at the 24-hour time-point. At the 48-hour time-point, in one of the experiments cells exhibited a trend similar to that of 24-hour time-point, albeit not statistically significant (Figure 4-15 A-B).

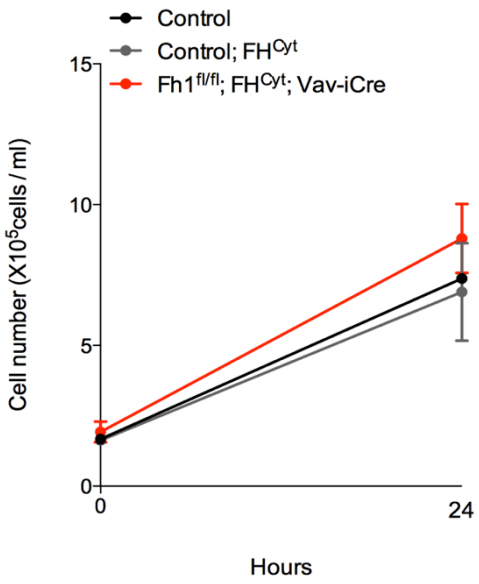

Figure 4-12. Proliferation rate of LICs lacking mitochondrial *Fh1*. Proliferation curves of LICs in liquid culture. Cell were seeded at a concentration of 150,000 cells/ml. Data are mean ± S.E.M. n = 3 biological replicates per genotype with 3 technical replicates ns, Unpaired t test.

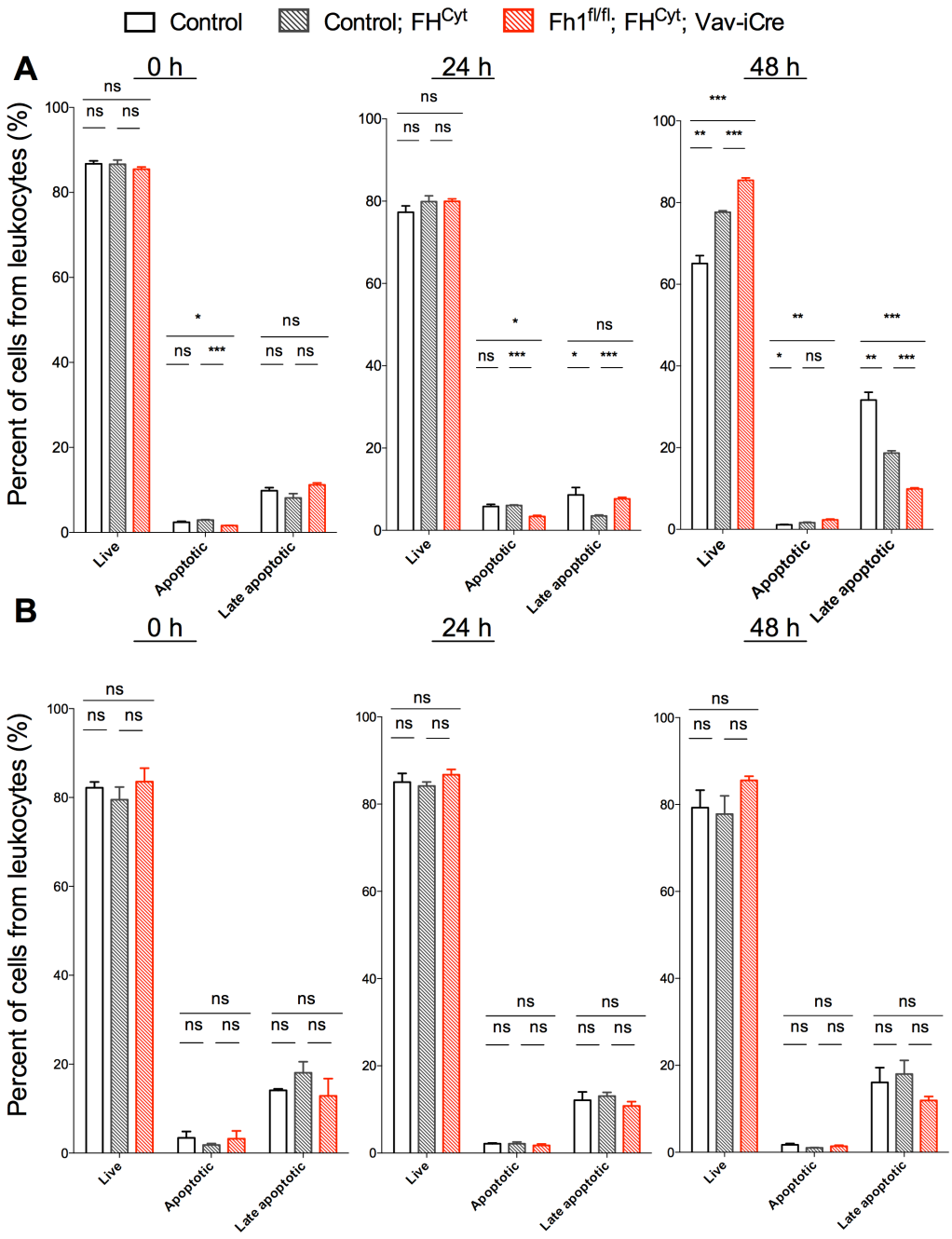

Figure 4-13. Apoptosis rate of LICs lacking mitochondrial *Fh1*. (A-B) Show experiment carried out twice using n = 1 biological replicate for (A) and n = 2 biological replicates for (B). Apoptosis assay using annexin V-FITC and DAPI staining and analysed using flow cytometry 0 (left), 24 (middle) and 48 hours (right) after seeding. Data are mean ± S.E.M, n = 3 technical replicates. LICs were isolated from the bone marrow of sick recipient mice at the point of sacrifice. LICs were sorted based on the CD45.2 and c-Kit markers ($CD45.2^{+}$/$c\text{-}Kit^{+}$). * $p<0.05$, **$p<0.01$, ***$p<0.001$ Unpaired t test.

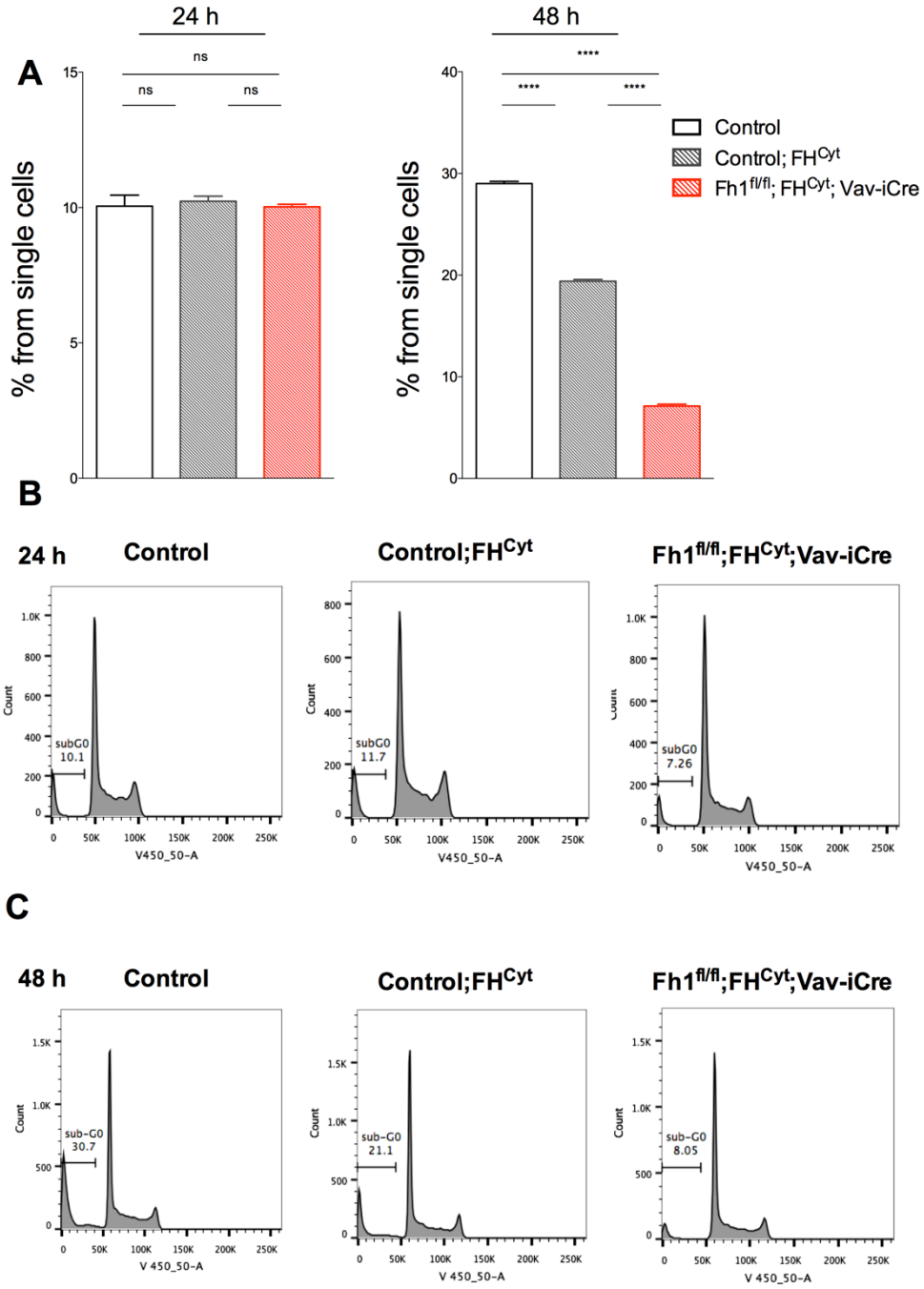

Figure 4-14. Sub-G0 phase of LICs with low SRC indicative of cell death rate. (A) Graphs indicate percentage of cells (from the single cell gate used to exclude doublets) in sub-G0 phase at 24 hours (left) and at 48 hours (right). The sub-G0 fraction was determined based on the DNA content of cells, using DAPI and analysing cells via flow cytometry. (B-C) Representative histograms indicating how the sub-G0 phase was determined at 24 hours (B) and at 48 hours (C) for *control* (left), *control; FH^{Cyt}* (middle) and *Fh1$^{fl/fl}$; FH^{Cyt}; Vav-iCre* (right). The graphs are representative of two independent experiments. n = 3 biological replicates per genotype. Data are mean ± S.E.M, **** p<0.0001, Unpaired t test.

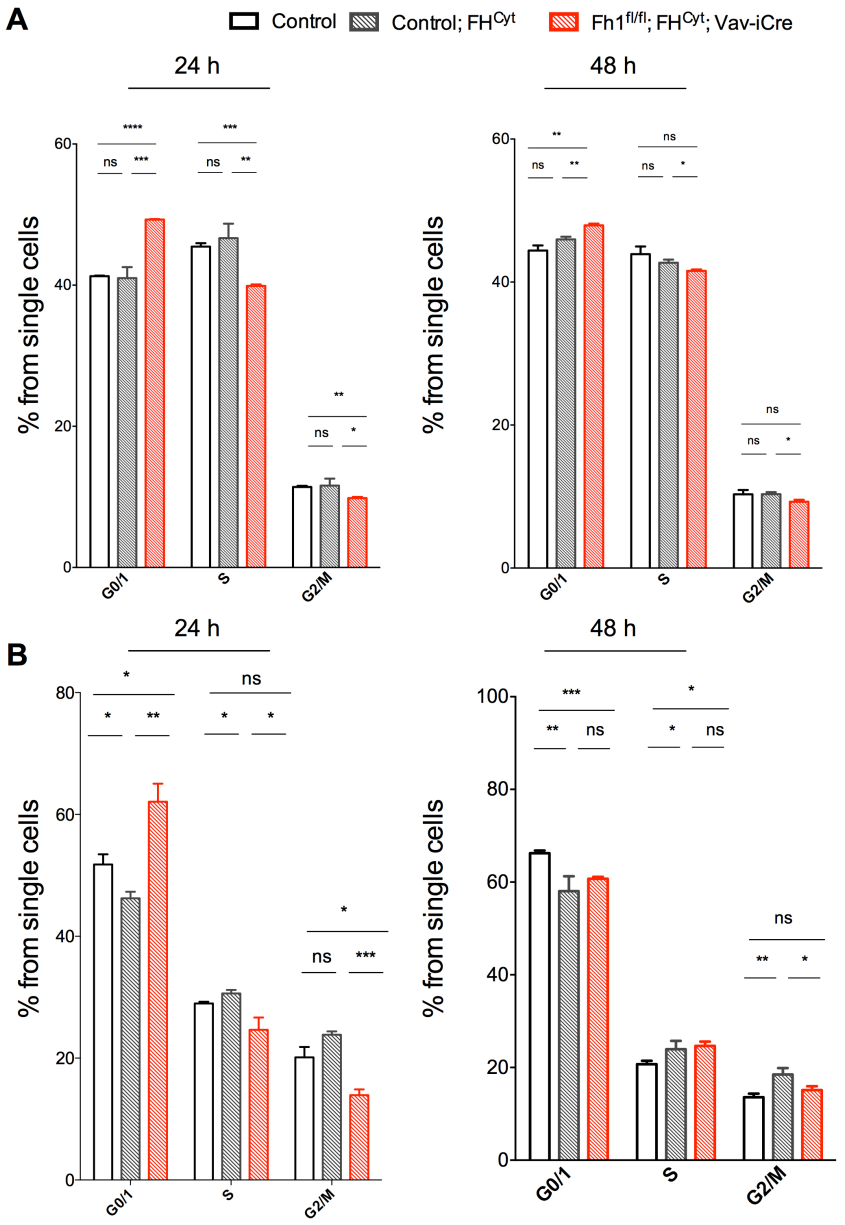

Figure 4-15. Cell cycle status of LICs with low SRC. Graph indicates percentage of cells at each stage of the cell cycle at 24 hours (left) and 48 hours (right). n = 1 biological replicate for (A) and n = 2 biological replicates for (B). Analysis was performed using DAPI staining (containing 0.1% Triton) and cells were analysed via flow cytometry. Data are mean ± S.E.M., n = 3 technical replicates per genotype. LICs were isolated from the bone marrow of sick recipient mice at the point of sacrifice. LICs were sorted based on the expression of CD45.2 and c-Kit markers ($CD45.2^+/C\text{-}Kit^+$). *p< 0.05, **p< 0.01, ***p<0.001, ****p<0.0001, Unpaired t test.

4.4.5 Mitochondrial Fh1 is not required for the long term self-renewal capacity of LICs

As described in the experimental design section (section 4.3), 100,000 pre-LCs of the *Mx1-Cre* background that were c-Kit^{+} and expressing Mac-1 and Gr1 (Figure 4-16), were transplanted into sub-lethally irradiated primary recipient mice. After the chimerism of LICs reached 20-30 % in the peripheral blood of the recipient mice, the mice were administered with 6 injections of poly (I:C) in order to induce the deletion of *Fh1*. Interestingly, the chimerism of LICs significantly decreased after the first three injections of poly (I:C) when compared to the LIC chimerism before poly (I:C) administration (Figure 4-17A-B). Deletion of mitochondrial *Fh1* was assessed before and after poly (I:C) administration (Figure 4-18 B). Of note, the chimerism of LICs in the *control* mice was not decreased, indicating that the decrease in chimerism was specifically due to deletion of mitochondrial *Fh1*. *Fh1$^{f/\Delta}$; FH^{Cyt}; Mx1-Cre* mice developed disease at a similar rate to *control* mice indicating that after LICs are established and generate AML in mice, the lack of mitochondrial *Fh1* does not affect their self-renewal capacity (Figure 4-18 A). On that note, the recipient mice that succumbed to leukaemia exhibited infiltration of LICs in their bone marrow and spleen (Figure 4-19A-D). LICs isolated from the bone marrow of sick recipient mice were also assessed for the deletion status of mitochondrial *Fh1* (Figure 4-19E).

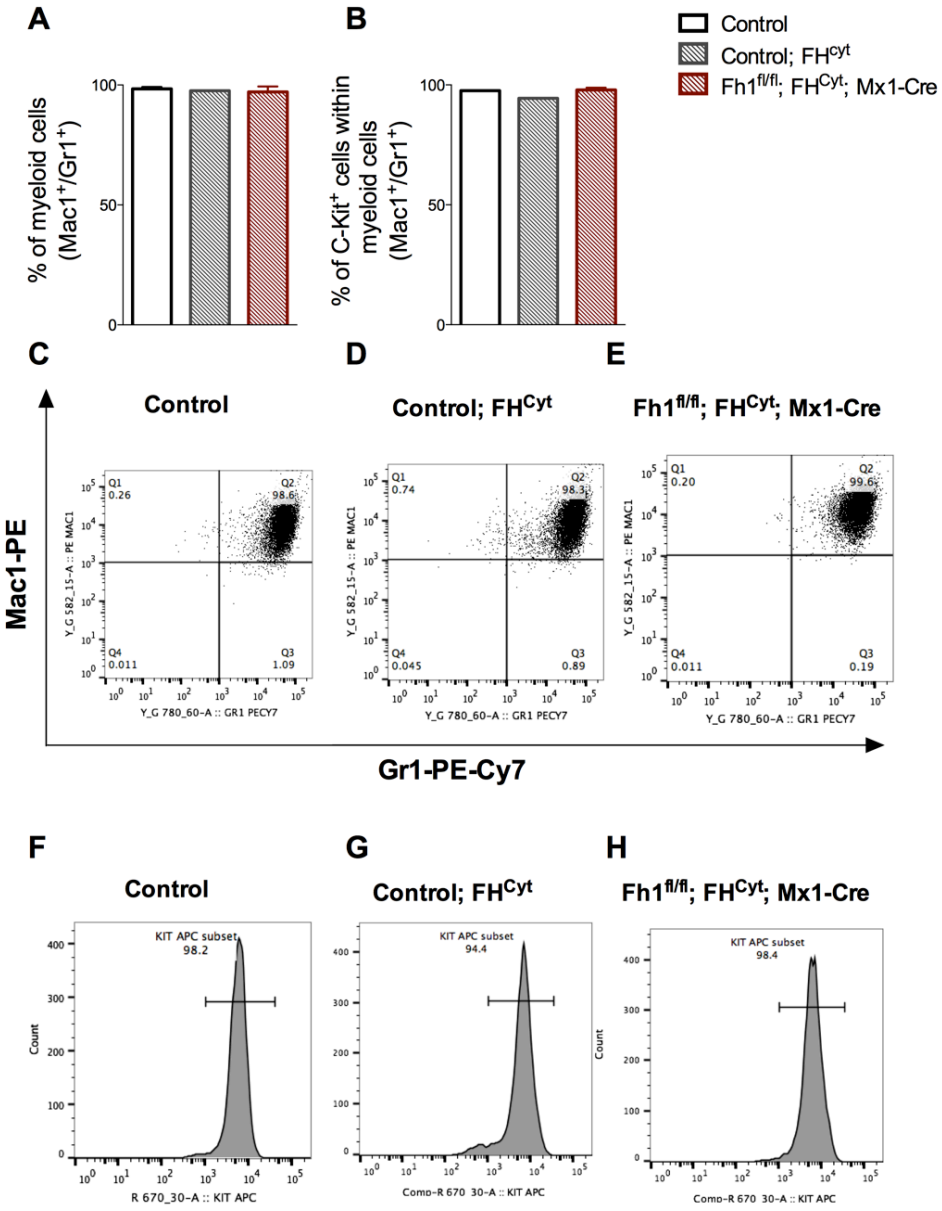

Figure 4-16. Flow cytometry profile of pre-LCs prior to transplantation in recipient mice. (A) Percentage of pre-LCs expressing myeloid markers (Mac-1^+/$Gr1^+$). Myeloid cells are defined as the sum of Mac-1^+/$Gr1^+$ and Mac-1^+. (B) Percentage of pre-LCs that are positive for c-Kit, within the myeloid compartment. Graphs show mean ± S.E.M. (C-E) Representative FACS dot plots of pre-LCs showing the expression of myeloid markers Mac-1 and Gr1. (C) *control*, (D) *control; FH^{Cyt}* and (E) *$Fh1^{fl/fl}$; FH^{Cyt}; Mx1-Cre* pre-LCs. (F-H) Representative FACS histogram showing the expression of c-Kit in *control* pre-LCs (F) *control; FH^{Cyt}* (G) and (H) *$Fh1^{fl/fl}$; FH^{Cyt}; Mx1-Cre* pre-LCs. No statistical analysis was performed as n = 2 for *control,* n = 1 for *control; FH^{Cyt}* and n = 2 for *$Fh1^{fl/fl}$; FH^{Cyt}; Mx1-Cre.* This is a representation of an experiment performed twice independently.

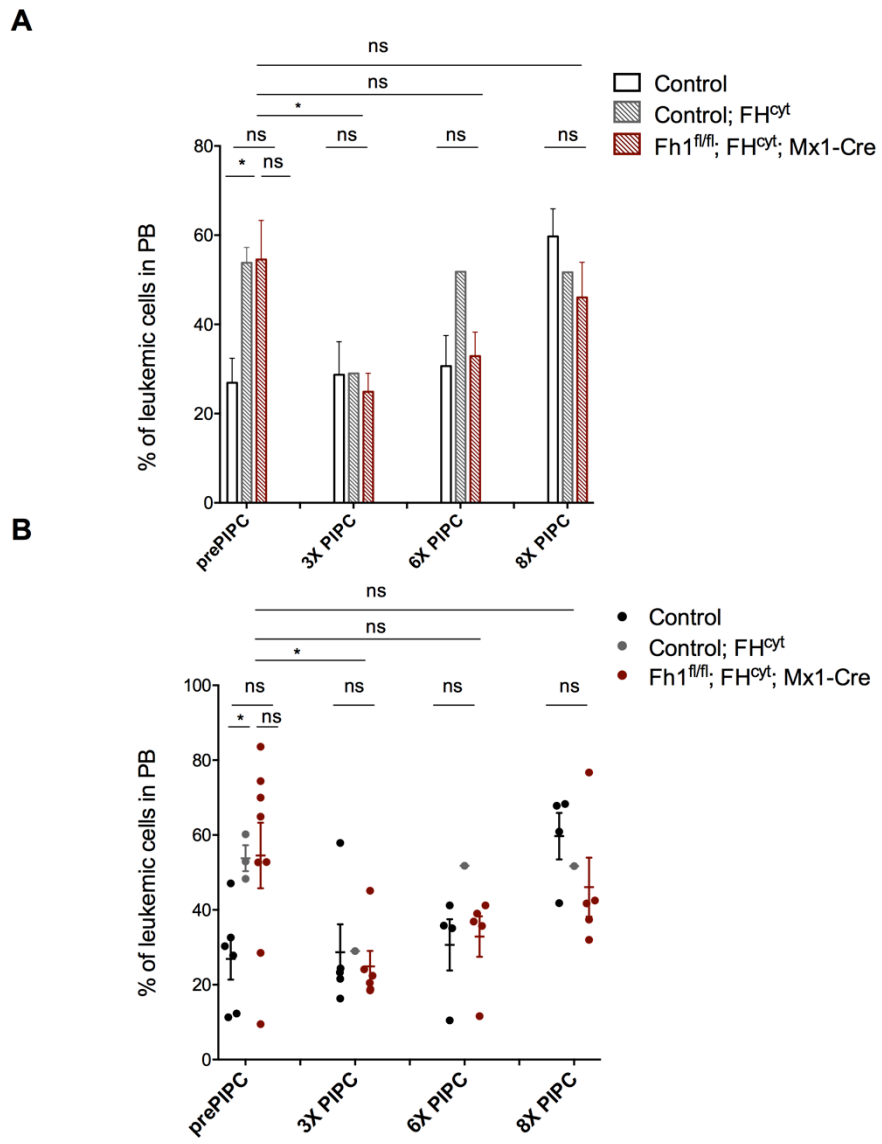

Figure 4-17. LIC chimerism during poly (I:C) administration in primary recipient mice. (A-B) Chimerism of leukaemic cells in the peripheral blood of recipient mice. Data are presented as summary (A) and for each individual recipient (B). Statistics were performed for *Fh1$^{fl/fl}$; FH^{Cyt}; Mx1-Cre* between pre-poly (I:C) and each time point onwards, and between genotypes at each time-point. No statistics were performed for *control; FH^{Cyt}* as there was only 1 recipient available after the initiation of poly (I:C). Graphs show mean ± S.E.M. This is a representation of an experiment performed independently twice. n = 2 biological replicates for *control*, n = 1 biological replicate for *control; FH^{Cyt}* and n = 2 biological replicates for *Fh1$^{fl/fl}$; FH^{Cyt}; Mx1-Cre*, n = 3-8 recipient mice per genotype. PIPC = poly (I:C). Mann-Whitney test, * $p < 0.05$.

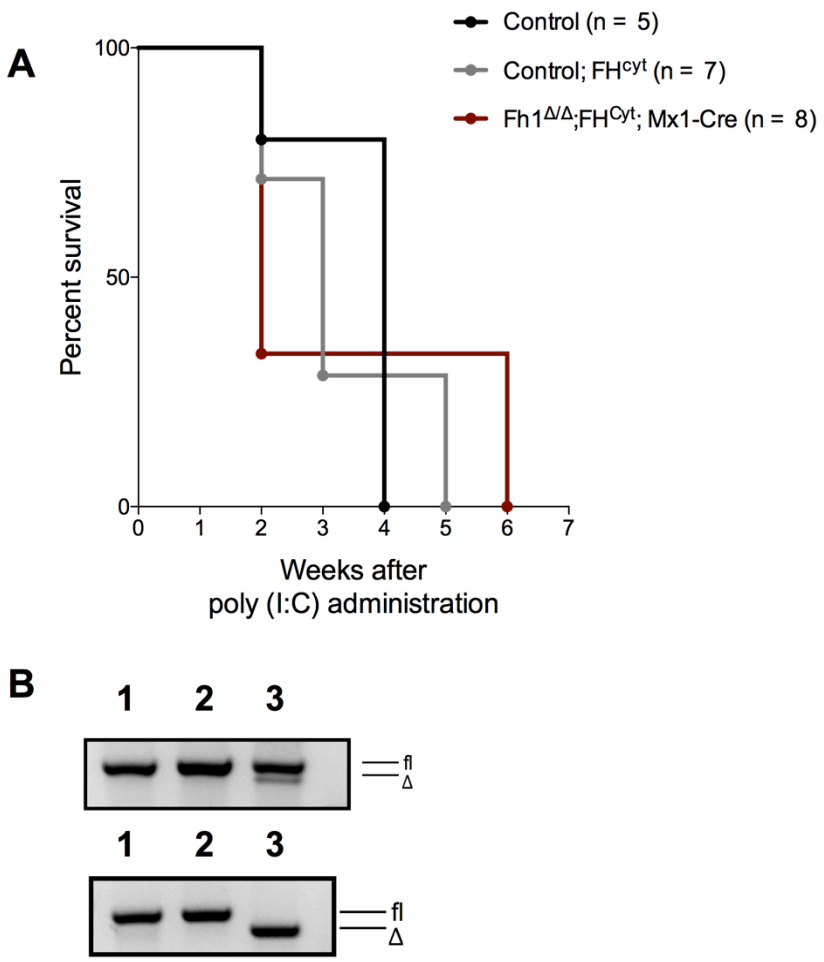

Figure 4-18. Mitochondrial *Fh1* is not required for self-renewal of LICs *in vivo*. (A) Kaplan-Meier survival curve of sub-lethally irradiated primary recipient mice transplanted with 100,000 c-Kit^{+} pre-leukaemic cells obtained from serial re-plating assays. (B) Representative genomic PCR assessing deletion of *Fh1* before poly (I:C) (top) and after poly (I:C) (bottom) administration. Lane 1 = *control*, lane 2 = *control; FH^{Cyt}*, lane 3 = *Fh1$^{fl/fl}$; FH^{Cyt}; Mx1-Cre*. n = 2 biological replicates for *control*, n = 2 biological replicate for *control; FH^{Cyt}* and n = 2 biological replicates for *Fh1$^{Δ/Δ}$; FH^{Cyt}; Mx1-Cre*, n = 5-8 recipient mice per genotype. Log-rank (Mantel-Cox) and Gehan-Breslow-Wicoxon tests were performed where data were statistically non-significant. fl- undeleted conditional allele, Δ- excised allele. This is a representation of an experiment carried out twice independently.

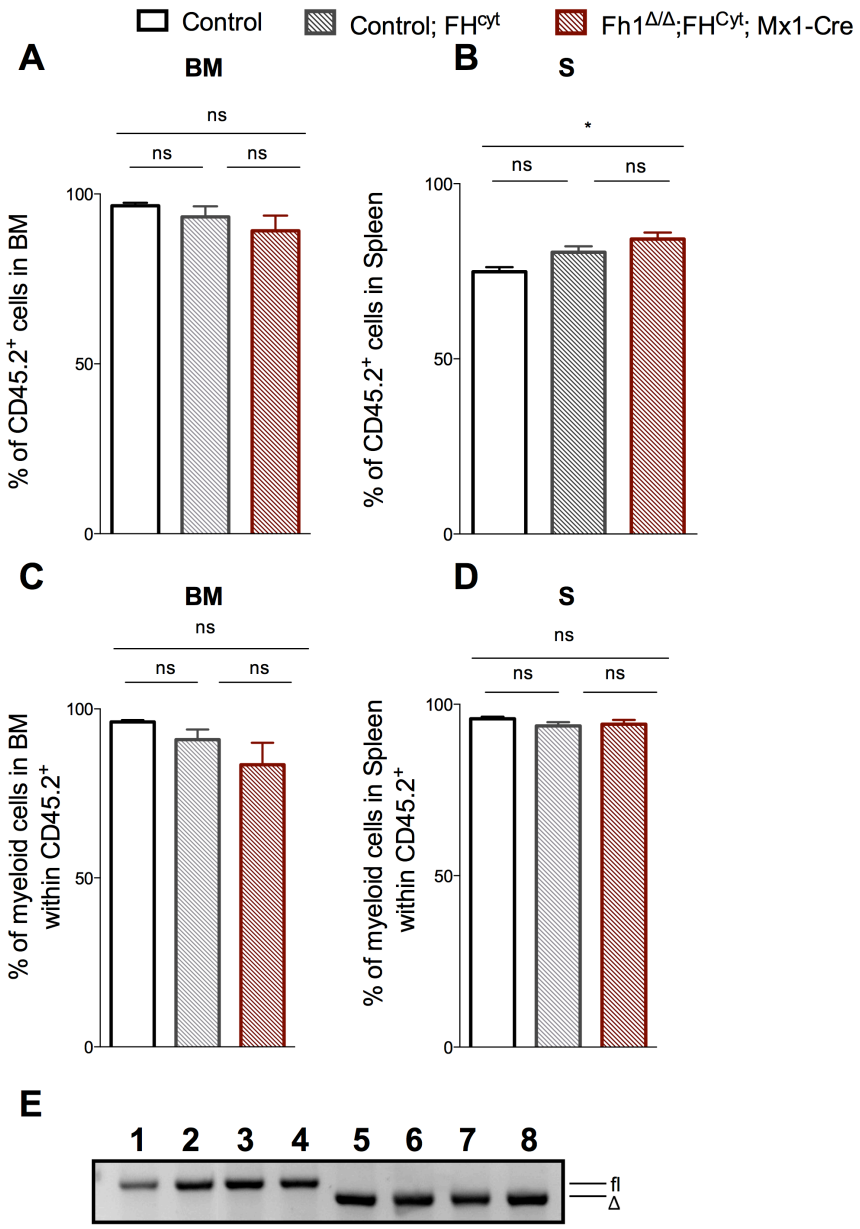

Figure 4-19. LIC infiltration in the bone marrow and spleen of primary recipient mice. Percentage of LICs ($CD45.2^+$) in bone marrow (A) and spleen (B) that express myeloid markers (myeloid cells are defined as the sum of $Mac\text{-}1^+/Gr1^+$ and $Mac\text{-}1^+$) in bone marrow (C) and spleen (D). Graphs show mean ± S.E.M. (E) Image of genomic PCR of *Fh1* in LICs isolated from the bone marrow of sick recipient mice. lanes 1-2 = control, lanes 3-4 = control*;* FH^{Cyt}, lanes 5-8 = $Fh1^{\Delta/\Delta}$*;* FH^{Cyt}*; Mx1-Cre.* n = 4-7 recipient mice analysed per genotype. Mann-Whitney test, * $p< 0.05$. fl- undeleted conditional allele, Δ- excised allele. This is a representation of an experiment carried out twice independently.

In order to assess whether mitochondrial *Fh1* is required for the long-term self-renewal capacity of LICs, I performed a secondary transplantation using LICs isolated from the bone marrow of sick primary recipient mice. Specifically, 10,000 LICs (CD45.2^{+}/ c-Kit^{+}) were transplanted into sub-lethally irradiated secondary recipient mice, after ensuring efficient deletion of mitochondrial *Fh1* (Figure 4-20B). Mice transplanted with control and *Fh1$^{f/f}$; FH^{Cyt}; Mx1-Cre* LICs developed disease at the same rate, demonstrating that mitochondrial Fh1 is not required for the long-term self-renewal capacity of LICs (Figure 4-20A). Of note, the cohort of the *control; FH^{Cyt}* mice succumbed to AML 21 days after transplantation compared to the other two cohorts that succumbed to AML at approximately 50 days post transplantation (Figure 4-20A). Similarly, to the previous experiment, fewer recipient mice for the *control; FH^{Cyt}* cohort were used and as a result, the survival curve could have been skewed. Recipient mice that succumbed to AML exhibited LIC infiltration in their bone marrow and spleen (Figure 4-21A-B). Finally, LICs isolated from the bone marrow of sick recipient mice were assessed for deletion of mitochondrial *Fh1* (Figure 4-21 C).

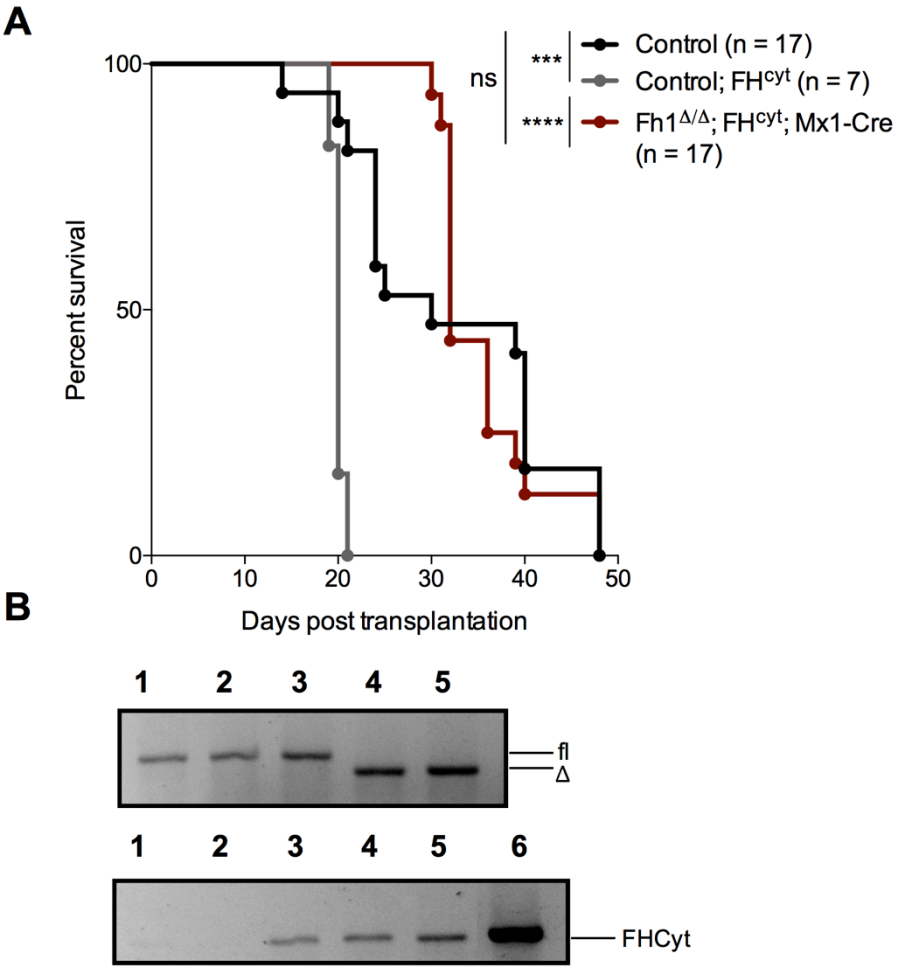

Figure 4-20. LICs lacking mitochondrial *Fh1* propagate AML in secondary recipient mice. (A) Kaplan- Meier survival curve of sub-lethally irradiated secondary recipient mice. 10,000 LICs ($CD45.2^{+}$/c-Kit^{+}) were isolated from primary recipient mice and transplanted into secondary recipient mice. (B) Gel images from genomic PCR performed to ensure deletion of *Fh1* (top) and presence of cytosolic isoform of *FH* (bottom) in LICs before the injection into secondary recipient mice. fl- undeleted conditional allele, Δ- excised allele, FH^{Cyt} - presence of mitochondial isoform of *FH.* Lane 1-2 = *control*, lane 3 = *control;* $FH^{Cyt,}$ lane 4-5 = $Fh1^{\Delta/\Delta}$; FH^{Cyt}; *Mx1-Cre,* lane 6 = positive control of FH^{Cyt}. n = 2 biological replicates for *control* and $Fh1^{\Delta/\Delta}$; FH^{Cyt}; *Mx1-Cre,* n = 1 for *control;* FH^{Cyt}. n = 7-17 recipient mice per genotype. *** p< 0.001, ****p< 0.0001, Log-rank (Mantel-Cox) and Gehan-Breslow-Wicoxon tests.

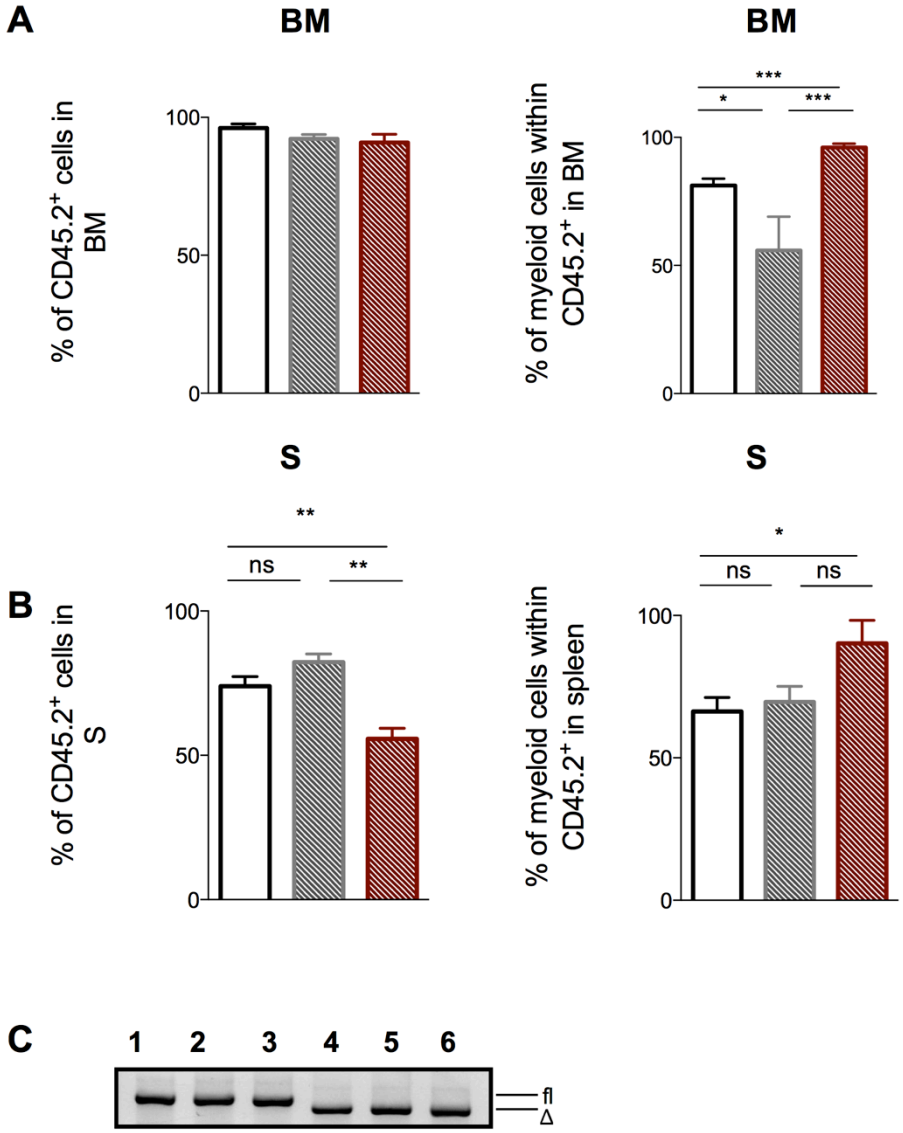

Figure 4-21. Infiltration of LICs in the bone marrow and spleen of secondary recipient mice. (A) Percentage of LICs ($CD45.2^+$) (left) that express myeloid markers (right) (myeloid cells are defined as the sum of $Mac\text{-}1^+/Gr1^+$ and $Mac\text{-}1^+$) in the bone marrow (A) and in the spleen (B). Graphs are mean ± S.E.M. (C) Image of genomic PCR of *Fh1* in LICs isolated from the bone marrow of sick recipient mice. lanes 1-2 = *control*, lane 3 = *control;* FH^{Cyt}, lanes 4-6 = $Fh1^{fl/fl}$*;* FH^{Cyt}*; Mx1-Cre*. n = 3-11 recipient mice analysed per genotype. Unpaired t test, * $p<0.05$, ** $p<0.01$, ***$p< 0.001$

4.4.6 *Fh1*$^{-/-}$; *FH*^{Cyt}; *Mx1-Cre* LICs exhibit low spare respiratory capacity

Mitochondrial *Fh1* causes a genetic truncation in the TCA cycle, and as a result could cause defects in mitochondrial respiration. One of the characteristics of such a defect is a low spare respiratory capacity (SRC). SRC was assessed by the Seahorse assay.

As expected, LICs lacking mitochondrial *Fh1* exhibited a very low SRC compared to *control* and *control; FH*^{Cyt} LICs (Figure 4-22A-B). Interestingly, when ECAR (which is indicative of the glycolysis rate of cells) was assessed, LICs lacking mitochondrial *Fh1* exhibited comparable ECAR rates to *control* and *control; FH*^{Cyt} LICs after the addition of 2-DG (Figure 4-23). These data indicate that LICs with the low SRC might be utilising another source other than glycolysis (such as fatty acid oxidation), in order to meet their energy demands under stressful conditions.

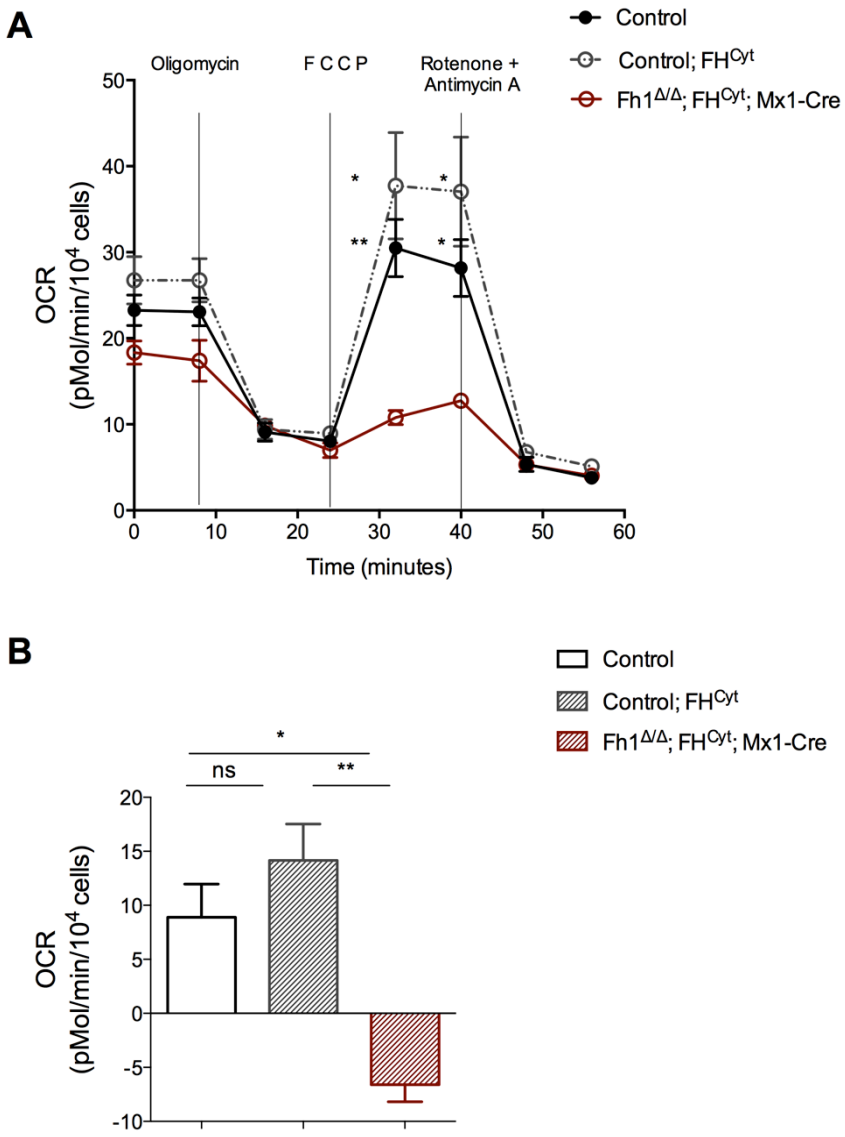

Figure 4-22. *Fh1$^{\Delta/\Delta}$; FH^{Cyt}; Mx1-Cre* LICs exhibit low SRC. (A) Oxygen consumption rate in LICs of the indicated genotypes under basal conditions and following sequential addition of the ATP synthase inhibitor oligomycin, the uncoupler FCCP, and the electron transport chain inhibitors antimycin alpha and rotenone. 250,000 cells/well were used. Values were normalised against the number of cells per well using either trypan blue discrimination or propidium ionide exclusion by flow cytometry. Stars indicate statistical significance between *control* and *Fh1$^{\Delta/\Delta}$; FH^{Cyt}; Mx1-Cre* or *control; FH^{Cyt}* and *Fh1$^{\Delta/\Delta}$; FH^{Cyt}; Mx1-Cre*. (B) Graph shows spare respiratory capacity (SRC) of indicated genotypes. SRC was calculated by substracting the value obtained right before the addition of oligomycin (i.e second measurement of basal respiration) from the value obtained after the addition of FCCP. OCR was measured using the Seahorse XF24 analyser. Data are mean ± S.E.M. n = 3-5 technical replicates per genotype. This is a representative graph of an experiment repeated 2 times using n = 1-2 biological replicates per genotype. *p< 0.05, ** p<0.01, Mann-Whitney test.

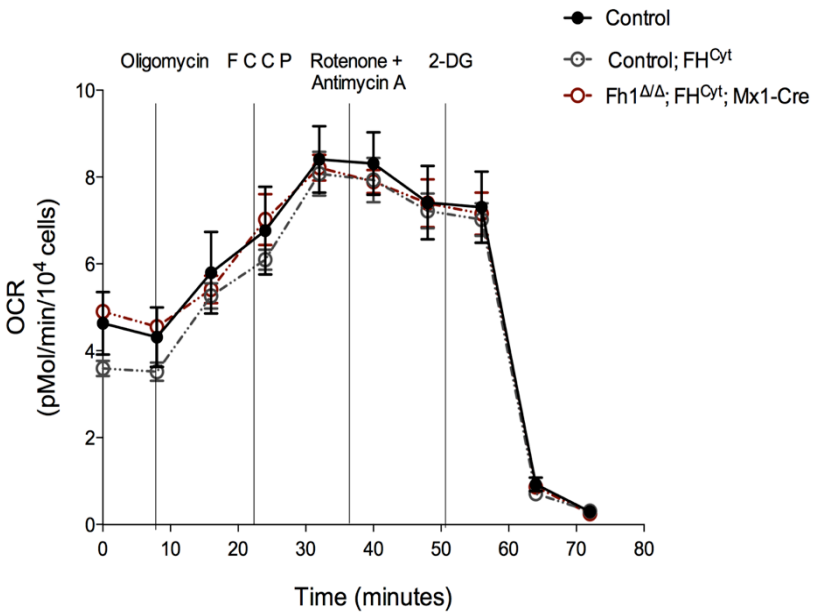

Figure 4-23. ECAR rate of *Fh1$^{\Delta/\Delta}$; FH^{Cyt}; Mx1-Cre* LICs. ECAR is the extracellular acidification rate and is indicative of the glycolysis rate. 2-DG is a non-specific inhibitor of glycolysis. 250,000 cells/well were used and normalisation was done using the cell number/well. Cell numbers were determined using either trypan blue discrimination or propidium ionide exclusion by flow cytometry. ECAR was measured using the Seahorse XF24 analyser. LICs were isolated from the bone marrow of primary sick recipient mice. Data are mean ± S.E.M. n = 3-5 technical replicates per genotype. This is a representative graph of an experiment repeated 2 times using n = 1-2 biological replicates per genotype. Statistics were performed for the values obtained after the addition of 2-DG. Data are non-significant, Mann-Whitney test.

4.4.7 $Fh1^{-/-}$; FH^{Cyt}; Mx1-Cre LICs exhibit normal apoptosis and cell cycle status

LICs that were isolated from the bone marrow of primary recipient mice were assessed for the cell cycle status as well as their apoptosis rates. In terms of apoptosis, LICs lacking mitochondrial *Fh1* exhibited a higher but non-significant percentage of apoptotic cells at the 24 hour time-point (Figure 4-24 figure axes changed).

On a similar note, LICs lacking mitochondrial *Fh1* only exhibited a higher percentage of cells in the G0/1 phase of the cell cycle and a lower percentage of cells in the G2/M phase (Figure 4-25).

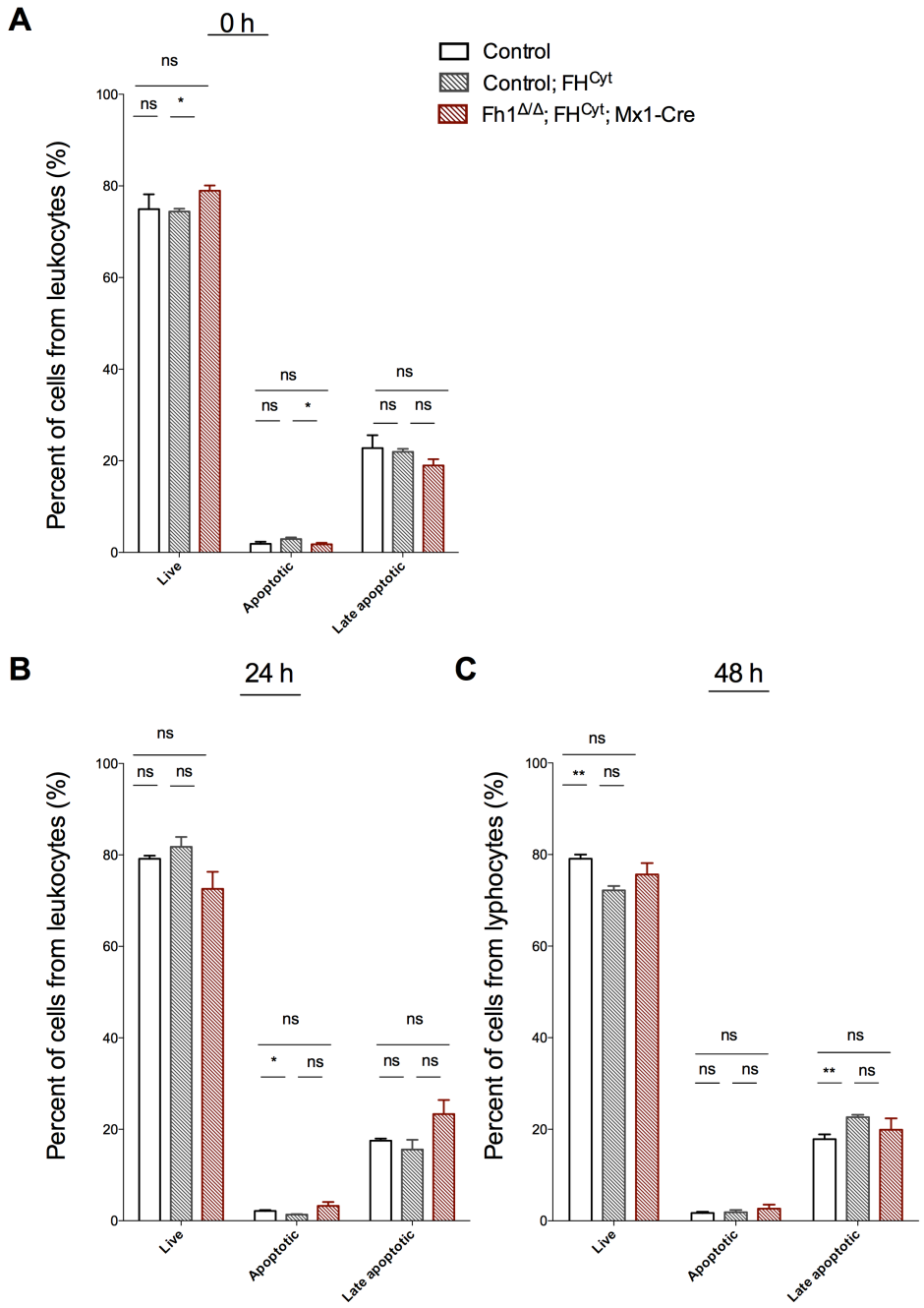

Figure 4-24. Apoptosis rate of *Fh1$^{\Delta/\Delta}$; FH^{Cyt}; Mx1-Cre* LICs. Graphs show percentage of cells. The apoptosis assay was performed using annexin V-FITC and DAPI staining, via flow cytometry at 0 hours (A), 24 hours (B) and at 48 hours (C). Data are mean ± S.E.M., n = 2 biological replicates for *control* and *Fh1$^{\Delta/\Delta}$; FH^{Cyt}; Mx1-Cre* and n = 1 for *control; FH^{Cyt}* with n = 4-6 technical replicates. LICs were isolated from the bone marrow of sick primary recipient mice at the point of sacrifice. LICs were sorted based on the expression of CD45.2 and c-Kit markers (CD45.2^{+}/c-Kit^{+}). * $p<0.05$, **$p<0.01$, Unpaired t test.

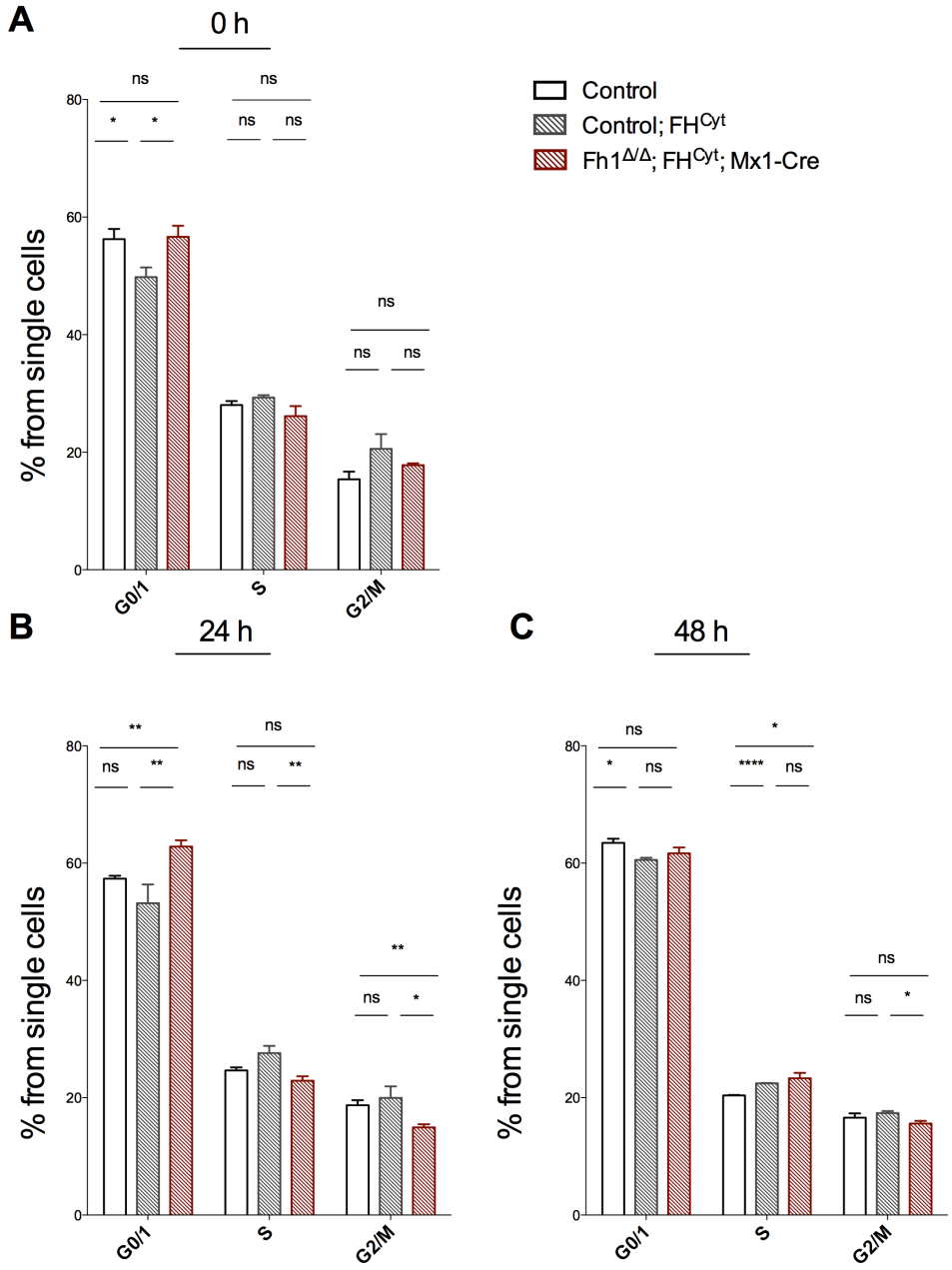

Figure 4-25. Cell cycle status of *Fh1$^{\Delta/\Delta}$; FH^{Cyt}; Mx1-Cre* LICs. Graphs indicate percentage of cells at each stage of the cell cycle at 0 hours (A), 24 hours (B) and 48 hours (C). Data are mean ± S.E.M., n = 2 biological replicates for *control* and *Fh1$^{\Delta/\Delta}$; FH^{Cyt}; Mx1-Cre* and n = 1 for *control; FH^{Cyt}* with n = 4-6 technical replicates. LICs were isolated from the bone marrow of sick primary recipient mice at the point of sacrifice. LICs were sorted based on the expression of CD45.2 and c-Kit markers (CD45.2^{+}/C-Kit^{+}). * p<0.05, **p<0.01, ****p< 0.0001, Unpaired t test.

4.5 Discussion

4.5.1 Mitochondrial Fh1 and genetically intact TCA are important for LIC generation in vivo

In this chapter I demonstrated that pre-LCs lacking mitochondrial *Fh1* generate AML at a much lower rate compared to *control* and *control; FH^{Cyt}* pre-LCs. Specifically, while 76 % of mice injected with LICs lacking mitochondrial *Fh1* survived, only 25 % and 30 % of *control* and *control; FH^{Cyt}* mice respectively survived. In that context, from the 6 biological replicates of *$Fh1^{fl/fl;}$ FH^{Cyt}; Vav-iCre* only 3 replicates generated disease in recipient mice.

Deletion of the mitochondrial isoform of *Fh1*, resulted in a genetic truncation in the TCA cycle. In order to assess the impact of the mitochondrial *Fh1* deletion on mitochondrial respiration, I utilised the seahorse assay. Interestingly, LICs lacking mitochondrial *Fh1* exhibited very low SRC compared to *control* and *control; FH^{Cyt}* LICs. This mitochondrial respiration deficit could potentially explain the inability of the pre-LCs to generate disease. In fact, recent studies have shown that oxidative phosphorylation (and mitochondrial respiration) are important for the survival of cancer cells. By using agents that blocked mitochondrial protein translation, specifically complexes of the electron transport chain, it was possible to decrease oxygen consumption and preferentially induce cell death in AML cell lines (Škrtić et al., 2011). In another study, knockdown of the mitochondrial proteasome member CIcP led to cell death of AML cell lines, as CIcP knockdown led to inhibition of oxidative phosphorylation and mitochondrial metabolism (Cole et al., 2015). The emerging studies have therefore indicated that mitochondrial respiration can be critical for the survival of leukaemic cells, thus offering new insight into the metabolic adaptation of cancer cells.

4.5.2 Mitochondrial Fh1 and a genetically intact TCA are not required for LIC maintenance in vivo

Furthering this study, I wanted to assess whether a genetically intact TCA is also important for the maintenance of LICs *in vivo.* To that end, I isolated *control*, *control; FH^{Cyt}* and *$Fh1^{fl/fl}$; FH^{Cyt}; Mx1-Cre* LSK cells and generated pre-LCs using the *Meis1/ Hoxa9* model. I then injected 100,000 c-Kit^{+} pre-LCs into sub-lethally

irradiated primary recipient mice. Once the LIC chimerism reached 20-30 % in the peripheral blood of recipient mice, I treated the mice with poly (I:C) in order to induce deletion of *Fh1*. Of note, in *Fh1$^{fl/fl}$; FH^{Cyt}; Mx1-Cre* cells, poly (I:C) treatment resulted in the deletion of mitochondrial *Fh1*. Deletion of mitochondrial *Fh1* did not affect the self-renewal capacity of LICs as mice succumbed to AML at a similar latency to mice injected with *control* or *control; FH^{Cyt}* LICs. Furthermore, upon transplantation into secondary recipient mice, *Fh1$^{\Delta/\Delta}$; FH^{Cyt}; Mx1-Cre* LICs generated AML at a similar rate to *control* LICs. These data indicate that mitochondrial *Fh1* (and effectively a genetically intact TCA) are not required for long term self-renewal capacity of LICs. Of note, the recipient mice injected with *control; FH^{Cyt}* LICs succumbed to AML faster compared to the other two cohorts. It is unlikely that the additional expression of fumarate hydratase (endogenous expression and the cytosolic transgene expression), exert a positive effect on LICs, as this was only observed in this particular experiment but was not observed in the transplantations using the *Vav Cre* model.

In summary, the data indicate that *Fh1* (and effectively genetically intact TCA) are important for the generation of LICs but are dispensable for the long-term self-renewal capacity of LICs and maintenance of AML. Indeed, there are genes/pathways that have been shown to be differentially required for the initial (pre-leukaemic) and later (fully leukaemic) stages of the disease. We have previously demonstrated in our lab that, *Hif-2a* deletion accelerated the development of LICs but had no impact on LIC maintenance in a knock-in model of *MLL-AF9* and the retroviral model of *Meis1/Hoxa9* (Vukovic et al., 2015). Furthermore, in another study, mTORC1 inactivation abolished the tumour-initiating capacity of LIC cells but did not affect their self-renewal capacity (Hoshii et al., 2012). Another study looked at the role of the polycomb repressive complex 2 (PRC2) component *EZH2* in the generation and maintenance of AML. Using the retroviral model of *MLL-AF9* the authors showed that *Ezh2*-null cells were unable to re-plate *in vitro* indicating that *Ezh2* impaired leukaemic colony formation (Neff et al., 2012). Interestingly, by using *Ezh2- MLL-AF9* cells of the *Mx1-Cre* background (thus allowing for inducible deletion of *Ezh2*), the cells generated disease *in vivo* at an equal rate as their wild type counterparts, but exhibited prolonged disease latency when transplanted in

secondary recipient mice. These data therefore indicated that *Ezh2* is required for the initiation of the disease but is dispensable once LICs are established.

The studies described above demonstrate that while some pathways/genes are critical for the initiation of AML, they are dispensable for the maintenance of AML and self-renewal capacity of LSCs. In a similar manner, mitochondrial *Fh1* and genetically intact TCA appear to be important for the initial stages of the disease but not thereafter.

4.5.3 LICs lacking mitochondrial Fh1 exhibit higher ECAR rates

Given the fact that cells lacking mitochondrial *Fh1* exhibited low SRC, which is through to reflect how well a cell can respond to high energy demands we wanted to assess whether these cells utilise more glycolysis in order to compensate for their inability to efficiently utilise mitochondrial respiration. For that we used the seahorse assay that offers simultaneous measurements of OCR and ECAR, reflecting mitochondrial respiration and glycolysis rates respectively. Based on 2 independent experiments, we observed that LICs with low SRC, appeared to have a sharper drop in ECAR after the addition of the glycolytic inhibitor 2-DG, and also exhibited higher basal ECAR rate. This could potentially indicate that LICs rely more on glycolysis compared to *control* and *control; FH^{Cyt}* LICs. However, it is important to consider that ECAR (which measures protons) arises from both lactate secretion (indicative of glycolysis) and respiratory acidification (in the form of CO_2) (Mookerjee et al., 2015). Therefore, ECAR is only indicative of glycolytic rates and validation experiments such as lactate measurements may be additionally informative.

4.5.4 Pre-LCs lacking mitochondrial Fh1 exhibit lower apoptosis rates

Pre-LCs lacking mitochondrial *Fh1* exhibited similar proliferation rates to *control* and *control; FH^{Cyt}* pre-LCs as well as similar cell cycle status. Interestingly, the cells lacking mitochondrial *Fh1* exhibited a lower percentage of apoptotic and late apoptotic cells in the span of 48 hours. Furthermore, the sub-G0 content of cells can provide information regarding the apoptotic/late apoptotic fraction of cells. That is

because cells in the late stage of apoptosis lose DNA content due to their membrane breaking down. With that in mind, it was interesting to see that pre-LCs lacking mitochondrial *Fh1* exhibited a significantly lower percentage of cells at sub-G0 at the 48-hour time-point, corroborating with the data from the annexin V assay.

Similarly, LICs lacking mitochondrial *Fh1* exhibited a trend of fewer apoptotic/late apoptotic cells as well as a significantly lower percentage of cells in the sub-G0 phase. Furthermore, LICs exhibited a higher percentage of G0/1 cells at the 24-hour time-point, potentially indicating that there is a larger fraction of the cells at a resting phase, compared to *control* and *control; FH^{Cyt}* LICs. However, if that were the case it would be expected that cells would have a lower proliferation rate, which was not observed.

It has been suggested that complete or partial OXPHOS defects may induce apoptosis resistance. Specifically, inhibition of the respiratory chain can suppress the activation of the pro-apoptotic BCL-2 proteins Bax and Bak (Tomiyama et al., 2006). Thus, the decreased apoptosis rate observed in *$Fh1^{fl/fl}$; FH^{Cyt}; Vav-iCre* cells could be attributed to the disruption of OXPHOS due to deletion of mitochondrial *Fh1*. Interestingly, evasion of apoptosis has been observed in *FH*-null renal cancer cells (Bardella et al., 2012). The authors found that AMPK activation, as a result of fumarate accumulation, led to an increase of the inhibitory phosphorylation of the pro-apoptotic protein BAD (Bardella et al., 2012). Based on those observations, the authors proposed that increased fumarate could activate G-protein coupled receptors, which may lead to activation of AMPK. It has been shown previously by others and by our lab that *FH^{Cyt}* expression metabolises the accumulated fumarate, as a result of mitochondrial *Fh1* deletion, thus bringing fumarate concentration to almost physiological levels. However, we have observed that fumarate is still significantly increased in *$Fh1^{fl/fl}$; FH^{Cyt}; Vav-iCre* compared to *control* cells. As a result, it is possible that elevated fumarate concentration is enough to activate AMPK and effectively inhibit BAD.

4.6 Summary

In summary, in this chapter the data indicate that *Fh1* (and effectively genetically intact TCA) are important for the generation of LICs but are dispensable for the long-term self-renewal capacity of LICs and maintenance of AML. Furthermore, LICs isolated from the bone marrow of sick recipient mice exhibited low SRC. Based on other studies, low SRC could be the reason why cells were unable to efficiently generate AML in mice, as SRC is thought to reflect how well cells can respond to high energy demands and also support long-term function. Additionally, LICs with low SRC could potentially utilise more glycolysis in order to compensate for their inability to efficiently utilise mitochondrial respiration. Finally, pre-LCs and LICs lacking mitochondrial *Fh1*, exhibited lower rates of apoptosis, that could be attributed to inhibition of pro-apoptotic proteins as a result of either OXPHOS disruption or AMPK activation. This chapter has provided insight about the role of oxidative respiration in AML cells in the *Meis1/Hoxa9* background. However, it will be informative to assess the role of *Fh1* and mitochondrial respiration using additional AML models.

CHAPTER 5

The role of *Fh1* in leukaemic transformation

5 The role of *Fh1* in leukaemic transformation

5.1 Introduction

5.1.1 FH in AML

AML is a clonal disease that is initiated from a small number of pre-leukaemic cells (pre-LCs) that have acquired initiating mutational events. Additional genetic hits lead to the generation of leukaemia-initiating cells (LICs). Pre-LCs consist of self-renewing haematopoietic stem and progenitor cells that can give rise to leukaemia *in vivo* with variable latency, and upon gradual accumulation of co-operative hits, LICs are functionally defined by their capacity to generate fully penetrant AML, with a short latency in murine models (Pandolfi et al., 2013).

Mutations of the metabolic enzyme IDH1/2 genes represent a novel class of mutations in AML, present in approximately 20 % of all AML cases (Mardis et al., 2009). IDH1 and IDH2 enzymes catalyse the oxidative decarboxylation of isocitrate to a-kegotlutarate in the cytoplasm and mitochondria respectively. Mechanistically, IDH1/2 mutations result in the accumulation of the metabolite 2-hydroxyglutarate. This metabolite accumulates at high concentrations in the cell at the expense of the metabolite a-ketoglutarate, thus leading to the inhibition of dioxygenase enzymes (that utilise a-ketoglutarate as a co-factor). Such enzymes include TET proteins and histone demethylases. The activity of the mutant IDH1/2 enzymes affect the energetic landscape of the cells, and the resultant generation of the 2-hydroxyglutarate (referred to as an "oncometabolite"), leads to epigenetic reprogramming, disruption of normal differentiation and contributes to a malignant phenotype (Rakheja et al., 2012). The identification of IDH mutations as a novel class of contributors to AML, opened the avenue to study metabolic enzymes and their role in malignant transformation.

Fh1 (FH in humans) is a *bona fide* tumour suppressor in kidney cancer and is an essential component of the TCA cycle (see section 1.11). However, its role in haematological malignancies has not been established. A study published in 1960 found that *FH* activity was significantly elevated in acute monocytic leukaemia as

well as moderately increased in acute granulocytic leukaemia. Interestingly, such increase was not observed in acute lymphocytic leukaemia cells (Tanaka et al., 1961). Similarly, a recent proteomics study identified that 7 out of 12 human AML patient samples that were studied had elevated *FH* protein levels. The study compared peripheral myeloid blast cells isolated from AML patients to $CD34^+$ cells isolated from healthy individuals (Elo et al., 2014).

Additionally, a search on Oncomine, a cancer genomics database, indicates that *FH* is both up- and down- regulated in different sub-types of AML with no apparent association with cytogenetics (oncomine.com). For instance, in a study looking at 43 AML patient samples, *FH* mRNA expression was deregulated in a fashion that was not consistent with FAB subtype, FLT3 mutation status or MLL re-arrangement status (Gutierrez et al., 2005).

The data obtained from different studies up to this point do not provide evidence to support whether the deregulation of the enzymatic activity of *FH* has a causal role in the generation of myeloid leukaemia or whether it is a consequence of the disease. Therefore, the aim of this chapter was to uncover the role of *Fh1* in AML using *in vivo* and *in vitro* murine models. The specific aims of the chapter are outlined below (See section 5.2).

5.2 Aims

The purpose of the following experiments was to determine the role of *Fh1* at different stages of leukaemic transformation. In particular, this chapter aims to determine the role of *Fh1*: In the generation of pre-leukaemic cells (pre-LCs)

In the maintenance of pre-LCs

In the maintenance of leukaemia-initiating cells (LICs):

By acute deletion of *Fh1 in vitro* utilising lentivirally expressed *Cre*

By acute inducible deletion of *Fh1 in vivo* utilizing the *Mx1-Cre* model

5.3 Experimental design

In order to address the aims of this chapter, the retroviral model of *Meis1/Hoxa9* was utilised, thus allowing for the assessment of the requirement of *Fh1* at different stages of leukaemic transformation. In this model primitive cells of the haematopoietic compartment are isolated and subsequently infected with retroviruses over-expressing *Meis1* and *Hoxa9*. The cells over-expressing *Meis1* and *Hoxa9* are then selected based on their antibiotic resistance to puromycin and neomycin, respectively. The experimental design was modified in order to address the above points individually, and are described via schematic representations below. Figure 5-1 describes the experimental design used to address whether *Fh1* plays a role in the generation of pre-LCs. Figure 5-2 describes the experimental design used to address whether *Fh1* plays a role in the maintenance of pre-LCs and LICs *in vitro*.

Finally, in order to address whether *Fh1* plays a role in the maintenance of LICs *in vivo*, the *Mx1-Cre* mouse model was used. *Mx1* (myxovirus resistance-1) is a vital part of the viral defence mechanism and its expression can be induced in response to interferon. Cre recombinase under the *Mx1* promoter can be activated by mimicking viral infection by the administration of the synthetic double-stranded RNA analogue poly:I:polyC (Kühn et al., 1995). A background activation of approximately 2-3 % is typically observed in the *Mx1-Cre* model as a result of endogenous interferon (Kühn et al., 1995). *Mx1-Cre* has been shown to be active in several tissues including heart, liver and kidney (Kühn et al., 1995). The experimental design is outlined in Figure 5-3.

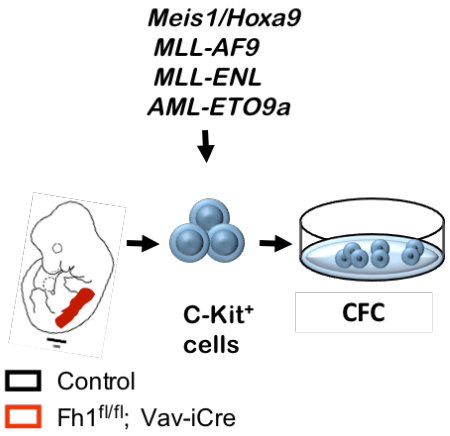

Figure 5-1. Experimental design. C-Kit^{+} cells isolated from 14.5dpc foetal livers were transduced with *Meis1/Hoxa9*, *MLL-AF9*, *MLL-ENL* and *AML-ETO9a* retroviruses and plated into methylcellulose, in order to assess their clonogenic potential. Specifically, 250,000 c-Kit^{+} cells underwent two rounds of infection with the respective viruses using retronectin-coated plates. After 48 hours, the cells were incubated with media containing antibiotics in order to select for the cells expressing the retroviruses (for *Meis1/Hoxa9* selection puromycin/neomycin was used. Neomycin was used for the rest of the plasmid-containing viruses). Following 48 hours of antibiotic selection, cells were seeded on semi-solid media (25,000 cells for *control,* and all surviving cells for *Fh1$^{fl/fl}$; Vav-iCre* cells). Colonies were counted 6 days after plating. This protocol was used to generate samples for figures 5-4 –5- 6.

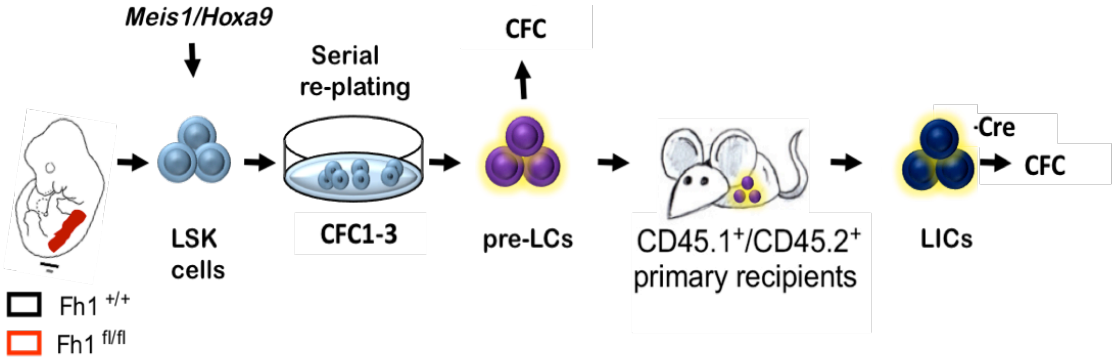

Figure 5-2. Experimental design. *Fh1*$^{+/+}$ and *Fh1*$^{fl/fl}$ (without *Vav-iCre*) LSK (lineage$^-$ Sca-1 $^+$ c-Kit$^+$) cells sorted from 14.5dpc foetal livers were co-transduced with *Meis1* and *Hoxa9* retroviruses and serially re-plated 3 times. The cells were subsequently infected with a bicistronic lentivirus expressing *Cre* and *iVenus* (or with lentivirus expressing the empty vector). *iVenus*$^+$ cells were sorted and plated into methylcellulose. In parallel, *Fh1*$^{+/+}$ and *Fh1*$^{fl/fl}$ pre-LCs were transplanted into recipient mice. LICs (CD45.2$^+$c-Kit$^+$ cells) were sorted from leukaemic recipients, transduced with *Cre* lentivirus (or with lentivirus expressing the empty vector) and after sorting, 25,000 cells were plated into methylcellulose. This protocol was used to generate figures 5-7 and 5-8.

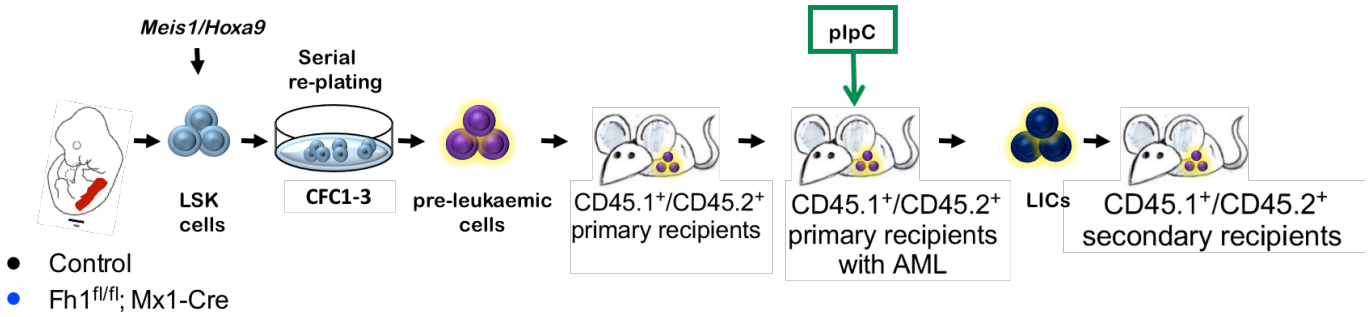

Figure 5-3. Experimental design. *Control* and *Fh1$^{fl/fl}$; Mx1-Cre* LSK (lineage$^-$ Sca-1 $^+$ c-Kit$^+$) cells sorted from 14.5dpc foetal livers were co-transduced with *Meis1* and *Hoxa9* retroviruses and were serially re-plated. The resultant pre-LCs were transplanted into sub-lethally irradiated CD45.1$^+$/CD45.2$^+$ recipients (100,000 cells per recipient). Once chimerism of leukaemic CD45.2$^+$ cells reached 20 % in the peripheral blood of recipient mice, mice were injected intra-peritoneally 6-8 times every alternate day with 300µg poly (I:C). Then 10,000 LICs (CD45.2$^+$c-Kit$^+$) from primary recipients were transplanted to secondary recipients. This protocol was used to generate figures 5-9 to 5-12.

5.4 Results

5.4.1 Fh1 is essential for the generation of pre-LCs

As described in Figure 5-1 stem and progenitor cells (c-Kit$^+$ cells) were isolated from the foetal liver of 14.5 dpc of *control* or *Fh1$^{fl/fl}$; Vav-iCre* embryos and were then infected with retroviruses expressing oncogenes or chromosomal translocations known to be involved in leukaemogenesis (described in section 1.9.3). When stem and progenitor cells lacking *Fh1* were transduced with *Meis1/Hoxa9*, *MLL-ENL*, *MLL-AF9* and *AML-ETO9a* retroviruses, they failed to generate colonies *in vitro,* indicating that cells require *Fh1* in order to undergo leukaemic transformation (Figure 5-4). Furthermore 48 hours post infection (and before the addition of antibiotics), there were fewer *Fh1$^{fl/fl}$; Vav-iCre* surviving cells compared to *control* cells indicating that expression of oncogenes/chromosomal translocations is not able to rescue the poor survival capacity of cells lacking *Fh1*(Figure 5-5; Figure 5-6).

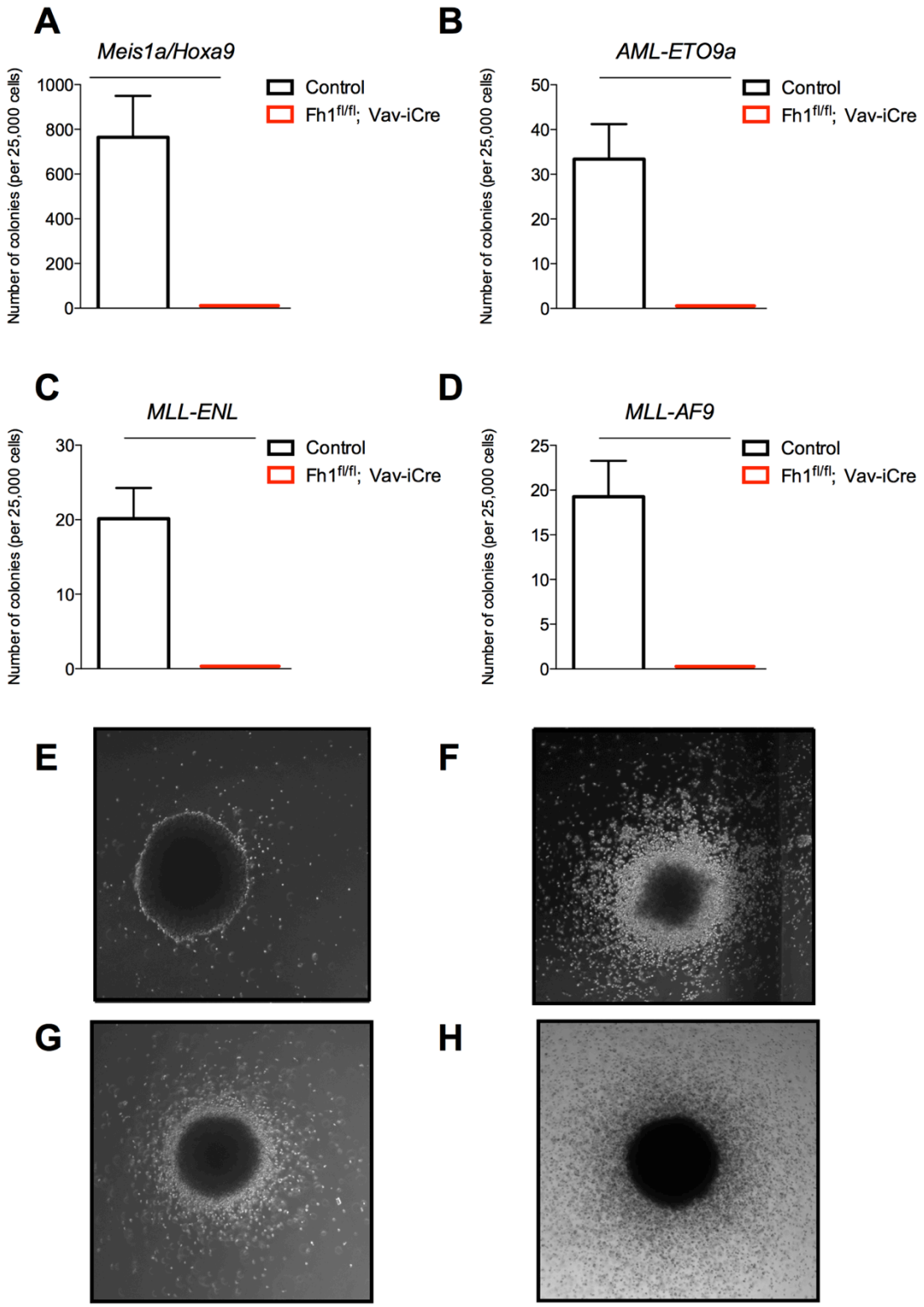

Figure 5-4. *Fh1*-deficient c-Kit^{+} cells fail to undergo transformation *in vitro*. (A-D) Shows colony counts 6 days after plating for retroviruses (A) *Meis1/Hoxa9*, (B) *AML-ETO9a,* (C) *MLL-ENL*, (D) *MLL-AF9*. (E-H) Shows representative colony images (10X magnification) (E) *Meis1/Hoxa9*, (F) *AML-ETO9a,* (G) *MLL-ENL*, (H) *MLL-AF9*. Data are mean ± S.E.M. n = 4-6 biological replicates per genotype.

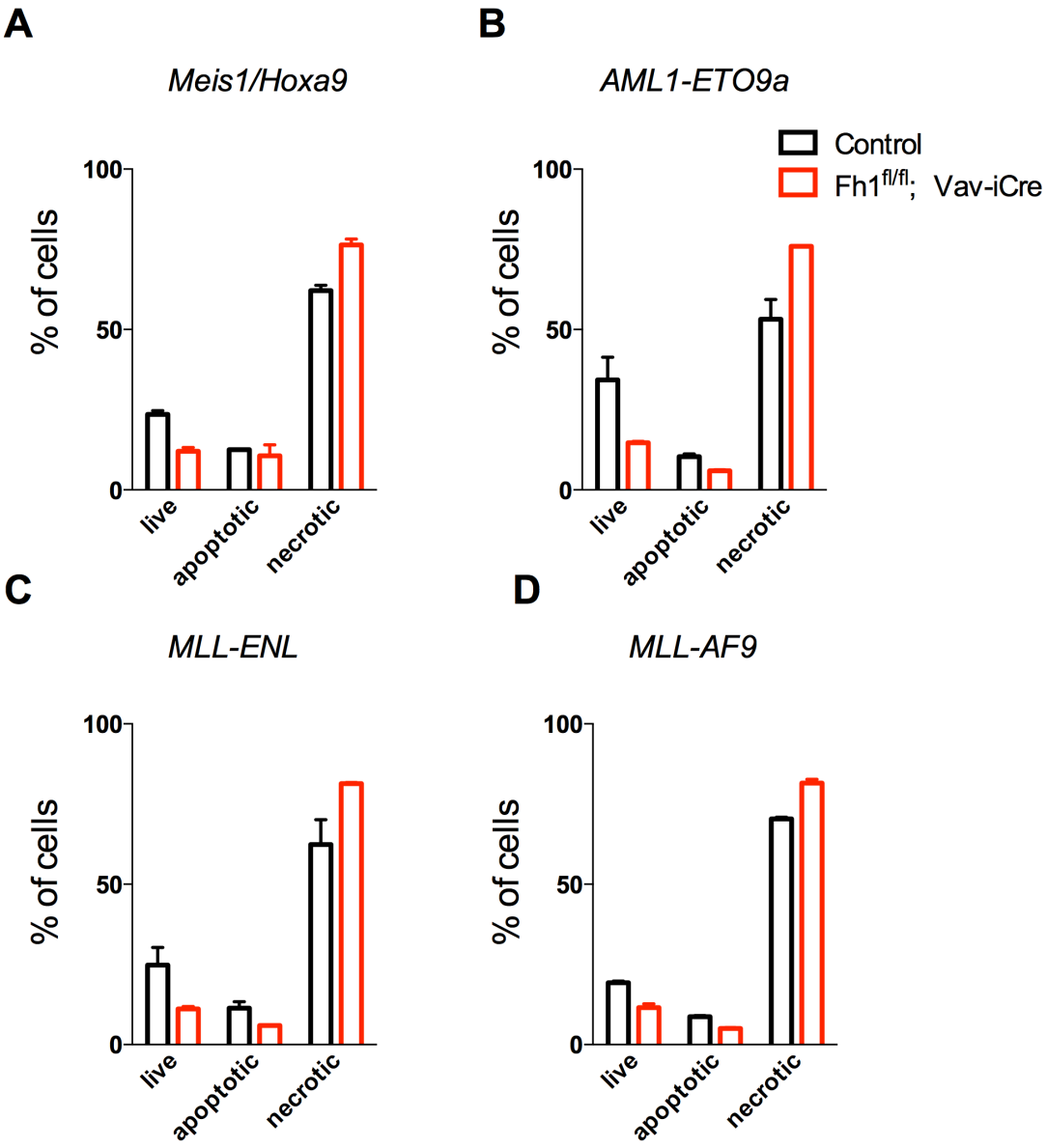

Figure 5-5. A higher percentage of *Fh1$^{fl/fl}$; Vav-iCre* cells undergo apotosis compared to *control* cells during leukaemic transformation. The percentage of cells that are annexinV^{-}DAPI^{-} (live), annexinV^{+}DAPI^{-} (apoptotic) and annexinV^{+}DAPI^{+} (late apoptotic) using the retroviruses (A) *Meis1/Hoxa9*, (B) *AML1-ETO9a*, (C) *MLL-ENL*, (D) *MLL-AF9*. The percentage indicates the fraction of cells from the parental gate (lymphocytes) during leukaemic transformation but before antibiotic selection. n = 2 biological replicates, Graphs show mean ± S.E.M.

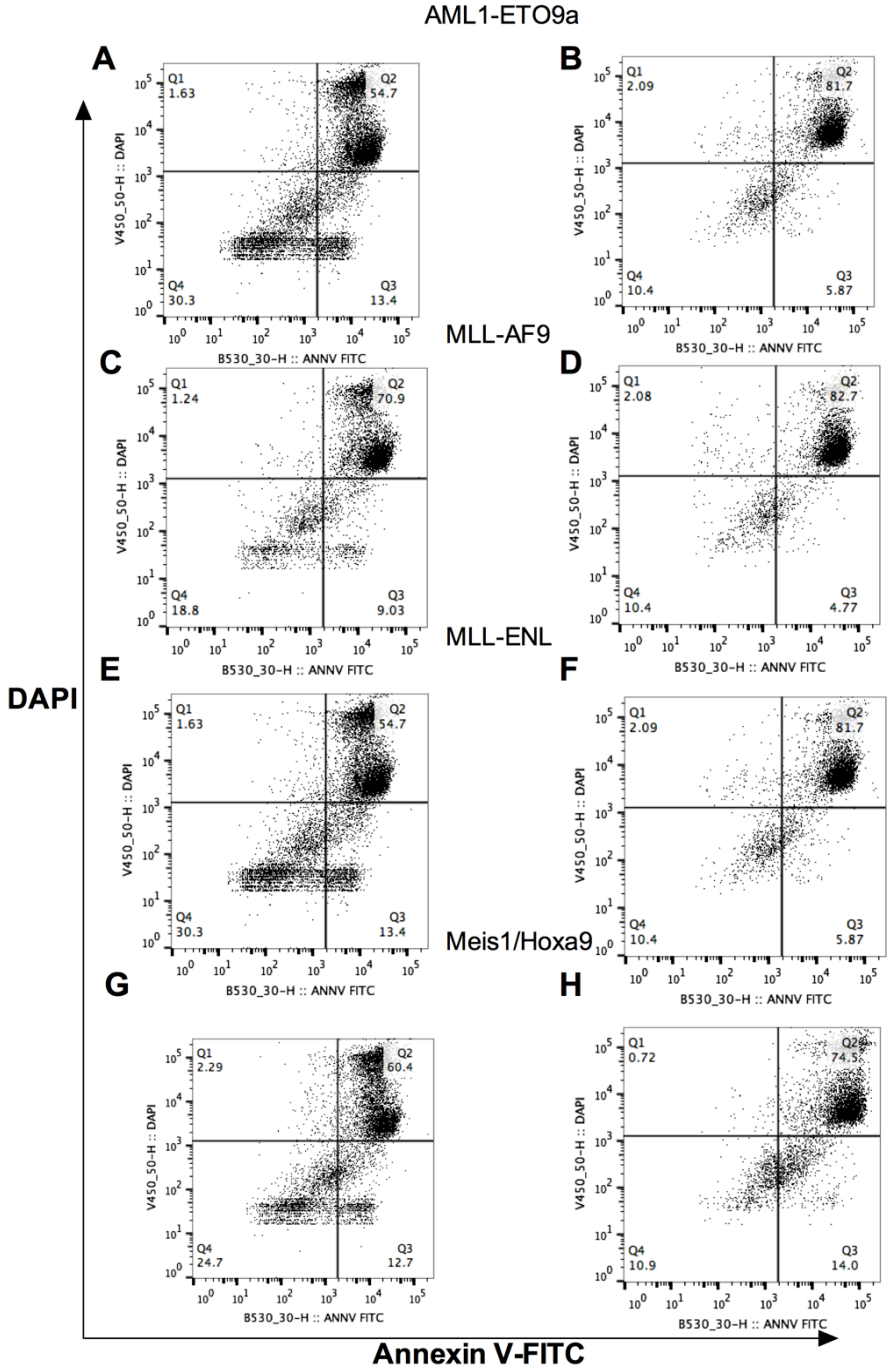

Figure 5-6. Representative FACS plots of annexinV staining during leukaemic transformation. (A-B) *AML1-ETO9a*, (C-D) *MLL-AF9*, (E-F) *MLL-ENL*, (G-H) *Meis1/Hoxa9*. In the left-hand panels apoptosis prolife of *control* cells 48 hours after retroviral infection. The apoptosis profile of *Fh1*$^{fl/fl}$*; Vav-iCre* cells is shown in the right-hand panels. The percentage of cells that are annexinV^{-}DAPI^{-} (live), annexinV^{+}DAPI^{-} (apoptotic) and annexinV^{+}DAPI^{+} (late apoptotic) using the retroviruses *AML1-ETO9a*, *MLL-AF9, MLL-ENL*, and *Meis1/Hoxa9.*

5.4.2 Fh1 is essential for the maintenance of pre-LCs

I next wanted to determine the impact of *Fh1* deletion on the colony formation capacity of pre-LCs. I transduced $Fh1^{+/+}$ (*Vav-iCre* negative) and $Fh1^{fl/fl}$ (*Vav-iCre* negative) foetal liver LSK (lineage$^-$ Sca-1$^+$ c-Kit$^+$) cells with *Meis1* and *Hoxa9* retroviruses. Following three rounds of serial re-plating, the cells were infected with *Cre –iVenus* lentivirus (or lentivirus containing the empty vector pRRL–*iVenus*), to acutely induce deletion of *Fh1* (for experimental design see Figure 5-2). Contrary to $Fh1^{+/+}$ cells expressing *Cre,* $Fh1^{fl/fl}$ cells failed to generate colonies but occasionally generated microscopic clusters that consisted of approximately 50-100 cells (Figure 5-7 B, C-D). Deletion of *Fh1* was assessed via genomic PCR of pre-LCs sorted based on *iVenus* positivity, 48 hours post-infection (Figure 5-7 E). Notably, $Fh1^{fl/fl}$ cells expressing the empty vector (pRRL-*iVenus*) generated significantly fewer colonies compared to $Fh1^{+/+}$ cells, potentially indicating lentiviral-related toxicity (Figure 5-7 A). These data therefore suggest that *Fh1* is critical for pre-LC maintenance.

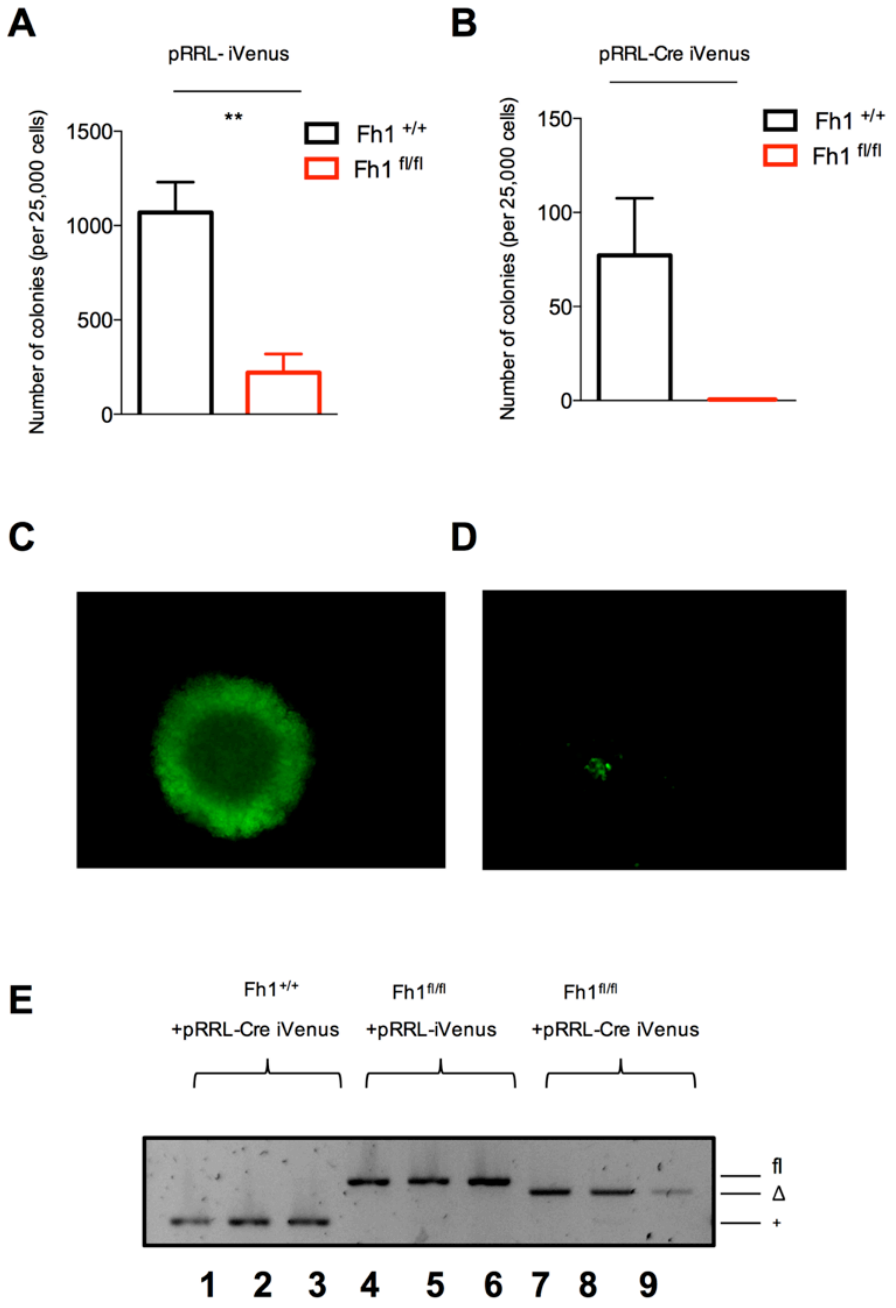

Figure 5-7. Acute deletion of *Fh1* in pre-LCs abolishes their clonogenic capacity. (A) Shows number of colonies generated by cells expressing the empty vector *pRRL-iVenus* at CFC3 (B) Shows number of colonies generated by *Cre*-expressing cells (*pRRL-Cre-iVenus*). Data are ± S.E.M., n = 3 biological replicates per genotype. (C-D) Representative images of colonies generated by $Fh1^{+/+}$ (C), or $Fh1^{fl/fl}$ cells (10x magnification) (D). (E) Representative gel showing PCR amplification of genomic DNA sorted from cells expressing either *pRRL-iVenus* emty vector or with *pRRL-*

Cre-iVenus (Lanes 1-3 = $Fh1^{+/+}$ infected with *pRRL-Cre-iVenus, lanes 4-6* = $Fh1^{fl/fl}$ infected with *pRRL-iVenus*, *lanes 7-9* = $Fh1^{fl/fl}$ infected *pRRL-Cre-iVenus*). fl-undeleted conditinal allele, Δ- excised allele, +-wild type allele. **p value< 0.005, Unpaired t test.

5.4.3 Fh1 is essential for the self-renewal capacity of LICs in vitro

In order to determine the requirement of *Fh1* for the maintenance of LICs, foetal liver LSK cells from $Fh1^{+/+}$ *(Vav-iCre negative*) and $Fh1^{fl/fl}$ *(Vav-iCre negative)* embryos were infected with *Meis1* and *Hoxa9* retroviruses. After three rounds of serial re-plating in semi-solid media the pre-LCs were transplanted into sub-lethally irradiated recipients. At the point where the primary recipient mice developed AML (i.e over 30 % of LIC chimerism in the peripheral blood of recipient mice), LICs were isolated and were then infected with lentiviruses expressing either *Cre* or the empty vector and were plated in semi-solid media to assess their clonogenic capacity (for experimental design see Figure 5-2).

Fh1-deficient LICs failed to generate colonies indicating that *Fh1* is required for LIC self-renewal (Figure 5-8 A, B). Similarly to pre-LCs, LICs lacking *Fh1* occasionally generated relatively small colonies compared to the large colonies generated by $Fh1^{+/+}$ cells expressing *Cre* (Figure 5-8 C, D*)*. Deletion of *Fh1* was confirmed by genomic PCR of LICs isolated based on *iVenus* positivity, 48 hours post-infection (Figure 5-8 E).

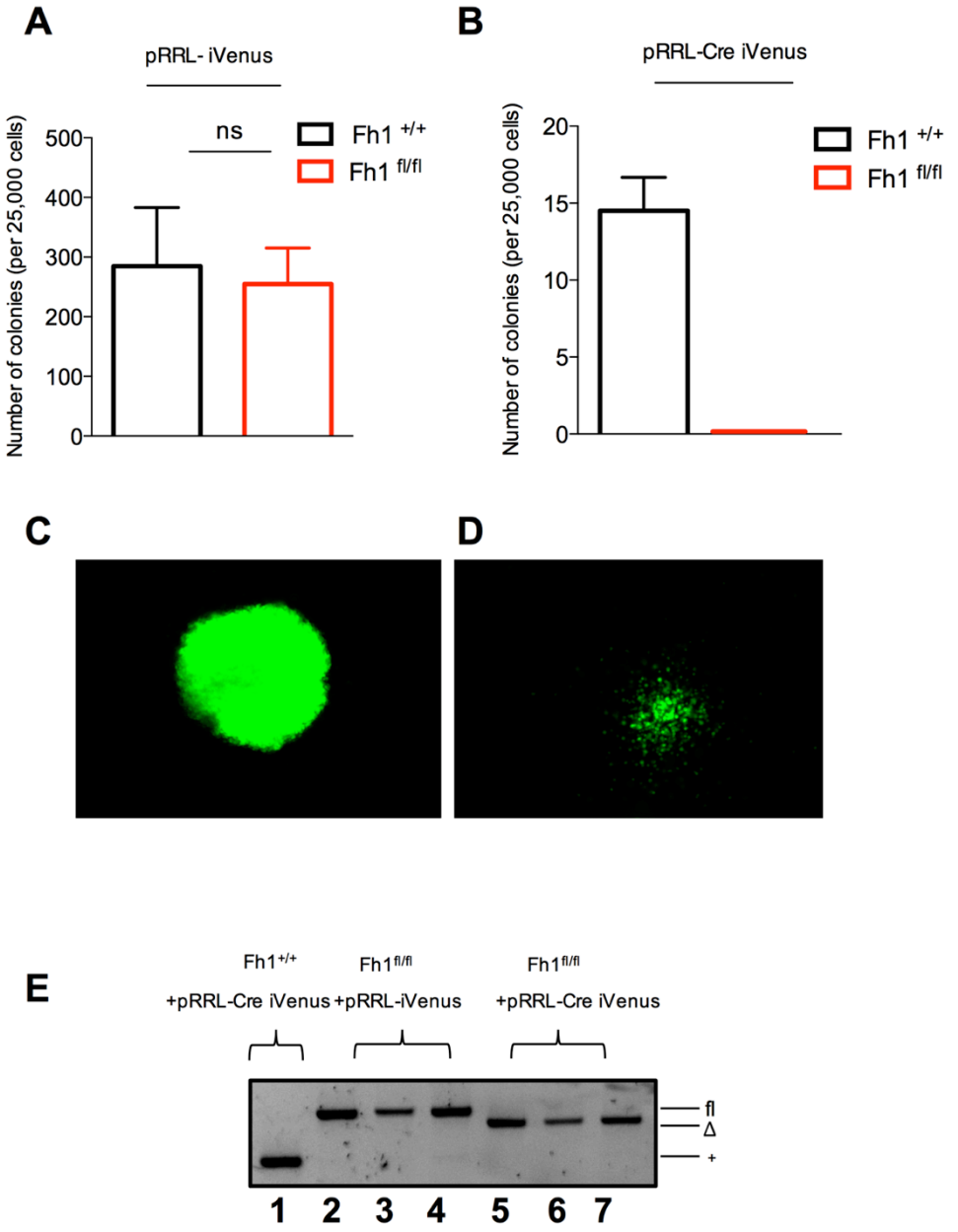

Figure 5-8. Acute deletion of *Fh1* in LICs abolishes their clonogenic capacity. *(A)* Shows number of colonies generated by cells expressing the empty vector. (B) Shows number of colonies generated by *Cre*-expressing cells. LICs were isolated from the bone marrow of mice that succumbed to AML and were then infected with lentivirally expressed *Cre*, to induce deletion of *Fh1*. Data are ± S.E.M. n = 3 biological replicates per genotype. (C-D) Representative images of colonies generated by $Fh1^{+/+}$ (C), or $Fh1^{fl/fl}$ cells (10x magnification). (E) Representative gel showing PCR amplification of genomic DNA sorted from cells expressing either empty vector (*pRRL-iVenus*) or *Cre* (*pRRL-Cre-iVenus)*. Lane 1 = $Fh1^{+/+}$ infected with *pRRL-Cre iVenus,* lanes 2-4 = $Fh1^{fl/fl}$ infected with *pRRL-iVenus,* lanes 5-7 =

Fh1$^{fl/fl}$ infected with *pRRL-Cre-iVenus*. fl- undeleted conditional allele, Δ- excised allele, + wild type allele. Unpaired t test.

5.4.4 Fh1 deletion can result in a decrease of LICs in vivo

To assess whether *Fh1* is required for the maintenance of LICs *in vivo,* LSK cells from 14.5 foetal liver embryos of the *Mx1-Cre* background were infected with retroviruses expressing *Meis1* and *Hoxa9* (For experimental design and description of the *Mx1-Cre* model, see section 5.3). After three rounds of serial re-plating 100,000 pre-LCs (c-Kit$^+$; double positive for Mac-1$^+$, Gr1$^+$) (see profile in Figure 5-9) were transplanted into primary recipient mice. The mice were monitored for clinical signs of AML, including hunched posture, slow movement, anaemia (white paws) and difficulty breathing. Once the chimerism of leukaemic cells (CD45.2$^+$) reached 20-30 % in the peripheral blood of recipient mice (CD45.1$^+$/CD45.2$^+$), mice were administered 6-8 intraperitoneal injections of poly (I:C) in order to induce deletion of *Fh1* within the leukaemic cell compartment (Figure 5-10; for more details on experimental design, see Figure 5-3). The primary recipient mice were monitored in order to assess the chimerism of the leukaemic cells in the peripheral blood. 10,000 LICs (CD45.2$^+$/c-Kit$^+$) LICs were then isolated from the bone marrow of primary recipient mice that succumbed to AML and were transplanted into sub-lethally irradiated secondary recipients. LICs are functionally defined by their capacity to generate fully penetrant AML, with a short latency in murine models (Pandolfi et al., 2013).

We found that upon administration of poly (I:C), the chimerism of *Fh1*$^{\Delta/\Delta}$*; Mx1-Cre* leukaemic cells (cells with deletion of *Fh1* after they were treated with poly (I:C)) decreased significantly after the third injection of poly (I:C) compared to chimerism of the *control* cells (Figure 5-10; A). Specifically, while *control* recipient mice exhibited increasingly high chimerism in their peripheral blood (20-30% before poly (I:C) compared to 50-60 % after 8 injections of poly (I:C)), *Fh1*$^{\Delta/\Delta}$*; Mx1-Cre* recipient mice exhibited decreased chimerism (40-60 % before poly (I:C) compared to 1-2 % after 8 injections of poly (I:C)). Notably, after the third injection of poly

(I:C), there was a decrease in the chimerism of the leukaemic cells in the *control* mice, indicative of the effect of poly (I:C) on leukaemic cells irrespective of the status of *Fh1* deletion (Figure 5-10; A).

Interestingly, two weeks after the last poly (I:C) injection the chimerism of $Fh1^{\Delta/\Delta}$; *Mx1-Cre* cells increased between 20-80 % (Figure 5-10; A). Recipient mice succumbed to AML as indicated by infiltration of LICs in the bone marrow and spleen (Figure 5-10; C, D). Genomic PCR performed on LICs isolated from the bone marrow of sick recipient mice at the point of sacrifice, indicated that *Fh1* deletion in the bone marrow was incomplete, suggesting that there might be two populations co-existing, one with undeleted *Fh1* and one with a complete deletion of *Fh1*(Figure 5-10; B). In order to assess whether the leukaemic cells with *Fh1* deletion could outcompete the other population and propagate leukaemia, we isolated $CD45.2^{+}$ c-Kit^{+} LICs from the bone marrow of primary recipient mice and transplanted them into sub-lethally secondary recipient mice (n = 1 *control*, n = 2 $Fh1^{\Delta/\Delta}$; *Mx1-Cre).* Recipients from both cohorts developed leukaemia at a similar same rate and bone marrow was largely populated by LICs (Figure 5-11 B). Genomic PCR analysis of LICs isolated from the peripheral blood of recipient mice, showed that some of the recipients injected with $Fh1^{\Delta/\Delta}$; *Mx1-Cre* LICs exhibited full deletion of *Fh1* (Figure 5-11A).

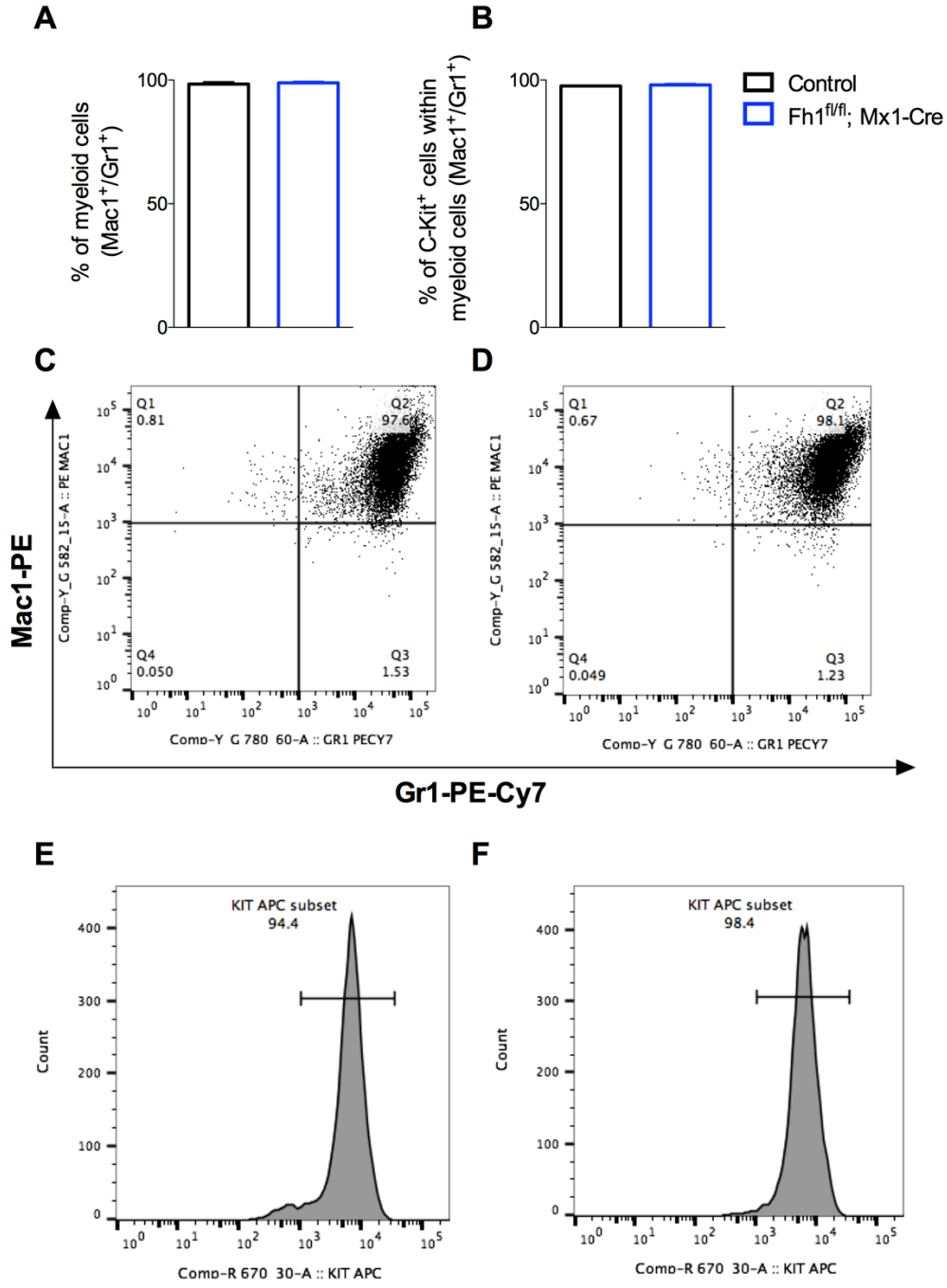

Figure 5-9. Flow cytometry profile of *control* and *Fh1$^{fl/fl}$; Mx1-Cre* pre-LCs prior to transplantation in recipient mice. (A) Percentage of pre-LCs expressing myeloid markers (Mac1^{+}/Gr1^{+}). (B) Percentage of pre-LCs that are positive for c-Kit, within the Mac1^{+}/Gr1^{+} compartment. (C-D) Representative FACS plots of *control* pre-LCs (C) and *Fh1$^{fl/fl}$; Mx1-Cre* pre-LCs (D) expressing the myeloid markers Mac1 and Gr1. (E-F) Representative FACS histogram showing the expression of c-Kit in *control* pre-LCs (E) and *Fh1*$^{fl/fl}$; *Mx1-Cre* pre-LCs (F). Data are ± S.E.M. with n = 2 biological replicates for *control* and n = 3 biological replicates for *Fh1$^{fl/fl}$; Mx1-Cre.*

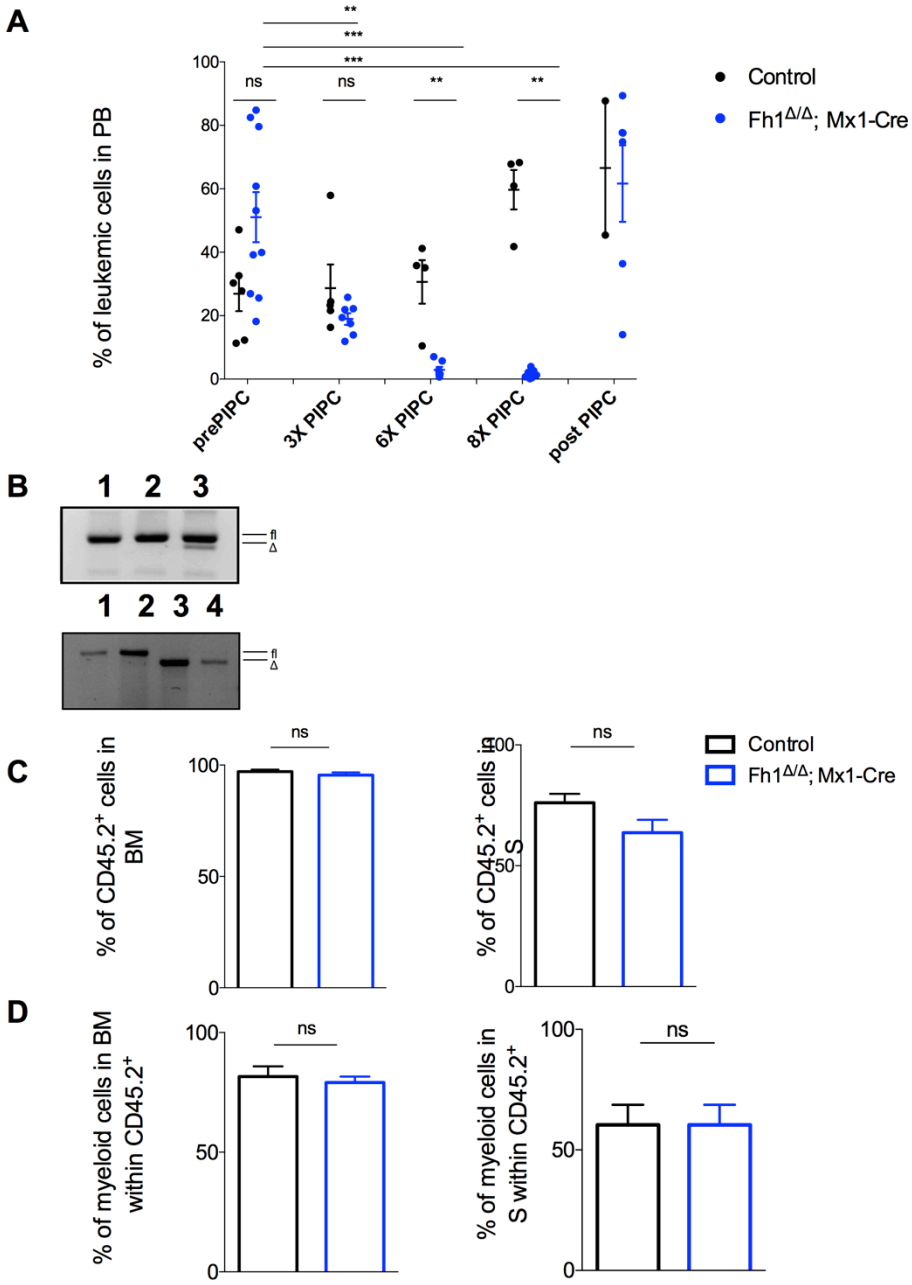

Figure 5-10. Acute deletion of *Fh1* in LICs reduces their self-renewal capacity *in vivo*. (A) Chimerism of leukaemic cells in the peripheral blood of recipient mice. Chimerism was assessed two days after each poly (I:C) administration and two weeks after the last injection. (B) Representative gel of genomic PCR assessing the deletion of *Fh1* before poly (I:C) treatment (top gel: lane 1= *Control*, lanes 2-3 = $Fh1^{fl/fl}$; *Mx1-Cre*) and after 6 doses of poly (I:C) treatment (bottom gel: lanes 1-2 = *Control*, lanes 3-4= $Fh1^{\Delta/\Delta}$; *Mx1-Cre.*) PCR was performed on leukaemic cells isolated from the peripheral blood of recipient mice that were sorted for $CD45.2^{+}$. (C) Chimerism of leukaemic cells in the bone marrow (left) and spleen (right) of recipient mice at the point of sacrifice. (D) Percentage of myeloid cells within the

CD45.2 compartment, in the bone marrow (left) and spleen (right) of recipient mice at point of sacrifice (myeloid cells are defined as the sum of $Mac1^{+}/Gr1^{+}$ and $Mac1^{+}$). n = 2-3 biological replicates per genotype, 6-10 recipient mice per genotype. PB – Peripheral Blood; BM – Bone Marrow; S – Spleen. PIPC – poly (I:C). Data are ± S.E.M. ** p< 0.005, *** p< 0.001. Mann-Whitney test.

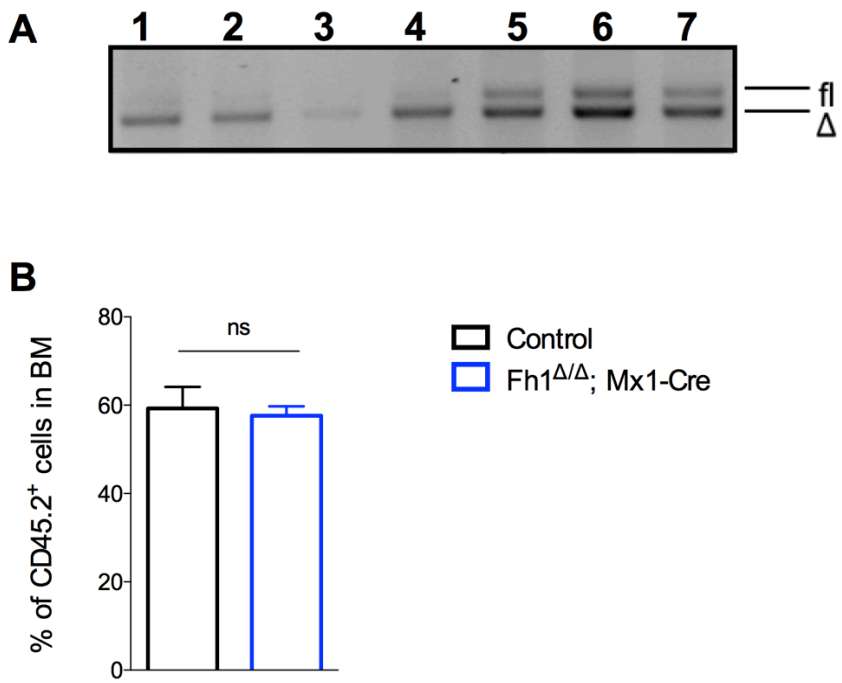

Figure 5-11. Assessing the role of *Fh1* in the maintenance of LICs. (A) Genomic PCR assessing the status of *Fh1* deletion from LICs isolated from the peripheral blood of secondary receipients. Bands represent individual recipients. Lanes 1-4 = LICs isolated from one biological sample (injected into 4 recipient mice), exhibiting full deletion of *Fh1*. Lanes 5-7 = LICs isolated from a second biological sample and exhibit incomplete deletion of *Fh1*. (B) Graph shows chimerism of leukaemic cells within the bone marrow of sick recipient mice at the point of sacrifice (n = 3 recipient mice for *control,* n= 9 recipient mice for $Fh1^{\Delta/\Delta}$; *Mx1-Cre* mice. Data are ± S.E.M. p = 0.075, Wilcoxon paired test. fl- undeleted conditional allele, Δ- excised allele.

Notably, all recipients were injected with LICs originating from the same biological sample. These data indicate that it is possible for LICs to survive without *Fh1* and generate AML in recipient mice. Given the fact that out of the three biological LIC samples, one was able to survive without *Fh1* I repeated the primary transplantation with two additional biological samples. Similarly to the first experiment, $Fh1^{\Delta/\Delta}$; *Mx1-Cre* LIC chimerism decreased after poly (I:C) administration (Figure 5-12 A) and *Fh1* deletion was confirmed via genomic PCR (Figure 5-12 B top before poly (I:C), bottom after poly (I:C)). Two weeks after the last poly (I:C) administration, mice succumbed to AML as indicated by infiltration of LICs ($CD45.2^+$; $Mac1^+/Gr1^+$) in the bone marrow and spleen (Figure 5-12 D, E). At the point of sacrifice LICs were isolated from the bone marrow of recipient mice in order to assess the deletion status of *Fh1*. Genomic PCR showed that *Fh1* was fully deleted in LICs (Figure 5-12 C). Collectively, it appears that lack of *Fh1* is not always detrimental to the long-term survival of LICs.

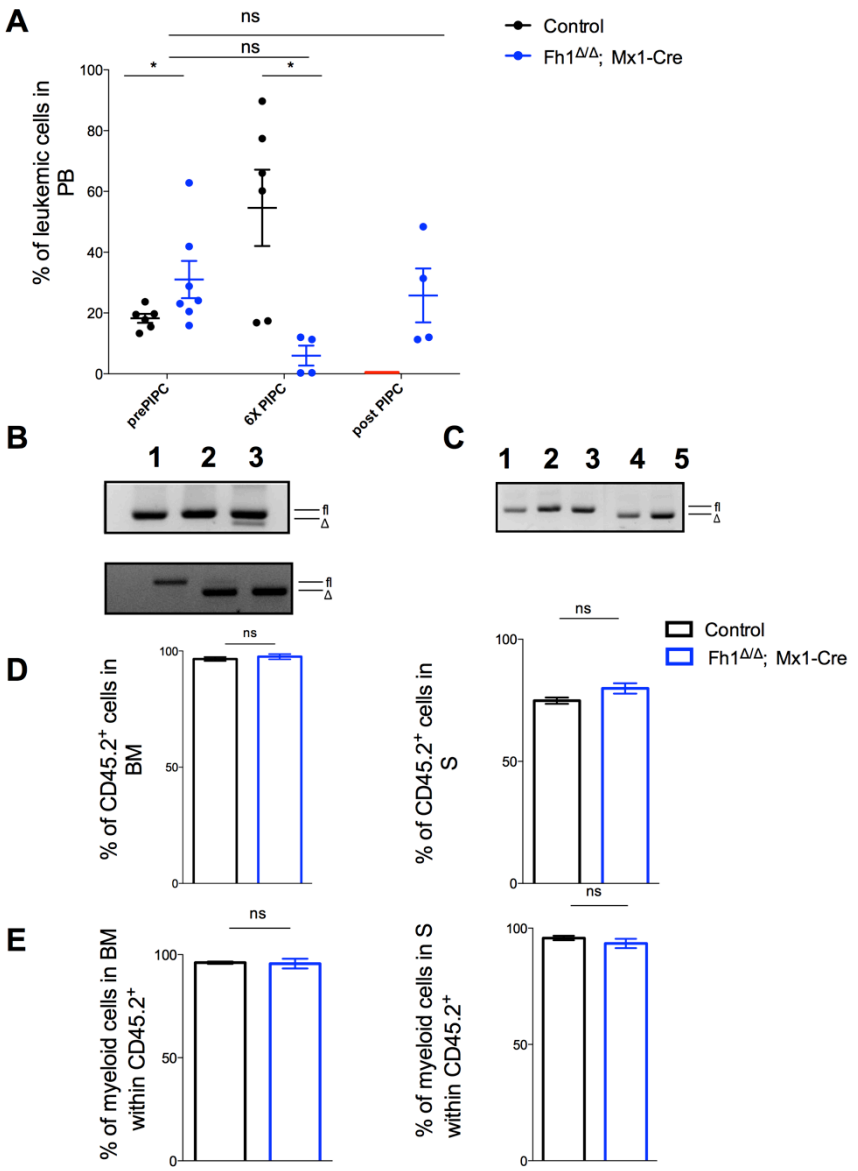

Figure 5-12. Acute deletion of *Fh1* in LICs results in reduction of their self-renewal capacity. (A) Chimerism of leukaemic cells in the peripheral blood of recipient mice. Chimerism was assessed two days after each poly (I:C) administration and two weeks after the last injection of poly (I:C). Of note, 2 weeks after poly (I:C) there were no remaining *control* mice. (B) Representative gel of genomic PCR assessing the deletion of *Fh1* before poly (I:C) treatment (top) and after 6 injections of poly (I:C) treatment (bottom). Top gel: lane 1 = control, lanes 2,3 = $Fh1^{fl/fl}$; *Mx1-Cre* mice. Bottom gel: lane 1= control, lanes 2,3 = $Fh1^{\Delta/\Delta}$; *Mx1-Cre* mice. (C) Genomic PCR assessing the deletion of *Fh1* in the bone marrow of recipient mice at the point of sacrifice. Lanes 1-3 = *Control,* lanes 4-5 = $Fh1^{\Delta/\Delta}$;

Mx1-Cre mice. (D) Chimerism of leukaemic cells in the bone marrow (left) and spleen (right) of recipient mice at the point of sacrifice. (E) Percentage of myeloid cells within the $CD45.2^+$ compartment, in the bone marrow (left) and spleen (right) of recipient mice at point of sacrifice (myeloid cells are defined as the sum of $Mac1^+/Gr1^+$ and $Mac1^+$). n = 2 biological replicates per genotype, 4 recipient mice per genotype. Data are ± S.E.M. Mann- Whitney, * $p< 0.05$.

5.5 Discussion

5.5.1 Fh1 is essential for the generation and maintenance of pre-LCs

In this chapter I assessed the requirement of *Fh1* in the generation of pre-LCs by infecting *control* or *Fh1$^{fl/fl}$; Vav-iCre* stem and progenitor cells with retroviruses expressing oncogenes or chromosomal translocation fragments known to be involved in AML development. In all cases, *Fh1$^{fl/fl}$; Vav-iCre* cells were unable to generate colonies indicating that *Fh1* is critical for the generation of pre-LCs.

However, given the fact the chromosomal translocations utilised above are frequently identified with other driver or secondary mutations in AML patients, it is possible that their expression alone would not be sufficient to rescue the effects that *Fh1* deletion would have. Therefore, it would be informative to express the oncogenes or chromosomal translocation fragments in combination in *Fh1$^{fl/fl}$*; *Vav-iCre* cells.

It is notable that *Fh1$^{fl/fl}$; Vav-iCre* cells exhibited decreased survival rates compared to *control* cells during the infection process before the addition of antibiotics indicating that cells lacking *Fh1* would eventually die, regardless of the oncogene they were expressing thus indicating that *Fh1* is essential for the survival of haematopoietic cells.

The requirement of *Fh1* in the maintenance of pre-LCs was assessed as well. For that pre-LCs were generated by isolating LSK cells from *Fh1$^{fl/fl}$* (*Vav-iCre negative)* and *Fh1$^{+/+}$* (*Vav-iCre negative)* embryos and infecting them with retroviruses expressing *Meis1* and *Hoxa9*. Established pre-LCs were then infected with lentivirus expressing *Cre* in order to induce deletion of *Fh1*. Following deletion of *Fh1*, pre-LCs were unable to generate colonies when plated in semi-solid media indicating that *Fh1* is required for pre-LCs to efficiently self-renew. It is notable that *Fh1$^{fl/fl}$* (*Vav-iCre negative)* cells infected with pRRL-empty vector exhibited a lower colony count compared to *Fh1$^{+/+}$* (*Vav-iCre negative)* (mean count of approximately 200 versus 800 colonies). This potentially indicates that the infection process itself had a

negative impact on the $Fh1^{fl/fl}$ (*Vav-iCre negative)* cells, as no background deletion was observed.

5.5.2 Fh1 deletion can result in drastic decrease of LICs in vivo

In order to assess the requirement of *Fh1* in the maintenance of LICs *in vivo,* I generated pre-LCs (as described above) of the *Mx1-Cre* background. Once the recipient mice exhibited LIC chimerism of 20-30 %, I initiated poly (I:C) injections. It is notable that after the third injection I observed a decrease in the chimerism of the leukaemic cells regardless of the status of *Fh1* deletion, indicating that poly (I:C) might have an effect on the survival of leukaemic cells. Indeed, when I performed a literature search, I found a scientific paper stating that poly (I:C) has a negative impact on the survival of leukaemic cells (Zeleznick and Bhuyan, 1969). The proposed mechanism is that poly (I:C) induces the host interferon response which slows the multiplication of the leukaemic cells, rather than exerting a cytotoxic effect on them(Zeleznick and Bhuyan, 1969). Furthermore, poly (I:C) elicits an interferon alpha response, and interferon alpha was used extensively to treat CML indicating that poly (I:C) would have an effect on leukaemic cells (Talpaz et al., 1983; 1986). Although the decrease in chimerism that I observed during the first three injections cannot be solely attributed to *Fh1* deletion, it is probable that the decrease observed beyond that point, was in fact attributed to *Fh1* deletion (as chimerism of *control* mice increased while it decreased in the $Fh1^{\Delta/\Delta}$*; Mx1-Cre* mice).

Moreover, when deleting *Fh1* acutely *in vitro* in LICs (using lentivirally expressed *Cre)*, I observed very small clusters (approximately 50 - 100 cells) indicating that LICs lacking *Fh1* can support minimal levels of their self-renewal capacity. In corroboration with this finding, following deletion of *Fh1* in LICs *in vivo*, I observed residual (1-2 %) and eventually full chimerism (60-80 %) of a mixed population of LICs, indicating that LICs lacking *Fh1* can survive for a period of time and fully expand and generate disease. We questioned whether the population of LICs with the

full deletion of *Fh1* would be able to propagate disease. In order to assess this point, we isolated LICs from the bone marrow of sick primary recipient mice and injected them into secondary recipients. At the point of sacrifice, we assessed the deletion of *Fh1* in LICs isolated from the bone marrow of sick recipient mice. Surprisingly, we found that some of the recipients (that were injected with LICs originating from the same biological sample), exhibited a full deletion of *Fh1*.

Given the fact that one biological sample out of the three was able to eventually expand and generate disease, we repeated the experiment using two additional biological samples. Similarly, once the LIC chimerism in primary recipient mice reached 20-30 %, we initiated poly (I:C) treatment. A few weeks after the last poly (I:C) treatment, $Fh1^{\Delta/\Delta}$; *Mx1-Cre* mice exhibited expanded LIC chimerism. At the point of sacrifice, the bone marrow cells of these mice were genotyped in order to assess the deletion of *Fh1*. To our surprise, all of the mice that were sacrificed exhibited a full deletion of *Fh1* in LICs.

Fh1 deletion, in combination with other mutations that could be occurring *in vivo,* offered a competitive survival advantage to the remaining LICs (as most LICs were eradicated after *Fh1* deletion), thus by-passing the potential metabolic defects as a result of *Fh1* deletion. Furthermore, although we have hypothesised that fumarate accumulation, as a result of *Fh1* deletion, has detrimental effects to haematopoietic cells (possibly due to inactivation of various proteins as a result of succination, or due to allosteric regulation of various enzymes by fumarate), it is nevertheless plausible that just like in the case of kidney cancer cells, fumarate acts as an oncometabolite in our retroviral *Meis1/ Hoxa9* model (Yang et al., 2012). It appears that in certain cases *Fh1* deletion selects for aggressive AML clones that are able to bypass the effects that *Fh1* deletion would have. Furthermore, this study potentially highlights the difference in metabolic requirements of pre-LCs and LICs as *Fh1* appears to be essential for the survival of pre-LCs but not for LICs.

In summary, *Fh1* is essential for the generation and maintenance of pre-LCs. The requirement of *Fh1* for LIC maintenance appears to be initially critical as the bulk population of AML cells were eradicated. However, in half of the cases observed the

remaining 1-2 % of LICs appeared to be able to repopulate the bone marrow of recipient mice, despite the deletion of *Fh1*. A certain percentage of AML patients after chemotherapy, exhibit relapse of AML due to "chemotherapy resistant" LICs. These LICs are often more aggressive than the initial AML clone, as chemotherapy is thought to select for these aggressive AML clones. In a similar manner, *Fh1* deletion could provide a selective advantage for certain AML clones within our murine model.

Furthermore, *Fh1* does not appear to be a tumour suppressor in AML, as opposed to in HLRCC. Finally, it is important to keep in mind that our findings were observed using one *in vivo* model and therefore conclusions about AML subtypes with varying genetic backgrounds cannot be generalised at this time.

CHAPTER 6
Discussion and final conclusions

6 Discussion and final conclusions

Previous work has focused on understanding how cell metabolism regulates HSC fates. During homeostasis, while HSCs utilize glycolysis to maintain their pool (Simsek et al., 2010), mitochondrial respiration plays a central role in the regulation of HSC quiescence and differentiation (Mantel et al., 2010; Gan et al., 2010; Nakada et al., 2010; Gurumurthy et al., 2010; Yu et al., 2012; Maryanovich et al., 2015). Furthermore, constitutively active OXPHOS, has been associated with HSC exhaustion (Maryanovich et al., 2015), and a recent study identified that deregulated mitochondrial activity is associated with HSC ageing (Mohrin et al., 2015).

Similarly, in an effort to better define the metabolic properties of malignant haematopoiesis, studies utilising primary AML samples, AML cell lines and transgenic mouse models, have identified several pathways that appear to be critical. Those pathways include glycolysis (Herst et al., 2011; Chen et al., 2014; Wang et al., 2014; Qin et al., 2016), fatty acid oxidation (Polet et al., 2016; Lee et al., 2015; Ricciardi et al., 2014; Samudio et al., 2010), and mitochondrial respiration (Skrtic et al., 2011; Sriskanthadevan et al., 2015; Cole et al., 2015).

This study, focused on uncovering the importance of mitochondrial respiration by genetically truncating the TCA cycle, through the deletion of the mitochondrial isoform of *Fh1*. *FH is a bone fide* tumour suppressor in HLRCC and previous work conducted in our lab has indicated that *Fh1* is essential for foetal and adult murine haematopoiesis. My project focused on two things; First to identify the importance of genetically intact TCA in non-malignant, aged haematopoiesis and in malignant haematopoiesis, by deleting the mitochondrial isoform of *Fh1*. Secondly, to understand whether, similarly to HLRCC, *Fh1* plays a tumour-suppressive role in malignant haematopoiesis.

6.1 Lack of mitochondrial *Fh1* affects the early progenitor compartment and the differentiated cell compartment in aged mice

Circulating white blood cells are programmed for distinct roles in normal physiology. As a result, each cell type requires different metabolic machineries in order to meet its energetic demands (MacIver et al., 2013; Caro-Maldonado et al., 2014; Doughty et al., 2006; Chacko et al., 2013). By genetically deleting the mitochondrial isoform of *Fh1* we generated a genetic perturbation of the TCA cycle and wanted to assess the impact it would have on the

haematopoietic system, after ageing mice for approximately 60 weeks. The key changes we observed in the primitive haematopoietic compartment were limited to an increase in the frequency of LSK cells and within the LSK population, we observed an increase in the frequency of the early progenitors HPC-1 and HPC-2. HPC-1 and HPC-2 cells are thought to contain a mixture of progenitor cells. Upon transplantation, HPC-1 cells are to transiently give rise to myeloid, B cells and T cells, and to a lesser extent platelets (Oguro et al., 2013). HPC-2 cells have limited reconstitution capacity and can give rise to erythrocytes and platelets, and to a lesser extent myeloid and B cells (Oguro et al., 2013). Interestingly, the expansion in these compartments did not translate to a deregulation in the downstream oligopotent progenitors, that would explain the drastic decrease in B cells and the myeloid bias B-cell depletion could result from the genetic truncation of the TCA cycle.

Both naïve and activated B cells (i.e. before and after the exposure to antigen) are known to rely on the TCA cycle but to different extents (Caro-Maldonado et al., 2014; Doughty et al., 2006). Naïve B cells heavily rely on the TCA cycle in order to meet their energetic demands as based on metabolite analysis, naïve B cells exhibit higher concentrations of the TCA metabolites fumarate and malate (Kunisawa et al., 2015). Furthermore, inhibition of mitochondrial respiration via the use of rotenone (that inhibits complex I of the electron transport chain), led to increased apoptosis of naïve B cells (Kunisawa et al., 2015). In addition, another study showed that naïve B cells use glucose-independent glutamine metabolism via the TCA cycle that is essential for their survival (Le et al., 2012). Activated B cells have been shown to utilise glycolysis and the TCA cycle at equal rates in order to meet their energetic demands, highlighting the importance of a fine balance between these two pathways (Kunisawa et al., 2015; Caro-Maldonado et al., 2014; Doughty et al., 2006).

In the aged mice, we observed a drastic depletion in the frequency of mature B cells in the bone marrow, peripheral blood and spleen. The B cell compartment was also depleted in terms of absolute numbers in the bone marrow. Collectively, my study is in agreement with previous reports, demonstrating that the TCA cycle is important for the development of B cells.

On the other hand, naïve T cells (i.e. T cells that have not encountered an antigen) utilise lipid oxidation and mitochondrial respiration in order to meet their energy demands, while T cell activation (i.e. engagement of the T cell receptor by the antigen-major histocompatibility complex) is generally associated with increased glucose uptake and glycolysis (Fox et al.,

2005; Frauwirth et al., 2002; MacIver et al., 2013; DeBernadinis et al., 2008; Michalek et al., 2011). We did not observe a drastic change in the frequency of T cells, especially in the thymus (which is the site for T cell development). As a result, our observations appear to be in line with other reports, in which T cells do not heavily rely on mitochondrial respiration and subsequently, mitochondrial *Fh1* deletion, does not impact on T cell survival.

6.2 The expansion of the myeloid compartment could be a result of a compensatory mechanism due to B-cell depletion in aged mice

The expansion of the myeloid compartment could either be a result of to the genetic block of the TCA or due to a compensatory mechanism of the haematopoietic, in response to B-cell depletion. In terms of metabolic properties, myeloid cells are known to exhibit a glycolytic rather than OXPHOS phenotype (Chacko et al., 2013). Therefore, a genetic truncation of the TCA cycle should not have a negative impact on the myeloid lineage. However, it is possible that other metabolic pathways such as glycolysis, could be upregulated due to the genetic truncation of the TCA cycle or fatty acid oxidation, thus providing a continuous energy source for myeloid cells. Consequently, the myeloid bias we observed is most likely attributed to the depletion of the B-cell lineage.

6.3 Aged mice lacking mitochondrial *Fh1* do not spontaneously develop AML

We observed that mice lacking mitochondrial *Fh1* displayed a bias towards the myeloid lineage in the peripheral blood from a young age (approximately 8 weeks). That prompted us to hypothesize that these mice could develop AML as they aged, and for that reason we left the mice to age up to approximately 60 weeks. Although the mice exhibited a persistently higher frequency of myeloid cells in their peripheral blood as they aged, they nevertheless did not spontaneously develop AML. AML is considered a "two-hit" disease, in which (at least) two lesions, each belonging to a different class, collaborate to generate AML, when neither is sufficient to do so in isolation (Gilliland and Griffin, 2002). The initiating lesions in AML are thought to be mutations that cause a block in normal differentiation, whereas secondary mutations are thought to provide a proliferative advantage. Given the fact that deletion of mitochondrial *Fh1* results in the expansion of the myeloid compartment with a parallel

depletion of B cells, it is possible that secondary "hits" are required to result to the development in AML.

6.4 Genetically intact TCA is differentially required for the generation and long-term self-renewal capacity of LICs in a retroviral *Meis1/Hoxa9* model

6.4.1 A genetically intact TCA is required for the efficient generation of LICs

Using the retroviral model of *Meis1/Hoxa9* we generated pre-LCs that were lacking the mitochondrial isoform of *Fh1,* resulting in a genetic truncation of the TCA cycle. The established pre-LCs were subsequently injected into sub-lethally irradiated primary recipient mice, in order to assess the importance of genetically intact TCA in the generation of LICs *in vivo*. Interestingly, we found that the survival rate of mice injected with pre-LCs with the genetic truncation of the TCA cycle, was significantly higher compared to the control cohorts of mice. More specifically, while only 25-30 % of the control mice cohorts survived, 76 % of the mice injected with pre-LCs with the genetic truncation of the TCA cycle, did not develop AML. This observation suggests that a genetically intact TCA is required for the efficient generation of LICs.

In an effort to understand the consequences that a genetic truncation of the TCA would have on overall mitochondrial respiration, we measured the oxygen consumption rate of LICs lacking mitochondrial *Fh1*. We found that LICs with the genetic truncation of the TCA exhibited a significant decrease in SRC, which based on the literature, is thought to reflect how well a cell can respond to high energy demand conditions (van der Windt et al., 2012; Choi et al., 2009; Ferrick et al., 2008; Nicholls, 2009). As a result, it is possible that the defect in SRC could play a causal role in the ability of the pre-LCs to generate disease as efficiently as pre-LCs with normal SRC and overall intact mitochondrial respiration. Indeed, as described earlier, recent studies have provided convincing evidence that mitochondrial respiration is important for the survival of several leukaemic cell lines as well as primary AML patient samples (Suganuma et al., 2010; Škrtić et al., 2011; Lagadinou et al., 2013; Cole et al., 2015). Furthermore, the importance of OXPHOS for cancer stem cells has been convincingly demonstrated in lung cancer, glioblastoma, pancreatic ductal adenocarcinoma and epithelial cancer stem cells (Ye et al., 2011; Janiszewska et al., 2012; Sancho et al., 2015; Pasto et al., 2014). Our data therefore provide additional evidence for the importance of mitochondrial respiration for cancer cells during disease initiation.

6.4.2 A genetically intact TCA is dispensable for the long-term self-renewal capacity of LICs

Interestingly, although the presence of genetically intact TCA played a role in the efficient generation of LICs from pre-LCs *in vivo*, it was dispensable for the long-term self-renewal capacity of LICs. We demonstrated this by using pre-LCs of the *Mx1-Cre* background, allowing inducible deletion of mitochondrial *Fh1*. Interestingly, once LICs were established, the genetic truncation of the TCA did not have an impact on LICs, as they generated AML in secondary recipient mice with similar latency to LICs of the control cohorts. Furthermore, LICs with the genetic truncation of the TCA exhibited a persistent defect in the SRC that did not appear to negatively impact their ability to generate AML in secondary recipient mice. These data demonstrate that LICs with the genetic truncation of the TCA cycle might be utilising alternate pathways in order to meet their energetic demands. It is plausible that those cells would rely more on glycolysis or fatty acid oxidation, since both pathways have been shown to be important for the survival of leukaemic cells. For instance, the self-renewal of both HSCs and LICs appears to be dependent on fatty acid oxidation (Samudio et al., 2010; Ito et al., 2012). Furthermore, glycolysis, appears to be the preferred energy source for many cancer (stem) cells as for example breast cancer stem cells. Specifically, it was demonstrated that the metabolic switch from OXPHOS to glycolysis was essential for the functionality of breast cancer stem cells (Dong et al., 2013). Similarly, glycolysis appears to be the preferred metabolic programme in cases of nasopharyngeal carcinoma stem cells (Shen et al, 2015), hepatocellular carcinoma (Chen et al., 2015), as well as leukaemic stem cells (Wang et al., 2014). Specifically, in a recent study, by deleting enzymes that affect aerobic glycolysis with different potencies (PKM2 or LDHA), the authors found that leukaemia initiation was impaired, highlighting the importance of glycolysis in an *MLL-AF9* mouse model and a CML model (Wang et al., 2014).

My data collectively demonstrate that a genetically intact TCA appears to be important for the initial stages of the disease (LIC generation), but is dispensable for later stages of the disease (LIC long-term self-renewal), indicating that during different stages of leukaemic transformation, the cells can undergo metabolic rewiring in order to meet their energetic demands, as for example observed in normal haematopoiesis during HSC differentiation (HSCs utilise primarily glycolysis but then switch to OXPHOS as the differentiation process takes place). A recent study carried from our lab showed that *Hif-2a* deletion accelerated the development of LICs but had no impact on LIC maintenance (Vukovic et al., 2015).

Similarly, in another study, the requirement of mTORC1 was critical for the tumour-initiating capacity of LICs but not for their self-renewal capacity (Hoshii et al., 2012). The PRC2 component, *EZH2* was similarly required for the initiation of LICs but was dispensable for their long-term self-renewal capacity (Neff et al., 2012). Therefore, my data is in agreement with other reports demonstrating that genes/pathways can be critical for initial stages of AML but dispensable for the later stages.

6.4.3 Fh1 is not a tumour suppressor in a retroviral Meis1/Hoxa9 model of AML

Germline loss-of-function mutations in the TCA cycle enzyme FH predispose affected individuals to benign cutaneous and uterine leiomyomata, renal cysts and hereditary leiomyomatosis and renal cell cancer, suggesting that, in this context, FH is a tumour suppressor (Tomlinson et al, 2002). FH-deficient cells and tumours have been shown to accumulate fumarate to very high levels with multiple consequences including the activation of multiple oncogenic pathways (Isaacs et al., 2005; Pollard et al., 2005). It has been previously postulated that tumorigenesis associated with *FH* deletion, might be driven by the upregulation of a number of oncogenic pathways driven by HIF (Gottlieb and Tomlinson, 2005). Indeed, it has been shown that fumarate competitively inhibits 2-oxoglutarate-dependent oxygenases, in particular PHDs, thus mimicking hypoxia and leading to the activation of oncogenic target genes (Isaacs et al., 2005). Furthermore, it has been shown that fumarate inhibits the activity and function of other members of the 2-oxoglutarate-dependent oxygenases including histone demethylase enzymes and TET proteins which are crucial in epigenetic regulation (Xiao et al., 2012), thus leading to epigenetic remodelling. In addition to its role as an allosteric regulator of 2-oxoglutarate-dependent oxygenases, fumarate is also an electrophile, spontaneously reacting with cysteine residues and forming S-2-succinyl-cysteine. This process is termed succination (Alderson et al., 2006). Accumulation of fumarate has been shown to directly correlate with an increase of succinated proteins, that could in part account for the oncogenic phenotype (Adam et al., 2011; Trnette et al., 2013). Studies have shown that fumarate accumulation leads to the succination (and therefore inactivation) of the Kelch-like ECH associated protein 1 (KEAP1), the negative regulator of the antioxidant nuclear factor-like 2 (NRF2) (Adam et al., 2011). As a result of all the effects that fumarate exerts, fumarate is considered an “oncometabolite” (Yang et al., 2012). An oncometabolite is a small molecule of normal metabolism whose accumulation causes metabolic dysregulation and effectively primes cells, allowing future progression to cancer

(Yan et al., 2012). The term oncometabolite was first coined to describe R-2-hydroxyglutarate (R-2HG). R-2HG is a by-product produced by the gain of function mutation of IDH1/2 (Leonardi et al., 2012).

The discovery of mutated metabolic enzymes (as for example FH and IDH) that lead to the accumulation of oncometabolites, has provided significant evidence that dysfunctional metabolism plays a direct role in oncogenesis. Given the fact that *FH* is considered a bona fide tumour suppressor in kidney cancer, we sought to determine whether *Fh1,* plays a similar role in leukaemogenesis.

To that end, we began by assessing its importance at the generation and maintenance of pre-LCs. We isolated *Fh1*-null stem and progenitor cells and infected them with retroviruses expressing oncogenes and chromosomal translocations known to be involved in AML development. The cells were then plated in semi-solid media in order to assess their clonogenic potential. Interestingly, cells lacking *Fh1* were unable to generate colonies. We then wanted to assess the importance of *Fh1* in the maintenance of pre-LCs. For that I generated pre-LCs, that had intact *Fh1*, using the *Meis1/Hoxa9* retroviruses. Acute deletion of *Fh1* in established pre-LCs led to the inability of the cells to generate any colonies. Overall these data indicate that *Fh1* is essential for the pre-leukaemic stage of the disease.

In order to assess the importance of *Fh1* in the later stages of the disease, I injected pre-LCs (in which *Fh1* was intact) into sub-lethally irradiated recipient mice. Once the mice succumbed to AML, I isolated the LICs and acutely deleted *Fh1* using lentivirally expressed *Cre*. Interestingly, following deletion of *Fh1*, LICs were unable to generate colonies *in vitro*, indicating that *Fh1* is essential for the maintenance of LICs *in vitro*.

Finally, I wanted to assess whether *Fh1* is important for the maintenance of LICs *in vivo*, by using the *Mx1-Cre* mouse model, that allows inducible deletion of *Fh1*. In this model, pre-LCs with intact *Fh1* were injected in sub-lethally irradiated recipient mice. Once the mice exhibited 20-30 % of LIC chimerism in the peripheral blood, I administered poly (I:C) in order to induce deletion of *Fh1* in LICs. As we were expecting, the chimerism of LICs was drastically decreased and recipient mice exhibited a very low percentage of LICs in their peripheral blood (0.5-2 %). To our surprise, approximately 2 weeks later, some of the recipient mice exhibited a very high LIC chimerism and succumbed to AML. Furthermore, when we assessed the deletion of *Fh1* in LICs, we found that LICs exhibited a complete

deletion of *Fh1*. This observation was very surprising as up to that point we observed that *Fh1* is essential for the initial stages of the disease as well as essential for the survival of LICs, at least *in vitro*. Furthermore, the drastic decrease in LIC chimerism as a result of *Fh1* deletion, resulted in half of the recipient mice to be "leukaemia-free", indicating that *Fh1* deletion can have a deleterious effect on the survival of LICs *in vivo*.

Based on these data, parallels can be drawn between the classical stages of AML in patients and in our mouse model. Typically, after patients are diagnosed with AML, they are treated with conventional chemotherapy drugs that eradicate the bulk population of AML cells, thus leading to clinical remission. However, in approximately 60 % of cases, the patients fall into relapse (Burnett et al., 2011). The patient relapse is thought to be a result of the insensitivity of leukaemic stem cells (LSCs) to the conventional chemotherapy drugs. Similarly, it is possible that via deletion of *Fh1*, we eradicated the bulk population of leukaemic cells but are simultaneously provided a selective advantage to the LIC clones that are able to survive and generate disease, despite the deletion of *Fh1*.

Overall, this study indicates that in the haematopoietic system, *Fh1* does not appear to play a tumour suppressive role, since in the pre-leukaemic stage and in half the cases at the leukaemic stage, deletion of both isoforms of *Fh1* halted the progression of the disease. Finally, this study highlights the differences that exist between kidney cancer and haematopoietic malignancy, supporting the notion that genes can play a tumour suppressive or tumour initiating role, depending on the biological system.

6.5 Future directions of the study

The overall conclusion of this project is that mitochondrial respiration has varying degrees of importance in aged, non-malignant haematopoiesis and in malignant haematopoiesis.

With respect to the truncation of the TCA cycle, it would be informative to biochemically validate that the deletion of mitochondrial *Fh1* causes a biochemical truncation of the TCA cycle, that could be verified by mass-spectrometry analysis. Additionally, despite the deletion of mitochondrial *Fh1*, the basal oxygen consumption rate of the cells is comparable to cells with intact TCA indicating that there are compensatory mechanisms rectifying for the genetic truncation of the TCA. Global metabolomic analyses could provide some insight for that. It would also be of considerable interest to study the role of genetically intact TCA using another *in vivo* model of AML, in order to identify whether my findings can be applicable to

different subtypes of AML. Furthermore, it would be important to understand why a genetically intact TCA appears to be required for the initial stages of the disease but not for the later stages. Flux metabolomics could help identify the metabolic rewiring that LICs have undergone in order to compensate for the genetic truncation of the TCA cycle, thus revealing their potential metabolic vulnerabilities.

With respect to the full deletion of *Fh1* (i.e. both the mitochondrial and cytosolic isoforms of *Fh1* using the *Vav-iCre* model), it would be informative to understand why it is detrimental to the survival of pre-LCs and LICs *in vitro*. The phenotype I observed could be attributed to different mechanisms, such as the fumarate-associated inhibition of a-KG-dependent dioxygenases such as TETs and KDMs. Similarly, identifying the key differences between *Fh1*$^{-/-}$ LICs that generated disease *in vivo* and the ones that did not, could offer a new insight about the tumour suppressive or oncogenic context associated with *Fh1* deletion.

CHAPTER 7
List of references

7 List of references

Adam, J., Hatipoglu, E., O'Flaherty, L., Ternette, N., Sahgal, N., Lockstone, H., Baban, D., Nye, E., Stamp, G.W., Wolhuter, K., et al. (2011). Renal cyst formation in Fh1-deficient mice is independent of the Hif/Phd pathway: roles for fumarate in KEAP1 succination and Nrf2 signalling. Cancer Cell *20*, 524–537.

Adam, J., Yang, M., Bauerschmidt, C., Kitagawa, M., O'Flaherty, L., Maheswaran, P., Özkan, G., Sahgal, N., Baban, D., Kato, K., et al. (2013). A Role for cytosolic fumarate hydratase in urea cycle metabolism and renal neoplasia. Cell Reports *3*, 1440–1448.

Adolfsson, J., Månsson, R., Buza-Vidas, N., Hultquist, A., Liuba, K., Jensen, C.T., Bryder, D., Yang, L., Borge, O.-J., Thoren, L.A.M., et al. (2005). Identification of Flt3+ lympho-myeloid stem cells lacking erythro-megakaryocytic potential a revised road map for adult blood lineage commitment. Cell *121*, 295–306.

Akashi, K., Traver, D., Miyamoto, T., and Weissman, I.L. (2000). A clonogenic common myeloid progenitor that gives rise to all myeloid lineages. Nature *404*, 193–197.

Alderson, N.L., Wang, Y., Blatnik, M., Frizzell, N., Walla, M.D., Lyons, T.J., Alt, N., Carson, J.A., Nagai, R., Thorpe, S.R., et al. (2006). S-(2-Succinyl)cysteine: a novel chemical modification of tissue proteins by a Krebs cycle intermediate. Arch. Biochem. Biophys. *450*, 1–8.

Anderson, G., and Jenkinson, E.J. (2001). Lymphostromal interactions in thymic development and function. Nat. Rev. Immunol. *1*, 31–40.

Andersson, A.K., Ma, J., Wang, J., Chen, X., Gedman, A.L., Dang, J., Nakitandwe, J., Holmfeldt, L., Parker, M., Easton, J., et al. (2015). The landscape of somatic mutations in infant MLL-rearranged acute lymphoblastic leukaemias. Nat. Genet. *47*, 330–337.

Arber, D.A., Orazi, A., Hasserjian, R., Thiele, J., Borowitz, M.J., Beau, M.M.L., Bloomfield, C.D., Cazzola, M., and Vardiman, J.W. (2016). The 2016 revision to the World Health Organization classification of myeloid neoplasms and acute leukaemia. Blood *127*, 2391–2405.

Argiropoulos, B., and Humphries, R.K. (2007). Hox genes in haematopoiesis and leukaemogenesis. Oncogene *26*, 6766–6776.

Argiropoulos, B., Yung, E., and Humphries, R.K. (2007). Unravelling the crucial roles of Meis1 in leukaemogenesis and normal haematopoiesis. Genes Dev. *21*, 2845–2849.

Ayton, P.M., and Cleary, M.L. (2003). Transformation of myeloid progenitors by MLL oncoproteins is dependent on Hoxa7 and Hoxa9. Genes Dev. *17*, 2298–2307.

Azcoitia, V., Aracil, M., Martínez-A, C., and Torres, M. (2005). The homeodomain protein Meis1 is essential for definitive haematopoiesis and vascular patterning in the mouse embryo. Developmental Biology *280*, 307–320.

Bank, A., Larsen, P.R., and Anderson, H.M. (1966). Di Guglielmo's syndrome after polycythemia. N. Engl. J. Med. *275*, 489–490.

Bardella, C., El-Bahrawy, M., Frizzell, N., Adam, J., Ternette, N., Hatipoglu, E., Howarth, K., O'Flaherty, L., Roberts, I., Turner, G., et al. (2011). Aberrant succination of proteins in fumarate hydratase-deficient mice and HLRCC patients is a robust biomarker of mutation status. J. Pathol. *225*, 4–11.

Bardella, C., Olivero, M., Lorenzato, A., Geuna, M., Adam, J., O'Flaherty, L., Rustin, P., Tomlinson, I., Pollard, P.J., and Di Renzo, M.F. (2012). Cells lacking the fumarase tumor suppressor are protected from apoptosis through a hypoxia-inducible factor-independent, AMPK-dependent mechanism. Mol. Cell. Biol. *32*, 3081–3094.

Beerman, I., Bhattacharya, D., Zandi, S., Sigvardsson, M., Weissman, I.L., Bryder, D., and Rossi, D.J. (2010). Functionally distinct haematopoietic stem cells modulate haematopoietic lineage potential during aging by a mechanism of clonal expansion. Proc. Natl. Acad. Sci. U.S.A. *107*, 5465–5470.

Bennett, J.M., Catovsky, D., Daniel, M.T., Flandrin, G., Galton, D.A., Gralnick, H.R., and Sultan, C. (1976). Proposals for the classification of the acute leukaemias. French-American-British (FAB) co-operative group. Br. J. Haematol. *33*, 451–458.

Benz, C., Copley, M.R., Kent, D.G., Wohrer, S., Cortes, A., Aghaeepour, N., Ma, E., Mader, H., Rowe, K., Day, C., et al. (2012). Haematopoietic stem cell subtypes expand differentially during development and display distinct lymphopoietic programs. Cell Stem Cell *10*, 273–283.

Bhatia, M., Wang, J.C., Kapp, U., Bonnet, D., and Dick, J.E. (1997). Purification of primitive human haematopoietic cells capable of repopulating immune-deficient mice. Proc. Natl. Acad. Sci. U.S.A. *94*, 5320–5325.

Biasco, L., Pellin, D., Scala, S., Dionisio, F., Basso-Ricci, L., Leonardelli, L., Scaramuzza, Baricordi, C., Ferrua, F., Cicalese, M.P., et al. (2016). *In vivo* tracking of human haematopoiesis reveals patterns of clonal dynamics during early and steady-state reconstitution phases. Cell Stem Cell *19*, 107–119.

Biswas, D., Milne, T.A., Basrur, V., Kim, J., Elenitoba-Johnson, K.S.J., Allis, C.D., and Roeder, R.G. (2011). Function of leukemogenic mixed lineage leukaemia 1 (MLL) fusion proteins through distinct partner protein complexes. Proc. Natl. Acad. Sci. U.S.A. *108*, 15751–15756.

Bosselut, R. (2004). CD4/CD8-lineage differentiation in the thymus: from nuclear effectors to membrane signals. Nature Reviews Immunology *4*, 529–540.

Bourgeron, T., Chretien, D., Poggi-Bach, J., Doonan, S., Rabier, D., Letouzé, P., Munnich, A., Rötig, A., Landrieu, P., and Rustin, P. (1994). Mutation of the fumarase gene in two siblings with progressive encephalopathy and fumarase deficiency. J Clin Invest *93*, 2514–2518.

Boyer, S.W., Schroeder, A.V., Smith-Berdan, S., and Forsberg, E.C. (2011). All haematopoietic cells develop from haematopoietic stem cells through Flk2/Flt3-positive progenitor cells. Cell Stem Cell *9*, 64–73.

Buchakjian, M.R., and Kornbluth, S. (2010). The engine driving the ship: metabolic steering of cell proliferation and death. Nat Rev Mol Cell Biol *11*, 715–727.

Buchi, F., Masala, E., Rossi, A., Valencia, A., Spinelli, E., Sanna, A., Gozzini, A., and Santini, V. (2014). Redistribution of H3K27me3 and acetylated histone H4 upon exposure to azacitidine and decitabine results in de-repression of the AML1/ETO target gene IL3. Epigenetics *9*, 387–395.

Burgess, R.J., Agathocleous, M., and Morrison, S.J. (2014). Metabolic regulation of stem cell function. J. Intern. Med. *276*, 12–24.

Burnett, A., Wetzler, M., and Löwenberg, B. (2011). Therapeutic advances in acute myeloid leukaemia. J. Clin. Oncol. *29*, 487–494.

Calvi, L.M., Adams, G.B., Weibrecht, K.W., Weber, J.M., Olson, D.P., Knight, M.C., Martin, R.P., Schipani, E., Divieti, P., Bringhurst, F.R., et al. (2003). Osteoblastic cells regulate the haematopoietic stem cell niche. Nature *425*, 841–846.

Cameron, E.R., and Neil, J.C. (2004). The Runx genes: lineage-specific oncogenes and tumor suppressors. Oncogene *23*, 4308–4314.

Cano, F., Drynan, L.F., Pannell, R., and Rabbitts, T.H. (2007). Leukaemia lineage specification caused by cell-specific Mll-Enl translocations. Oncogene *27*, 1945–1950.

Carapeti, M., Aguiar, R.C., Goldman, J.M., and Cross, N.C. (1998). A novel fusion between MOZ and the nuclear receptor coactivator TIF2 in acute myeloid leukaemia. Blood *91*, 3127–3133.

Caro-Maldonado, A., Wang, R., Nichols, A.G., Kuraoka, M., Milasta, S., Sun, L.D., Gavin, A.L., Abel, E.D., Kelsoe, G., Green, D.R., et al. (2014). Metabolic reprogramming is required for antibody production that is suppressed in anergic but exaggerated in chronically BAFF-exposed B cells. J Immunol *192*, 3626–3636.

Castro-Vega, L.J., Buffet, A., De Cubas, A.A., Cascón, A., Menara, M., Khalifa, E., Amar, L., Azriel, S., Bourdeau, I., Chabre, O., et al. (2014). Germline mutations in FH confer predisposition to malignant pheochromocytomas and paragangliomas. Hum. Mol. Genet. *23*, 2440–2446.

Celso, C. Lo, Fleming, H.E., Wu, J.W., Zhao, C.X., Miake-Lye, S., Fujisaki, J., Côté, D., Rowe, D.W., Lin, C.P., and Scadden, D.T. (2009). Live-animal tracking of individual haematopoietic stem/progenitor cells in their niche. Nature *457*, 92–96.

Cesta, M.F. (2006). Normal structure, function, and histology of the spleen. Toxicol Pathol *34*, 455–465.

Chacko, B.K., Kramer, P.A., Ravi, S., Johnson, M.S., Hardy, R.W., Ballinger, S.W., and Darley-Usmar, V.M. (2013). Methods for defining distinct bioenergetic profiles in platelets, lymphocytes, monocytes, and neutrophils, and the oxidative burst from human blood. Laboratory Investigation *93*, 690–700.

Challen, G.A., Boles, N.C., Chambers, S.M., and Goodell, M.A. (2010). Distinct haematopoietic stem cell subtypes are differentially regulated by TGF-β1. Cell Stem Cell *6*, 265–278.

Chance, B., Sies, H., and Boveris, A. (1979). Hydroperoxide metabolism in mammalian organs. Physiol. Rev. *59*, 527–605.

Chen W-L, Wang J-H, Zhao A-H, et al. A distinct glucose metabolism signature of acute myeloid leukaemia with prognostic value. (2014). Blood. 2014;124(10):1645-1654. Blood *124*, 2893–2893.

Chen, C.-L., Uthaya Kumar, D.B., Punj, V., Xu, J., Sher, L., Tahara, S.M., Hess, S., and Machida, K. (2016). Metabolically reprograms tumor-initiating stem-like cells through tumorigenic changes in oxidative phosphorylation and fatty acid metabolism. Cell Metab. *23*, 206–219.

Chen, C., Liu, Y., Liu, R., Ikenoue, T., Guan, K.-L., Liu, Y., and Zheng, P. (2008). TSC–mTOR maintains quiescence and function of haematopoietic stem cells by repressing mitochondrial biogenesis and reactive oxygen species. J. Exp. Med. *205*, 2397–2408.

Chen, H., Yang, T., Zhu, L., and Zhao, Y. (2015). Cellular Metabolism on T-Cell Development and Function. International Reviews of Immunology *34*, 19–33.

Chen, J., Astle, C.M., and Harrison, D.E. (2000). Genetic regulation of primitive haematopoietic stem cell senescence. Experimental Haematology *28*, 442–450.

Chen, Y., Xu, Q., Ji, D., Wei, Y., Chen, H., Li, T., Wan, B., Yuan, L., Huang, R., and Chen, G. (2016). Inhibition of pentose phosphate pathway suppresses acute myelogenous leukaemia. Tumour Biol. *37*, 6027–6034.

Cho, R.H., Sieburg, H.B., and Muller-Sieburg, C.E. (2008). A new mechanism for the aging of haematopoietic stem cells: aging changes the clonal composition of the stem cell compartment but not individual stem cells. Blood *111*, 5553–5561.

Choi, S.W., Gerencser, A.A., and Nicholls, D.G. (2009). Bioenergetic analysis of isolated cerebrocortical nerve terminals on a microgram scale: spare respiratory capacity and stochastic mitochondrial failure. Journal of Neurochemistry *109*, 1179–1191.

Chute, J.P., Muramoto, G.G., Dressman, H.K., Wolfe, G., Chao, N.J., and Lin, S. (2006). Molecular profile and partial functional analysis of novel endothelial cell-derived growth factors that regulate haematopoiesis. Stem Cells *24*, 1315–1327.

Clapp, D.W., Freie, B., Lee, W.H., and Zhang, Y.Y. (1995). Molecular evidence that in situ-transduced foetal liver haematopoietic stem/progenitor cells give rise to medullary haematopoiesis in adult rats. Blood *86*, 2113–2122.

Cole, A., Wang, Z., Coyaud, E., Voisin, V., Gronda, M., Jitkova, Y., Mattson, R., Hurren, R., Babovic, S., Maclean, N., et al. (2015). Inhibition of the mitochondrial protease ClPP as a therapeutic strategy for human acute myeloid leukaemia. Cancer Cell *27*, 864–876.

Copley, M.R., Beer, P.A., and Eaves, C.J. (2012). Haematopoietic stem cell heterogeneity takes centre stage. Cell Stem Cell *10*, 690–697.

Corces-Zimmerman, M.R., Hong, W.-J., Weissman, I.L., Medeiros, B.C., and Majeti, R. (2014). Pre leukaemic mutations in human acute myeloid leukaemia affect epigenetic regulators and persist in remission. Proc. Natl. Acad. Sci. U.S.A. *111*, 2548–2553.

Cozzio, A., Passegué, E., Ayton, P.M., Karsunky, H., Cleary, M.L., and Weissman, I.L. (2003). Similar MLL-associated leukaemias arising from self-renewing stem cells and short-lived myeloid progenitors. Genes Dev. *17*, 3029–3035.

Dahl, R., Iyer, S.R., Owens, K.S., Cuylear, D.D., and Simon, M.C. (2007). The transcriptional repressor GFI-1 antagonizes PU.1 activity through protein-protein interaction. J. Biol. Chem. *282*, 6473–6483.

Davis, J.N., McGhee, L., and Meyers, S. (2003). The ETO (MTG8) gene family. Gene *303*, 1–10.

De Boer, J., Walf-Vorderwülbecke, V., and Williams, O. (2013). In focus: MLL-rearranged leukaemia. Leukaemia *27*, 1224–1228.

De Boer, J., Williams, A., Skavdis, G., Harker, N., Coles, M., Tolaini, M., Norton, T., Williams, K., Roderick, K., Potocnik, A.J., et al. (2003). Transgenic mice with haematopoietic and lymphoid specific expression of Cre. Eur. J. Immunol. *33*, 314–325.

De Craene, B., and Berx, G. (2013). Regulatory networks defining EMT during cancer initiation and progression. Nat. Rev. Cancer *13*, 97–110.

De Kouchkovsky, I., and Abdul-Hay, M. (2016). "Acute myeloid leukaemia: a comprehensive review and 2016 update." Blood Cancer J *6*, e441.

De Thé, H., Chomienne, C., Lanotte, M., Degos, L., and Dejean, A. (1990). The t (15;17) translocation of acute promyelocytic leukaemia fuses the retinoic acid receptor alpha gene to a novel transcribed locus. Nature *347*, 558–561.

DeBerardinis, R.J., Lum, J.J., Hatzivassiliou, G., and Thompson, C.B. (2008). The biology of cancer: metabolic reprogramming fuels cell growth and proliferation. Cell Metabolism *7*, 11–20.

Degner, S.C., Verma-Gaur, J., Wong, T.P., Bossen, C., Iverson, G.M., Torkamani, A., Vettermann, C., Lin, Y.C., Ju, Z., Schulz, D., et al. (2011). CCCTC-binding factor (CTCF) and cohesin influence the genomic architecture of the Igh locus and antisense transcription in pro-B cells. Proc. Natl. Acad. Sci. U.S.A. *108*, 9566–9571.

Dick JE, MagliMC, HuszarD, PhillipsRA, BernsteinA. Introduction of a selectable gene into primitive stemcells capable of long-termreconstitution of the haemopoietic system of W/Wv mice. Cell. (1985); 42:71–79.

DiMartino, J.F., Ayton, P.M., Chen, E.H., Naftzger, C.C., Young, B.D., and Cleary, M.L. (2002). The AF10 leucine zipper is required for leukaemic transformation of myeloid progenitors by MLL-AF10. Blood *99*, 3780–3785.

Ding, L., and Morrison, S.J. (2013). Haematopoietic stem cells and early lymphoid progenitors occupy distinct bone marrow niches. Nature *495*, 231–235.

Ding, L., Ley, T.J., Larson, D.E., Miller, C.A., Koboldt, D.C., Welch, J.S., Ritchey, J.K., Young, M.A., Lamprecht, T., McLellan, M.D., et al. (2012). Clonal evolution in relapsed acute myeloid leukaemia revealed by whole-genome sequencing. Nature *481*, 506–510.

Ding, L., Saunders, T.L., Enikolopov, G., and Morrison, S.J. (2012). Endothelial and perivascular cells maintain haematopoietic stem cells. Nature *481*, 457–462.

Djabali, M., Selleri, L., Parry, P., Bower, M., Young, B.D., and Evans, G.A. (1992). A trithorax-like gene is interrupted by chromosome 11q23 translocations in acute leukaemias. Nat. Genet. *2*, 113–118.

Döhner, K., Schlenk, R.F., Habdank, M., Scholl, C., Rücker, F.G., Corbacioglu, A., Bullinger, L., Fröhling, S., and Döhner, H. (2005). Mutant nucleophosmin (NPM1) predicts favorable prognosis in younger adults with acute myeloid leukaemia and normal cytogenetics: interaction with other gene mutations. Blood *106*, 3740–3746.

Dombret, H., and Gardin, C. (2016). An update of current treatments for adult acute myeloid leukaemia. Blood *127*, 53–61.

Dong, C., Yuan, T., Wu, Y., Wang, Y., Fan, T.W.M., Miriyala, S., Lin, Y., Yao, J., Shi, J., Kang, T., et al. (2013). Loss of FBP1 by Snail-mediated repression provides metabolic advantages in basal-like breast cancer. Cancer Cell *23*, 316–331.

Doughty, C.A., Bleiman, B.F., Wagner, D.J., Dufort, F.J., Mataraza, J.M., Roberts, M.F., and Chiles, T.C. (2006). Antigen receptor-mediated changes in glucose metabolism in B lymphocytes: role of phosphatidylinositol 3-kinase signalling in the glycolytic control of growth. Blood *107*, 4458–4465.

Doulatov, S., Notta, F., Laurenti, E., and Dick, J.E. (2012). Haematopoiesis: a human perspective. Cell Stem Cell *10*, 120–136.

Drissen, R., Buza-Vidas, N., Woll, P., Thongjuea, S., Gambardella, A., Giustacchini, A., Mancini, E., Zriwil, A., Lutteropp, M., Grover, A., et al. (2016). Distinct myeloid progenitor-differentiation pathways identified through single-cell RNA sequencing. Nat Immunol *17*, 666–676.

Dull, T., Zufferey, R., Kelly, M., Mandel, R.J., Nguyen, M., Trono, D., and Naldini, L. (1998). A third-generation lentivirus vector with a conditional packaging system. J. Virol. *72*, 8463–8471.

Dykstra, B., Kent, D., Bowie, M., McCaffrey, L., Hamilton, M., Lyons, K., Lee, S.-J., Brinkman, R., and Eaves, C. (2007). Long-term propagation of distinct haematopoietic differentiation programs *in vivo*. Cell Stem Cell *1*, 218–229.

Dykstra, B., Olthof, S., Schreuder, J., Ritsema, M., and Haan, G. de (2011). Clonal analysis reveals multiple functional defects of aged murine haematopoietic stem cells. J. Exp. Med. *208*, 2691–2703.

Elo, L.L., Karjalainen, R., Öhman, T., Hintsanen, P., Nyman, T.A., Heckman, C.A., and Aittokallio, T. (2014). Statistical detection of quantitative protein biomarkers provides insights into signalling networks deregulated in acute myeloid leukaemia. Proteomics *14*, 2443–2453.

Elvidge, G.P., Glenny, L., Appelhoff, R.J., Ratcliffe, P.J., Ragoussis, J., and Gleadle, J.M. (2006). Concordant Regulation of Gene Expression by Hypoxia and 2-Oxoglutarate-dependent Dioxygenase Inhibition. J. Biol. Chem. *281*, 15215–15226.

Ema, H., Sudo, K., Seita, J., Matsubara, A., Morita, Y., Osawa, M., Takatsu, K., Takaki, S., and Nakauchi, H. (2005). Quantification of self-renewal capacity in single haematopoietic stem cells from normal and Lnk-deficient mice. Dev. Cell *8*, 907–914.

Epstein, A.C., Gleadle, J.M., McNeill, L.A., Hewitson, K.S., O'Rourke, J., Mole, D.R., Mukherji, M., Metzen, E., Wilson, M.I., Dhanda, A., et al. (2001). C. elegans EGL-9 and mammalian homologs define a family of dioxygenases that regulate HIF by prolyl hydroxylation. Cell *107*, 43–54.

Erickson, P., Gao, J., Chang, K.S., Look, T., Whisenant, E., Raimondi, S., Lasher, R., Trujillo, J., Rowley, J., and Drabkin, H. (1992). Identification of breakpoints in t(8;21) acute myelogenous leukaemia and isolation of a fusion transcript, AML1/ETO, with similarity to Drosophila segmentation gene, runt. Blood *80*, 1825–1831.

Estey, E., and Döhner, H. (2006). Acute myeloid leukaemia. Lancet *368*, 1894–1907.

Falini, B., Mecucci, C., Tiacci, E., Alcalay, M., Rosati, R., Pasqualucci, L., La Starza, R., Diverio, D., Colombo, E., Santucci, A., et al. (2005). Cytoplasmic nucleophosmin in acute myelogenous leukaemia with a normal karyotype. N. Engl. J. Med. *352*, 254–266.

Ferrick, D.A., Neilson, A., and Beeson, C. (2008). Advances in measuring cellular bioenergetics using extracellular flux. Drug Discovery Today *13*, 268–274.

Field, A.K., Tytell, A.A., Lampson, G.P., and Hilleman, M.R. (1967). Inducers of interferon and host resistance. II. Multistranded synthetic polynucleotide complexes. Proceedings of the National Academy of Sciences *58*, 1004–1010.

Figueroa, M.E., Abdel-Wahab, O., Lu, C., Ward, P.S., Patel, J., Shih, A., Li, Y., Bhagwat, N., Vasanthakumar, A., Fernandez, H.F., et al. (2010). Leukaemic IDH1 and IDH2 mutations result in a hypermethylation phenotype, disrupt TET2 function, and impair haematopoietic differentiation. Cancer Cell *18*, 553–567.

Fine, B.M., Stanulla, M., Schrappe, M., Ho, M., Viehmann, S., Harbott, J., and Boxer, L.M. (2004). Gene expression patterns associated with recurrent chromosomal translocations in acute lymphoblastic leukaemia. Blood *103*, 1043–1049.

Fogal, V., Richardson, A.D., Karmali, P.P., Scheffler, I.E., Smith, J.W., and Ruoslahti, E. (2010). Mitochondrial p32 Protein is a critical regulator of tumour metabolism via maintenance of oxidative phosphorylation. Molecular and Cellular Biology *30*, 1303–1318.

Folmes, C.D.L., Dzeja, P.P., Nelson, T.J., and Terzic, A. (2012). Metabolic plasticity in stem cell homeostasis and differentiation. Cell Stem Cell *11*, 596–606.

Forristal, C.E., Nowlan, B., Jacobsen, R.N., Barbier, V., Walkinshaw, G., Walkley, C.R., Winkler, I.G., and Levesque, J.P. (2015). HIF-1α is required for haematopoietic stem cell mobilization and 4-prolyl hydroxylase inhibitors enhance mobilization by stabilizing HIF-1α. Leukaemia *29*, 1366–1378.

Forsberg, E.C., Serwold, T., Kogan, S., Weissman, I.L., and Passegué, E. (2006). New evidence supporting megakaryocyte-erythrocyte potential of flk2/flt3+ multipotent haematopoietic progenitors. Cell *126*, 415–426.

Fox, C.J., Hammerman, P.S., and Thompson, C.B. (2005). Fuel feeds function: energy metabolism and the T-cell response. Nat Rev Immunol *5*, 844–852.

Frauwirth, K.A., Riley, J.L., Harris, M.H., Parry, R.V., Rathmell, J.C., Plas, D.R., Elstrom, R.L., June, C.H., and Thompson, C.B. (2002). The CD28 signalling pathway regulates glucose metabolism. Immunity *16*, 769–777.

Frezza, C., Zheng, L., Folger, O., Rajagopalan, K.N., MacKenzie, E.D., Jerby, L., Micaroni, M., Chaneton, B., Adam, J., Hedley, A., et al. (2011). Haem oxygenase is synthetically lethal with the tumour suppressor fumarate hydratase. Nature *477*, 225–228.

Galloway, J.L., Wingert, R.A., Thisse, C., Thisse, B., and Zon, L.I. (2005). Loss of gata1 but not gata2 converts erythropoiesis to myelopoiesis in zebrafish embryos. Dev. Cell *8*, 109–116.

Gan, B., Hu, J., Jiang, S., Liu, Y., Sahin, E., Zhuang, L., Fletcher-Sananikone, E., Colla, S., Wang, Y.A., Chin, L., et al. (2010). Lkb1 regulates quiescence and metabolic homeostasis of haematopoietic stem cells. Nature *468*, 701–704.

Garcia-Cuellar, M.-P., Büttner, C., Bartenhagen, C., Dugas, M., and Slany, R.K. (2016). Leukaemogenic MLL-ENL Fusions Induce Alternative Chromatin States to Drive a Functionally Dichotomous Group of Target Genes. Cell Reports *15*, 310–322.

Gatenby, R.A., and Gillies, R.J. (2004). Why do cancers have high aerobic glycolysis? Nature Reviews Cancer *4*, 891–899.

Giampaolo, A., Sterpetti, P., Bulgarini, D., Samoggia, P., Pelosi, E., Valtieri, M., and Peschle, C. (1994). Key functional role and lineage-specific expression of selected HOXB genes in purified haematopoietic progenitor differentiation. Blood *84*, 3637–3647.

Goardon, N., Marchi, E., Atzberger, A., Quek, L., Schuh, A., Soneji, S., Woll, P., Mead, A., Alford, K.A., Rout, R., et al. (2011). Coexistence of LMPP-like and GMP-like Leukaemia Stem Cells in Acute Myeloid Leukaemia. Cancer Cell *19*, 138–152.

Golub, T.R., Slonim, D.K., Tamayo, P., Huard, C., Gaasenbeek, M., Mesirov, J.P., Coller, H., Loh, M.L., Downing, J.R., Caligiuri, M.A., et al. (1999). Molecular classification of cancer: class discovery and class prediction by gene expression monitoring. Science *286*, 531–537.

Gottlieb, E., and Tomlinson, I.P.M. (2005). Mitochondrial tumour suppressors: a genetic and biochemical update. Nat Rev Cancer *5*, 857–866.

Greenbaum, A., Hsu, Y.-M.S., Day, R.B., Schuettpelz, L.G., Christopher, M.J., Borgerding, J.N., Nagasawa, T., and Link, D.C. (2013). CXCL12 in early mesenchymal progenitors is required for haematopoietic stem-cell maintenance. Nature *495*, 227–230.

Griffin, J.D., and Löwenberg, B. (1986). Clonogenic cells in acute myeloblastic leukaemia. Blood *68*, 1185–1195.

Grimwade, D., Hills, R.K., Moorman, A.V., Walker, H., Chatters, S., Goldstone, A.H., Wheatley, K., Harrison, C.J., Burnett, A.K., and National Cancer Research Institute Adult Leukaemia Working Group (2010). Refinement of cytogenetic classification in acute myeloid leukaemia: determination of prognostic significance of rare recurring chromosomal abnormalities among 5876 younger adult patients treated in the United Kingdom Medical Research Council trials. Blood *116*, 354–365.

Grimwade, D., Ivey, A., and Huntly, B.J.P. (2016). Molecular landscape of acute myeloid leukaemia in younger adults and its clinical relevance. Blood *127*, 29–41.

Grinenko, T., Arndt, K., Portz, M., Mende, N., Günther, M., Cosgun, K.N., Alexopoulou, D., Lakshmanaperumal, N., Henry, I., Dahl, A., et al. (2014). Clonal expansion capacity defines two consecutive developmental stages of long-term haematopoietic stem cells. J. Exp. Med. *211*, 209–215.

Gu, T.-P., Guo, F., Yang, H., Wu, H.-P., Xu, G.-F., Liu, W., Xie, Z.-G., Shi, L., He, X., Jin, S., et al. (2011). The role of Tet3 DNA dioxygenase in epigenetic reprogramming by oocytes. Nature *477*, 606–610.

Guenechea, G., Gan, O.I., Dorrell, C., and Dick, J.E. (2001). Distinct classes of human stem cells that differ in proliferative and self-renewal potential. Nat. Immunol. *2*, 75–82.

Guitart, A.V., Subramani, C., Armesilla-Diaz, A., Smith, G., Sepulveda, C., Gezer, D., Vukovic, M., Dunn, K., Pollard, P., Holyoake, T.L., et al. (2013). Hif-2α is not essential for cell-autonomous haematopoietic stem cell maintenance. Blood *122*, 1741–1745.

Gurumurthy, S., Xie, S.Z., Alagesan, B., Kim, J., Yusuf, R.Z., Saez, B., Tzatsos, A., Ozsolak, F., Milos, P., Ferrari, F., et al. (2010). The Lkb1 metabolic sensor maintains haematopoietic stem cell survival. Nature *468*, 659–663.

Gutiérrez, N.C., López-Pérez, R., Hernández, J.M., Isidro, I., González, B., Delgado, M., Fermiñán, E., García, J.L., Vázquez, L., González, M., et al. (2005). Gene expression profile reveals deregulation of genes with relevant functions in the different subclasses of acute myeloid leukaemia. Leukaemia *19*, 402–409.

Hanahan, D., and Weinberg, R.A. (2011). Hallmarks of cancer: the next generation. Cell *144*, 646–674.

Harrison, D.E., Zhong, R.K., Jordan, C.T., Lemischka, I.R., and Astle, C.M. (1997). Relative to adult marrow, foetal liver repopulates nearly five times more effectively long-term than short-term. Exp. Hematol. *25*, 293–297.

Harrison, D.E., Astle, C.M., and Stone, M. (1989). Numbers and functions of transplantable primitive immunohaematopoietic stem cells. Effects of age. Journal of Immunology *142*, 3833–3840.

Heaney, M.L., and Soriano, G. (2013). Acute Myeloid Leukaemia Following a Myeloproliferative Neoplasm: Clinical characteristics, genetic features and effects of therapy. Curr Hematol Malig Rep *8*, 116–122.

Herst, P.M., Howman, R.A., Neeson, P.J., Berridge, M.V., and Ritchie, D.S. (2011). The level of glycolytic metabolism in acute myeloid leukaemia blasts at diagnosis is prognostic for clinical outcome. J. Leukoc. Biol. *89*, 51–55.

Hock, H., Hamblen, M.J., Rooke, H.M., Schindler, J.W., Saleque, S., Fujiwara, Y., and Orkin, S.H. (2004). Gfi-1 restricts proliferation and preserves functional integrity of haematopoietic stem cells. Nature *431*, 1002–1007.

Hoekstra, A.S., de Graaff, M.A., Briaire-de Bruijn, I.H., Ras, C., Seifar, R.M., van Minderhout, I., Cornelisse, C.J., Hogendoorn, P.C.W., Breuning, M.H., Suijker, J., et al. (2015). Inactivation of SDH and FH cause loss of 5hmC and increased H3K9me3 in paraganglioma/pheochromocytoma and smooth muscle tumours. Oncotarget *6*, 38777–38788.

Hole, P.S., Darley, R.L., and Tonks, A. (2011). Do reactive oxygen species play a role in myeloid leukaemias? Blood *117*, 5816–5826.

Hole, P.S., Pearn, L.,

Hole, P.S., Zabkiewicz, J., Munje, C., Newton, Z., Pearn, L., White, P., Marquez, N., Hills, R.K., Burnett, A.K., Tonks, A., et al. (2013). Overproduction of NOX-derived ROS in AML promotes proliferation and is associated with defective oxidative stress signalling. Blood *122*, 3322–3330.

Hope, K.J., Jin, L., and Dick, J.E. (2004). Acute myeloid leukaemia originates from a hierarchy of leukaemic stem cell classes that differ in self-renewal capacity. Nat. Immunol. *5*, 738–743.

Hoshii, T., Tadokoro, Y., Naka, K., Ooshio, T., Muraguchi, T., Sugiyama, N., Soga, T., Araki, K., Yamamura, K., and Hirao, A. (2012). mTORC1 is essential for leukaemia propagation but not stem cell self-renewal. J Cl*122*, 2114–2129.

Hossfeld, D.K. (2002). E.S. Jaffe, N.L. Harris, H. Stein, J.W. Vardiman (eds). World Health Organization Classification of Tumours: Pathology and genetics of tumours of haematopoietic and lymphoid tissues. Ann Oncol *13*, 490–491.

Huntly, B.J.P., and Gilliland, D.G. (2005). Leukaemia stem cells and the evolution of cancer-stem-cell research. Nat. Rev. Cancer *5*, 311–321.

Huntly, B.J.P., Shigematsu, H., Deguchi, K., Lee, B.H., Mizuno, S., Duclos, N., Rowan, R., Amaral, S., Curley, D., Williams, I.R., et al. (2004). MOZ-TIF2, but not BCR-ABL, confers properties of leukaemic stem cells to committed murine haematopoietic progenitors. Cancer Cell *6*, 587–596.

Ikuta, K., and Weissman, I.L. (1992). Evidence that haematopoietic stem cells express mouse c-kit but do not depend on steel factor for their generation. Proc Natl Acad Sci U S A *89*, 1502–1506.

Imamura, T., Morimoto, A., Takanashi, M., Hibi, S., Sugimoto, T., Ishii, E., and Imashuku, S. (2002). Frequent co-expression of HoxA9 and Meis1 genes in infant acute lymphoblastic leukaemia with MLL rearrangement. Br. J. Haematol. *119*, 119–121.

Isaacs, J.S., Jung, Y.J., Mole, D.R., Lee, S., Torres-Cabala, C., Chung, Y.-L., Merino, M., Trepel, J., Zbar, B., Toro, J., et al. (2005). HIF overexpression correlates with biallelic loss of fumarate hydratase in renal cancer: novel role of fumarate in regulation of HIF stability. Cancer Cell *8*, 143–153.

Ito, K., and Suda, T. (2014). Metabolic requirements for the maintenance of self-renewing stem cells. Nat Rev Mol Cell Biol *15*, 243–256.

Ito, K., Carracedo, A., Weiss, D., Arai, F., Ala, U., Avigan, D.E., Schafer, Z.T., Evans, R.M., Suda, T., Lee, C.-H., et al. (2012). A PML–PPAR-δ pathway for fatty acid oxidation regulates haematopoietic stem cell maintenance. Nat. Med. *18*, 1350–1358.

Ito, K., Hirao, A., Arai, F., Takubo, K., Matsuoka, S., Miyamoto, K., Ohmura, M., Naka, K., Hosokawa, K., Ikeda, Y., et al. (2006). Reactive oxygen species act through p38 MAPK to limit the lifespan of haematopoietic stem cells. Nat. Med. *12*, 446–451.

Jaakkola, P., Mole, D.R., Tian, Y.M., Wilson, M.I., Gielbert, J., Gaskell, S.J., von Kriegsheim, A., Hebestreit, H.F., Mukherji, M., Schofield, C.J., et al. (2001). Targeting of HIF-alpha to the von Hippel-Lindau ubiquitylation complex by O2-regulated prolyl hydroxylation. Science *292*, 468–472.

Jacque, N., Ronchetti, A.M., Larrue, C., Meunier, G., Birsen, R., Willems, L., Saland, E., Decroocq, J., Maciel, T.T., Lambert, M., et al. (2015). Targeting glutaminolysis has antileukaemic activity in acute myeloid leukaemia and synergizes with BCL-2 inhibition. Blood *126*, 1346–1356.

Jan, M., Snyder, T.M., Corces-Zimmerman, M.R., Vyas, P., Weissman, I.L., Quake, S.R., and Majeti, R. (2012). Clonal evolution of pre leukaemic haematopoietic stem cells precedes human acute myeloid leukaemia. Sci Transl Med *4*, 149ra118.

Jang, M.K., Mochizuki, K., Zhou, M., Jeong, H.-S., Brady, J.N., and Ozato, K. (2005). The bromodomain protein Brd4 is a positive regulatory component of P-TEFb and stimulates RNA polymerase II-dependent transcription. Mol. Cell *19*, 523–534.

Jang, Y.-Y., and Sharkis, S.J. (2007). A low level of reactive oxygen species selects for primitive haematopoietic stem cells that may reside in the low-oxygenic niche. Blood *110*, 3056–3063.

Janiszewska, M., Suva, M.L., Riggi, N., Houtkooper, R.H., Auwerx, J., Clement-Schatlo, V., Radovanovic, I., Rheinbay, E., Provero, P., and Stamenkovic, I. (2012). Imp2 controls oxidative phosphorylation and is crucial for preserving glioblastoma cancer stem cells. Genes & Development *26*, 1926–1944.

Janzen, V., Forkert, R., Fleming, H.E., Saito, Y., Waring, M.T., Dombkowski, D.M., Cheng, T., DePinho, R.A., Sharpless, N.E., and Scadden, D.T. (2006). Stem-cell ageing modified by the cyclin-dependent kinase inhibitor p16 INK4a. Nature *443*, 421–426.

Jayavelu, A.K., Müller, J.P., Bauer, R., Böhmer, S.-A., Lässig, J., Cerny-Reiterer, S., Sperr, W.R., Valent, P., Maurer, B., Moriggl, R., et al. (2016). NOX4-driven ROS formation mediates PTP inactivation and cell transformation in FLT3ITD-positive AML cells. Leukaemia *30*, 473–483.

Jing, Y. (2004). The PML-RARalpha fusion protein and targeted therapy for acute promyelocytic leukaemia. Leuk. Lymphoma *45*, 639–648.

Jitschin, R., Hofmann, A.D., Bruns, H., Gie\s sl, A., Bricks, J., Berger, J., Saul, D., Eckart, M.J., Mackensen, A., and Mougiakakos, D. (2014). Mitochondrial metabolism contributes to oxidative stress and reveals therapeutic targets in chronic lymphocytic leukaemia. Blood *123*, 2663–2672.

Johnson, G.R., and Moore, M. a. S. (1975). Role of stem cell migration in initiation of mouse foetal liver haemopoiesis. Nature *258*, 726–728.

Jordan, C.T., McKearn, J.P., and Lemischka, I.R. (1990). Cellular and developmental properties of foetal haematopoietic stem cells. Cell *61*, 953–963.

Jung, Y., Wang, J., Schneider, A., Sun, Y.-X., Koh-Paige, A.J., Osman, N.I., McCauley, L.K., and Taichman, R.S. (2006). Regulation of SDF-1 (CXCL12) production by osteoblasts; a possible mechanism for stem cell homing. Bone *38*, 497–508.

Kagey, M.H., Newman, J.J., Bilodeau, S., Zhan, Y., Orlando, D.A., van Berkum, N.L., Ebmeier, C.C., Goossens, J., Rahl, P.B., Levine, S.S., et al. (2010). Mediator and cohesin connect gene expression and chromatin architecture. Nature *467*, 430–435.

Kamminga, L.M., van Os, R., Ausema, A., Noach, E.J.K., Weersing, E., Dontje, B., Vellenga, E., and de Haan, G. (2005). Impaired haematopoietic stem cell functioning after serial transplantation and during normal aging. Stem Cells *23*, 82–92.

Katayama, Y., Battista, M., Kao, W.-M., Hidalgo, A., Peired, A.J., Thomas, S.A., and Frenette, P.S. (2006). Signals from the Sympathetic Nervous System Regulate Haematopoietic Stem Cell Egress from Bone Marrow. Cell *124*, 407–421.

Katsura, Y., and Kawamoto, H. (2001). Stepwise lineage restriction of progenitors in lympho-myelopoiesis. Int. Rev. Immunol. *20*, 1–20.

Kawagoe, H., Humphries, R.K., Blair, A., Sutherland, H.J., and Hogge, D.E. (1999). Expression of Hox genes, Hox-cofactors, and MLL in phenotypically and functionally defined subpopulations of leukaemic and normal human haematopoietic cells. Leukaemia *13*, 687–698.

Kawamoto, H., Ohmura, K., and Katsura, Y. (1997). Direct evidence for the commitment of haematopoietic stem cells to T, B and myeloid lineages in murine foetal liver. Int. Immunol. *9*, 1011–1019.

Keller G, Paige C, Gilboa E, Wagner EF. Expression of a foreign gene in myeloid and lymphoid cells derived from multipotent haematopoietic precursors. Nature. (1985);318:149–154.

Khwaja, A., Bjorkholm, M., Gale, R.E., Levine, R.L., Jordan, C.T., Ehninger, G., Bloomfield, C.D., Estey, E., Burnett, A., Cornelissen, J.J., et al. (2016). Acute myeloid leukaemia. Nat Rev Dis Primers *2*, 16010.

Kiel, M.J., Yilmaz, Ö.H., Iwashita, T., Yilmaz, O.H., Terhorst, C., and Morrison, S.J. (2005). SLAM Family Receptors Distinguish Haematopoietic Stem and Progenitor Cells and Reveal Endothelial Niches for Stem Cells. Cell *121*, 1109–1121.

Kim, E., Ilagan, J.O., Liang, Y., Daubner, G.M., Lee, S.C.-W., Ramakrishnan, A., Li, Y., Chung, Y.R., Micol, J.-B., Murphy, M.E., et al. (2015). SRSF2 mutations contribute to myelodysplasia by mutant-specific effects on exon recognition. Cancer Cell *27*, 617–630.

Kim, I., He, S., Yilmaz, Ö.H., Kiel, M.J., and Morrison, S.J. (2006). Enhanced purification of foetal liver haematopoietic stem cells using SLAM family receptors. Blood *108*, 737–744.

Kim, J.H., Chu, S.C., Gramlich, J.L., Pride, Y.B., Babendreier, E., Chauhan, D., Salgia, R., Podar, K., Griffin, J.D., and Sattler, M. (2005). Activation of the PI3K/mTOR pathway by BCR-ABL contributes to increased production of reactive oxygen species. Blood *105*, 1717–1723.

Kingston, R.E., Chen, C.A., and Rose, J.K. (2003). Calcium phosphate transfection. Curr Protoc Mol Biol *Chapter 9*, Unit 9.1.

Kirito, K., Fox, N., Komatsu, N., and Kaushansky, K. (2005). Thrombopoietin enhances expression of vascular endothelial growth factor (VEGF) in primitive haematopoietic cells through induction of HIF-1α. Blood *105*, 4258–4263.

Kohlmann, A., Schoch, C., Schnittger, S., Dugas, M., Hiddemann, W., Kern, W., and Haferlach, T. (2003). Molecular characterisation of acute leukaemias by use of microarray technology. Genes Chromosomes Cancer *37*, 396–405.

Kon, A., Shih, L.-Y., Minamino, M., Sanada, M., Shiraishi, Y., Nagata, Y., Yoshida, K., Okuno, Y., Bando, M., Nakato, R., et al. (2013). Recurrent mutations in multiple components of the cohesin complex in myeloid neoplasms. Nat. Genet. *45*, 1232–1237.

Kondo, M., Weissman, I.L., and Akashi, K. (1997). Identification of clonogenic common lymphoid progenitors in mouse bone marrow. Cell *91*, 661–672.

Koptyra, M., Falinski, R., Nowicki, M.O., Stoklosa, T., Majsterek, I., Nieborowska-Skorska, M., Blasiak, J., and Skorski, T. (2006). BCR/ABL kinase induces self-mutagenesis via reactive oxygen species to encode imatinib resistance. Blood *108*, 319–327.

Krivtsov, A.V., Figueroa, M.E., Sinha, A.U., Stubbs, M.C., Feng, Z., Valk, P.J.M., Delwel, R., Döhner, K., Bullinger, L., Kung, A.L., et al. (2013). Cell of origin determines clinically relevant subtypes of MLL-rearranged AML. Leukaemia *27*, 852–860.

Krivtsov, A.V., Twomey, D., Feng, Z., Stubbs, M.C., Wang, Y., Faber, J., Levine, J.E., Wang, J., Hahn, W.C., Gilliland, D.G., et al. (2006). Transformation from committed progenitor to leukaemia stem cell initiated by MLL-AF9. Nature *442*, 818–822.

Kroon, E., Krosl, J., Thorsteinsdottir, U., Baban, S., Buchberg, A.M., and Sauvageau, G. (1998). Hoxa9 transforms primary bone marrow cells through specific collaboration with Meis1a but not Pbx1b. The EMBO Journal *17*, 3714–3725.

Kühn, R., Schwenk, F., Aguet, M., and Rajewsky, K. (1995). Inducible gene targeting in mice. Science *269*, 1427–1429.

Kumaravelu, P., Hook, L., Morrison, A.M., Ure, J., Zhao, S., Zuyev, S., Ansell, J., and Medvinsky, A. (2002). Quantitative developmental anatomy of definitive haematopoietic stem cells/long-term repopulating units (HSC/RUs): role of the aorta-gonad-mesonephros (AGM) region and the yolk sac in colonisation of the mouse embryonic liver. Development *129*, 4891–4899.

Kunisaki, Y., Bruns, I., Scheiermann, C., Ahmed, J., Pinho, S., Zhang, D., Mizoguchi, T., Wei, Q., Lucas, D., Ito, K., et al. (2013). Arteriolar niches maintain haematopoietic stem cell quiescence. Nature *502*, 637–643.

Kunisawa, J., Sugiura, Y., Wake, T., Nagatake, T., Suzuki, H., Nagasawa, R., Shikata, S., Honda, K., Hashimoto, E., Suzuki, Y., et al. (2015). Mode of bioenergetic metabolism during B cell differentiation in the intestine determines the distinct requirement for vitamin B1. Cell Reports *13*, 122–131.

Kwon, K., Hutter, C., Sun, Q., Bilic, I., Cobaleda, C., Malin, S., and Busslinger, M. (2008). Instructive role of the transcription factor E2A in early B lymphopoiesis and germinal center B cell development. Immunity *28*, 751–762.

Lacaud, G., Carlsson, L., and Keller, G. (1998). Identification of a foetal haematopoietic precursor with B cell, T cell, and macrophage potential. Immunity *9*, 827–838.

Lagadinou, E.D., Sach, A., Callahan, K., Rossi, R.M., Neering, S.J., Minhajuddin, M., Ashton, J.M., Pei, S., Grose, V., O'Dwyer, K.M., et al. (2013). BCL-2 inhibition targets oxidative phosphorylation and selectively eradicates quiescent human leukaemia stem cells. Cell Stem Cell *12*, 329–341.

Lam, K., and Zhang, D.-E. (2012). RUNX1 and RUNX1-ETO: roles in haematopoiesis and leukaemogenesis. Front Biosci (Landmark Ed) *17*, 1120–1139.

Lapidot, T., Sirard, C., Vormoor, J., Murdoch, B., Hoang, T., Caceres-Cortes, J., Minden, M., Paterson, B., Caligiuri, M.A., and Dick, J.E. (1994). A cell initiating human acute myeloid leukaemia after transplantation into SCID mice. Nature *367*, 645–648.

Larochelle, A., Vormoor, J., Hanenberg, H., Wang, J.C., Bhatia, M., Lapidot, T., Moritz, T., Murdoch, B., Xiao, X.L., Kato, I., et al. (1996). Identification of primitive human haematopoietic cells capable of repopulating NOD/SCID mouse bone marrow: implications for gene therapy. Nat. Med. *2*, 1329–1337.

Laukka, T., Mariani, C.J., Ihantola, T., Cao, J.Z., Hokkanen, J., Kaelin, W.G., Godley, L.A., and Koivunen, P. (2016). Fumarate and Succinate Regulate Expression of Hypoxia-inducible Genes via TET Enzymes. J. Biol. Chem. *291*, 4256–4265.

Lawrence, H.J., Helgason, C.D., Sauvageau, G., Fong, S., Izon, D.J., Humphries, R.K., and Largman, C. (1997). Mice bearing a targeted interruption of the homeobox gene HOXA9 have defects in myeloid, erythroid, and lymphoid haematopoiesis. Blood *89*, 1922–1930.

Le, A., Lane, A.N., Hamaker, M., Bose, S., Gouw, A., Barbi, J., Tsukamoto, T., Rojas, C.J., Slusher, B.S., Zhang, H., et al. (2012). Glucose-independent glutamine metabolism via tca cycling for proliferation and survival in B Cells. Cell Metabolism *15*, 110–121.

Lee, E.A., Angka, L., Rota, S.-G., Hanlon, T., Mitchell, A., Hurren, R., Wang, X.M., Gronda, M., Boyaci, E., Bojko, B., et al. (2015). Targeting mitochondria with avocatin B induces selective leukaemia Cell Death. Cancer Res. *75*, 2478–2488.

Lemischka, I.R., Raulet, D.H., and Mulligan, R.C. (1986). Developmental potential and dynamic behavior of haematopoietic stem cells. Cell *45*, 917–927.

Leonardi, R., Subramanian, C., Jackowski, S., and Rock, C.O. (2012). Cancer-associated Isocitrate Dehydrogenase mutations inactivate NADPH-dependent reductive carboxylation. J. Biol. Chem. *287*, 14615–14620.

Ley, T.J., Ding, L., Walter, M.J., McLellan, M.D., Lamprecht, T., Larson, D.E., Kandoth, C., Payton, J.E., Baty, J., Welch, J., et al. (2010). DNMT3A mutations in acute myeloid leukaemia. N. Engl. J. Med. *363*, 2424–2433.

Ley, T.J., Mardis, E.R., Ding, L., Fulton, B., McLellan, M.D., Chen, K., Dooling, D., Dunford-Shore, B.H., McGrath, S., Hickenbotham, M., et al. (2008). DNA sequencing of a cytogenetically normal acute myeloid leukaemia genome. Nature *456*, 66–72.

Li, C.L., and Johnson, G.R. (1995). Murine haematopoietic stem and progenitor cells: I. Enrichment and biologic characterisation. Blood *85*, 1472–1479.

Liang, Y., Van Zant, G., and Szilvassy, S.J. (2005). Effects of ageing on the homing and engraftment of murine haematopoietic stem and progenitor cells. Blood *106*, 1479–1487.

Licht, J.D. (2006). Reconstructing a disease: What essential features of the retinoic acid receptor fusion oncoproteins generate acute promyelocytic leukaemia? Cancer Cell *9*, 73–74.

Lieu, Y.K., and Reddy, E.P. (2009). Conditional c-myb knockout in adult haematopoietic stem cells leads to loss of self-renewal due to impaired proliferation and accelerated differentiation. Proc. Natl. Acad. Sci. U.S.A. *106*, 21689–21694.

Lindsley, R.C., Mar, B.G., Mazzola, E., Grauman, P.V., Shareef, S., Allen, S.L., Pigneux, A., Wetzler, M., Stuart, R.K., Erba, H.P., et al. (2015). Acute myeloid leukaemia ontogeny is defined by distinct somatic mutations. Blood *125*, 1367–1376.

Liu, P., Tarlé, S.A., Hajra, A., Claxton, D.F., Marlton, P., Freedman, M., Siciliano, M.J., and Collins, F.S. (1993). Fusion between transcription factor CBF beta/PEBP2 beta and a myosin heavy chain in acute myeloid leukaemia. Science *261*, 1041–1044.

Lo, C.G., Lu, T.T., and Cyster, J.G. (2003). Integrin-dependence of lymphocyte entry into the splenic white pulp. J. Exp. Med. *197*, 353–361.

Loschen, G., Azzi, A., Richter, C., and Flohé, L. (1974). Superoxide radicals as precursors of mitochondrial hydrogen peroxide. FEBS Lett. *42*, 68–72.

Loughran, S.J., Kruse, E.A., Hacking, D.F., de Graaf, C.A., Hyland, C.D., Willson, T.A., Henley, K.J., Ellis, S., Voss, A.K., Metcalf, D., et al. (2008). The transcription factor Erg is essential for definitive haematopoiesis and the function of adult haematopoietic stem cells. Nat Immunol *9*, 810–819.

Löwenberg, B., Downing, J.R., and Burnett, A. (1999). Acute myeloid leukaemia. N. Engl. J. Med. *341*, 1051–1062.

Lu, M., Kawamoto, H., Katsube, Y., Ikawa, T., and Katsura, Y. (2002). The common myelolymphoid progenitor: a key intermediate stage in hemopoiesis generating T and B cells. J. Immunol. *169*, 3519–3525.

Luchsinger, L.L., de Almeida, M.J., Corrigan, D.J., Mumau, M., and Snoeck, H.-W. (2016). Mitofusin 2 maintains haematopoietic stem cells with extensive lymphoid potential. Nature *529*, 528–531.

Ludin, A., Gur-Cohen, S., Golan, K., Kaufmann, K.B., Itkin, T., Medaglia, C., Lu, X.-J., Ledergor, G., Kollet, O., and Lapidot, T. (2014). Reactive oxygen species regulate haematopoietic stem cell self-renewal, migration and development, as well as their bone marrow microenvironment. Antioxid. Redox Signal. *21*, 1605–1619.

Luis, T.C., Luc, S., Mizukami, T., Boukarabila, H., Thongjuea, S., Woll, P.S., Azzoni, E., Giustacchini, A., Lutteropp, M., Bouriez-Jones, T., et al. (2016). Initial seeding of the embryonic thymus by immune-restricted lympho-myeloid progenitors. Nat Immunol *17*, 1424–1435.

Lutterbach, B., and Hiebert, S.W. (2000). Role of the transcription factor AML-1 in acute leukaemia and haematopoietic differentiation. Gene *245*, 223–235.

Lutterbach, B., Hou, Y., Durst, K.L., and Hiebert, S.W. (1999). The inv(16) encodes an acute myeloid leukaemia 1 transcriptional corepressor. Proc Natl Acad Sci U S A *96*, 12822–12827.

Lymperi, S., Horwood, N., Marley, S., Gordon, M.Y., Cope, A.P., and Dazzi, F. (2008). Strontium can increase some osteoblasts without increasing haematopoietic stem cells. Blood *111*, 1173–1181.

MacIver, N.J., Michalek, R.D., and Rathmell, J.C. (2013). Metabolic regulation of T lymphocytes. Ann. Rev. Imm. *31*, 259–283.

Månsson, R., Hultquist, A., Luc, S., Yang, L., Anderson, K., Kharazi, S., Al-Hashmi, S., Liuba, K., Thorén, L., Adolfsson, J., et al. (2007). Molecular evidence for hierarchical transcriptional lineage priming in foetal and adult stem cells and multipotent progenitors. Immunity *26*, 407–419.

Mantel, C., Messina-Graham, S., and Broxmeyer, H.E. (2010). Upregulation of nascent mitochondrial biogenesis in mouse haematopoietic stem cells parallels upregulation of CD34 and loss of pluripotency: a potential strategy for reducing oxidative risk in stem cells. Cell Cycle *9*, 2008–2017.

Mardis, E.R., Ding, L., Dooling, D.J., Larson, D.E., McLellan, M.D., Chen, K., Koboldt, D.C., Fulton, R.S., Delehaunty, K.D., McGrath, S.D., et al. (2009). Recurring mutations found by sequencing an acute myeloid leukaemia genome. N. Engl. J. Med. *361*, 1058–1066.

Marschalek, R. (2010). Mixed lineage leukaemia: roles in human malignancies and potential therapy. FEBS Journal *277*, 1822–1831.

Martin, M.E., Milne, T.A., Bloyer, S., Galoian, K., Shen, W., Gibbs, D., Brock, H.W., Slany, R., and Hess, J.L. (2003). Dimerization of MLL fusion proteins immortalizes haematopoietic cells. Cancer Cell *4*, 197–207.

Maryanovich, M., Zaltsman, Y., Ruggiero, A., Goldman, A., Shachnai, L., Zaidman, S.L., Porat, Z., Golan, K., Lapidot, T., and Gross, A. (2015). An MTCH2 pathway repressing mitochondria metabolism regulates haematopoietic stem cell fate. Nature Communications *6*, 7901.

Masson, N., Willam, C., Maxwell, P.H., Pugh, C.W., and Ratcliffe, P.J. (2001). Independent function of two destruction domains in hypoxia-inducible factor-alpha chains activated by prolyl hydroxylation. EMBO J. *20*, 5197–5206.

McCrann, D.J., Eliades, A., Makitalo, M., Matsuno, K., and Ravid, K. (2009). Differential expression of NADPH oxidases in megakaryocytes and their role in polyploidy. Blood *114*, 1243–1249.

McCulloch, E.A. (1983). Stem cells in normal and leukaemic hemopoiesis (Henry Stratton Lecture, 1982). Blood *62*, 1–13.

McLaughlin, F., Ludbrook, V.J., Cox, J., Carlowitz, I. von, Brown, S., and Randi, A.M. (2001). Combined genomic and antisense analysis reveals that the transcription factor Erg is implicated in endothelial cell differentiation. Blood *98*, 3332–3339.

McMahon, K.A., Hiew, S.Y.-L., Hadjur, S., Veiga-Fernandes, H., Menzel, U., Price, A.J., Kioussis, D., Williams, O., and Brady, H.J.M. (2007). Mll has a critical role in foetal and adult haematopoietic stem cell self-renewal. Cell Stem Cell *1*, 338–345.

Mead, A.J., Linch, D.C., Hills, R.K., Wheatley, K., Burnett, A.K., and Gale, R.E. (2007). FLT3 tyrosine kinase domain mutations are biologically distinct from and have a significantly more favorable prognosis than FLT3 internal tandem duplications in patients with acute myeloid leukaemia. Blood *110*, 1262–1270.

Mebius, R.E., Miyamoto, T., Christensen, J., Domen, J., Cupedo, T., Weissman, I.L., and Akashi, K. (2001). The foetal liver counterpart of adult common lymphoid progenitors gives rise to all lymphoid lineages, CD45+CD4+CD3- cells, as well as macrophages. J. Immunol. *166*, 6593–6601.

Medvinsky, A., and Dzierzak, E. (1996). Definitive haematopoiesis is autonomously initiated by the AGM region. Cell *86*, 897–906.

Mendelson, A., and Frenette, P.S. (2014). Haematopoietic stem cell niche maintenance during homeostasis and regeneration. Nat. Med. *20*, 833–846.

Méndez-Ferrer, S., Michurina, T.V., Ferraro, F., Mazloom, A.R., MacArthur, B.D., Lira, S.A., Scadden, D.T., Ma'ayan, A., Enikolopov, G.N., and Frenette, P.S. (2010). Mesenchymal and haematopoietic stem cells form a unique bone marrow niche. Nature *466*, 829–834.

Metallo, C.M., Gameiro, P.A., Bell, E.L., Mattaini, K.R., Yang, J., Hiller, K., Jewell, C.M., Johnson, Z.R., Irvine, D.J., Guarente, L., et al. (2012). Reductive glutamine metabolism by IDH1 mediates lipogenesis under hypoxia. Nature *481*, 380–384.

Metcalf and M. A. S. Moore. (1972). Haemopoietic Cells. North-Holland, Amsterdam, and Elsevier, New York, 1971. xiv, 550 pp. Frontiers of Biology, vol. 24. Science *178*, 974–975.

Metzeler, K.H., Herold, T., Rothenberg-Thurley, M., Amler, S., Sauerland, M.C., Görlich, D., Schneider, S., Konstandin, N.P., Dufour, A., Bräundl, K., et al. (2016). Spectrum and prognostic relevance of driver gene mutations in acute myeloid leukaemia. Blood *128*, 686–698.

Meyer, C., Kowarz, E., Hofmann, J., Renneville, A., Zuna, J., Trka, J., Ben Abdelali, R., Macintyre, E., De Braekeleer, E., De Braekeleer, M., et al. (2009). New insights to the MLL recombinome of acute leukaemias. Leukaemia *23*, 1490–1499.

Meyers, S., Lenny, N., and Hiebert, S.W. (1995). The t(8;21) fusion protein interferes with AML-1B-dependent transcriptional activation. Mol Cell Biol *15*, 1974–1982.

Michalek, R.D., Gerriets, V.A., Jacobs, S.R., Macintyre, A.N., MacIver, N.J., Mason, E.F., Sullivan, S.A., Nichols, A.G., and Rathmell, J.C. (2011). Cutting edge: distinct glycolytic and lipid oxidative metabolic programs are essential for effector and regulatory CD4+ T cell subsets. J. Immunol. *186*, 3299–3303.

Miller, T., Krogan, N.J., Dover, J., Erdjument-Bromage, H., Tempst, P., Johnston, M., Greenblatt, J.F., and Shilatifard, A. (2001). COMPASS: A complex of proteins associated with a trithorax-related SET domain protein. Proc Natl Acad Sci U S A *98*, 12902–12907.

Milne, T.A., Kim, J., Wang, G.G., Stadler, S.C., Basrur, V., Whitcomb, S.J., Wang, Z., Ruthenburg, A.J., Elenitoba-Johnson, K.S.J., Roeder, R.G., et al. (2010). Multiple interactions recruit MLL1 and MLL1 fusion proteins to the HOXA9 locus in leukaemogenesis. Mol. Cell *38*, 853–863.

Miyamoto, T., Weissman, I.L., and Akashi, K. (2000). AML1/ETO-expressing non leukaemic stem cells in acute myelogenous leukaemia with 8;21 chromosomal translocations. PNAS *97*, 7521–7526.

Mohan, M., Lin, C., Guest, E., and Shilatifard, A. (2010). Licensed to elongate: a molecular mechanism for MLL-based leukaemogenesis. Nat. Rev. Cancer *10*, 721–728.

Mohrin, M., Shin, J., Liu, Y., Brown, K., Luo, H., Xi, Y., Haynes, C.M., and Chen, D. (2015). Stem cell aging. A mitochondrial UPR-mediated metabolic checkpoint regulates haematopoietic stem cell ageing. Science *347*, 1374–1377.

Mookerjee, S. A., Brand, M. D. (2015) Measurement and analysis of extracellular acid production to determine glycolytic rate. J. Vis. Exp. (106), e53464, doi:10.3791/53464 (2015).

Morita, Y., Ema, H., and Nakauchi, H. (2010). Heterogeneity and hierarchy within the most primitive haematopoietic stem cell compartment. J. Exp. Med. *207*, 1173–1182.

Morrison, S.J., and Weissman, I.L. (1994). The long-term repopulating subset of haematopoietic stem cells is deterministic and isolatable by phenotype. Immunity *1*, 661–673.

Morrison, S.J., Hemmati, H.D., Wandycz, A.M., and Weissman, I.L. (1995). The purification and characterisation of foetal liver haematopoietic stem cells. Proc Natl Acad Sci U S A *92*, 10302–10306.

Morrison, S.J., Wandycz, A.M., Akashi, K., Globerson, A., and Weissman, I.L. (1996). The ageing of haematopoietic stem cells. Nat. Med. *2*, 1011–1016.

Morrison, S.J., Wandycz, A.M., Hemmati, H.D., Wright, D.E., and Weissman, I.L. (1997). Identification of a lineage of multipotent haematopoietic progenitors. Development *124*, 1929–1939.

Moskow, J.J., Bullrich, F., Huebner, K., Daar, I.O., and Buchberg, A.M. (1995). Meis1, a PBX1-related homeobox gene involved in myeloid leukaemia in BXH-2 mice. Mol. Cell. Biol. *15*, 5434–5443.

Motohashi, H., Kimura, M., Fujita, R., Inoue, A., Pan, X., Takayama, M., Katsuoka, F., Aburatani, H., Bresnick, E.H., and Yamamoto, M. (2010). NF-E2 domination over Nrf2 promotes ROS accumulation and megakaryocytic maturation. Blood *115*, 677–686.

Mrózek, K., and Bloomfield, C.D. (2008). Clinical significance of the most common chromosome translocations in adult acute myeloid leukaemia. J Natl Cancer Inst Monogr *2008*, 52–57.

Mullen, A.R., Wheaton, W.W., Jin, E.S., Chen, P.-H., Sullivan, L.B., Cheng, T., Yang, Y., Linehan, W.M., Chandel, N.S., and DeBerardinis, R.J. (2012). Reductive carboxylation supports growth in tumour cells with defective mitochondria. Nature *481*, 385–388.

Müller-Sieburg, C.E., Cho, R.H., Thoman, M., Adkins, B., and Sieburg, H.B. (2002). Deterministic regulation of haematopoietic stem cell self-renewal and differentiation. Blood *100*, 1302–1309.

Muller-Sieburg, C.E., Sieburg, H.B., Bernitz, J.M., and Cattarossi, G. (2012). Stem cell heterogeneity: implications for ageing and regenerative medicine. Blood *119*, 3900–3907.

Munnich, A. (2008). Casting an eye on the Krebs cycle. Nat. Genet. *40*, 1148–1149.

Murakami, K., Mavrothalassitis, G., Bhat, N.K., Fisher, R.J., and Papas, T.S. (1993). Human ERG-2 protein is a phosphorylated DNA-binding protein--a distinct member of the ets family. Oncogene *8*, 1559–1566.

Nakada, D., Saunders, T.L., and Morrison, S.J. (2010). Lkb1 regulates cell cycle and energy metabolism in haematopoietic stem cells. Nature *468*, 653–658.

Nakajima, E.C., and Van Houten, B. (2013). Metabolic symbiosis in cancer: refocusing the Warburg lens. Molecular Carcinogenesis *52*, 329–337.

Nakamura, Y., Arai, F., Iwasaki, H., Hosokawa, K., Kobayashi, I., Gomei, Y., Matsumoto, Y., Yoshihara, H., and Suda, T. (2010). Isolation and characterisation of endosteal niche cell populations that regulate haematopoietic stem cells. Blood *116*, 1422–1432.

Nasmyth, K., and Haering, C.H. (2009). Cohesin: its roles and mechanisms. Ann. Rev. Genet. *43*, 525–558.

Naveiras, O., Nardi, V., Wenzel, P.L., Hauschka, P.V., Fahey, F., and Daley, G.Q. (2009). Bone-marrow adipocytes as negative regulators of the haematopoietic microenvironment. Nature *460*, 259–263.

Neff, T., Sinha, A.U., Kluk, M.J., Zhu, N., Khattab, M.H., Stein, L., Xie, H., Orkin, S.H., and Armstrong, S.A. (2012). Polycomb repressive complex 2 is required for MLL-AF9 leukaemia. Proc Natl Acad Sci U S A *109*, 5028–5033.

Network, T.C.G.A.R. (2013). Genomic and epigenomic landscapes of adult de novo acute myeloid leukaemia. N. Engl. J. Med. *368*, 2059–2074.

Ng, A.P., Loughran, S.J., Metcalf, D., Hyland, C.D., de Graaf, C.A., Hu, Y., Smyth, G.K., Hilton, D.J., Kile, B.T., and Alexander, W.S. (2011). Erg is required for self-renewal of haematopoietic stem cells during stress haematopoiesis in mice. Blood *118*, 2454–2461.

Nicholls, D.G. (2009). Spare respiratory capacity, oxidative stress and excitotoxicity. Biochemical Society Transactions *37*, 1385–1388.

Nilsson, S.K., Johnston, H.M., and Coverdale, J.A. (2001). Spatial localisation of transplanted haematopoietic stem cells: inferences for the localisation of stem cell niches. Blood *97*, 2293–2299.

Nolte, M.A., Hamann, A., Kraal, G., and Mebius, R.E. (2002). The strict regulation of lymphocyte migration to splenic white pulp does not involve common homing receptors. Immunology *106*, 299–307.

Nombela-Arrieta, C., Pivarnik, G., Winkel, B., Canty, K.J., Harley, B., Mahoney, J.E., Park, S.-Y., Lu, J., Protopopov, A., and Silberstein, L.E. (2013). Quantitative imaging of haematopoietic stem and progenitor cell localization and hypoxic status in the bone marrow microenvironment. Nat Cell Biol *15*, 533–543.

North, T., Gu, T.L., Stacy, T., Wang, Q., Howard, L., Binder, M., Marin-Padilla, M., and Speck, N.A. (1999). Cbfa2 is required for the formation of intra-aortic haematopoietic clusters. Development *126*, 2563–2575.

North, T.E., Stacy, T., Matheny, C.J., Speck, N.A., and de Bruijn, M.F.T.R. (2004). Runx1 is expressed in adult mouse haematopoietic stem cells and differentiating myeloid and lymphoid cells, but not in maturing erythroid cells. Stem Cells *22*, 158–168.

Notta, F., Zandi, S., Takayama, N., Dobson, S., Gan, O.I., Wilson, G., Kaufmann, K.B., McLeod, J., Laurenti, E., Dunant, C.F., et al. (2016). Distinct routes of lineage development reshape the human blood hierarchy across ontogeny. Science *351*.

Nutt, S.L., and Kee, B.L. (2007). The transcriptional regulation of B cell lineage commitment. Immunity *26*, 715–725.

O'Flaherty, L., Adam, J., Heather, L.C., Zhdanov, A.V., Chung, Y.-L., Miranda, M.X., Croft, J., Olpin, S., Clarke, K., Pugh, C.W., et al. (2010). Dysregulation of hypoxia pathways in fumarate hydratase-deficient cells is independent of defective mitochondrial metabolism. Hum. Mol. Genet. *19*, 3844–3851.

Oburoglu, L., Tardito, S., Fritz, V., de Barros, S.C., Merida, P., Craveiro, M., Mamede, J., Cretenet, G., Mongellaz, C., An, X., et al. (2014). Glucose and glutamine metabolism regulate human haematopoietic stem cell lineage specification. Cell Stem Cell *15*, 169–184.

Oguro, H., Ding, L., and Morrison, S.J. (2013). SLAM family markers resolve functionally distinct subpopulations of haematopoietic stem cells and multipotent progenitors. Cell Stem Cell *13*, 102–116.

Okada, Y., Feng, Q., Lin, Y., Jiang, Q., Li, Y., Coffield, V.M., Su, L., Xu, G., and Zhang, Y. (2005). hDOT1L links histone methylation to leukaemogenesis. Cell *121*, 167–178.

Omatsu, Y., Sugiyama, T., Kohara, H., Kondoh, G., Fujii, N., Kohno, K., and Nagasawa, T. (2010). The essential functions of adipo-osteogenic progenitors as the haematopoietic stem and progenitor cell niche. Immunity *33*, 387–399.

Ooi, A., Wong, J.-C., Petillo, D., Roossien, D., Perrier-Trudova, V., Whitten, D., Min, B.W.H., Tan, M.-H., Zhang, Z., Yang, X.J., et al. (2011). An antioxidant response phenotype shared between hereditary and sporadic type 2 papillary renal cell carcinoma. Cancer Cell *20*, 511–523.

Orkin, S.H., and Zon, L.I. (2008). Haematopoiesis: An evolving paradigm for stem cell biology. Cell *132*, 631–644.

Osawa, M., Hanada, K., Hamada, H., and Nakauchi, H. (1996). Long-term lymphohaematopoietic reconstitution by a single CD34-low/negative haematopoietic stem cell. Science *273*, 242–245.

Paiushina, O.V., Domaratskaia, E.I., and Starostin, V.I. (2012). Cellular composition and regulatory function of foetal liver stroma. Tsitologiia *54*, 369–380.

Pandolfi, A., Barreyro, L., and Steidl, U. (2013). Concise Review: Pre leukaemic stem cells: molecular biology and clinical implications of the precursors to leukaemia stem cells. Stem Cells Translational Medicine *2*, 143–150.

Papa, S., Martino, P.L., Capitanio, G., Gaballo, A., De Rasmo, D., Signorile, A., and Petruzzella, V. (2012). The oxidative phosphorylation system in mammalian mitochondria. Adv. Exp. Med. Biol. *942*, 3–37.

Papaemmanuil, E., Cazzola, M., Boultwood, J., Malcovati, L., Vyas, P., Bowen, D., Pellagatti, A., Wainscoat, J.S., Hellstrom-Lindberg, E., Gambacorti-Passerini, C., et al. (2011). Somatic SF3B1 mutation in myelodysplasia with ring sideroblasts. N. Engl. J. Med. *365*, 1384–1395.

Papaemmanuil, E., Gerstung, M., Bullinger, L., Gaidzik, V.I., Paschka, P., Roberts, N.D., Potter, N.E., Heuser, M., Thol, F., Bolli, N., et al. (2016). Genomic classification and prognosis in acute myeloid leukaemia. N. Engl. J. Med. *374*, 2209–2221.

Papaemmanuil, E., Gerstung, M., Malcovati, L., Tauro, S., Gundem, G., Van Loo, P., Yoon, C.J., Ellis, P., Wedge, D.C., Pellagatti, A., et al. (2013). Clinical and biological implications of driver mutations in myelodysplastic syndromes. Blood *122*, 3616–3627; quiz 3699.

Parmar, K., Mauch, P., Vergilio, J.-A., Sackstein, R., and Down, J.D. (2007). Distribution of haematopoietic stem cells in the bone marrow according to regional hypoxia. Proc. Natl. Acad. Sci. U.S.A. *104*, 5431–5436.

Pastò, A., Bellio, C., Pilotto, G., Ciminale, V., Silic-Benussi, M., Guzzo, G., Rasola, A., Frasson, C., Nardo, G., Zulato, E., et al. (2014). Cancer stem cells from epithelial ovarian cancer patients privilege oxidative phosphorylation, and resist glucose deprivation. Oncotarget *5*, 4305–4319.

Pearce, E.L., and Pearce, E.J. (2013). Metabolic Pathways in Immune Cell Activation and Quiescence. Immunity *38*, 633–643.

Pedersen, M., Löfstedt, T., Sun, J., Holmquist-Mengelbier, L., Påhlman, S., and Rönnstrand, L. (2008). Stem cell factor induces HIF-1alpha at normoxia in haematopoietic cells. Biochem. Biophys. Res. Commun. *377*, 98–103.

Peterlin, B.M., and Price, D.H. (2006). Controlling the elongation phase of transcription with P-TEFb. Mol. Cell *23*, 297–305.

Petrie, H.T. (2002). Role of thymic organ structure and stromal composition in steady-state postnatal T-cell production. Immunological Reviews *189*, 8–20.

Piccoli, C., Agriesti, F., Scrima, R., Falzetti, F., Di Ianni, M., and Capitanio, N. (2013). To breathe or not to breathe: the haematopoietic stem/progenitor cells dilemma. Br J Pharmacol *169*, 1652–1671.

Piccoli, C., Ria, R., Scrima, R., Cela, O., D'Aprile, A., Boffoli, D., Falzetti, F., Tabilio, A., and Capitanio, N. (2005). Characterisation of mitochondrial and extra-mitochondrial oxygen consuming reactions in human haematopoietic stem cells novel evidence of the occurrence of NADPH oxidase activity. J. Biol. Chem. *280*, 26467–26476.

Pineault, N., Helgason, C.D., Lawrence, H.J., and Humphries, R.K. (2002). Differential expression of Hox, Meis1, and Pbx1 genes in primitive cells throughout murine haematopoietic ontogeny. Experimental Hematology *30*, 49–57.

Polet, F., Corbet, C., Pinto, A., Rubio, L.I., Martherus, R., Bol, V., Drozak, X., Grégoire, V., Riant, O., and Feron, O. (2015). Reducing the serine availability complements the inhibition of the glutamine metabolism to block leukaemia cell growth. Oncotarget *7*, 1765–1776.

Pollard, P.J., Brière, J.J., Alam, N.A., Barwell, J., Barclay, E., Wortham, N.C., Hunt, T., Mitchell, M., Olpin, S., Moat, S.J., et al. (2005). Accumulation of Krebs cycle intermediates and over-expression of HIF1alpha in tumours which result from germline FH and SDH mutations. Hum. Mol. Genet. *14*, 2231–2239.

Pollard, P.J., Spencer-Dene, B., Shukla, D., Howarth, K., Nye, E., El-Bahrawy, M., Deheragoda, M., Joannou, M., McDonald, S., Martin, A., et al. (2007). Targeted inactivation of Fh1 causes proliferative renal cyst development and activation of the hypoxia pathway. Cancer Cell *11*, 311–319.

Porcher, C., Swat, W., Rockwell, K., Fujiwara, Y., Alt, F.W., and Orkin, S.H. (1996). The T cell leukaemia oncoprotein SCL/tal-1 is essential for development of all haematopoietic lineages. Cell *86*, 47–57.

Pronk, C.J.H., Rossi, D.J., Månsson, R., Attema, J.L., Norddahl, G.L., Chan, C.K.F., Sigvardsson, M., Weissman, I.L., and Bryder, D. (2007). Elucidation of the phenotypic, functional, and molecular topography of a myeloerythroid progenitor cell hierarchy. Cell Stem Cell *1*, 428–442.

Qian, H., Buza-Vidas, N., Hyland, C.D., Jensen, C.T., Antonchuk, J., Månsson, R., Thoren, L.A., Ekblom, M., Alexander, W.S., and Jacobsen, S.E.W. (2007). Critical role of thrombopoietin in maintaining adult quiescent haematopoietic stem cells. Cell Stem Cell *1*, 671–684.

Qin, L., Tian, Y., Yu, Z., Shi, D., Wang, J., Zhang, C., Peng, R., Chen, X., Liu, C., Chen, Y., et al. (2015). Targeting PDK1 with dichloroacetophenone to inhibit acute myeloid leukaemia (AML) cell growth. Oncotarget *7*, 1395–1407.

Querfurth, E., Schuster, M., Kulessa, H., Crispino, J.D., Döderlein, G., Orkin, S.H., Graf, T., and Nerlov, C. (2000). Antagonism between C/EBPβ and FOG in eosinophil lineage commitment of multipotent haematopoietic progenitors. Genes Dev. *14*, 2515–2525.

Rakheja, D., Konoplev, S., Medeiros, L.J., and Chen, W. (2012). IDH mutations in acute myeloid leukaemia. Human Pathology *43*, 1541–1551.

Rampal, R., Alkalin, A., Madzo, J., Vasanthakumar, A., Pronier, E., Patel, J., Li, Y., Ahn, J., Abdel-Wahab, O., Shih, A., et al. (2014). DNA hydroxymethylation profiling reveals that WT1 mutations result in loss of TET2 function in acute myeloid leukaemia. Cell Rep *9*, 1841–1855.

Rao, R.C., and Dou, Y. (2015). Hijacked in cancer: the KMT2 (MLL) family of methyltransferases. Nat. Rev. Cancer *15*, 334–346.

Reya, T., Morrison, S.J., Clarke, M.F., and Weissman, I.L. (2001). Stem cells, cancer, and cancer stem cells. Nature *414*, 105–111.

Rhodes, J., Hagen, A., Hsu, K., Deng, M., Liu, T.X., Look, A.T., and Kanki, J.P. (2005). Interplay of pu.1 and gata1 determines myelo-erythroid progenitor cell fate in zebrafish. Dev. Cell *8*, 97–108.

Ricciardi, M.R., Mirabilii, S., Allegretti, M., Licchetta, R., Calarco, A., Torrisi, M.R., Foà, R., Nicolai, R., Peluso, G., and Tafuri, A. (2015). Targeting the leukaemia cell metabolism by the CPT1a inhibition: functional preclinical effects in leukaemias. Blood *126*, 1925–1929.

Riether, C., Schürch, C.M., and Ochsenbein, A.F. (2015). Regulation of haematopoietic and leukaemic stem cells by the immune system. Cell Death & Differentiation *22*, 187–198.

Rossi, D.J., Bryder, D., Zahn, J.M., Ahlenius, H., Sonu, R., Wagers, A.J., and Weissman, I.L. (2005). Cell intrinsic alterations underlie haematopoietic stem cell ageing. Proc. Natl. Acad. Sci. U.S.A. *102*, 9194–9199.

Rothenberg, E.V. (2007). Negotiation of the T lineage fate decision by transcription-factor interplay and microenvironmental signals. Immunity *26*, 690–702.

Rowley, J.D. (1973). Identificaton of a translocation with quinacrine fluorescence in a patient with acute leukaemia. Ann. Genet. *16*, 109–112.

Rowley, J.D., Golomb, H.M., and Dougherty, C. (1977). 15/17 translocation, a consistent chromosomal change in acute promyelocytic leukaemia. Lancet *1*, 549–550.

Rozovskaia, T., Feinstein, E., Mor, O., Foa, R., Blechman, J., Nakamura, T., Croce, C.M., Cimino, G., and Canaani, E. (2001). Upregulation of Meis1 and HoxA9 in acute lymphocytic leukaemias with the t(4 : 11) abnormality. Oncogene *20*, 874–878.

Russell, E.S., and Bernstein, S.E. (1966). Blood and blood formation. in biology of the laboratory mouse, second edition, E.L. Green, ed. (New York: McGraw–Hill), pp. 351–372.

Russler-Germain, D.A., Spencer, D.H., Young, M.A., Lamprecht, T.L., Miller, C.A., Fulton, R., Meyer, M.R., Erdmann-Gilmore, P., Townsend, R.R., Wilson, R.K., et al. (2014). The R882H DNMT3A mutation associated with AML dominantly inhibits wild-type DNMT3A by blocking its ability to form active tetramers. Cancer Cell *25*, 442–454.

Samudio, I., Fiegl, M., and Andreeff, M. (2009). Mitochondrial uncoupling and the Warburg effect: molecular basis for the reprogramming of cancer cell metabolism. Cancer Res. *69*, 2163–2166.

Samudio, I., Fiegl, M., McQueen, T., Clise-Dwyer, K., and Andreeff, M. (2008). The Warburg effect in leukaemia-stroma cocultures is mediated by mitochondrial uncoupling associated with uncoupling protein 2 activation. Cancer Res *68*, 5198–5205.

Samudio, I., Harmancey, R., Fiegl, M., Kantarjian, H., Konopleva, M., Korchin, B., Kaluarachchi, K., Bornmann, W., Duvvuri, S., Taegtmeyer, H., et al. (2010). Pharmacologic inhibition of fatty acid oxidation sensitizes human leukaemia cells to apoptosis induction. J. Clin. Inv.*120*, 142–156.

Sancho, P., Burgos-Ramos, E., Tavera, A., Bou Kheir, T., Jagust, P., Schoenhals, M., Barneda, D., Sellers, K., Campos-Olivas, R., Graña, O., et al. (2015). MYC/PGC-1α balance determines the metabolic phenotype and plasticity of pancreatic cancer stem cells. Cell Metabolism *22*, 590–605.

Sanjuan-Pla, A., Macaulay, I.C., Jensen, C.T., Woll, P.S., Luis, T.C., Mead, A., Moore, S., Carella, C., Matsuoka, S., Bouriez Jones, T., et al. (2013). Platelet-biased stem cells reside at the apex of the haematopoietic stem-cell hierarchy. Nature *502*, 232–236.

Sass, E., Blachinsky, E., Karniely, S., and Pines, O. (2001). Mitochondrial and cytosolic isoforms of yeast fumarase are derivatives of a single translation product and have identical amino termini. J. Biol. Chem. *276*, 46111–46117.

Sattler, M., Verma, S., Shrikhande, G., Byrne, C.H., Pride, Y.B., Winkler, T., Greenfield, E.A., Salgia, R., and Griffin, J.D. (2000). The BCR/ABL tyrosine kinase induces production of reactive oxygen species in haematopoietic cells. J. Biol. Chem. *275*, 24273–24278.

Sauvageau, G., Lansdorp, P.M., Eaves, C.J., Hogge, D.E., Dragowska, W.H., Reid, D.S., Largman, C., Lawrence, H.J., and Humphries, R.K. (1994). Differential expression of homeobox genes in functionally distinct CD34+ subpopulations of human bone marrow cells. Proceedings of the National Academy of Sciences *91*, 12223–12227.

Schaaf, C.A., Kwak, H., Koenig, A., Misulovin, Z., Gohara, D.W., Watson, A., Zhou, Y., Lis, J.T., and Dorsett, D. (2013). Genome-wide control of RNA polymerase II activity by cohesin. PLoS Genet. *9*, e1003382.

Schnittger, S., Schoch, C., Kern, W., Mecucci, C., Tschulik, C., Martelli, M.F., Haferlach, T., Hiddemann, W., and Falini, B. (2005). Nucleophosmin gene mutations are predictors of favorable prognosis in acute myelogenous leukaemia with a normal karyotype. Blood *106*, 3733–3739.

Schödel, J., Oikonomopoulos, S., Ragoussis, J., Pugh, C.W., Ratcliffe, P.J., and Mole, D.R. (2011). High-resolution genome-wide mapping of HIF-binding sites by ChIP-seq. Blood *117*, e207–e217.

Schofield, R. (1978). The relationship between the spleen colony-forming cell and the haemopoietic stem cell. Blood Cells *4*, 7–25.

Sciacovelli, M., Gonçalves, E., Johnson, T.I., Zecchini, V.R., da Costa, A.S.H., Gaude, E., Drubbel, A.V., Theobald, S.J., Abbo, S.R., Tran, M.G.B., et al. (2016). Fumarate is an epigenetic modifier that elicits epithelial-to-mesenchymal transition. Nature *537*, 544–547.

Seet, C.S., Brumbaugh, R.L., and Kee, B.L. (2004). Early B cell factor promotes B lymphopoiesis with reduced interleukin 7 responsiveness in the absence of E2A. J. Exp. Med. *199*, 1689–1700.

Segal, A.W. (2005). How neutrophils kill microbes. Ann. Rev. Immunol. *23*, 197–223.

Semenza, G.L. (2000). Hypoxia, clonal selection, and the role of HIF-1 in tumor progression. Crit. Rev. Biochem. Mol. Biol. *35*, 71–103.

Shen, W.-F., Montgomery, J.C., Rozenfeld, S., Moskow, J.J., Lawrence, H.J., Buchberg, A.M., and Largman, C. (1997). AbdB-like Hox proteins stabilize DNA binding by the Meis1 homeodomain proteins. Molecular and Cellular Biology *17*, 6448–6458.

Shen, Y.-A., Wang, C.-Y., Hsieh, Y.-T., Chen, Y.-J., and Wei, Y.-H. (2015). Metabolic reprogramming orchestrates cancer stem cell properties in nasopharyngeal carcinoma. Cell Cycle *14*, 86–98.

Shin, J.Y., Hu, W., Naramura, M., and Park, C.Y. (2014). High c-Kit expression identifies haematopoietic stem cells with impaired self-renewal and megakaryocytic bias. J. Exp. Med. *211*, 217–231.

Shinohara, A., Imai, Y., Nakagawa, M., Takahashi, T., Ichikawa, M., and Kurokawa, M. (2014). Intracellular reactive oxygen species mark and influence the megakaryocyte-erythrocyte progenitor fate of common myeloid progenitors. Stem Cells *32*, 548–557.

Shirai, C.L., Ley, J.N., White, B.S., Kim, S., Tibbitts, J., Shao, J., Ndonwi, M., Wadugu, B., Duncavage, E.J., Okeyo-Owuor, T., et al. (2015). Mutant U2AF1 expression alters haematopoiesis and pre - mRNA splicing *in vivo*. Cancer Cell *27*, 631–643.

Shlush, L.I., Zandi, S., Mitchell, A., Chen, W.C., Brandwein, J.M., Gupta, V., Kennedy, J.A., Schimmer, A.D., Schuh, A.C., Yee, K.W., et al. (2014). Identification of pre-leukaemic haematopoietic stem cells in acute leukaemia. Nature *506*, 328–333.

Shurtleff, S.A., Meyers, S., Hiebert, S.W., Raimondi, S.C., Head, D.R., Willman, C.L., Wolman, S., Slovak, M.L., Carroll, A.J., and Behm, F. (1995). Heterogeneity in

CBF beta/MYH11 fusion messages encoded by the inv(16)(p13q22) and the t(16;16)(p13;q22) in acute myelogenous leukaemia. Blood *85*, 3695–3703.

Sieburg, H.B., and Müller-Sieburg, C.E. (2004). Classification of short kinetics by shape. In Silico Biology *4*, 209–217.

Sieburg, H.B., Cho, R.H., Dykstra, B., Uchida, N., Eaves, C.J., and Muller-Sieburg, C.E. (2006). The haematopoietic stem compartment consists of a limited number of discrete stem cell subsets. Blood *107*, 2311–2316.

Signer, R.A.J., and Morrison, S.J. (2013). Mechanisms that regulate stem cell ageing and life span. Cell Stem Cell *12*, 152–165.

Simsek, T., Kocabas, F., Zheng, J., Deberardinis, R.J., Mahmoud, A.I., Olson, E.N., Schneider, J.W., Zhang, C.C., and Sadek, H.A. (2010). The distinct metabolic profile of haematopoietic stem cells reflects their location in a hypoxic niche. Cell Stem Cell *7*, 380–390.

Škrtić, M., Sriskanthadevan, S., Jhas, B., Gebbia, M., Wang, X., Wang, Z., Hurren, R., Jitkova, Y., Gronda, M., Maclean, N., et al. (2011). Inhibition of mitochondrial translation as a therapeutic strategy for human acute myeloid leukaemia. Cancer Cell *20*, 674–688.

Skversky, N.J., Yarrow, M.W., and Lewinn, E.B. (1957). Phenylbutazone in the treatment of deep-vein thrombophlebitis; a preliminary report. J Albert Einstein Med Cent (Phila) *5*, 268–271.

Smith, T.G., Robbins, P.A., and Ratcliffe, P.J. (2008). The human side of hypoxia-inducible factor. Br. J. Haematol. *141*, 325–334.

Somervaille, T.C.P., and Cleary, M.L. (2006). Identification and characterisation of leukaemia stem cells in murine MLL-AF9 acute myeloid leukaemia. Cancer Cell *10*, 257–268.

Sourbier, C., Ricketts, C.J., Matsumoto, S., Crooks, D.R., Liao, P.-J., Mannes, P.Z., Yang, Y., Wei, M.-H., Srivastava, G., Ghosh, S., et al. (2014). Targeting ABL1-mediated oxidative stress adaptation in fumarate hydratase-deficient cancer. Cancer Cell *26*, 840–850.

Spangrude, G.J., Heimfeld, S., and Weissman, I.L. (1988). Purification and characterisation of mouse haematopoietic stem cells. Science *241*, 58–62.

Spencer, J.A., Ferraro, F., Roussakis, E., Klein, A., Wu, J., Runnels, J.M., Zaher, W., Mortensen, L.J., Alt, C., Turcotte, R., et al. (2014). Direct measurement of local oxygen concentration in the bone marrow of live animals. Nature *508*, 269–273.

Speth, J.M., Hoggatt, J., Singh, P., and Pelus, L.M. (2014). Pharmacologic increase in HIF1α enhances haematopoietic stem and progenitor homing and engraftment. Blood *123*, 203–207.

Sriskanthadevan, S., Jeyaraju, D.V., Chung, T.E., Prabha, S., Xu, W., Skrtic, M., Jhas, B., Hurren, R., Gronda, M., Wang, X., et al. (2015). AML cells have low spare

reserve capacity in their respiratory chain that renders them susceptible to oxidative metabolic stress. Blood *125*, 2120–2130.

Starck, J., Cohet, N., Gonnet, C., Sarrazin, S., Doubeikovskaia, Z., Doubeikovski, A., Verger, A., Duterque-Coquillaud, M., and Morle, F. (2003). Functional Cross-Antagonism between Transcription Factors FLI-1 and EKLF. Mol. Cell. Biol. *23*, 1390–1402.

Stein, E.M., and Tallman, M.S. (2016). Emerging therapeutic drugs for AML. Blood *127*, 71–78.

Suda, T., Takubo, K., and Semenza, G.L. (2011). Metabolic Regulation of Haematopoietic Stem Cells in the Hypoxic Niche. Cell Stem Cell *9*, 298–310.

Sudarshan, S., Sourbier, C., Kong, H.-S., Block, K., Romero, V.A.V., Yang, Y., Galindo, C., Mollapour, M., Scroggins, B., Goode, N., et al. (2009). Fumarate hydratase deficiency in renal cancer induces glycolytic addiction and hypoxia-inducible transcription factor 1α stabilization by glucose-dependent generation of reactive oxygen species. Mol Cell Biol *29*, 4080–4090.

Suganuma, K., Miwa, H., Imai, N., Shikami, M., Gotou, M., Goto, M., Mizuno, S., Takahashi, M., Yamamoto, H., Hiramatsu, A., et al. (2010). Energy metabolism of leukaemia cells: glycolysis *versus* oxidative phosphorylation. Leukaemia & Lymphoma *51*, 2112–2119.

Suh, Y.A., Arnold, R.S., Lassegue, B., Shi, J., Xu, X., Sorescu, D., Chung, A.B., Griendling, K.K., and Lambeth, J.D. (1999). Cell transformation by the superoxide-generating oxidase Mox1. Nature *401*, 79–82.

Sullivan, L.B., Garcia-Martinez, E., Nguyen, H., Mullen, A.R., Dufour, E., Sudarshan, S., Licht, J.D., Deberardinis, R.J., and Chandel, N.S. (2013). The proto-oncometabolite fumarate binds glutathione to amplify ROS dependent signaling. Mol Cell *51*, 236–248.

Sun, J., Ramos, A., Chapman, B., Johnnidis, J.B., Le, L., Ho, Y.-J., Klein, A., Hofmann, O., and Camargo, F.D. (2014). Clonal dynamics of native haematopoiesis. Nature *514*, 322–327.

Swansbury, G.J., Slater, R., Bain, B.J., Moorman, A.V., and Secker-Walker, L.M. (1998). Haematological malignancies with t(9;11)(p21-22;q23): a laboratory and clinical study of 125 cases. European 11q23 Workshop participants. Leukaemia *12*, 792–800.

Swerdlow SH, Campo E, Harris NL, et al, eds. WHO Classification of tumours of haematopoietic and lymphoid tissues. Lyon: IARC; (2008).

Tahiliani, M., Koh, K.P., Shen, Y., Pastor, W.A., Bandukwala, H., Brudno, Y., Agarwal, S., Iyer, L.M., Liu, D.R., Aravind, L., et al. (2009). Conversion of 5-methylcytosine to 5-hydroxymethylcytosine in mammalian DNA by MLL partner TET1. Science *324*, 930–935.

Takubo, K., Goda, N., Yamada, W., Iriuchishima, H., Ikeda, E., Kubota, Y., Shima, H., Johnson, R.S., Hirao, A., Suematsu, M., et al. (2010). Regulation of the HIF-1alpha level is essential for haematopoietic stem cells. Cell Stem Cell *7*, 391–402.

Takubo, K., Nagamatsu, G., Kobayashi, C.I., Nakamura-Ishizu, A., Kobayashi, H., Ikeda, E., Goda, N., Rahimi, Y., Johnson, R.S., Soga, T., et al. (2013). Regulation of glycolysis by Pdk functions as a metabolic checkpoint for cell cycle quiescence in haematopoietic stem cells. Cell Stem Cell *12*, 49–61.

Talpaz, M., Kantarjian, H.M., McCredie, K., Trujillo, J.M., Keating, M.J., and Gutterman, J.U. (1986). Haematologic remission and cytogenetic improvement induced by recombinant human interferon alpha A in chronic myelogenous leukaemia. N. Engl. J. Med. *314*, 1065–1069.

Talpaz, M., McCredie, K.B., Mavligit, G.M., and Gutterman, J.U. (1983). Leukocyte interferon-induced myeloid cytoreduction in chronic myelogenous leukaemia. Blood *62*, 689–692.

Tanaka KR, Valentine WN. Fumarase activity of human leukocytes and erythrocytes. Blood 17, 328-333 (1961).

Tannahill, G.M., Curtis, A.M., Adamik, J., Palsson-McDermott, E.M., McGettrick, A.F., Goel, G., Frezza, C., Bernard, N.J., Kelly, B., Foley, N.H., et al. (2013). Succinate is an inflammatory signal that induces IL-1β through HIF-1α. Nature *496*, 238–242.

Taoudi, S., Bee, T., Hilton, A., Knezevic, K., Scott, J., Willson, T.A., Collin, C., Thomas, T., Voss, A.K., Kile, B.T., et al. (2011). ERG dependence distinguishes developmental control of haematopoietic stem cell maintenance from haematopoietic specification. Genes Dev. *25*, 251–262.

Teitell, M.A., and Mikkola, H.K.A. (2006). Transcriptional activators, repressors, and epigenetic modifiers controlling haematopoietic stem cell development. Pediatr. Res. *59*, 33R – 9R.

Ternette, N., Yang, M., Laroyia, M., Kitagawa, M., O'Flaherty, L., Wolhulter, K., Igarashi, K., Saito, K., Kato, K., Fischer, R., et al. (2013). Inhibition of mitochondrial aconitase by succination in fumarate hydratase deficiency. Cell Reports *3*, 689–700.

TeSlaa, T., and Teitell, M.A. (2014). Techniques to monitor glycolysis. Methods in Enzymology, (Elsevier), pp. 91–114.

Thiede, C., Koch, S., Creutzig, E., Steudel, C., Illmer, T., Schaich, M., and Ehninger, G. (2006). Prevalence and prognostic impact of NPM1 mutations in 1485 adult patients with acute myeloid leukaemia (AML). Blood *107*, 4011–4020.

Thol, F., Bollin, R., Gehlhaar, M., Walter, C., Dugas, M., Suchanek, K.J., Kirchner, A., Huang, L., Chaturvedi, A., Wichmann, M., et al. (2014). Mutations in the cohesin complex in acute myeloid leukaemia: clinical and prognostic implications. Blood *123*, 914–920.

Thorsteinsdottir, U., Kroon, E., Jerome, L., Blasi, F., and Sauvageau, G. (2001). Defining Roles for *HOX* and *MEIS1* genes in induction of acute myeloid leukaemia. Molecular and Cellular Biology *21*, 224–234.

Thorsteinsdottir, U., Mamo, A., Kroon, E., Jerome, L., Bijl, J., Lawrence, H.J., Humphries, K., and Sauvageau, G. (2002). Overexpression of the myeloid leukaemia–associated *Hoxa9* gene in bone marrow cells induces stem cell expansion. Blood *99*, 121–129.

Thota, S., Viny, A.D., Makishima, H., Spitzer, B., Radivoyevitch, T., Przychodzen, B., Sekeres, M.A., Levine, R.L., and Maciejewski, J.P. (2014). Genetic alterations of the cohesin complex genes in myeloid malignancies. Blood *124*, 1790–1798.

Till, J.E., McCulloch, E.A., and Siminovitch, L. (1964). a stochastic model of stem cell proliferation, based on the growth of spleen colony-forming cells. Proc Natl Acad Sci U S A *51*, 29–36.

Tkachuk, D.C., Kohler, S., and Cleary, M.L. (1992). Involvement of a homolog of Drosophila trithorax by 11q23 chromosomal translocations in acute leukaemias. Cell *71*, 691–700.

Tomiyama, A., Serizawa, S., Tachibana, K., Sakurada, K., Samejima, H., Kuchino, Y., and Kitanaka, C. (2006). Critical role for mitochondrial oxidative phosphorylation in the activation of tumor suppressors Bax and Bak. J. Natl. Cancer Inst. *98*, 1462–1473.

Tomlinson, I.P.M., Alam, N.A., Rowan, A.J., Barclay, E., Jaeger, E.E.M., Kelsell, D., Leigh, I., Gorman, P., Lamlum, H., Rahman, S., et al. (2002). Germline mutations in FH predispose to dominantly inherited uterine fibroids, skin leiomyomata and papillary renal cell cancer. Nature Genetics *30*, 406–410.

Tong, W.-H., Sourbier, C., Kovtunovych, G., Jeong, S.Y., Vira, M., Ghosh, M., Romero, V.V., Sougrat, R., Vaulont, S., Viollet, B., et al. (2011). The glycolytic shift in fumarate-hydratase-deficient kidney cancer lowers AMPK levels, increases anabolic propensities and lowers cellular iron levels. Cancer Cell *20*, 315–327.

Traver, D., Miyamoto, T., Christensen, J., Iwasaki-Arai, J., Akashi, K., and Weissman, I.L. (2001). Foetal liver myelopoiesis occurs through distinct, prospectively isolatable progenitor subsets. Blood *98*, 627–635.

Tregoning, S., Salter, W., Thorburn, D.R., Durkie, M., Panayi, M., Wu, J.Y., Easterbrook, A., and Coman, D.J. (2013). Fumarase deficiency in dichorionic diamniotic twins. Twin Res Hum Genet *16*, 1117–1120.

Tsutsumi, S., Taketani, T., Nishimura, K., Ge, X., Taki, T., Sugita, K., Ishii, E., Hanada, R., Ohki, M., Aburatani, H., et al. (2003). Two distinct gene expression signatures in pediatric acute lymphoblastic leukaemia with MLL rearrangements. Cancer Res *63*, 4882–4887.

Ugale, A., Norddahl, G.L., Wahlestedt, M., Säwén, P., Jaako, P., Pronk, C.J., Soneji, S., Cammenga, J., and Bryder, D. (2014). Haematopoietic stem cells are intrinsically protected against MLL-ENL-mediated transformation. Cell Rep *9*, 1246–1255.

Usui, T., Preiss, J.C., Kanno, Y., Yao, Z.J., Bream, J.H., O'Shea, J.J., and Strober, W. (2006). T-bet regulates Th1 responses through essential effects on GATA-3 function rather than on IFNG gene acetylation and transcription. J. Exp. Med. *203*, 755–766.

van der Windt, G.J.W., Everts, B., Chang, C.-H., Curtis, J.D., Freitas, T.C., Amiel, E., Pearce, E.J., and Pearce, E.L. (2012). Mitochondrial respiratory capacity is a critical regulator of CD8+ T cell memory development. Immunity *36*, 68–78.

Visnjic, D., Kalajzic, Z., Rowe, D.W., Katavic, V., Lorenzo, J., and Aguila, H.L. (2004). Haematopoiesis is severely altered in mice with an induced osteoblast deficiency. Blood *103*, 3258–3264.

Vukovic, M., Guitart, A.V., Sepulveda, C., Villacreces, A., O'Duibhir, E., Panagopoulou, T.I., Ivens, A., Menendez-Gonzalez, J., Iglesias, J.M., Allen, L., et al. (2015). Hif-1α and Hif-2α synergize to suppress AML development but are dispensable for disease maintenance. J. Exp. Med. *212*, 2223–2234.

Vukovic, M., Guitart, A.V., Sepulveda, C., Villacreces, A., O'Duibhir, E., Panagopoulou, T.I., Ivens, A., Menendez-Gonzalez, J., Iglesias, J.M., Allen, L., et al. (2015). Hif-1α and Hif-2α synergize to suppress AML development but are dispensable for disease maintenance. J. Exp. Med. *212*, 2223–2234.

Walter, M.J., Shen, D., Ding, L., Shao, J., Koboldt, D.C., Chen, K., Larson, D.E., McLellan, M.D., Dooling, D., Abbott, R., et al. (2012). Clonal architecture of secondary acute myeloid leukaemia. N. Engl. J. Med. *366*, 1090–1098.

Wang, J.C.Y., and Dick, J.E. (2005). Cancer stem cells: lessons from leukaemia. Trends Cell Biol. *15*, 494–501.

Wang, Q., Wu, G., Mi, S., He, F., Wu, J., Dong, J., Luo, R.T., Mattison, R., Kaberlein, J.J., Prabhakar, S., et al. (2011). MLL fusion proteins preferentially regulate a subset of wild-type MLL target genes in the leukaemic genome. Blood *117*, 6895–6905.

Wang, Y.-H., Israelsen, W.J., Lee, D., Yu, V.W.C., Jeanson, N.T., Clish, C.B., Cantley, L.C., Vander Heiden, M.G., and Scadden, D.T. (2014). Cell-state-specific metabolic dependency in haematopoiesis and leukaemogenesis. Cell *158*, 1309–1323.

Wang, Y., Xiao, M., Chen, X., Chen, L., Xu, Y., Lv, L., Wang, P., Yang, H., Ma, S., Lin, H., et al. (2015). WT1 recruits TET2 to regulate its target gene expression and suppress leukaemia cell proliferation. Mol. Cell *57*, 662–673.

Warburg, O. (1956). On the origin of cancer cells. Science *123*, 309–314.

Watson, J.V., Chambers, S.H., and Smith, P.J. (1987). A pragmatic approach to the analysis of DNA histograms with a definable G1 peak. Cytometry *8*, 1–8.

Weinberg, F., Hamanaka, R., Wheaton, W.W., Weinberg, S., Joseph, J., Lopez, M., Kalyanaraman, B., Mutlu, G.M., Budinger, G.R.S., and Chandel, N.S. (2010). Mitochondrial metabolism and ROS generation are essential for Kras-mediated tumorigenicity. Proc. Natl. Acad. Sci. *107*, 8788–8793.

Weissman, I.L. (2000). Stem cells: Units of development, units of regeneration, and units in evolution. Cell *100*, 157–168.

Weissman, I.L., Anderson, D.J., and Gage, F. (2001). Stem and progenitor cells: origins, phenotypes, lineage commitments, and transdifferentiations. Ann. Rev. Cell Dev. Biol. *17*, 387–403.

Wilson, A., Laurenti, E., Oser, G., van der Wath, R.C., Blanco-Bose, W., Jaworski, M., Offner, S., Dunant, C.F., Eshkind, L., Bockamp, E., et al. (2008). Haematopoietic stem cells reversibly switch from dormancy to self-renewal during homeostasis and repair. Cell *135*, 1118–1129.

Winkler, I.G., Barbier, V., Nowlan, B., Jacobsen, R.N., Forristal, C.E., Patton, J.T., Magnani, J.L., and Lévesque, J.-P. (2012). Vascular niche E-selectin regulates haematopoietic stem cell dormancy, self renewal and chemoresistance. Nat Med *18*, 1651–1657.

Wise, D.R., Ward, P.S., Shay, J.E.S., Cross, J.R., Gruber, J.J., Sachdeva, U.M., Platt, J.M., DeMatteo, R.G., Simon, M.C., and Thompson, C.B. (2011). Hypoxia promotes isocitrate dehydrogenase-dependent carboxylation of α-ketoglutarate to citrate to support cell growth and viability. PNAS *108*, 19611–19616.

Wong, P., Iwasaki, M., Somervaille, T.C.P., So, C.W.E., and Cleary, M.L. (2007). Meis1 is an essential and rate-limiting regulator of MLL leukaemia stem cell potential. Genes Dev *21*, 2762–2774.

Wong, T.N., Ramsingh, G., Young, A.L., Miller, C.A., Touma, W., Welch, J.S., Lamprecht, T.L., Shen, D., Hundal, J., Fulton, R.S., et al. (2015). Role of TP53 mutations in the origin and evolution of therapy-related acute myeloid leukaemia. Nature *518*, 552–555.

Xiao, M. et al. (2012). Inhibition of α -KG-dependent histone and DNA demethylases byfumarate and succinate that are accumulated in mutations of FH and SDH tumor suppressors. Genes Dev. 26, 1326–1338.

Xiao, M., Yang, H., Xu, W., Ma, S., Lin, H., Zhu, H., Liu, L., Liu, Y., Yang, C., Xu, Y., et al. (2012). Inhibition of α-KG-dependent histone and DNA demethylases by fumarate and succinate that are accumulated in mutations of FH and SDH tumor suppressors. Genes Dev. *26*, 1326–1338.

Xie, Y., Yin, T., Wiegraebe, W., He, X.C., Miller, D., Stark, D., Perko, K., Alexander, R., Schwartz, J., Grindley, J.C., et al. (2009). Detection of functional haematopoietic stem cell niche using real-time imaging. Nature *457*, 97–101.

Yamada, Y., Warren, A.J., Dobson, C., Forster, A., Pannell, R., and Rabbitts, T.H. (1998). The T cell leukaemia LIM protein Lmo2 is necessary for adult mouse haematopoiesis. Proc. Natl. Acad. Sci. U.S.A. *95*, 3890–3895.

Yamamoto, R., Morita, Y., Ooehara, J., Hamanaka, S., Onodera, M., Rudolph, K.L., Ema, H., and Nakauchi, H. (2013). Clonal analysis unveils self-renewing lineage-restricted progenitors generated directly from haematopoietic stem cells. Cell *154*, 1112–1126.

Yamazaki, S., Ema, H., Karlsson, G., Yamaguchi, T., Miyoshi, H., Shioda, S., Taketo, M.M., Karlsson, S., Iwama, A., and Nakauchi, H. (2011). Non myelinating schwann cells maintain haematopoietic stem cell hibernation in the bone marrow niche. Cell *147*, 1146–1158.

Yang, L., Bryder, D., Adolfsson, J., Nygren, J., Månsson, R., Sigvardsson, M., and Jacobsen, S.E.W. (2005). Identification of Lin ($^-$) Sca1($^+$) kit ($^+$) CD34 ($^+$) Flt3($^-$) short-term haematopoietic stem cells capable of rapidly reconstituting and rescuing myeloablated transplant recipients. Blood *105*, 2717–2723.

Yang, M., Soga, T., Pollard, P.J., and Adam, J. (2012). The emerging role of fumarate as an oncometabolite. Front Oncol *2*, 85.

Ye, X.-Q., Li, Q., Wang, G.-H., Sun, F.-F., Huang, G.-J., Bian, X.-W., Yu, S.-C., and Qian, G.-S. (2011). Mitochondrial and energy metabolism-related properties as novel indicators of lung cancer stem cells. International Journal of Cancer *129*, 820–831.

Yeoh, E.-J., Ross, M.E., Shurtleff, S.A., Williams, W.K., Patel, D., Mahfouz, R., Behm, F.G., Raimondi, S.C., Relling, M.V., Patel, A., et al. (2002). Classification, subtype discovery, and prediction of outcome in pediatric acute lymphoblastic leukaemia by gene expression profiling. Cancer Cell *1*, 133–143.

Yogev, O., Yogev, O., Singer, E., Shaulian, E., Goldberg, M., Fox, T.D., and Pines, O. (2010). Fumarase: A mitochondrial metabolic enzyme and a cytosolic/nuclear component of the DNA damage response. PLoS Biology *8*, e1000328.

Yokoyama, A., Lin, M., Naresh, A., Kitabayashi, I., and Cleary, M.L. (2010). A higher-order complex containing AF4 and ENL family proteins with P-TEFb facilitates oncogenic and physiologic MLL-dependent transcription. Cancer Cell *17*, 198–212.

Yoshida K, Sanada M, Shiraishi Y, et al. (2011). Frequent pathway mutations of splicing machinery in myelodysplasia. Nature; 478(7367):64-69.

Yoshihara, H., Arai, F., Hosokawa, K., Hagiwara, T., Takubo, K., Nakamura, Y., Gomei, Y., Iwasaki, H., Matsuoka, S., Miyamoto, K., et al. (2007). Thrombopoietin/MPL signalling regulates haematopoietic stem cell quiescence and interaction with the osteoblastic niche. Cell Stem Cell *1*, 685–697.

Yu, W.-M., Liu, X., Shen, J., Jovanovic, O., Pohl, E.E., Gerson, S.L., Finkel, T., Broxmeyer, H.E., and Qu, C.-K. (2013). Metabolic regulation by the mitochondrial phosphatase PTPMT1 is required for haematopoietic stem cell differentiation. Cell Stem Cell *12*, 62–74.

Zanjani, E.D., Ascensao, J.L., and Tavassoli, M. (1993). Liver-derived foetal haematopoietic stem cells selectively and preferentially home to the foetal bone marrow. Blood *81*, 399–404.

Zeisig, B.B., and Wai Eric So, C. (2009). Retroviral/Lentiviral transduction and transformation assay in leukaemia, C.W. Eric So, ed. (Totowa, NJ: Humana Press), pp. 207–229.

Zeisig, B.B., Milne, T., García-Cuéllar, M.-P., Schreiner, S., Martin, M.-E., Fuchs, U., Borkhardt, A., Chanda, S.K., Walker, J., Soden, R., et al. (2004). Hoxa9 and

Meis1 are key targets for MLL-ENL-mediated cellular immortalization. Mol. Cell. Biol. *24*, 617–628.

Zeleznick, L.D., and Bhuyan, B.K. (1969). Treatment of leukaemic (L-1210) mice with double-stranded polyribonucleotides. Proc. Soc. Exp. Biol. Med. *130*, 126–128.

Zeng, H., Yücel, R., Kosan, C., Klein-Hitpass, L., and Möröy, T. (2004). Transcription factor Gfi1 regulates self-renewal and engraftment of haematopoietic stem cells. EMBO J *23*, 4116–4125.

Zhang, J., Niu, C., Ye, L., Huang, H., He, X., Tong, W.-G., Ross, J., Haug, J., Johnson, T., Feng, J.Q., et al. (2003). Identification of the haematopoietic stem cell niche and control of the niche size. Nature *425*, 836–841.

Zheng, L., Cardaci, S., Jerby, L., MacKenzie, E.D., Sciacovelli, M., Johnson, T.I., Gaude, E., King, A., Leach, J.D.G., Edrada-Ebel, R., et al. (2015). Fumarate induces redox-dependent senescence by modifying glutathione metabolism. Nat Commun *6*, 6001.

Zheng, L., MacKenzie, E.D., Karim, S.A., Hedley, A., Blyth, K., Kalna, G., Watson, D.G., Szlosarek, P., Frezza, C., and Gottlieb, E. (2013). Reversed argininosuccinate lyase activity in fumarate hydratase-deficient cancer cells. Cancer Metab *1*, 12.

Zhong, D., Xiong, L., Liu, T., Liu, X., Liu, X., Chen, J., Sun, S.-Y., Khuri, F.R., Zong, Y., Zhou, Q., et al. (2009). The glycolytic inhibitor 2-deoxyglucose activates multiple prosurvival pathways through IGF1R. J. Biol. Chem. *284*, 23225–23233.

Ziemin-van der Poel, S., McCabe, N.R., Gill, H.J., Espinosa, R., Patel, Y., Harden, A., Rubinelli, P., Smith, S.D., Le Beau, M.M., and Rowley, J.D. (1991). Identification of a gene, MLL, that spans the breakpoint in 11q23 translocations associated with human leukaemias. Proc. Natl. Acad. Sci. U.S.A. *88*, 10735–10739.

Zuber, J., Radtke, I., Pardee, T.S., Zhao, Z., Rappaport, A.R., Luo, W., McCurrach, M.E., Yang, M.-M., Dolan, M.E., Kogan, S.C., et al. (2009). Mouse models of human AML accurately predict chemotherapy response. Genes & Development *23*, 877–889.